EXCIPIENT CHARACTERIZATION AND PARTICLE ENGINEERING TO DEVELOP DIRECTLY COMPRESSED ORALLY DISINTEGRATING TABLETS

ALI AHMED ALI AL-KHATTAWI

Doctor of Philosophy

ASTON UNIVERSITY

September 2014

Aston University

Excipient Characterization and Particle Engineering to Develop Directly Compressed Orally Disintegrating Tablets

Ali Ahmed Ali Al-Khattawi

Doctor of Philosophy

Thesis Summary

ODTs have emerged as a novel oral dosage form with a potential to deliver a wide range of drug candidates to paediatric and geriatric patients. Compression of excipients offers a cost-effective and translatable methodology for the manufacture of ODTs. Though, technical challenges prevail such as difficulty to achieve suitable tablet mechanical strength while ensuring rapid disintegration in the mouth, poor compressibility of preferred ODT diluent D-mannitol, and limited use for modified drug-release.

The work investigates excipients' functionality in ODTs and proposes new methodologies for enhancing material characteristics via process and particle engineering. It also aims to expand ODT applications for modified drug-release. Preformulation and formulation studies employed a plethora of techniques/tests including AFM, SEM, DSC, XRD, TGA, HSM, FTIR, hardness, disintegration time, friability, stress/strain and Heckel analysis. Tableting of D-mannitol and cellulosic excipients utilised various compression forces, material concentrations and grades. Engineered D-mannitol particles were made by spray drying mannitol with pore former NH_4HCO_3. Coated microparticles of model API omeprazole were prepared using water-based film forming polymers.

The results of nanoscopic investigations elucidated the compression profiles of ODT excipients. Strong densification of MCC (Py is 625 MPa) occurs due to conglomeration of physico-mechanical factors whereas D-mannitol fragments under pressure leading to poor compacts. Addition of cellulosic excipients (L-HPC and HPMC) and granular mannitol to powder mannitol was required to mechanically strengthen the dosage form (hardness >60 N, friability <1%) and to maintain rapid disintegration (<30 sec). Similarly, functionality was integrated into D-mannitol by fabrication of porous, yet, resilient particles which resulted in upto 150% increase in the hardness of compacts. The formulated particles provided resistance to fracture under pressure due to inherent elasticity while promoted tablet disintegration (50-77% reduction in disintegration time) due to porous nature. Additionally, coated microparticles provided an ODT-appropriate modified-release coating strategy by preventing drug (omeprazole) release.

Keywords: Mannitol, tablet, functionality, compressibility, modified-release

Dedication

I dedicate this work to my family members especially my father 'Dr Ahmed Ali Ibrahim Al-Khattawi' and my mother 'Dr Hanaa Dawood Salman Alghallay' whom without, I wouldn't be able to achieve this. It has been a tough journey and I couldn't have imagined myself getting to this stage without your encouragement and support. You have strengthened me, stood by my side, prayed for me and backed me with all resources. No matter how much I try, words fail to express my love and gratitude to you.

List of Contents

Chapter 1

Chapter 2

List of Tables

List of Figures

13

15

19

Abbreviations List

°C	Degree celsius
μg	Microgram
μl	Micro litre
μm	Micro metre
2θ	Angular range
AAPS	American association of pharmaceutical scientists
AFM	Atomic force microscopy
ANOVA	Analysis of variance
API	Active pharmaceutical ingredient
ATR	Attenuated total reflectance
AUC	Area under curve
$CaOH_2$	Calcium hydroxide
CCF	Central composite face-centred
CDER	Centre for drug evaluation and research
CHMP	Committee for medicinal products for human use
cm	Centimetre
CMC	Critical micelle concentration
CO_2	Carbone dioxide
Copt	Optical concentration
D_2O	Deuterium oxide (heavy water)
Dmod Y	Distance to model Y
DOE	Design of experiments
DSC	Differential scanning calorimetry
EDQM	European directorate for the quality of medicines
EE	Encapsulation efficiency
EMA	European medicines agency
FDA	Food and drug administration
FIP	International pharmaceutical federation
FTIR	Fourier-transform infrared spectroscopy
g	Gram
GERD	Gastro-oesophageal reflux disease
GIT	Gastro-intestinal tract
h	Hour
H_2O	Water
H-bonding	Hydrogen bonding
HCl	Hydrochloric acid
HPMC	Hydroxypropyl methylcellulose
HPMCAS	Hydroxypropyl methylcellulose acetate succinate
HSM	Hot stage microscopy
ICH	International conference on harmonisation
kg	Kilogram
kN	Kilo Newton
kV	Kilo Volts
L-HPC	Low-substituted hydroxypropyl cellulose
LLOD	Lower limit of detection
LLOQ	Lower limit of quantification
m	Metre
M	Molar
mA	Milliampere
MCC	Microcrystalline cellulose
mg	Milligram
min	Minute

MJ	Mega Joule
mJ	Milli joule
mL	Millilitre
mm	Millimetre
Mod	Modification
MPa	Mega pascal
MβCD	Methyl-β-cyclodextrin
N	Newton
N	Normal
$NaHCO_3$	Sodium bicarbonate
NaOH	Sodium hydroxide
NH_3	Ammonia
NH_4HCO_3	Ammonium bicarbonate
nm	Nanometre
nN	Nano Newton
NSAID	Non-steroidal anti-inflammatory drug
o/w	Oil-in-water
ODT	Orally disintegrating tablet
PBS	Phosphate buffered saline
PEG	Polyethylene glycol
Ph. Eur.	European pharmacopeia
PLS	Partial least squares
PPI	Proton pump inhibitor
ppm	Parts per million
PVA	Polyvinyl alcohol
PVP	Polyvinylpyrrolidone
Py	Yield pressure
Q^2	Predictability
QbD	Quality by design
Ra	Average roughness
RH	Relative humidity
RP-HPLC	Reversed-Phase High Performance Liquid Chromatography
Rpm	Rounds per minute
SD	Standard deviation
sec	Second
SEM	Scanning electron microscopy
$t_{1/2}$	Half life
Tg	Glass transition temperature
TGA	Thermogravimetric analysis
TPGS	α-tocopheryl polyethylene glycol 1000 succinate
USP	United states pharmacopeia
UV PDA	Ultraviolet photo diode array
v/v	Volume per volume
VMD	Volume mean diameter
w/v	weight per volume
w/w	weight per weight
XRD	X-ray diffraction

Awards/Poster Prizes

1- International Pharmaceutical Excipients Council (IPEC) Graduate Award for Excellence of Research on Excipients, Texas 2013 (first recipient from the UK).

2- Academy of Pharmaceutical Sciences of Great Britain – GlaxoSmithKline Poster Prize Award, Edinburgh 2013.

3- Royal Society of Chemistry Process Technology Group Award, London 2011.

Publication List

Articles and Reviews:

1- Ali Al-Khattawi, Hamad Alyami, Bill Townsend, Xianghong Ma and Afzal R Mohammed (2014) Evidence-Based Nanoscopic and Molecular Framework for Excipient Functionality in Compressed Orally Disintegrating Tablets. *PLOS ONE*, 9(7): e101369.

2- Ali Al-Khattawi, Affiong Iyire, Tom Dennison, Eman Dahmash, Clifford J Bailey, Julian Smith, Chris Martin, Peter Rue and Afzal R Mohammed (2014) Systematic Screening of Compressed ODT Excipients: Cellulosic Versus Non-Cellulosic. *Current Drug Delivery*, 11(4):486-500.

3- Ali Al-Khattawi and Afzal R Mohammed (2013) Compressed Orally Disintegrating Tablets: Excipients Evolution and Formulation Strategies. *Expert Opinion on Drug Delivery*, 10(5): 651-663.

4- Ali Al-Khattawi, Hamad Alyami, Afzal R Mohammed (2013) A Systematic Investigation of D-Mannitol Functionality in the Development of Age-Appropriate Formulations *CRS newsletter*, (April).

5- Ali Al-Khattawi, Ahmad Aly, Yvonne Perrie, Peter Rue and Afzal R Mohammed (2012) Multi Stage Strategy to Reduce Friability of Directly Compressed Orally Disintegrating Tablets. *Drug Delivery Letters*, 2(3): 195-201.

6- Ali Al-Khattawi and Afzal R Mohammed (2014) Excipients in Medicines for Children: Scientific and Regulatory Paradigms. *European Pharmaceutical Review*, 19(2), 67-70.

7- Ali Al-Khattawi and Afzal R Mohammed (2014) Challenges and Emerging Solutions in the Development of Compressed Orally Disintegrating Tablets. *Expert Opinion on Drug Discovery*, doi:10.1517/17460441.2014.941802.

Book Chapters:

1- Imran Saleem and Ali Al-Khattawi (2013) Surface Phenomena. In Pharmaceutics the science of medicine design. Denton P and Rostron C (Eds.). (13 vols.). Oxford University Press.

2- Ali Al-Khattawi, Tom Dennison, David Terry and Afzal R Mohammed (2014) Extemporaneous Preparation of Medicines for Children - *Neonatal and Paediatric prescribing* – (submitted).

3- Tom Dennison, Ali Al-Khattawi, David Terry and Afzal R Mohammed (2014) Developing medicines for children, with emphasis on the implications of the regulations and development process for the prescriber – *Neonatal and Paediatric prescribing* – (submitted).

Oral Presentations:

1- The Power of AFM Characterization in the Development of Novel Solid Pharmaceutical Dosage Forms. *4th International Workshop on Advanced Atomic Force Microscopy Techniques, Karlsruhe Institute of Nanotechnology (KIT-INT), Germany, March 2013.*

2- Microstructure Property and Adhesion Profiling to Elucidate Compaction Mechanisms of Pharmaceutical Materials. *UK PharmSci, Edinburgh, September 2013.*

3- Formulation Development of Orally Disintegrating Tablets: An Opportunity to Address Swallowing Difficulties in Geriatric Patients. *Geriatric Safe Medicines Summit, London, September 2013.*

4- Directly Compressed Orally Disintegrating Tablets for Paediatric Drug Delivery: A Novel Heat-Cool Process Strategy. *UK PharmSci, Nottingham, September 2012.*

Conference Proceedings

1- Ali Al-Khattawi, Peter Rue, Yvonne Perrie and Afzal R Mohammed. Engineered Dual Functional Mannitol for Age-Appropriate Formulation Development. *UK PharmSci, Hertfordshire, 2014.*

2- Ali Al-Khattawi, Peter Rue, Yvonne Perrie and Afzal R Mohammed. Particle Engineering Strategy For Controlled Porosity, Surface Habit and Functionality of Pharmaceutical Excipients. *UKICRS, Cork, 2014.*

3- Ali Al-Khattawi, Hamad Alyami, Bill Townsend, Xianghong Ma, Afzal R Mohammed. A Novel Approach to Improve Tableting Process Robustness and De-risk Formulation Development of Compressed Orally Disintegrating Tablets. *AAPS, Texas, 2013.*

Chapter 1

Introduction to Compressed ODTs, Excipients, Formulation Challenges and Emerging Solutions

1.1. Introduction

Oral delivery of active pharmaceutical ingredients has historically been associated with conventional formulations such as tablets, capsules and liquid dosage forms due to the ease of manufacture and financial viability. However, the last couple of decades have seen the emergence of a new paradigm focussed on the development of "patient-centred" dosage forms which has been the precursor to the advent of novel technologies such as modified release systems, needle free injections and others with an ultimate objective of enhancing medication concordance and maintenance of market exclusivity (Stegemann et al., 2012).

An orally disintegrating tablet (ODT) is a patient-friendly dosage form which disintegrates in the mouth upon contact with saliva thereby obviating the need to swallow tablets. ODTs are an ideal dosage form to deliver medicines to various patient populations, including the elderly and children, who usually have compromised swallowing ability due to various physiological and psychological factors (Sumiya et al., 2000; Varia et al., 2007).

The development in the field of orodispersible products has seen the emergence of different dosage forms besides ODTs such as oral lyophilisates and orodispersible films. According to EMA's Committee for Medicinal Products for Human Use (CHMP), orodispersible dosage forms have a 'great promise for children' (EMA CHMP, 2006). Moreover, previous surveys and clinical trials have shown that ODTs are well received by patients and healthcare professionals (MacGregor et al., 2003; Carnaby-Mann and Crary, 2005; Ibañez et al., 2007; LeBourgeois et al., 1999). Some of the marketed ODT products can be seen in Table 1.1 (from Jeong et al., 2010):

Table 1.1: ODTs patented technologies and examples of marketed products.

Patented Technology	Process Used	Product Example
Zydis	Solution or dispersion of drug and excipients (e.g. gelatine, saccharide) prepared and filled into blisters then freeze dried	Claritin Reditab contains loratadine (anti-histamine)
OraSolv	Tablets are prepared from effervescent powder at low compression force, used in combination with PackSolv technology as the tablets are friable	Remeron SolTab contains mirtazapine (anti-depressant)
DuraSolv	Similar to OraSolv except that tablets are prepared at higher compression forces so they can be packed in bottles	Zomig-ZMT contains zolmitriptan (anti-migraine)
WOW Tab	Granulation of low-mouldable saccharides (e.g. mannitol) and high-mouldable saccharides (e.g. sorbitol) then compression into tablets followed by moisture treatment	Gaster D contains famotidine (anti-ulcer)
Flashdose	A floss-like crystalline structure called 'cotton candy' is produced by a unique spinning mechanism before compressing it with the drug and other excipients to form tablets	Nurofen Meltlet contains ibuprofen (NSAID)
Frosta	Plastic granules made then mixed with wet binder and compressed	Fortecal contains calcium (supplement)
Pharmaburst	Dry blending of co-processed excipients with API, flavour and lubricant	Staxyn contains vardenafil hydrochloride (erectile dysfunction)

The increasing demand for ODTs as manifested by substantial market share (estimated to be $ 9 billion in 2012) has led to the development of multiple formulation strategies, including the cost-effective approach of direct compression (Chang, 2000; Harmon, 2007). This process is a convenient methodology to produce ODTs with adequate structural integrity necessary for optimal product performance. However, the relatively low porosity of a compressed ODT matrix may prolong the time required for the tablet to disintegrate, signifying the vital role of excipient selection in promoting disintegration (Al-Khattawi et al., 2012).

Compression technology has always relied on the use of mono functional excipients such as lactose and starch which ultimately influence a single outcome in the resultant tablet. This has led to the inclusion of several excipients within the formulation mix/blend to obtain multiple

outcomes such as high hardness, low friability and faster disintegration. Often this approach is not preferable for ODT formulations as it limits drug loading capacity, increases product intra variability and affects the cost of final dosage form.

Consequently, the evolution of multifunctional excipients has overcome some of the disadvantages of using mono functional excipients leading to the development of filler/binder-disintegrant systems such as microcrystalline cellulose (MCC) and silicified MCC. Usually, multifunctional excipients are engineered/co-processed to provide a synergistic effect of the individual excipients they are comprised of (Tobyn et al., 1998). The multi-functionality provided by these excipients is interesting as it often results in better compactability (i.e. capacity to produce tablets with sufficient strength under the effect of densification), dilution potential and possibly faster disintegration. Densification refers to the increase in particle density under the applied shear forces of the compression process. Similarly the inclusion of sugar alcohols/polyols such as mannitol in ODTs has resulted in the production of ODT with superior mouth feel (Yoshinari et al., 2002).

In this work, the collation and consolidation of published literature of the last 17 years has been presented in a systematic order with a view to make available various principles and considerations in the design and formulation of ODT both for fundamental and translatable research. This chapter has been broadly classified into two compartments. The first segment (sections 1.2 and 1.3) focuses on excipient features that have been modified over the years in order to meet the criterion for an ODT. Literature analysis in this section is primarily focused on the rationale for selection of excipients from different classes of naturally occurring compounds with the ultimate objective of providing the reader with the framework necessary to develop and modify novel materials. This segment also evaluates the technologies investigated towards enhancement of product characteristics including hardness and disintegration time. Various techniques including their fundamental scientific rationale for development have been discussed in detail. The objective was to highlight the techniques investigated in the past for

enhancing product profiling, which can be achieved through the application of novel analytical as well as production facilities.

The second segment (section 1.4) provides further insights into the challenges and realistic problems faced during formulation development of compressed ODTs. The information contained in this part was derived from issues encountered during formulation development of compressed ODTs in our laboratory and from problems reported in the literature. The work reports the development of a suitable taste masked particles, solubility enhancement of active pharmaceutical ingredients (APIs) in ODTs, dose capacity within the ODT platform and the development of modified release technologies to be introduced into the compressed ODT matrix. This segment also highlights the main processing related aspects including the challenges associated with poor flowability of powders and segregation during direct compression in addition to the lubrication sensitivity faced when using different classes of excipients.

1.2. Excipient features and compression technology for ODT development

The development of an ODT using compression can be broadly defined as a two stage technology platform which involves blending of excipients with the active ingredient followed by compaction of the powder blend into tablets. Blending and compression offers a wide range of benefits including lower production cost and time, faster turnaround of batch production and a substantial reduction in packaging costs (Fu et al., 2004). Pre-treatment/pre-processing of the powder mix is occasionally carried out prior to compaction, which is primarily influenced by either drug specific characteristics (e.g. brittleness or poor compressibility) or process related requirements (e.g. poor flowability of the powder mixture into the die). The most commonly employed pre processing strategies include granulation (including roller compaction), spray drying, hot-melt extrusion, extrusion/spheronization and milling.

Based on our findings from extensive investigation of the published literature on compressed ODTs over the last two decades, it is clear that excipient selection criteria are based on either functionality or chemical structure. The focus of ODT design in the early nineties was on the inclusion of mono functional excipients, such as cellulose derivatives as binders, which later resulted in the development of bi functional materials exhibiting binder-disintegrant properties. The chemical basis for evolution of excipient usage in ODTs saw the shift from cellulose based materials (primarily crystalline cellulose) towards the extensive use of sugar/polyol based excipients. This trend was recognized when reviewing the literature on ODTs between 1995 and 2010 which showed an increase in the number of publications stating sugar alcohols (mainly mannitol) as the main ODT excipients and a reduction in the number of publications mentioning cellulosic excipients (Figure 1.1).
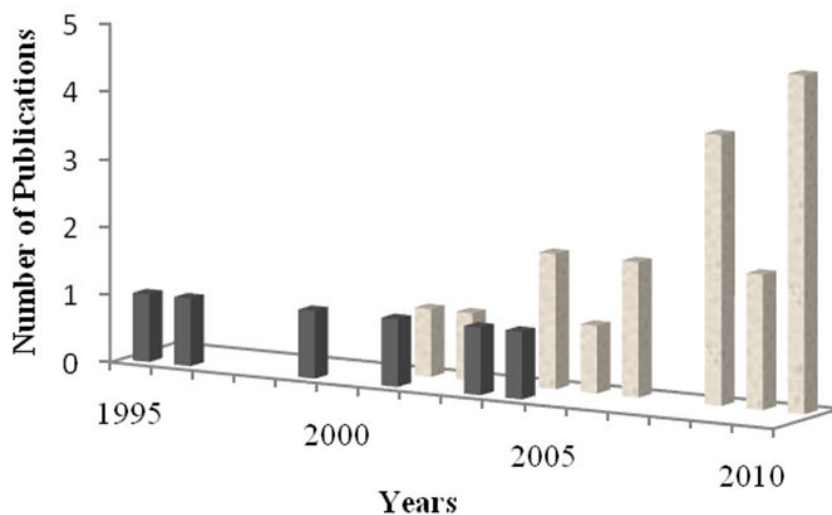
Figure 1.1: The development of compressed ODTs between 1995 and 2010 based on research using cellulose based excipients ■ or sugar/polyol based excipients ▩.

One of the first articles on the formulation of compressed ODTs was published by Watanabe et al. in 1995 describing the use of crystalline cellulose and low-substituted hydroxypropyl cellulose (L-HPC). In that work, crystalline cellulose was used as a binder and filler along with L-HPC as a disintegrant. Results from that study showed that ODTs prepared from crystalline

32

cellulose have sufficient mechanical strength for practical use and provided the basis for further development of cellulose based excipients such as microcrystalline cellulose (MCC) which has improved flow and compaction properties. MCC is currently the most widely used cellulose based excipient. The material has an exceptionally strong binding property resulting in high dilution potential, and equally has a rapid disintegration profile attributed to swelling or capillary action (Nogami et al., 1969). The strong binding property of MCC is a result of its plastic deformation under pressure. Generally, plastic deformation occurs if the applied shear forces overcome (crystal structure or shape is changed under compression) the intermolecular forces which work to restore the crystal features to its original form (elastic deformation) (Hess, 1978; York, 1983). However, MCC was reported to have a unique plastic deformation mechanism which occurs through hydrogen bonding to adjacent MCC particles as suggested by Hüttenrauch (1971). In fact, the studies discussed in this thesis have revealed other mechanistic information on MCC plastic deformation behaviour (See Chapter 2 2.3.2.1 for more details). Another aspect to consider in the selection of MCC for ODTs is that MCC is insoluble in water/saliva and as a result particle surface texture plays a role in determining its mouth feel properties. The earlier grades of MCC had a rough texture (Figure 1.2 a) which adversely affected the mouth feel of the excipient when used in an ODT.

In the following year, Bi et al. (1996) studied the feasibility of using MCC (as a binder) within ODTs due to its high compactability and pleasant taste upon tablet disintegration. The study concluded that optimisation of binder: disintegrant concentration is essential in reducing the disintegration time of the tablets. Although the study investigated the disintegration profile of the tablets in human volunteers to obtain a correlation with the *in vitro* results, issues associated with poor mouth feel (grittiness) of large particle size of MCC after tablet disintegration were not reported. The next significant development in particle engineering of MCC based excipients was the study by Ishikawa et al. (2001), on spherical MCC particles with a mean particle size of 7 μm. Development of spherical particles with reduced size significantly improved the flow properties of MCC with the added benefit of having a pleasant mouth feel.

Following the nineties decade, research into ODTs and more specifically into compressed ODTs increased significantly. Many ready-to-use powder blends were developed commercially which contained sugar and polyols such as sucrose, mannitol, xylitol, sorbitol and maltodextrin as the key ODT excipients.

The distinct advantages offered by sugar/polyol based excipients were the superior mouth feel, sweetening flavour and their application as fillers. The most favoured diluent in the development of ODTs was the sugar alcohol mannitol which is prepared by catalytic reduction of sugars. Mannitol has a negative heat of solution which provides a cooling sensation in the mouth. Furthermore, mannitol has been studied for the development of ODT formulations as it offers a creamy mouth feel upon disintegration of the tablet, a sweet taste regardless of low sugar content and is non-hygroscopic (Yoshinari et al., 2002). However, the main drawback of the commonly used polymorph of mannitol (Mod I, also denoted β) in tablet formulations is its low compactability. Mannitol undergoes fragmentation under pressure leading to the formation of weak compacts, unlike other fragmenting materials such as lactose which produce stronger compacts as a result of the formation of new clean surfaces/contact points (Ilkka and Paronen, 1993). Results in Chapter 2 (2.3.2.2) also confirmed the fragmentation behaviour of mannitol through the use of advanced surface analysis techniques. Furthermore, our previous research suggested that the longitudinal/needle shaped particles of mannitol (Figure 1.2 b) are implicated in its low compactability which is manifested by the production of friable tablets (Al-Khattawi et al., 2012). To overcome processing disadvantages, the development of mannitol grades with improved physical attributes has been investigated using spray drying and co-processing approaches (discussed in section 1.3.2.2 and in Chapter 4).
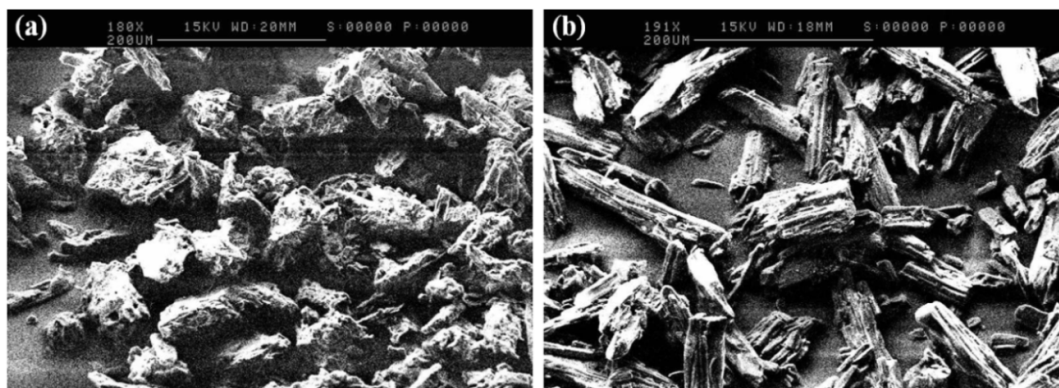
Figure 1.2: Scanning electron microscopy image of (a) microcrystalline cellulose (MCC) powder and (b) D-mannitol powder.

Other diluents such as lactose, xylitol, sorbitol, erythritol and maltodextrin have also been studied in ODT development by admixing them with mannitol or MCC to improve processability of the formulation. For example, the addition of α-lactose monohydrate to MCC improves the flow properties of directly compressed mixtures (Bi et al., 1999). Similarly, sorbitol or xylitol can be added to mannitol to improve the hardness profile of ODTs as they have better compactability than mannitol alone but cannot be completely substituted for mannitol due to their relatively high hygroscopicity (Alderborn and Nyström, 1996).

A major problem associated with the development of ODTs (especially freeze dried ODTs) is their low mechanical hardness which requires the use of specialized primary packaging such as double-foil blister pack with a peelable aluminium lidding (John Wyeth and Brother Ltd, 1981). Binders and disintegrants are used alongside diluents to produce mechanically strong ODTs while maintaining a short disintegration time. Despite that, very few technologies depend solely on the existing properties of diluents such as the high hardness and short disintegration associated with MCC, whereas others require the addition of binders/disintegrants to improve the hardness of ODTs and/or to reduce disintegration time.

Low-substituted hydroxypropyl cellulose (L-HPC), starch and cross-linked polyvinylpyrrolidone (also called crospovidone) have a dual functionality, i.e. they work as both binders and disintegrants (Shu et al., 2002; Shimizu et al., 2003 b; Morales et al., 2010). L-

HPC is partially substituted hydroxypropyl ether of cellulose obtained from purified wood pulp. It has a fibrous cellulosic structure which aids in the formation of strong bonds when used as a dry binder in tablets thereby preventing capping/lamination. Moreover, investigation of the compaction properties of various L-HPC grades has shown that it undergoes plastic deformation similar to MCC and other cellulosic polymers (Alvarez-Lorenzo et al., 2000 a). In addition, the low degree of substitution and the presence of hydroxyl groups on the cellulose backbone offer the necessary environment for imbibing water into the polymer network which provides the basis for its role as a disintegrant upon contact with water. In research conducted by Gissinger and Stamm (1980), L-HPC was shown to have ten times more swelling capacity than that of MCC. This was attributed to the far lower crystallinity of L-HPC compared to that of MCC which could result in superior water uptake to the amorphous regions of the polymer. Furthermore, L-HPC was approved for nutraceutical applications because of its natural origin. However, the rheological properties of L-HPC powder must be considered during formulation development, especially during direct compression, as it has poor flow properties when compared to MCC (Alvarez-Lorenzo et al., 2000 a).

Crospovidone is a synthetic disintegrant which has been widely used in ODTs as it enhances the fast disintegration of ODTs due to its capillary action and swelling ability (Kornblum and Stoopak, 1973). Microscopic imaging of crospovidone has shown the presence of small aggregates forming a sponge-like porous structure (Shah and Augsburge, 2001) which provides the basis for its role as a disintegrant through capillary action (wicking). Furthermore, research has shown that crospovidone containing tablets retain lower disintegration time than tablets prepared with other disintegrants such as croscarmellose and sodium starch glycolate. An added benefit of incorporating crospovidone is its wide applicability in delivering cationic, anionic and non-ionic drugs due to its neutral characteristics unlike croscarmellose and sodium starch glycolate which are anionic in nature (Fransén et al., 2008). Dual functionality of crospovidone as a binder-disintegrant system was reported when used in high concentrations due to its ability

to reduce friability of the tablet considerably together with reduction in disintegration time (Soh et al., 2013).

Starch in different forms such as partly pregelatinized or corn starch has also been extensively studied in ODT development. Starch deforms by plastic deformation under pressure and swells upon contact with water through wicking which provides the basis for its dual functionality as a binder–disintegrant excipient. The only drawback reported in literature for ODT development with starch is its sensitivity and physical incompatibility upon mixing with lubricants such as magnesium stearate which forms a film between starch particles and has a detrimental impact on the resultant tablet hardness (Bos et al., 1991; Mimura et al., 2011).

1.3. Formulation and Process Strategies for Compressed ODT development

The development of an ODT with an acceptable hardness which does not require specialist packaging and disintegration time within the limits stipulated by the various national formularies together with high drug payload can be obtained through different formulation and process related strategies. While no regulatory limits were stated for mechanical strength of ODTs, a disintegration time of 30 seconds and a weight of less than 500 mg were the main criteria required for a successful ODT formulation according to FDA (FDA CDER, 2008). On the other hand, the Ph. Eur. specified a longer time for orodispersible tablets disintegration of 3 minutes. The FDA guidelines seemed to be more stringent with the definition requirement of orally disintegrating tablets in contrast to Ph. Eur. guidelines which specifies similar disintegration time limit (3 min) for all of orodispersible, dispersible and soluble tablets (EMA EDQM, 2005). The formulation methodologies of compressed ODTs were categorized into (a) strategies for inducing fast disintegration of ODTs and (b) strategies for producing hard tablets without compromising disintegration time. These different formulation avenues and the approaches used to achieve them are illustrated in Figure 1.3 and discussed in sections 1.3.1 and 1.3.2.
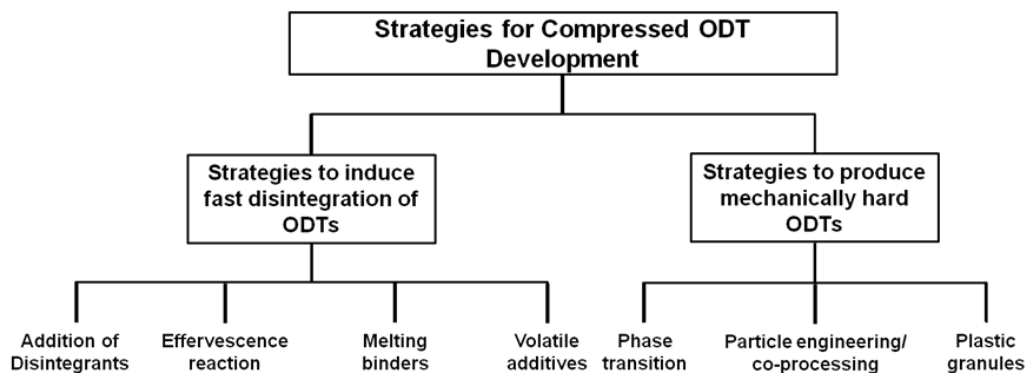
Figure 1.3: Strategic development of ODTs using the compression method.

1.3.1. Strategies to induce fast disintegration of ODTs

1.3.1.1. Incorporation of disintegrants

Disintegrants or superdisintegrants are used in the development of ODTs to reduce the disintegration time to an acceptable level. In addition to the disintegrant/binder systems mentioned earlier, another area that has been the centre of ODT development is the feasibility of utilising naturally occurring materials such as agar powders and amino acids as disintegrants/superdisintegrants.

Agar powders which are naturally occurring saccharides were first used as ODT disintegrants in 1996 by Ito and Sugihara. Agar powders absorb water and induce swelling without becoming gelatinous in water at ambient temperatures. Agar was treated by allowing it to swell in water followed by drying and grinding to allow the production of a disintegrant with good swelling properties. The reduction of particle size through grinding resulted in a faster rate of particle swelling which was reported to be 22 times quicker than that of non-treated powder leading to rapid disintegration of ODTs (Ito and Sugihara, 1996).

Amino acids due to their high wettability are another class of materials that have been investigated for use as disintegration promoters for both oral lyophilisates as well as directly compressed ODTs. Alhusban et al. (2010) investigated the use of proline and serine as disintegration enhancers for lyophilised orally disintegrating tablets mainly due to their high

wettability. Furthermore, various amino acids including L-lysine HCl, L-alanine, glycine and L-tyrosine were studied for their suitability as disintegrants in an ODT prepared by compression method (Fukami et al., 2005). The results from the study showed that inclusion of amino acids promoted faster disintegration of the resultant tablet. It was hypothesised that surface energy of amino acids based on their ratio of polar and dispersion components had a significant influence on tablet performance. An amino acid with an increased dispersion component (non-polar) produced faster disintegration when in contact with water (polar). This was interpreted in accordance with the theory proposed by Matsumaru on the generation of a force separating the hydrophobic and hydrophilic surfaces upon penetration of water into the tablet (Fukami et al., 2005).

The order and stage of disintegrant addition varies depending on the formulation requirements. Broadly, they can be either blended directly with the mixture of excipients or indirectly via techniques such as granulation or spray coating. While the direct addition and blending is a straightforward process, granulation and spray coating involve multiple stages but often result in improvement in ODT properties. Spray coating of mannitol by a suspension of disintegrants (corn starch and crospovidone) using fluidized bed granulator led to the development of an ODT system with superior properties over the physical mixing procedure. The produced granules possessed extremely large surface area as a result of deposition of fine disintegrant particles onto the surface of mannitol particle. This large surface area was responsible for the fast disintegration of ODT as well as for the formation of hard compacts due to increased contact area between particles. Interestingly, this research also concluded that hard particles of crospovidone resisted plastic deformation under pressure causing less change in the internal pore structure of the ODT after tableting (Okuda et al., 2009).

Details of other disintegrants including starch, crospovidone and L-HPC have already been discussed in the section above (1.2).

39

1.3.1.2. The use of effervescent reaction to promote ODT disintegration

One of the earliest ODTs was produced by compression of effervescent agents into a tablet. In 1991, Wehling et al developed a tablet that had a rapid disintegration in the oral cavity which even though not classed as an ODT at that time, in principle could be considered an ODT. The dosage form was developed for paediatrics to achieve two goals: firstly to enable the delivery of oral medicines to children who are unable to swallow/chew tablets and secondly to produce a distinct sensation of effervescence to help mask the unpleasant taste of bitter compounds (Cima Labs, 1991).

Effervescent ODTs are very similar to conventional effervescent tablets in terms of the mechanism of disintegration i.e. they use the same principle of effervescence. Release of carbon dioxide as a result of chemical reaction between acids such as citric, tartaric, malic, fumaric, or succinic acids and alkali metal carbonate/bicarbonate such as sodium bicarbonate upon contact with water/saliva forms the fundamental principle of effervescence. Generation of carbon dioxide promotes ODT disintegration into smaller fragments and accounts for the 'fizzing' sensation in the mouth (Jacob et al., 2009). The only difference between the effervescent ODT and conventional effervescent tablet is the method of administration as the ODT is intended for disintegration in the mouth while effervescent tablets are usually dissolved/dispersed in solution before administration as an oral liquid. The key drawback of this strategy is the high hygroscopicity of the resultant tablets which requires specialist packaging to avoid moisture sorption. Few products are available in the market based on the effervescent ODT strategy such as acetaminophen alone or in combination with antihistamines as well as antidepressant mirtazapine.

1.3.1.3. Hydrophilic melting binders in ODTs

Melting binders (binders that melt at body temperature) were primarily used to improve the dissolution profile of poorly soluble drugs such as ibuprofen through melt granulation technique

and for the development of sustained release multiple unit dosage forms (Ghebre-Sellassie, 1994; Passerini et al., 2002). Abdelbary et al (2004) exploited this property to develop compressed ODTs following granulation of hydrophilic waxy binder PEG-6-stearate. The binder was included during granulation either from solution (wet granulation) or by melting with the rest of excipients (melt granulation). ODTs with hardness of less than 60 N disintegrated within 40-50 sec. In addition, inclusion of croscarmellose as a disintegrating agent resulted in further reduction of disintegration time. Similar approach was also studied within our laboratories investigating the suitability of α-tocopheryl polyethylene glycol 1000 succinate (TPGS) as a hydrophilic melt binder. TPGS melts at body temperature (37°C) and forms micelles in solution which facilitates the inclusion of poorly soluble drugs into ODTs. The disintegration time of TPGS-containing ODTs were less than 3 min and the addition of crospovidone improved the disintegration time further along with the added advantage of reduction in tablet friability (Al-Khattawi et al., 2012). Generally, the disintegration time of ODTs produced by this method is longer than disintegration time of ODTs produced by other techniques as the rate limiting step in tablet disintegration can be the speed with which the binder melts at body temperature when in contact with saliva.

1.3.1.4. Porous tablets incorporating volatile additives

The paradigm for generating a porous network within the tablet for quick disintegration in the mouth was originally applied for oral lyophilisates prepared by freeze drying. These tablets disintegrate faster due to rapid penetration of water through capillary action into the porous framework of freeze dried matrix (Jones et al., 2011). The generation of a porous infrastructure which accounts for nearly 90% of the total volume of the tablet results in weak tablets which requires specialist packaging to preserve their integrity (Verley and Yarwood, 1990; Seager, 1998).

Tablets prepared by compression have good mechanical strength due to deformation of particles under pressure creating dense compacts with a resultant substantial reduction in porosity.

41

Inclusion of subliming agents prior to tablet compaction would however have a dual impact. Firstly, compression of material under pressure would result in the formation of dense compacts and secondly sublimation of excipients upon tablet formation would generate a relatively wider porous network within the tablet (Boehringer Mannheim, 1975). The commonly investigated subliming agents in literature include camphor, ammonium bicarbonate, menthol and thymol.

Koizumi et al. (1997) developed a porous tablet of mannitol using a direct compression method. Camphor was blended with mannitol before compressing into an ODT. This was followed by heating the tablets at 80°C for 30 min to obtain ODTs with approximately 30% porosity. The ODTs produced by this method dissolved in the mouth within 20 seconds without leaving any gritty sensation. Similarly, Roser et al. (1998) developed a soluble oral tablet using ammonium bicarbonate as the volatile component. The excipients including binders were mixed with the volatile salt and compacted into tablets. The tablets were subjected to reduced pressure using vacuum drying (1.5 torr) and a temperature of 60°C. The use of vacuum drying helped to reduce the pressure and accordingly lowered the temperature required for sublimation. The dissolution time of the tablets was reduced from 15 to 1 min after inclusion of ammonium bicarbonate. Furthermore, binders were added to improve the hardness of the tablets to avoid loss of mechanical hardness upon sublimation of ammonium bicarbonate. In another study, the effect of sublimation of granules on tablet properties was compared to that of sublimation from the intact tablet. Similar to the approach proposed by Roser et al. (1998) vacuum drying of the granules prior to compaction as well as the resultant tablet were studied with a view to understanding pore network retention upon application of high compression forces. The study concluded that pores formed in the granules due to sublimation collapse upon tableting and retard the disintegration time when compared to tablets exposed to sublimation (Gohel et al., 2004). This low mechanical strength issue was addressed in Chapter 4 by the development of porous non-brittle particles for fast disintegration and high mechanical strength.

Unlike the ODTs produced by effervescent method, moisture sorption is not an issue with the tablets produced by sublimation/evaporation technique as they do not dissolve if exposed to high humidity levels (Gohel et al., 2004). However, the use of temperature for sublimation is impractical for the manufacturing of ODTs containing heat-sensitive drugs. Moreover, friability might be an issue for the ODTs produced by this method as the internal structure of the tablet is weakened by the formation of very fine canals or pores (Patel et al., 2008).

1.3.2. Strategies to produce mechanically hard ODTs without compromising the disintegration time

1.3.2.1. Phase transition methods to improve mechanical strength

Phase transition involves the preparation of ODTs by low compression forces to ensure high tablet porosity followed by post manufacture treatment of the tablets using either heat or humidity to improve the mechanical properties. Employing the crystalline transition method, freeze dried amorphous sucrose was mixed with mannitol and compressed into tablets at low compression forces (10 - 150 MPa). This was followed by subjecting the tablets to a humid environment to initiate the transition of sucrose from the amorphous to crystalline state. Molecular transition upon exposure to high humidity is due to the plasticizing effect which reduces the glass transition temperature of amorphous sucrose leading to its conversion from glassy to rubbery state. The rubbery state is a high energy state that favours formation of crystalline sucrose. This was supported by evidence from thermal analysis and powder x-ray diffraction which showed that amorphous sucrose had completely converted into crystalline form creating new internal points of contact in the tablet resulting in a tablet with high tensile strength (tensile strength is used to express hardness of compacts regardless of their dimensions) (Newton et al., 1971) coupled with retention of original porosity (Sugimoto et al., 2001). In another study, the principle of crystal transition was further improved to allow the manufacture of ODTs using fluidized bed granulation. Water content in granules and temperature control during granulation process resulted in the formation of amorphous sucrose within the granules. Upon storage, amorphous sucrose would change into a crystalline form

resulting in hard tablet compacts. It is noticeable that, using this approach, the researchers were able to develop a simpler technology which could be used to produce ODTs commercially; however, amorphous sucrose in the granules may start to crystallize if the granules are not compressed into tablets immediately after production. This was evident in the significant increase of tensile strength for tablets compressed immediately after granulation compared to the small increase in tensile strength for tablets compressed from granules after prolonged storage (Sugimoto et al., 2006).

Another amendment to the above approach was to convert materials in solid state to molten and back to solid state upon a heat/cool cycle which resulted in an increase in hardness and pore size of ODTs without a change in crystal form. Low-melting point sugar alcohol (trehalose or xylitol) was blended with high-melting point sugar alcohol (erythritol) followed by heating. Heat was used to melt the low melting point sugar alcohol which permitted its diffusion between the granules or powder particles of the high-melting point sugar alcohol. This was followed by a cooling step in order for the molten material to solidify (Figure 1.4). The solidification caused a significant increase in hardness of the tablets possibly due to the formation of solid bridges or inter-particle bonds between powder particles (Kuno et al., 2008 a). This research was focused on increasing the diffusion of a material in the tablet to enhance the interparticulate bonding upon solidification without a change in original crystal form, unlike the process of transition from amorphous to crystalline phase mentioned earlier which increased ODT hardness by a change in crystal structure.
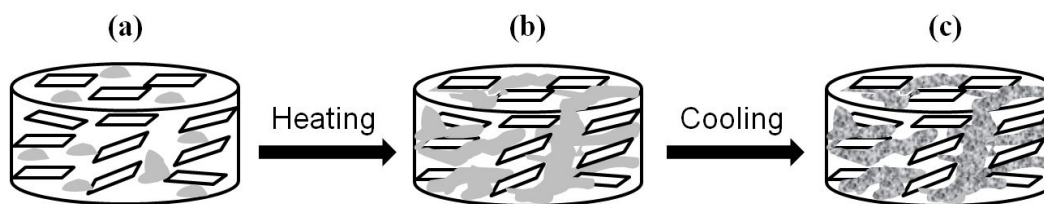
Figure 1.4: Phase transition method for production of compressed ODTs. (a) Tablet before heating showing scattered low-melting point excipient (grey). (b) The low-melting excipient is molten and distributed between high-melting point excipient. (c) Solidification of molten excipient takes place increasing the mechanical strength of ODT.

Despite the novel approach in these studies, there are several issues associated with these systems: firstly the transition from amorphous to crystalline phase may involve the formation of a new crystal form that differs in properties from the original material. This requires rigorous testing for the properties of the new crystal form to ensure the stability of the product with no toxicity. Moreover, the use of humidity or heat treatment is very likely to compromise the stability and suitability of the methods for water-sensitive or heat-sensitive drugs respectively.

1.3.2.2. Particle engineering and co-processing of excipients

Particle engineering allows the design and development of new multifunctional excipients i.e. excipient combinations that play a role as filler, binder and disintegrant (Duriez and Joshi, 2004). Co-processing strategies such as blending, co-grinding and spray drying were used to prepare excipients with improved mechanical or disintegration properties for incorporation into ODTs. In these processes, a change in particle size, morphology or crystal habit (plates, needles, irregular, etc.) may occur. Furthermore, the adsorption of excipients to each other or simply the combination of two or more favourable properties of individual excipients in a powder blend could be considered a co-processing approach. This usually results in materials with alternate physical properties to that of the individual excipients before co-processing due to increase in surface area, improvement in wetting properties, better compaction (due to different deformation mechanism under pressure), faster disintegration and enhanced dissolution (York, 1983). Some of the common ODT excipients are available in the market in the form of mannitol co-processed with starch or crospovidone as well as MCC co-processed with silicone dioxide.

Mizumoto et al. (2005) investigated the disintegration and compaction properties of saccharides in ODTs. They categorized them according to compressibility level, which is the ability of a material to undergo reduction in volume as a result of applied pressure (see example in chapter 3 section 3.3.1) , into low compressibility and high compressibility saccharides. The low compressibility saccharides included sucrose, lactose, glucose, xylitol, mannitol and erythritol

whereas maltose, sorbitol, trehalose and maltitol were chosen as high compressibility saccharides. The ODT formulation approach involved granulating a low compressibility excipient such as mannitol which provides fast disintegration with a high compressibility excipient such as maltose which produces strong compacts with the resultant formulation exhibiting high tensile strength and faster disintegration.

In another study, a suspension of microcrystalline cellulose (98%) with colloidal silicon dioxide (2%) was dried to obtain silicified microcrystalline cellulose. The produced co-processed excipient is a result of intimate physical association between MCC and silicon dioxide with no chemical or polymorphic change (Platteeuw et al., 2004). Silicified MCC is claimed to have superior flow properties attained from silicon dioxide as well as good compactability (compactability refers to the ability of a material to produce tablets with sufficient strength under the effect of densification, see example in chapter 3 section 3.3.1) provided by MCC. Moreover, silicified microcrystalline cellulose is stated to provide fast tablet disintegration in less than 60 sec if blended with an active ingredient at a 50:50 ratio. This is assisted due to the porous structure of silica and swelling ability of MCC enabling fast disintegration (Jivraj et al., 2000).

Another strategy that was employed for co-processing was co-grinding. In a research conducted by Shu et al. (2002), D-mannitol and crospovidone were co-ground prior to blending with non-ground crospovidone and lubricant followed by tableting using direct compression. The specific surface area of D-mannitol during grinding was increased in the presence of crospovidone. The increase in surface area improved the hardness of the tablets due to the creation of new surfaces of contact in the tablet. However, the disintegration time was delayed possibly due to reduced porosity (increased hardness), but was resolved with the extra granular addition of crospovidone (Shu et al., 2002).

Co-grinding of polysaccharides agar and guar gum with mannitol was also investigated as previous research suggested that treated agars have favourable disintegration properties (see

section 1.3.1.1). Previous research showed that guar gum by itself is not compressible and forms weak compacts (Schiermeier and Schmidt, 2002). Mannitol-agar or Mannitol-guar gum was suspended in water to allow swelling to occur; this was followed by drying and grinding of the swollen mass to obtain a co-ground powder. The co-processed mannitol-agar/guar gum was assessed as an ODT excipient and yielded good compaction/disintegration properties when MCC was added to the mix (Sharma et al., 2008).

Spray drying is considered a valuable tool for the development of tableting excipients. It involves rapid drying of a drop of liquid of drug/excipients sprayed from a nozzle of controlled diameter at controlled temperature and process parameters. It is a one-step continuous process used to produce particles with spherical shape and controlled size distribution (Figure 1.5) (Masters, 1991). Spray drying was utilized to produce a wide range of extensively used tableting excipients such as MCC and spray dried lactose (Gohel, 2005). Spray drying induces compactability in the excipients as a result of the plasticity imparted to spray dried products. Plastic deformation of spray dried materials is hypothesized to occur as the produced amorphous form is less prone to fragmentation and more deformable than original crystalline particles which in turn provide a significant improvement in compaction properties. In addition to plastic deformation, the spherical shape of spray dried particles provides better rearrangement of the particles in the die during tableting leading to enhanced compaction characteristics (Gonnissen et al., 2007; Rojas and Kumar, 2012 b). Other advantages of spray drying include improved flow properties of spherical shaped particles and low moisture content in the final dried product. However, it may not be suitable for materials which are heat-sensitive and could result in a change of the crystallinity of excipients forming less stable amorphous forms.

(a) **(b)**
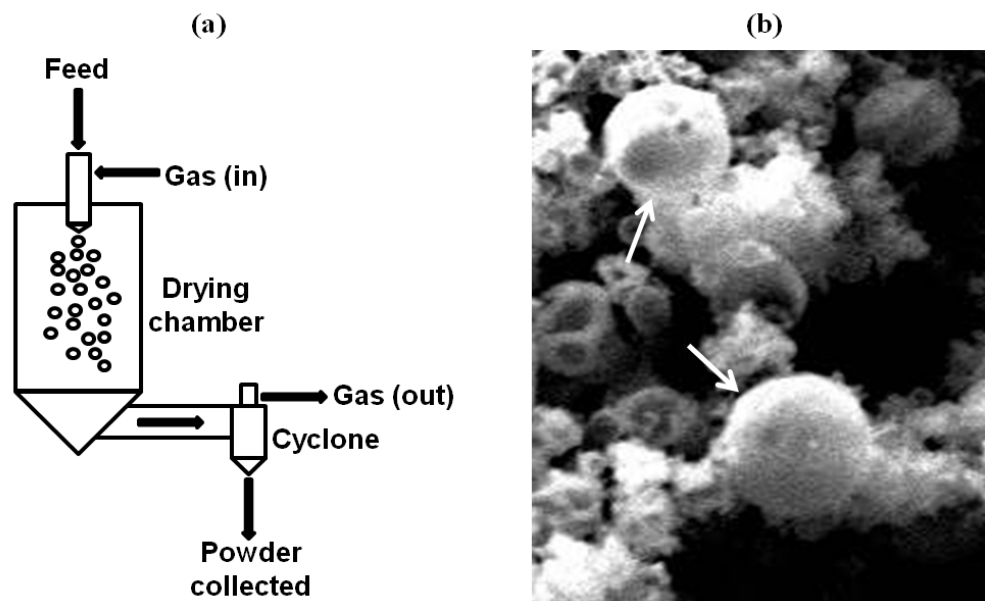
Figure 1.5: The use of spray drying for manufacture of ODT excipients. (a) Schematic of spray drier equipment showing atomized droplets and powder collection. (b) Spherical morphology of produced spray dried particles.

Co-processing by spray drying was mainly used to develop directly compressed ODT matrix agents with enhanced physical properties. The main co-processing combinations described in literature consist of mannitol or MCC as the primary component in the spray dryer feed in addition to other additives such as a disintegrating agent. Spray drying was used by Allen et al. in 1996 to develop matrix excipient with porous structures. The formulation comprised of mannitol, gelatine and other bulking agents which were dissolved in water and alcohol (such as ethanol) followed by spray drying. The dried powder was porous due to the channels formed during the evaporation of ethanol. These porous particles could be mixed with the drug and other excipients before compressing into tablets. A coating polymer such as polyvinyl alcohol (PVA) was applied on the formed compacts to enhance the hardness as the tablets tend to be fragile and breakable due to their high porosity (The Board of Regents of the University of Oklahoma, 1996). However, the use of organic solvents during excipients fabrication is not preferred due to their negative environmental impact; as a result, Chapter 4 describes an aqueous-based spray drying method for creating porous mannitol particles.

In another research, spray drying was used for processing mannitol with various disintegrants/superdisintegrants such as crospovidone. The combined effect of higher porosity of spray dried powders along with the wicking/swelling action of crospovidone resulted in ODTs disintegrating in less than 1 min. Furthermore, the co-processed powder showed better flow properties than physical mixtures of mannitol and disintegrants which was attributed to the spherical shape of particles produced in spray drying (Mishra et al., 2006).

Spray drying was also used to prepare a co-processed excipient by coating mannitol over calcium silicate. The latter is a porous excipient which functions as a dispersing agent. Mannitol was dissolved in water at elevated temperature followed by suspending calcium silicate to achieve a ratio of 75:25 for mannitol and calcium silicate respectively. The slurry formed was spray dried to obtain a co-processed powder of calcium silicate coated by mannitol. The powder was used as a matrix forming powder for ODTs and showed fast disintegration (Rubicon Research Private, 2009).

Furthermore, co-processing of a new polymorph of cellulose, microcrystalline cellulose II (MCC II) with fumed silica using spray drying and wet granulation was studied. The compactability of the co-processed excipient as well as flow properties and dilution potential were significantly improved due to the alteration of the fibre morphology of MCC II to more regularly shaped particles. The result was an improvement in the binding properties after silicification of the MCC II which in turn reduced the elastic recovery of the excipient that is associated with tableting problems such as capping and lamination (Rojas and Kumar, 2012 a).

Milling (grinding) and spray drying could generate amorphous forms of the processed materials (Bhandari et al., 1997; Yu, 2001). Although the application of particle engineering/co-processing technologies can yield amorphous materials which offer better dissolution characteristics (Hancock and Parks, 2000), stability considerations to prevent the conversion of high energy amorphous form into crystalline form should be extensively tested (Hancock and Zografi, 1997).

1.3.2.3. Manufacture of plastic granules for the development of ODTs

Porous granules that deform into plastic state under pressure were prepared by wet granulation. The granules were made by mixing a ready-to-use excipient composed of maltodextrin and corn syrup solids with spray dried mannitol followed by spraying sucrose as a liquid binder. The granules retained high porosity due to the maltodextrin grade which caused fast disintegration and assisted plastic deformation at relatively low compression forces. Furthermore, spray dried mannitol increased the mechanical strength of the granules as an increase in hardness was observed upon increase in its proportion. The increased hardness is in turn associated with the nature of spray dried materials which generally deform through plastic deformation. On the other hand, an increase in spray dried mannitol also increased the disintegration time therefore optimum proportion of spray dried mannitol was chosen in the formulation.

The other important aspect of this invention is the use of penetration enhancer which attracts water into the pores/capillaries within the plastic granules thus leading to fast disintegration. Additionally, the use of plastic polymeric materials to fabricate the granules is associated with the formation of a viscous layer due to gelation on the surface of tablet. This viscous layer could retard water penetration and disintegration of tablet and for that reason penetration enhancer was incorporated within the granules to maximize water penetration into the tablet core. A binder (sucrose) was included within the granules to enhance the durability of the ODTs which had friability of less than 1% and to maintain the porous structure of granules during wet granulation (Jeong et al., 2005). Although a penetration enhancer was critical for the fast disintegration of ODT produced by this method, however, it is equally possible that it would attract moisture into the formulation therefore negatively impacting on the stability of drug/excipients if no special packaging is provided.

1.4. Challenges of compressed ODTs and emerging solutions

Like any other emerging technology, a number of limitations and challenges arise especially when applying the ODT formulation strategies to APIs which have less favourable physico-chemical or organoleptic properties. Table 1.2 summarises the main characteristics of ODTs and associated challenges discussed in the next sections.

Table 1.2: Characteristics of ODTs.

Property	Explanation	Challenge
Palatability	Flavours could be used for mildly unpleasant tastes and other taste masking technologies for highly unpalatable compounds. Mouthfeel is another determining factor as particle size and shape dictate the texture of materials and sensation in mouth.	Taste masking using flavours may not always succeed. Introduction of coatings may hinder dissolution and/or affect bioequivalence. For mouthfeel, large particles can produce a gritty/chalky feeling. Similar situation happens in some non-spherical particles.
Disintegration time	Recommended ODT disintegration in < 30 sec according to USP or 3 min according to Ph. Eur.	While commercial ready-to-use powders can achieve that, mechanical strength of tablet (example high friability) is usually the compromise. Additionally, no universal method for assessment exists
Tablet weight	500 mg for water soluble components	Limited use for high dose insoluble APIs due to difficulty of swallowing large insoluble slurries
Dose capacity	1/3 of tablet weight using directly compressible excipients	Due to low dilution capacity (compressibility) of available ODT platforms, only nearly 1/3 of tablet weight comprises the drug itself
Processing and practicality	Powders for direct compression must be flowable, MCC containing mixtures are free flowing	Limited by the use of cohesive APIs
Release profile	ODTs commonly have immediate release profile	Limited use for delayed/extended release APIs

1.4.1. Taste masking issues and available technologies

Taste masking constitutes a challenge for the development of ODTs as well as other orodispersible dosage forms. The challenge is represented in the difficulty to conceal the taste of unpalatable medicines (as will be discussed in 1.4.1.1) or related to unavailability of suitable *in vitro*/preclinical taste assessment methodologies (sec 1.4.1.2).

1.4.1.1. Taste masking approaches

One of the common issues with ODTs is the difficulty of administering bitter tasting drugs when the tablet disintegrates in the mouth (Brown, 2001). As a result, several approaches were made available for the taste masking of bitter tasting compounds in compressible ODTs. These include the addition of taste modifiers such as sweeteners and flavours, coating by conventional spray coaters or dry coating, complexation with ion-exchange resins and fabrication of microspheres by spray drying.

Taste masking of furosemide was achieved by the addition of maltitol (sweet) or yogurt (sour) powder as taste modifiers to the other excipients during granulation. This method depends on the extent of corrective action of the taste modifiers on the bitter unpleasant taste and is usually simple to develop. However, some drugs are intensely bitter, which require taste masking by coating (spray coating), encapsulation using spray drying or via complexation approach (Kawano et al., 2010).

Taste masking methods that introduce a physical barrier between the drug and taste buds of the tongue should meet certain criteria. These are either process related such as cost-effectiveness and scalability of the taste masking approach or product related attributes. The latter mainly include the size of coated particles, which should be small enough (generally < 500 μm) to avoid grittiness in the mouth, the coating layer that should dissolve/rupture (after shielding the drug in the mouth) to achieve bioequivalence with the original formulation, the mechanical strength of the coating polymer which should withstand the compression pressure thus avoiding

premature release and finally the amount of coating polymer which should not affect the weight of the final dosage form significantly.

Spray coating is one of the conventional technologies which could produce a physical barrier between the drug and taste buds of the tongue. The drug particles are either coated by pan coating with a spray gun or using fluidised bed which involves a stream of air to disperse the drug and a spray gun to atomise the coating polymer. In one coating method, the core which may include the drug, a sweetening agent and a binder was sprayed with a coating polymer that retards dissolution in the mouth. This was followed by drying to obtain the coated microparticles (Cima Labs, 1997). The microparticles were compressed into ODT using a low compression force to avoid breakage of the coating layer and subsequent drug leakage.

Another taste masking technology reported in the literature was based on the method of Ozeki et al. (2003) which involved multilayer compression technology. The first compressed layer is a base which potentially functions as a cushioning component followed by compressing the taste masked particles (core) under low pressure and finally compression of a second layer which forms a matrix around the first layer and the core. The key advantage of using this process is to reduce the effect of compression pressure on the coating layer of the taste masked particles which prevents particle rupture and premature release of the bitter drug in the mouth. On the other hand, process development requires the use of sophisticated equipment suitable for multilayer compression with a special die/punch set.

Several researchers used spray drying to produce taste masked microspheres (Bora et al., 2008; Xu et al., 2008; Mizumoto et al., 2008; Sheshala et al., 2011). Spray drying applies a coat on the bitter tasting drug from solution/suspension with the capability of controlling particle size and shape necessary for optimum mouthfeel. Furthermore, the ability to produce microspheres rapidly and in a continuous manner gives it an advantage over the other coating methods. Spray drying is also used when other coating methods are unsuccessful. Famotidine taste masking using fluidised bed coating was not reproducible due to poor flowability of the drug; thus, spray

drying was carried out as an alternative coating method (Mizumoto et al., 2008). However, care should be taken when using this process as spray drying can also result in poorly flowable powders if the density of the particles is too low.

Furthermore, pH sensitive polymers can be used for coating by spray drying. Yan et al. (2010) prepared taste masked microspheres of Donepezil hydrochloride (a bitter tasting drug) using a methacrylate based polymer which is only soluble at pH below 5.5; therefore, microspheres prevented the release of drug in the mouth at the salivary pH of 6.2. Nevertheless, the drug is released in stomach at pH 1.2 for subsequent absorption in the small intestine. The work in Chapter 5 also utilises spray drying of pH-responsive polymer hydroxypropyl methylcellulose acetate succinate (HPMCAS) to achieve taste masking in addition to enteric coating of model poorly soluble drug omeprazole.

Ion-exchange resins have also been employed for taste masking of several bitter tasting drugs formulated into ODTs (Devireddy et al., 2009; Shukla et al., 2009; Bhoyar et al., 2010; Samprasit et al., 2012). Masking the bitter taste takes place by adsorption of the bitter drug onto ion-exchange resin (cationic or anionic exchange resin) via weak ionic bonds forming an adsorption complex called Resinate. The latter is insoluble at the pH of saliva and is therefore tasteless upon disintegration of ODT. After swallowing the resinate, drug is released by exchanging with ions present in stomach or intestine, hence allowing the drug absorption to occur (Shukla et al., 2009).

Additionally, a multiple-taste masking strategy was carried out by Sugiura et al. (2012) which involved physical approach by spray coating of intensely bitter famotidine with ethylcellulose together with organoleptic approach by addition of flavours and sweeteners. The palatability of famotidine was improved as the two approaches seemed to function cooperatively.

A combination of the previously explained methods could be useful in masking the aversive taste of bitter drugs due to possible synergism of effects. Although the available technologies

address some of the issues of taste masking, unpalatability of drug formulations still represent an unresolved issue that affects medicine compliance in paediatrics.

1.4.1.2. Taste assessment approaches

Taste assessment of ODTs is mainly performed using human panel volunteers who taste the tablet upon placing in the mouth and after full disintegration (Nakano et al., 2013). The method itself provides the best information on ODTs taste and after-taste; however, associated costs due to recruitment and training of healthy volunteers and the risk of ingestion/pregastric absorption demand alternatives for human testing.

Usually, drug release studies are employed as an indirect method for taste assessment by checking if a formulation can hinder drug release in a mouth-simulated environment. The main limitation of this method is the lack of actual information about taste of materials and/or intensity of taste. For example, a small amount of bitter compound that is well compensated for by adding sweeteners/taste modifiers may still show a failing formulation using the drug release approach.

An interesting development was the introduction of artificial taste sensors, also referred as electronic tongues. These utilise electrochemical sensing (electrical potential difference between blank and sample liquids) coupled with chemometrics software to differentiate between tastants (Valle, 2010). It was reported that it is difficult to provide absolute statements regarding the taste of a specific compound using electronic tongues as the instruments do not take into account a lot of the physiological conditions in the mouth (Woertz et al., 2011). In addition, the cost of analysis using these instruments is considerably high. Other approaches such as animal preference testing or cell culture/physiological methods are still under development.

1.4.2. Solubilisation and incorporation of poorly soluble drugs into ODTs

Solubility enhancement of drugs formulated into ODTs has become an increasingly important subject since nearly 40% of the drugs in the development pipeline are poorly water soluble (Keck and Müller, 2006). The main explored solubilisation techniques for ODTs are solid dispersion and milling.

Solid dispersion technique uses hydrophilic excipients such as polyvinylpyrrolidone (PVP) and polyethylene glycol (PEG) as carriers for poorly water soluble drugs. Blending of the poorly soluble drug with a carrier polymer using a suitable dispersion technique may result in insertion of drug particles within the matrix of the carrier polymer. The dissolution of the drug is usually enhanced by increased amorphicity or improved wettability due to wicking action of the carrier polymer. Solid dispersions for ODTs reported in the literature were prepared using solvent evaporation technique, hot-melt extrusion and milling. Poorly soluble drug rofecoxib was formulated as a solid dispersion with PVP using solvent evaporation method. This was followed by incorporation of the dispersion along with disintegrants and volatile additives into ODT prepared by compression. The dissolution of the drug showed an improvement due to change of the drug phase from crystalline to amorphous form which is known to be more water soluble (Sammour et al., 2006).

Risperidone solid dispersion was also prepared by solvent evaporation method, however, with methyl-β-cyclodextrin (MβCD) as the highly water soluble excipient. The reformulated drug showed 99 fold increase in solubility as a result of formation of solid dispersion complex with MβCD. The hydrophobic drug formed an inclusion complex with MβCD molecule thus exposing only hydrophilic parts to the surrounding water. In addition, solid state examination showed that (in some formulations) resperidone converted from the poorly soluble crystalline form to the amorphous form which resulted in better solubility (Rahman et al., 2010). Hydroxypropyl-β-cyclodextrin was also used to form an inclusion complex with clozapine by an evaporation method. The complex was then formulated into ODT by direct compression and

showed an enhanced *in vitro* dissolution rate (Zeng et al., 2013). Similar approach was reported for perphenazine to improve the dissolution rate of this practically insoluble drug before incorporation into ODTs (Wang et al., 2013).

Hot-melt extrusion was used to prepare solid dispersion of ibuprofen by embedding the drug in methacrylate copolymer matrix. The extrudate of the poorly soluble drug and carrier polymer was produced by melting ibuprofen using high temperature. Characterization of the obtained granules showed a glassy solution of ibuprofen molecularly dispersed within methacrylate copolymer matrix. Subsequently, solid dispersions were incorporated into ODTs prepared by direct compression technique (Gryczke et al., 2011).

Processing of solid dispersions provides a potential solubilisation approach for ODTs; however, sometimes the powders produced by this technique suffer from poor flowability and compressibility issues (Serajuddin, 1999). Furthermore, the use of evaporation and heating steps may not be suitable for heat-sensitive drugs. Finally, the polymorphic transitions are not ruled out when using this approach which may require extensive testing of the product using thermal profiling and crystallography techniques such as differential scanning calorimetry (DSC) and x-ray diffraction (XRD).

Milling was also used to enhance the dissolution of poorly soluble drugs for ODT development. Upon milling, particle size of the drug is reduced which in turn would increase the overall surface area and subsequently increases the dissolution rate of a poorly water soluble drug (Hu et al., 2004). This approach was applied to finofibrate which is a poorly soluble drug intended for administration as an ODT. Fine drug powder (6 μm) was produced by air jet milling process following different orders of milling and blending to optimise the formulation. The results showed improved dissolution of the drug due to increased wettability and hydrophilicity. However, granulation was needed to improve the processability of the fine cohesive powder produced by milling. This was followed by compressing the granules of the drug and various other excipients into ODTs.

57

1.4.3. Limited dose capacity for ODTs

One of the issues with ODTs manufactured by freeze drying (first generation ODTs) is their very low dose capacity (< 50 mg for water soluble drugs) as higher doses could impact the hardness of the compact. Similarly, ODTs produced by compression have a maximum dose capacity approaching 30-40% of the tablet weight. This is an important consideration as it restricts the use of ODTs for low dose drugs only (Harmon, 2007).

US FDA recommends that the whole ODT weight should not exceed 500 mg unless the constituents are highly water soluble (FDA CDER, 2008). This presents an additional challenge as it would affect the quantity of a poorly soluble drug or insoluble excipient to be used in an ODT. Moreover, the final weight of the ODT may exceed 750 mg - 1 g using some of the existing ODT technologies especially when incorporating high dose drugs such as acetaminophen. Furthermore, bitter tasting drugs undergo similar issue because the taste masking technologies (which form one or more coating layers) increase the weight/size of the drug particle and in turn affect the final weight of the ODT. In addition, it was shown that poorly soluble drugs may affect the disintegration time of compressed ODTs upon increasing the concentration of the drug (Crowley et al., 2013). This issue is particularly relevant with the rising number of poorly soluble drugs in the drug discovery pipeline.

Solutions to improve the dose capacity of ODTs are unavailable currently due to lack of materials that can provide a high dilution potential and disintegrate rapidly at the same time.

1.4.4. Development of fast disintegrating ODTs with modified release kinetics

The development of multiple-unit dosage form, also called multiparticulates, technologies in tandem with formulation of ODT base/matrix is an area of primary focus from both academia and pharmaceutical industry. This is mainly due to the immediate release profile of ODTs as the dosage form disintegrates rapidly within few seconds. Rapid release is a general property of all mouth disintegrating/dissolving dosage forms such as chewable/suckable tablets and thin films.

Sometimes, pregastric absorption enhances the release of the drug when administered as an ODT (Corapcioglu and Sarper, 2005). To expand the ODT platform for drugs to be released in a delayed/sustained fashion to achieve alternative pharmacokinetics, new accompanying technologies are being incorporated within the ODT fast disintegrating base. The schematic in Figure 1.6 illustrates the different technologies used for developing modified release ODTs.
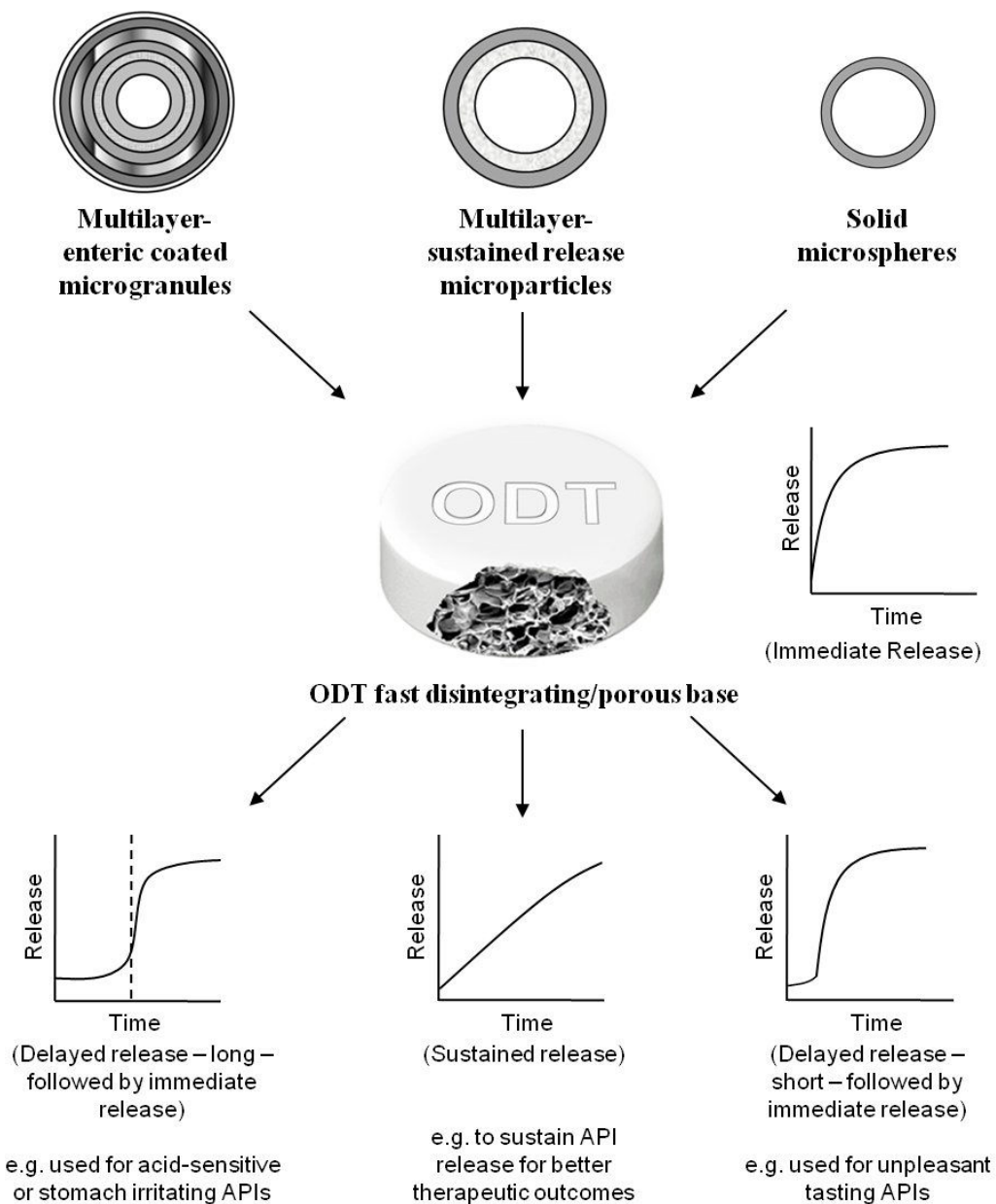
Figure 1.6: A schematic representing some of the reported approaches for modifying the release of APIs from ODTs (generally immediate release). Microgranules, microparticles or microspheres containing the API are incorporated into fast disintegrating/porous ODT base to achieve desired release profile. The achieved release profiles are outlined above with examples of possible applications.

Some drugs are difficult to incorporate into an existing ODT matrix without introducing a coating layer or sometimes several coating layers over the drug particle or granule. Multiparticulate drug delivery systems are formulated to achieve desired pharmacokinetics. These release systems can protect the drug from the acidic environment of stomach, target drugs to certain parts of the intestine for better absorption, provide longer duration of action or reduce frequency of administration of a drug (Alhusban et al., 2011).

Another advantage of developing multiparticulates is to overcome the shortcomings of single-unit dosage forms such as monolithic coated tablets (Shimizu et al., 2003 a). It is sometimes claimed that multiparticulates are more suitable for controlled release of drugs because the particles are widely dispersed in the gastro-intestinal tract (GIT) after administration; therefore maximising the absorption from different parts of the intestine (Davis et al., 1984). It was also claimed that food does not affect the gastric emptying of multiple units smaller than 2 mm in size in contrast to single-unit dosage forms which are affected due to their large size (Marvola et al., 1989).

Antacid containing ODTs present a substantial case for formulation development as significant proportion of patients with dysphagia (swallowing difficulty) have acid-related disorders such as gastro-oesophageal reflux disease (GERD), which are managed best with proton pump inhibitors (PPIs) (Howden, 2004). Incorporation of PPIs into ODTs is challenging as the drug undergoes quick acidic degradation in stomach; therefore, enteric coating is required to achieve delayed release of the drug. Shimizu et al. (2003 b) developed an ODT formulation of lansoprazole (PPI) and studied the effect of different formulation and process variables on the properties of the ODTs. One of the main challenges was the development of enteric coated microparticles that could withstand the compression force used to make ODTs. The other challenge was to provide good taste in the mouth and reduce the grittiness upon tablet disintegration. For the above reasons, different enteric coating layers were used to protect the

drug from premature release in stomach as well as to prevent the bitter taste and unpleasant gritty feeling of some of the used excipients (Shimizu et al., 2003 b and c).

Mizumoto (2008) and Maeda et al. (2011) developed sustained release microparticles of tamsulosin hydrochloride using fluidized bed coating processes. Initial investigations were centred on layering the drug around MCC core followed by sustained release coating composed of water soluble and water insoluble polymers and finally applying an enteric coat over the sustained release layer. In another study, a matrix type microparticle was developed by dissolving the drug in water and mixing with sustained release polymers aquacoat and methacrylate. The microparticles were incubated overnight at 80ºC before coating with another layer of methacrylate polymer and plasticiser. Both methods produced microparticles with a diameter of 200 μm, necessary for optimum mouth feel. Furthermore, the microparticles were successful in providing a sustained release profile similar to the existing commercial pellet. The dissolution profile of microparticles produced by the first method was assessed before and after incorporation into ODT. The results showed no difference in dissolution as the technology used to compress the microparticles utilised low compression pressure which in turn did not affect the coating layer integrity.

Metoclopramide HCl sustained release microspheres were prepared by emulsification-solvent evaporation technique. The drug was dissolved in benzyl alcohol whereas the sustained release polymer (ethyl cellulose) dissolved in dichloromethane. Both solutions were mixed together to provide the organic phase. PVA was dissolved in water to constitute the outer aqueous phase. The two phases, oil and water, were homogenised at different speeds for 10 min to obtain an oil-in-water (o/w) emulsion. This was followed by washing, filtration and drying steps to obtain solid microspheres. The latter were incorporated into ODT prepared by wet granulation which showed a sustained release of metoclopromide HCl in Wistar rats over 20 h compared to the release of drug from conventional tablet formulation which was not detected after 8 h (Kasliwal et al., 2011).

Limited number of methods is available to fabricate modified release multiparticulates for compressed ODTs. Additionally, these processes are accompanied by many drawbacks and practicality issues such as the use of organic solvents and plasticisers for dissolution/film formation of coating polymers. Moreover, the use of many coating steps can complicate the scale-up and have a bearing on the operational costs. Consequently, modified release microparticles were developed for taste masking and enteric coating of model drug omeprazole (as a poorly water soluble PPI) utilising two-step aqueous spray drying process (Chapter 5).

1.4.5. Powder flow issues and relevant improvements

Powders intended for ODT compression require good flowability to allow easy handling during blending/processing and to permit continuous flow through the hoppers into the die of the tablet press. Granulated powders used to prepare ODTs usually have good flow properties as a result of the uniform large particle size and the low number of fines produced (Juppo et al., 1995). In contrast, powders prepared by blending or processing for direct compression of ODTs generally have poor flowability due to their smaller particle size or wider size distribution, non-uniform shape and possibly irregular surface texture. The latter properties lead to interparticulate interaction by electrostatic charges, Van der Waals forces, local chemical bonds and bridging forces which in turn impact flow (Castellanos, 2005).

Another problem associated with flow properties of directly compressible powders is segregation due to variation in particle size of excipients such that fine particles sift between the coarser particles during hopper flow. Consequently, variation in bulk density and issues in weight uniformity of the final dosage form may occur (Parsons, 1976).

The flowability of directly compressible powders could be assessed during the primary stages of product development and should be part of the product design strategy. It is essential that no large differences in particle size exist between the drug and excipients during mixing to avoid segregation of the blend (Jivraj, 2000). In addition, particle shape is understood to have an

impact on bulk properties and flowability of powders (Fu et al., 2012). In particular, spherical shaped particles show better flow properties than fibre or needle shaped particles. The development of spherical shaped particles of MCC was utilised to improve the flow properties of powder in the ODT technology by Ishikawa et al. (2001). In another study, spherical sugar granules were added to the mixture of MCC and L-HPC to enhance the flowability. Moreover, the development of spray drying technology as an adjuvant method for the production of flowable powders has attracted a great deal of research due to the spherical shape of spray dried particles as well as their uniform narrow size distribution (Masters, 1991).

The improvement in flow properties was also achieved by mixing poorly flowing excipients such as MCC (older grades) with lactose which has better flow properties to produce an ODT powder blend that could be directly compressed on a rotary tablet press (Alderborn and Nyström, 1996; Sunada and Bi, 2002). Similarly, MCC was co-processed with silicon dioxide to produce silicified MCC as a directly compressible excipient which has good flow properties (Tobyn et al., 1998).

Furthermore, a fundamental research into the development of non-segregating materials was carried out by Staniforth et al. (1981) who investigated a crystallisation method of mannitol for the production of excipient with better physical properties. A highly porous surfaced mannitol was prepared by modification of mannitol crystal habit. This mannitol seemed to be useful as a non-segregating excipient during direct compression applications.

In fact, it is essential to point out that changing powder bulk properties is not always possible especially during the late stages of process development; therefore, some of the flowability issues related to cohesive powders such as arching and ratholing could be minimized by changing the design of the hoppers to allow mass flow of the powders (Prescott and Hossfeld, 1994). In addition, the introduction of force feeders to improve the flow of powders/granules is considered a significant development in the field of direct compression technology (Lieberman et al., 1989).

1.4.6. Lubricant sensitivity and available solutions

A lubricant is added during the manufacture of tablets as it reduces the friction between the tablet and machine die/punch. Magnesium stearate is the most commonly used lubricant in the preparation of tablets due to availability and low cost. Nevertheless, it is well documented that magnesium stearate is associated with a reduction in tablets' mechanical strength depending on the degree of sensitivity of excipients to the lubricant (Zuurman et al., 1999). For example, plastic deforming materials show higher lubricant sensitivity to mixing with magnesium stearate due to formation of a lubricant film between the excipient particles which reduce inter-particle interaction.

MCC is one of the preferred excipients for developing ODTs due to its good mechanical strength and fast disintegration. However, it is highly affected by the addition of magnesium stearate which causes a significant reduction in the hardness of MCC containing tablets (Zuurman et al., 1999). Moreover, some reports indicated that magnesium stearate could prolong the disintegration time and delay the dissolution of tablets due to its hydrophobic nature (Bolhuis et al., 1981).

To reduce the negative effects of magnesium stearate on ODT performance, an ODT technology that uses a tablet press with an external lubrication system was developed. In this technology, the lubricant is applied on the outside only and thus negative effects of magnesium stearate on the interparticulate interactions of excipients were minimised. This in turn allowed compressing the ODTs at much lower forces resulting in higher porosity which is necessary for rapid disintegration (Kyowa Hakko Kogyo Co., 1994). Despite this, the approach reported is probably an expensive one as it uses a proprietary external lubrication technology.

Research into ODTs also utilised alternative lubricants such as talc and sodium stearyl fumarate instead of magnesium stearate and found talc as the most desirable lubricant for ODTs prepared by phase transition method due to its minimal effect on disintegration time (Kuno et al., 2008

b). Nevertheless, using talc as a lubricant has its downside as it may produce a chalky mouthfeel when the ODT disintegrates.

1.4.7. Development of a physiologically relevant disintegration test

Disintegration time of ODTs can be determined in the oral cavity (*in vivo*) by placing the tablet in the mouth and recording the time needed for disintegration without drinking water or chewing on the tablet (Mishra and Amin, 2009). Clearly, this method requires human volunteers and ethical approvals besides the fact that it is not suitable for potent drugs due to pregastric absorption concerns. As a result, a cost-effective and representative method is needed for the assessment of disintegration time *in vitro* during the early stages of ODT development.

Currently, the only regulatory approved *in vitro* test for measurement of disintegration time of ODTs is the United States pharmacopeia (USP) method <701> (USP Convention, 2005). This test uses 800 - 900 mL of disintegration medium and a vigorously oscillating basket which provides disintegration conditions far from those in the oral cavity. Fang et al. (2006) from the FDA presented a simple and rapid method for the assessment of disintegration time and compared four different products to check suitability for labelling as ODTs. In their method, a disposable syringe was used to directly deliver 1 mL of water on a tablet placed on a flat surface. An incomplete disintegration within 30 sec indicates that further laboratory testing or justification may be required for the tablet to be labelled as ODT. However, there was no *in vitro/in vivo* correlation data reported in this research and the determination of disintegration end point is subjective.

Since the introduction of ODT concept, scientists developed many *in-house* disintegration tests claimed to be suitable for ODTs. Bi et al. (1996) proposed a disintegration test called 'the paddle method' which was used later on by other research groups (Que et al., 2006). This method uses the dissolution apparatus assembly for the measurement of disintegration time. A tablet is inserted into a cylindrical sinker (perforated pocket) attached on the inside wall of a

disintegration beaker containing 900 mL of disintegration medium. A paddle stirs the disintegration medium at 100 rpm while time was recorded from the start of process until the whole tablet disintegrated and passed through the screen of the cylindrical sinker. Although the method shows a good correlation with *in vivo* disintegration time, it uses a large volume of disintegration medium which possibly does not reflect the small amount of salivary fluid present in the mouth. Also, it does not account for the small force exerted by the tongue and upper palate of the mouth on the ODT.

Shibata and colleagues (2004) developed a method for predicting the *in vivo* disintegration time of ODTs using compaction analyzer. The researchers claimed that disintegration time in the mouth is influenced by powder compactability. Using the compaction analyzer, different compaction profiles were obtained and correlated with the disintegration time of ODT in the mouth. A good correlation was found between stationary time of upper punch displacement and disintegration time in the mouth. Although a good association was established, the prediction method is excipient-specific as different excipients exhibit different compression behaviours, and second it requires the use of an advanced compaction simulator.

Several researchers and companies used texture analysers to apply a small force which simulates the pressure applied by the tongue or the upper palate on the ODT (Dor and Fix, 2000; Mesdjian et al., 2001; Abdelbary et al., 2005). This force is considered important in enhancing the disintegration of ODT and is not accounted for in the official disintegration test. Simply, the probe of the texture analyser descends on the tablet which is placed in a small container filled with a specific amount of disintegration medium. A constant force is applied on the tablet where probe penetration into the tablet takes place. The texture analyser records time-displacement curves which could be used to determine the starting and completion times of disintegration. An excellent correlation between disintegration time in the texture analyser and in the mouth was reported in the literature (Abdelbary et al., 2005).

Harada et al. (2006) developed a disintegration apparatus which uses a rotating shaft to apply a weight of 10 to 15 g on the ODT. The ODT itself is placed on a stainless steel plate comprising small holes in the middle to allow water penetration to the ODT from a reservoir underneath. Upon complete ODT disintegration, the weight (conductive material) touches the stainless steel plate producing an electrical signal that indicates the end of test. This method has shown excellent correlation with the human disintegration test. The concept of applying a weight on the tablet was also used in the Kyoto-model disintegration test which classifies ODTs according to water permeability and indicates test completion when two weights (outer and inner) touch a filter paper beneath ODT tested (Kakutani et al., 2010). Moreover, recently a device discussed by Yoshita et al. (2013) showed a positive correlation with *in vivo* data. The ODT is placed between two meshes (lower and upper), on which artificial saliva is dripped from above. The end point of the disintegration test is recorded when the tablet completely disintegrates and two meshes touch each other.

1.5. Research aims and objectives

The research aims to understand the main physico-mechanical properties of commonly used ODT excipients to tackle product challenges and enable robust/cost-effective formulation development. The research will cover the following main ODT challenges/gaps in the knowledge:

1- Several reports have dealt with the assessment of functionality of direct compression ODT excipients on the macro/bulk-scale (such as by identification of material plastic, elastic or fragmentation behaviour under pressure). However, evidence on the micro/nano-scale features and inter-particle adhesion forces of tableting excipients is very limited and more mechanistic data are required to accelerate preformulation activities.

2- The development of ODTs using direct compression usually employs excipient pre-blends which are commercially available. Limited knowledge is available to the formulator on the type and level of excipients that must be used, compression force optimal range, particle size effect, process additives and stability considerations. Moreover, there is insufficient information in the literature on the formulation stages that must be followed to achieve a balance between fast disintegration (< 30 sec) and good mechanical strength (usually 60-70 N).

3- In contrast to cellulosic excipients, mannitol based (non-processed) ODT products suffer poor mechanical properties due to brittle fracture under pressure. This has led to a number of formulation issues, especially the resultant ODTs exhibit low hardness (which impacts processing/costs of packaging and patient handling) and sometimes fail to meet the regulatory specified disintegration time (30 sec limit according to USP or 3 min according to Ph. Eur.).

4- The domain for modified release ODT technologies is very limited currently, despite the potential advantages that could be attained e.g. for enteric coating or taste masking of APIs within ODTs. Accordingly, several challenges should be addressed during formulation

69

development of ODT accompanying technologies. These are: drug-specific challenges such as stability and solubility profile, formulation challenges such as development of optimal particle properties for good mouth-feel and process challenges such as the development of aqueous process (eco-friendly).

The objectives of the thesis were categorized according to the experimental chapters as follows:

Chapter 2:

- To provide evidence-based understanding of the physico-mechanical properties of commonly used ODT excipients, mannitol and MCC.

- To understand the factors governing the adhesion between particles during compression.

- To elucidate the excipients specific functionalities in relation to target product profile for ODTs and foresee possible shortcomings during the manufacture of ODTs.

Chapter 3:

- To develop directly compressible ODT base/blend using a multi-stage approach for the inclusion of mannitol and novel cellulosic excipients (such as L-HPC NBD-022 grade).

- To develop an ODT blend that disintegrates in < 30 sec while retaining good mechanical strength (Hardness > 60 N).

- To assess the optimum levels of excipients and compression forces in order to develop a successful ODT formulation.

- To investigate the effect of particle size of excipients and different processed mannitol grades on the final ODT properties.

- To test the formulated blend and tablets for physico-chemical and mechanical stability over 6 months according to ICH guidelines.

Chapter 4:

- To integrate better tableting functionality into the main ODT diluent D-mannitol via engineering its particle characteristics including densification profile and porosity.

- To overcome the shortcomings of the commonly used powder mannitol in ODT products such as low hardness and long disintegration time.

- To fabricate robust particles of mannitol that would resist brittle fracture during tableting.

- To develop porous particles that can promote tablet disintegration through 'wicking'.

- To understand the effect of formulation mixture composition and spray drying temperature on the resultant particles tableting functionality.

Chapter 5:

- To develop a modified release technology suitable for ODTs, that can be used for taste masking and enteric coating of poorly soluble compounds.

- To develop an encapsulation process which involves few steps, is aqueous-based, and has high encapsulation efficiency.

- To optimise the excipients' concentrations and identify the appropriate drug: polymer ratio that achieves suitable encapsulation efficiency.

- To carry out process optimisation using mathematical design of experiments (DOE).

- To incorporate the resultant encapsulated drug into an ODT base (from Chapter 3) and assess its drug release properties.

Chapter 2

Preformulation of ODTs: Evidence-Based Nanoscopic and Molecular Framework for Excipient Functionality

2.1. Introduction

The inclusion of excipient in formulations has seen an evolution from the traditional concept of inert component alongside the active ingredient to the functional and essential constituent of pharmaceutical dosage forms (Pifferi et al., 1999). The production of orally disintegrating tablets (ODTs) is usually achieved by direct compression of drug and excipients into hard compacts where the meticulous choice of excipients plays an integral role in determining product attributes such as porosity, friability and taste (Al-Khattawi et al., 2012). For example, microcrystalline cellulose imparts plasticity to compressed ODTs and enhances fast disintegration while D-mannitol improves mouth feel due to its sweet taste and creamy texture.

In-depth structural analysis of pharmaceutical excipients is necessary to improve resultant product characteristics and to predict product functionality through rational formulation design. For tablets, the understanding of major powder densification mechanisms under pressure and its effect on tablet properties is considered vital (Al-Khattawi and Mohammed, 2013). In general, tableting excipients deform elastically, plastically or by brittle fracture under pressure resulting in either strong and durable tablets or friable and fragile ones depending on the type of excipient/s employed (Roberts and Rowe, 1987 a). Furthermore, porosity and, indirectly, disintegration rate are affected by the mechanism of densification of tablets as the harder compacts have lower porosity and vice versa. Moreover, other aspects of tablet formulation/process such as lubricant sensitivity and punch velocity are known to affect tablet properties based on the densification mechanisms of excipients involved. For example, fragmenting materials are less susceptible to changes in compaction velocity when compared to materials undergoing plastic deformation (Roberts and Rowe, 1985).

The widely utilised model of Heckel (1961) for powder deformation under pressure provided the scientific community with an important tool for understanding the mechanical properties of excipients (Heckel, 1961). However, the model has also been criticised for its suitability for pharmaceutical applications as it was originally developed for research in metallurgy

73

(Sonnergaard, 1999). In accordance, other methods are needed in conjunction with the Heckel profile analysis to depict the full picture of powder interaction at the interparticulate and intermolecular levels. In addition, a fundamental knowledge of solid-state properties and their relationships to physico-mechanical aspects of excipients is required to understand the tableting behaviour (York, 1983).

The influence of particles/crystals morphology on the mechanical properties of powders has been considered earlier using microscopic techniques. However, conclusions are difficult to establish due to lack of supporting information on the nano-topographical features of excipients and the nature of adhesive forces that exist at the inter-particle interfaces (Van Veen et al., 2000). Tablets are formed from the densification and deformation of the powder particles, and the formation of inter-particle bonds due to adhesive forces. Hence, evidence of the micro/nano-scale features and adhesion forces of tableting excipients is crucial to develop a mechanistic understanding of their functionality in formulation development of ODTs.

The current study aims to investigate the interparticulate adhesive/cohesive interactions of commonly used ODT excipients including microcrystalline cellulose (MCC) and D-mannitol to understand the mechanisms affecting product functionality, specifically the effect on binding capacity and processability. In addition, two model active pharmaceutical ingredients (APIs) with different mechanical and physico-chemical properties were chosen to investigate the adhesion within tablets.

- The objective is to reveal the nano forces and surface energies within excipients/APIs using atomic force microscopy (AFM).

- Functionalised AFM probe with an excipient/API particle is used to obtain force-distance curves when indented upon another particle.

- AFM was used to understand the factors governing the adhesion between particles during compression.

74

- The generated data on adhesion forces is to be compared to the bulk tablet characteristics including their influence on tabletability (i.e. capacity to produce tablets of sufficient strength, example section 2.3.3).

- Surface topography and particle roughness were examined using AFM and SEM for the nano and microscopic features respectively.

- The effect on Heckel profiles and solid state polymorphic and thermal properties will also be investigated.

2.2. Materials and methods

2.2.1. Materials

Microcrystalline cellulose (MCC) Avicel grade PH-102 was obtained from FMC BioPolymer (Philadelphia, USA). D-mannitol, theophylline and magnesium stearate were purchased from Sigma-Aldrich (Pool, UK). Ibuprofen DC grade was obtained from Shasun Pharmaceuticals Limited (Chennai, India). All the ingredients were of pharmaceutical grade and used as received.

2.2.2. Methods

2.2.2.1. Powder flow assessment by Carr's index (bulk/tapped density)

Powder flow properties of the excipients and APIs were assessed using Carr's index. Bulk and tapped densities were obtained using a Sotax tap density USP I apparatus (Allschwil, Switzerland). The initial volume (volume at zero tap or bulk volume) was recorded for 10 g of powder poured into a 50 mL measuring cylinder. The machine operated for 10, 500 and 1250 taps and tapped volumes recorded. Triplicate measurements were made followed by calculation of Carr's index from bulk/tapped densities. Equations shown below:

$$\text{Tapped density} = \frac{\text{Mass of powder}}{\text{final powder volume}}$$

$$\text{Bulk density} = \frac{\text{Mass of powder}}{\text{Initial powder volume}}$$

$$\text{Carr's index} = \frac{(\text{Tapped density} - \text{Bulk density})}{\text{Tapped density}} \times 100$$

2.2.2.2. Atomic force microscopy (AFM)

AFM analysis was carried out using Veeco Dimension 3100 AFM with Nanoscope IVa controller and Nanoscope software (version 6.13r1) from Bruker (Massachusetts, USA). Two modes of analysis were conducted: contact mode for measurement of inter-particle adhesion forces and tapping mode for the examination of topography and surface roughness of the analysed powders. Silicon nitride cantilevers (model DNP, Bruker) were used for contact mode while silicon cantilevers (model TESP, Bruker) were used for tapping mode. All experiments were carried out under air and at room temperature (20-25°C).

2.2.2.2.1.   AFM contact mode

AFM contact mode was used to record force-distance curves for each pair of particles tested. The AFM cantilever was functionalised with a single particle using epoxy glue that cures within 5 min. The procedure was carried out by picking up a minimal amount of glue from a drop placed on a plate under the AFM probe using the engage/withdraw mode. This was followed by quickly attaching the excipient/API particle on to the probe by repeating the engage/withdraw cycle. The functionalised (sample) cantilever was left for ≈ 10 min in order for the glue to cure fully (Eve et al., 2002).

Before undertaking the particle-particle contact phase of the experiment, and in order to obtain accurate force measurements, the spring constant of the sample cantilever was determined using a calibration cantilever with a known spring constant (i.e. a known capacity for the cantilever to

bend under applied pressure). The spring constant of the sample cantilever was calculated using the formula below:

$$k = k_{ref}\left(\frac{S_{ref}}{S_{hard}} - 1\right)\left(\frac{L}{L - \Delta L}\right)^3$$

Where k and k_{ref} are the spring constants of the sample and reference cantilevers respectively. S_{ref} and S_{hard} are the deflection sensitivities of the sample cantilever on the reference cantilever and a hard surface respectively. L is the length of the reference cantilever while ΔL is the offset of the tip of the sample cantilever from the end of the reference cantilever. The spring constant of DNP cantilevers varied between 0.06 - 0.35 N/m, while it was 42 N/m for TESP cantilevers.

After obtaining the spring constant, the sample cantilever was engaged on another particle which was placed in a plate on the microscope stage. The force of adhesion was calculated by the Nanoscope software using Hooke's law:

$$F = k \times z$$

Where F is the adhesion force, k is spring constant for the sample cantilever and z is the vertical distance travelled by the sample cantilever upon retraction from the particle on the plate.

Force-distance curves were generated when the cantilever particle approaches the particle on the plate and upon leaving it. Figure 2.1 a shows a typical force-distance curve where the adhesion force F is represented on the Y-axis and the vertical distance moved by the sample cantilever (z) on the X-axis. Control runs were performed before each sample analysis by indenting the functionalised cantilever on an empty plate and recording the force-distance curve. Figure 2.1 b shows a control run whereby a small adhesion force was observed due to capillary forces resulting from a thin film of moisture existing on surfaces under standard room temperatures (20-25°C).
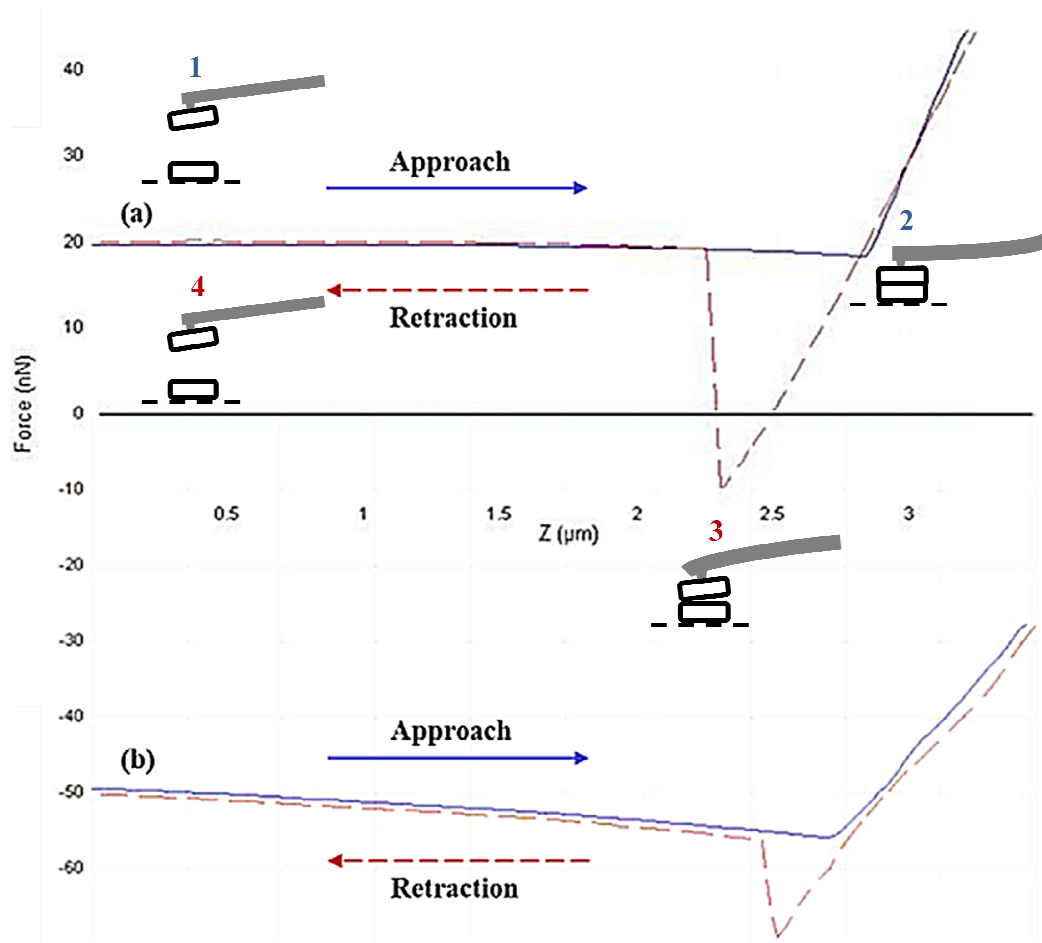
Figure 2.1: Force-distance curves. (a) Approach and retraction curves of the cantilever with attached particle upon indentation on another particle placed under the AFM. The illustration cartoon represents the four stages of the force-distance curve generation. These are: 1) Functionalised cantilever (with glued particle) approaches 2nd particle on the plate, 2) particle on cantilever is in contact with particle on the plate, 3) Cantilever particle detaches (snaps off) from the 2nd particle underneath and 4) Cantilever fully retracted. (b) Control run representing the indentation of cantilever with particle on an empty plate. The graphs show adhesion force on the y-axis and vertical distance travelled by cantilever (z) on x-axis.

Various combinations of particles of MCC, D-mannitol, ibuprofen and theophylline were tested for intermolecular adhesion/cohesion forces. Triplicate measurements were performed on a single area of a particle and were repeated on at least 6 different particles (6-10 particles) resulting in an overall 18 – 30 points for each adhesion pair (Camesano and Logan, 2000; Chaw et al., 2005). Data for force measurement were expressed as mean ± SD. The dependence of adhesion force on contact area between particles was minimized by choosing particles with similar size (ranging between 30 – 50 μm). Moreover, the indentation process was carried out

78

such that the particle attached to the cantilever formed a cross with the particle on the plate resulting in a total area of contact between 135 - 625 μm^2. Both approach and pulling velocities were kept identical in all experiments (Roberts, 2005) between 3000 nm/s to 6000 nm/s and a step size of 0.972 μm was used. Surface energy measurements between the pairs of particles were derived from the adhesion forces (pull-off forces) using the JKR model (Johnson et al., 1971) and following the procedure by Grierson et al. (2005).

2.2.2.2.2. AFM tapping mode

Tapping mode was carried out to obtain the detailed surface topography and roughness of MCC, D-mannitol, ibuprofen and theophylline. The cantilever (silicon TESP cantilever with tip radius of 8 nm) was tuned and driven to resonance frequency before scanning the surface. The scan rate was maintained at 1 Hz on a varied scan size between 10 μm^2 and 100 nm^2 with a frame resolution of 512x512. During scanning, the applied force of the cantilever on the sample was minimised by adjusting drive amplitude and feedback settings. Three dimensional images were obtained for the surface of particles using mixed mode which produces images based on height and amplitude feedback during scanning. Average roughness (Ra) was obtained based on spatial resolution/frequency of surface features using the Nanoscope software for a 10 μm^2 section of each particle. Roughness data for 1 μm^2 sections were not useful for interpretation due to surfaces smoothness and interference with noise.

2.2.2.3. Preparation of tablets

2.2.2.3.1. Tablet preparation for out-of-die Heckel analysis

MCC, D-mannitol, ibuprofen and theophylline powders were individually compacted into 500 mg tablets under compression forces between 5 and 30 kN. The tablet press utilised for preparing the tablets was a bench-top hydraulic press from Specac ltd. (Slough, UK) equipped with flat-faced dies 13 mm in diameter. Dies were lubricated externally using magnesium stearate dispersed in acetone (5% w/v).

Out-of-die Heckel profile was used to examine powder densification mechanisms and to obtain mean yield pressure (Py) values. Out-of-die analysis involves compacting the tablets at different pressures and measuring the porosity after ejection of the tablets. Py was obtained from the reciprocal of the slope (K) of the linear portion of the Heckel plot. Heckel model is represented by the equation of densification which follows first-order kinetics.

$$Ln[1/(1-D)] = P \times K + A$$

Where Ln(1/(1-D)) (D being the relative density of compact) is represented on the Y-axis and P (compaction pressure) on the X-axis. A and K are the intercept and slope of the linear portion of the curve respectively.

2.2.2.3.2. Preparation of ODTs from binary and ternary mixtures

The first phase of this study involved the assessment of MCC, D-mannitol, ibuprofen and theophylline tabletability. Tablets (500 mg) were prepared from each powder using the same tableting machine mentioned previously. Magnesium stearate (0.5% w/w) was added to each powder, blended for 1 min in a plastic tub, followed by compression between 10 and 40 kN. Tensile strength of the tablets was obtained from hardness measurements (see section 2.2.2.10) which were plotted against compaction pressure to produce tabletability profile. Three tablets were prepared at each compression force.

The second phase was carried out to examine the influence of MCC on ODT properties based on different ratios of MCC (2 – 99.5% w/w), varying D-mannitol concentration and fixed 0.5% w/w magnesium stearate. Powder blending was carried out by manual shaking of the powders in a plastic tub for 5 min before further blending with magnesium stearate for 1 min. Tableting was performed using the same tablet press at a fixed compression force of 20 kN. Three tablets were prepared for each MCC concentration followed by testing for hardness.

The third phase was performed to assess the effect of varying ratios of ibuprofen and theophylline on the hardness and disintegration time of ODTs. Both APIs were incorporated at

concentrations ranging from 10 to 40% w/w using a fixed concentration 50% w/w of MCC, a varying concentration of D-mannitol and 0.5% w/w magnesium stearate. Blending of the drug and excipients was carried out by manual shaking for 5 min followed by adding magnesium stearate and continuous blending for 1 min. The tablets (500 mg) were prepared at a fixed compression force of 20 kN for 30 sec. Six tablets were prepared at each drug concentration, three were used for hardness and three for disintegration test.

2.2.2.4. Scanning electron microscopy (SEM)

The morphology of MCC, D-mannitol, ibuprofen and theophylline powder particles as well as cross sections of compacted specimens of each were examined by scanning electron microscopy (SEM) Stereoscan 90 from Cambridge Instruments (Crawley, UK). For the powders, approximately 1 mg of each material was placed onto a double-sided adhesive strip on an aluminium stub. For the tablets, each of the 500 mg compacts was dissected with a blade then a thin layer was obtained to improve gold coating of the specimen. The specimen stub was coated with a thin layer of gold using a sputter coater Polaron SC500 from Polaron Equipment ltd. (Watford, UK) at 20 mA for 3 min followed by sample examination using SEM. The acceleration voltage (kV) and the magnification can be seen on each micrograph.

2.2.2.5. Attenuated total reflectance-fourier transform infrared spectroscopy (ATR-FTIR)

Investigation of hydrogen bonding within MCC and theophylline tablets as well as identification of the polymorphic forms of all four molecules was carried out using Nicolet IS5 FTIR spectrometer equipped with an iD5 attenuated total reflectance (ATR) diamond from Thermo Fisher Scientific (Massachusetts, USA). FTIR spectra were captured in the region 400-4000 cm^{-1}. Approximately 50 mg of neat powders as well as 50 mg MCC and theophylline compacts (5 mm in diameter) made at compression forces between 5 and 20 kN were placed on the diamond plate followed by 16 scans / sample (n=3). For MCC, the H-bonding investigation involved mathematical self-deconvolution and curve fitting of the broad OH band between

3000-3500 cm^{-1} according to the method reported in (Oh et al., 2005; Janardhnan and Sain, 2011). The deconvoluted bands were assigned to inter/intramolecular H-bonding. The area under curve was calculated for the individual peaks and ratio of intermolecular: intramolecular H-bonding used as an indication of any molecular changes during compression of MCC powder.

2.2.2.6. X-ray diffraction (XRD)

X-ray diffraction was carried out on MCC powder to investigate the presence of amorphous/crystalline phases using a D2 Phaser diffractometer from Bruker (Massachusetts, USA). The angular range (2θ) was 4 – 50° with increments steps of 0.02° and measured at 0.25 sec/step. Diffractive patterns were generated as counts per step and thereafter analyzed using Eva 18.0.0.0 software (Bruker, AXS). Runs were carried out in triplicate and representative results shown.

2.2.2.7. Thermogravimetric analysis (TGA)

A thermogravimetric analyzer Pyris 1 TGA from Perkin Elmer (Massachusetts, USA) was used to measure the moisture content and decomposition temperature of all powders. 2 mg of each sample was loaded onto the TGA pan and heated between 30-300°C at a scanning rate of 10°C/min under nitrogen stream. Pyris Manager Software (version 5.00.02) was used for analysing the obtained thermograms. Moisture content was obtained by calculating Δy for each run between 30°C and 120°C. Also, by drawing tangents on the weight (%) versus temperature curve, the onset of decomposition temperature was obtainable. The latter was indirectly used to help choose the upper temperature in DSC runs (section 2.2.2.8). Triplicate scans were carried out for each of the analysed samples.

2.2.2.8. Differential scanning calorimetry (DSC)

DSC Q 200, from TA Instruments (Delaware, USA) was used to determine the thermal properties of powders. Accurately weighed samples (5 mg) of MCC, D-mannitol, ibuprofen and theophylline were transferred into crimped Tzero aluminium pans and heated in the range of 30 - 300°C at a rate of 10°C/min under a nitrogen purge. For MCC, a pin hole was introduced into the sample and reference DSC pans to allow moisture evaporation to occur. MCC was also analysed using cyclic mode whereby consecutive heating and cooling runs were conducted between 30°C and 180°C at a rate of 20°C/min. This was followed by analysis of resulting graphs using TA instruments universal analysis 2000 software (V 4.5A).

2.2.2.9. Particle size analysis

Particle size of powders was measured by laser diffraction technique using particle size analyzer HELOS/BR and dry disperser RODOS with feeder VIBRI/L from Sympatec (Clausthal-Zellerfeld, Germany). The measuring range of the lens was 0 - 175 μm. Approximately 2 g of each powder was placed in the feeder tray and the run started at trigger condition of 2% Copt (optical concentration) for 10 sec with powder dispensing pressure of 3 bar. Volume mean diameter (VMD) was recorded for all four powders and all the measurements were carried out in triplicate.

2.2.2.10. Tablet crushing strength

Crushing strength of tablets (also referred as hardness) was measured immediately after compression using 4M tablet hardness tester from Schleuniger (Thun, Switzerland). Tensile strength was calculated using the equation:

$$\sigma = \frac{(2 \times \text{Hardness})}{\pi \times d \times h}$$

Where σ is the tensile strength, d is the diameter of tablet and h is the tablet thickness. All measurements were carried out in triplicate and the values reported as mean ± SD.

2.2.2.11. Tablet disintegration time

The disintegration time was determined for 3 tablets using the United States Pharmacopeia (USP) moving basket disintegration apparatus (USP Convention, 2005). Disintegration test apparatus used was ZT3 from Erweka (Heusenstamm, Germany). A tablet was placed in the disintegration basket (without using a disk) which was raised and lowered at a constant frequency of 30 cycles/min in the disintegration medium. Distilled water (800 mL) maintained at 37°C was used as the medium of disintegration while disintegration time was recorded for one tablet at a time to improve accuracy of recording. Time of disintegration was recorded when all the disintegrated fractions of tablet passed through the mesh of disintegration basket. Measurements were carried out in triplicate and values were reported as mean ± SD.

2.2.2.12. Tablet porosity

Tablet porosity was measured using helium pycnometry, Multipycnometer from Quantachrome Instruments (Syosset, USA). The true volume of tablet was measured based on Archimedes principle of fluid displacement. The fluid used in the instrument was helium gas which has the ability to penetrate tiny pores approaching one angstrom (10^{-10} m) in diameter. One tablet was placed in a micro sample cell of the instrument and the true volume V_t was obtained using the equation:

$$V_t = V_C - V_R(P1/P2 - 1)$$

Where V_t is true volume of the sample, V_C is volume of the sample cell, V_R is the known reference volume, P1 is atmospheric pressure and P2 is pressure change during determination. V_t was used to calculate the true density of the tablet by weighing the tablet and substituting the values into:

$$\text{True density} = \text{Weight of tablet/True volume}$$

Porosity (ε) was calculated using the equation:

$$\varepsilon = 1 - (\text{Bulk density/True density})$$

Bulk density was acquired from:

$$\text{Bulk density} = \text{Weight of tablet/Bulk volume}$$

Bulk volume was obtained by measuring the radius (r) and thickness (h) of the tablet using a digital calliper and substituting in the equation for volume of a flat-faced tablet:

$$V = \pi \times r^2 \times h$$

All porosity measurements were carried out in triplicate.

2.2.2.13. Statistical analysis

Student t-test and analysis of variance (ANOVA) were carried out using GraphPad Prism 6.02 software (California, USA). Statistical significant difference was considered at a p value <0.05. Where applicable, all results are presented as mean $\pm$ SD (SD; standard deviation) to account for the noise encountered within the experiments.

2.3. Results and discussion

Functionalised AFM probe with an excipient/API particle (shown in Figure 2.2 a and b) was used to obtain force-distance curves when indented upon another particle. AFM force-distance data are rich in information about the intermolecular interactions between particles including weak non-covalent and short ranged forces such as hydrogen bonding, van der Waals, electrostatic and capillary forces (Butt et al., 1991).
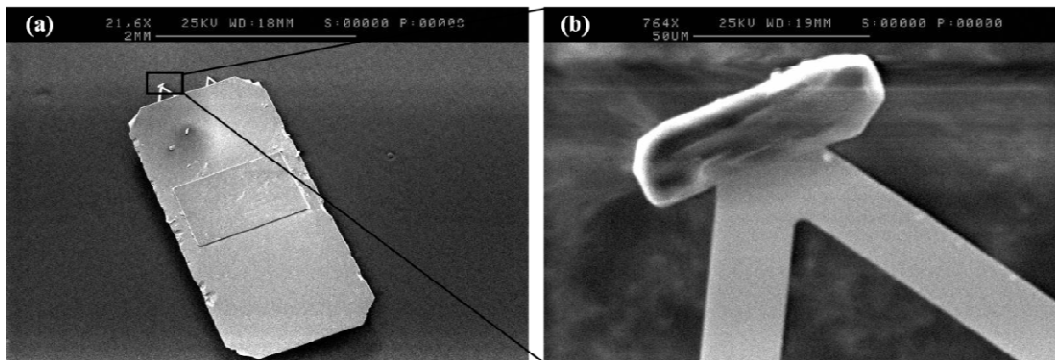
Figure 2.2: AFM cantilever. (a) Full size of cantilever and (b) higher magnification showing a particle attached on the nano tip of the probe.

To ensure reproducibility of the measured adhesion forces, the study involved calibrating the functionalised cantilever before each force-distance cycle measurement (section 2.2.2.2.1.). The control measurements showed very low adhesion forces (approximately 10 nN) conforming to the presence of a very thin film of moisture on air-exposed surfaces. This is a common feature of operating AFM in air which could be considered a drawback if the purpose was to detect weak van der Waals forces, however, the magnitude of these forces is usually too low to accommodate for the strong adhesion experienced during compression of powders. Furthermore, the operation in air would simulate the actual manufacturing environment during tableting/processing of pharmaceutical powders. Moreover, the excipients used in ODT development are usually less hygroscopic in air to avoid abrupt disintegration or dissolution of the usually porous dosage form during storage.

Other appropriate measures such as controlling contact area between particles and approach/retraction speeds of cantilever were also undertaken to reduce inter-particulate variation observed in AFM measurements (Roberts, 2005) as outlined in the methodology section.

The results of adhesion/cohesion forces and surface energies shown in Table 2.1 below will be interpreted in the next sections in relation to individual excipient properties or for combination

of excipients/APIs. The sensitivity of AFM was exploited to examine local variations (i.e. larger standard deviation) that occurred between two particle pairs (MCC-MCC and Theophylline-Theophylline) (Roberts, 2005). This was attributed to the rough surface of MCC (discussed in section 2.3.2.1) and the extrapolation of theophylline adhesion curve (flat retraction curve discussed in section 2.3.2.4).

Table 2.1: AFM adhesive/cohesive forces and surface energies of various interaction pairs of MCC, D-mannitol, ibuprofen and theophylline. Triplicate measurements were performed on a single area of a particle and were repeated on at least 6 different particles (6-10 particles) resulting in an overall 18 – 30 points for each adhesion pair. Results reported as mean ± SD.

Particle–Particle Interaction Pair	Adhesion/Cohesion Force (nN)	Surface Energy γ (mJ/m^2)
MCC-MCC	45.15 ± 23.65	1.39 ± 0.73
MCC-Ibuprofen	67.12 ± 8.48	2.07 ± 0.26
MCC-Theophylline	62.93 ± 7.36	1.94 ± 0.23
D-mannitol-D-mannitol	31.88 ± 9.38	0.77 ± 0.23
D-mannitol-MCC	11.22 ± 7.69	0.27 ± 0.19
D-mannitol-Ibuprofen	30.83 ± 10.93	0.75 ± 0.29
D-mannitol-Theophylline	29.82 ± 0.76	0.72 ± 0.02
Ibuprofen-Ibuprofen	24.45 ± 5.96	0.76 ± 0.18
Theophylline-Theophylline	136.33 ± 26.85*	2.40 ± 0.53

*Cohesive force for Theophylline-Theophylline combination was indirectly obtained by extrapolation as the full force which was very high was beyond instrument measuring limit as maximum deflection of cantilever was reached.

Additionally, the approach for measuring adhesion forces reported herein was successful in deriving important statistical trends discussed in the different sections. The findings on

densification mechanisms discussed in this work were mostly in agreement with the Heckel profiles (Figure 2.3) and SEM results. The preformulation characteristics for the different excipients and APIs were compiled in Table 2.2 below and will be discussed in conjunction with the literature reported on densification mechanisms and nanoscopic information obtained from the current AFM study.
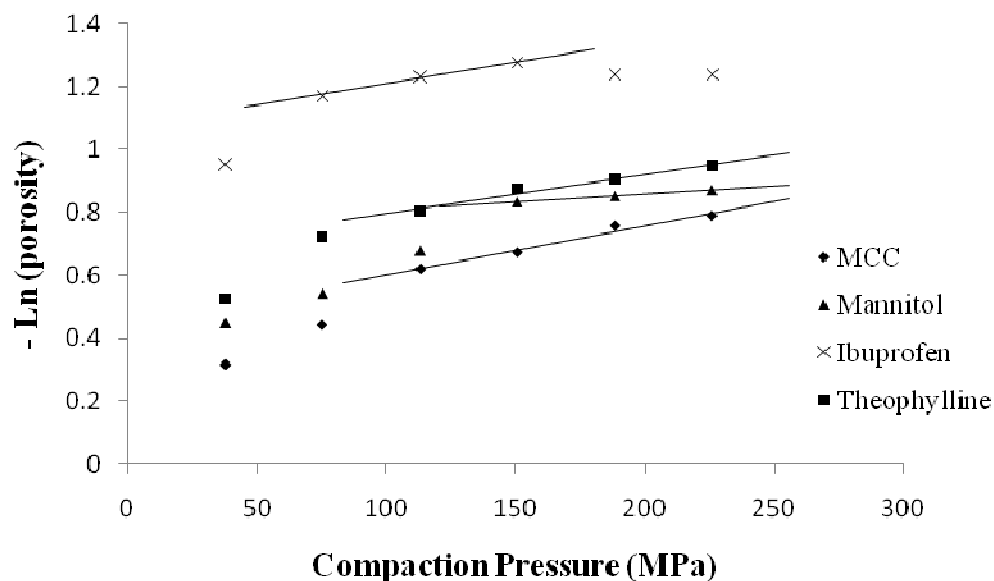
Figure 2.3: Overlaid Heckel plots for MCC, D-mannitol, ibuprofen and theophylline. The trend lines are used to find the mean yield pressure of the materials. Each point represents triplicate measurements of porosity (n=3).

Table 2.2: Physico-chemical and mechanical properties of MCC, D-mannitol, ibuprofen and theophylline. Where applicable, results reported as mean ± SD (n=3).

Material	AFM Average Roughness (Ra)	Melting Peak (°C)	Solid State/ Polymorphic Modification	Crystal Habit/ Morphology	Heckel plot analysis		Moisture Content (%)	Particle Size VMD (μm)	Carr's Index (%)
					Mean Yield Pressure (MPa)	R^2 of Linear Portion			
MCC	1079	N/A Chars at 260-270	Crystalline/ Amorphous	Irregular /microfibrillar structure	625	0.97	3.46 ± 0.17	92.27 ± 2.74	16.00 ± 3.03
D-mannitol	333	168.43 ± 0.06	mod I	Elongated with multiple surface asperities	2000	0.99	0.4 ± 0.17	37.78 ± 1.05	39.50 ± 1.56
Ibuprofen	273	77.40 ± 0.08	Crystalline	Elongated with smooth surfaces	714	0.99	0.41 ± 0.35	32.15 ± 1.24	32.75 ± 0.52
Theophylline	321	270.71 ± 0.89	Anhydrous polymorph II	Columnar composed of multiple crystallites	833	0.97	0.22 ± 0.04	96.67 ± 2.25	29.01 ± 1.77

2.3.1. Flow properties of excipients/APIs

Flow properties of the materials were mainly dominated by the effect of particle size as well as adhesion profile. The results of Carr's index in Table 2.2 showed that only MCC exhibited good flow properties (Carr's index between 12-16%) whereas the rest of the materials exhibited poor cohesive to very poor flow behaviour (Carr's index range 28-40%).

The reason for the good flowability of MCC is its relatively large particle size (92.27 ± 2.74 µm) and agglomerate-like particle morphology (Figure 2.4 a). The microfibril structure of MCC was probably responsible for some intercalation (discussed in detail in section 2.3.2.1) which may negatively impact flow. Hence, MCC did not exhibit excellent flow (Carr's index for excellent flow range 5-10%) and the effect of intercalation was ultimately minimised by the large particle size and agglomerate-like morphology. The adhesion force of MCC (45.15 ± 23.65 nN) could not be utilised for explaining the flow behaviour due to the accompanying variation resulting from intercalation (explained in section 2.3.2.1).
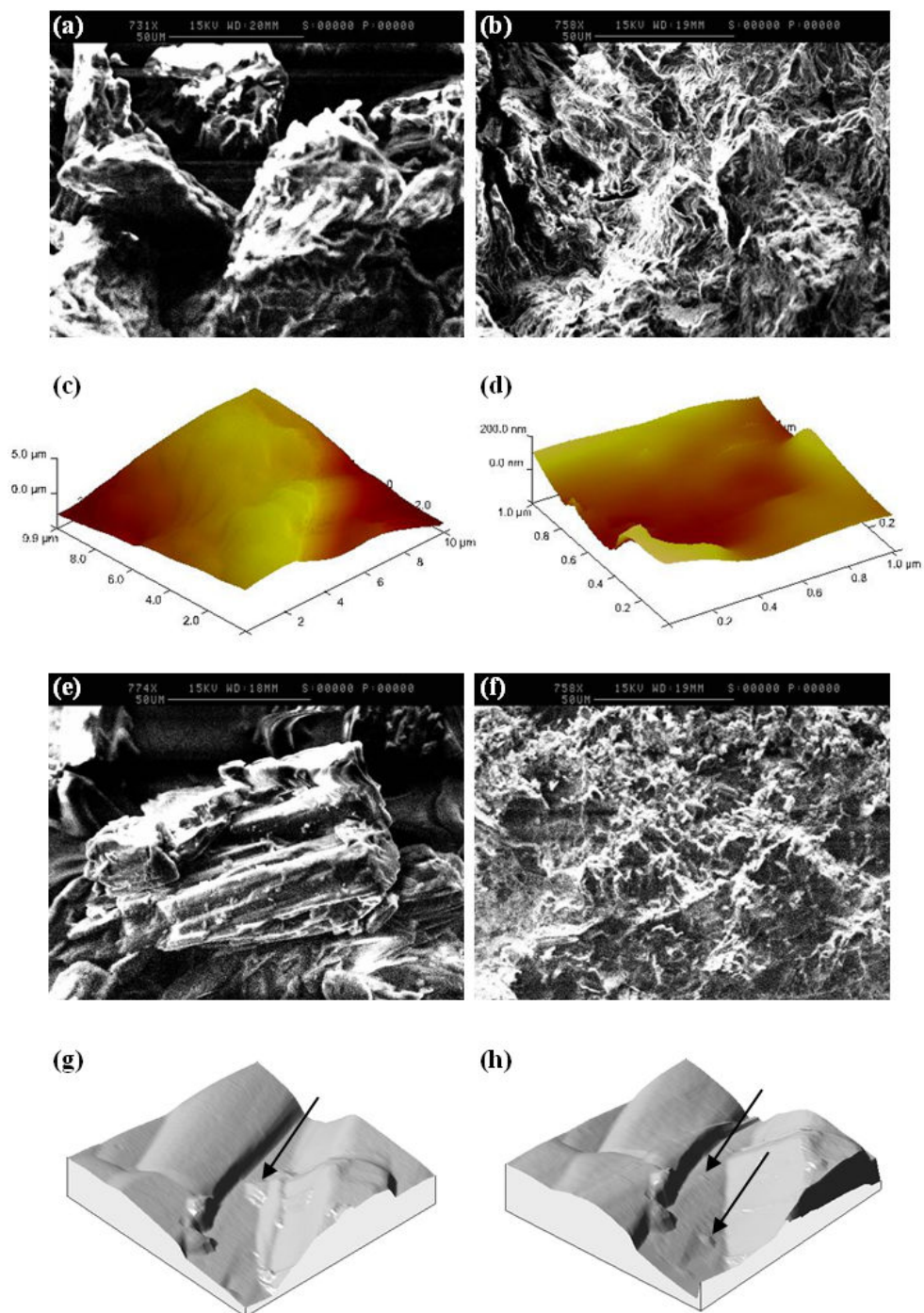
Figure 2.4: Micro and nano structural features of MCC and D-mannitol from SEM and AFM. (a) and (b) show SEM images of MCC particles before and after compression into tablet respectively, (c) and (d) show AFM topographical images of MCC single microfibril of one particle and pore/channel between adjacent MCC microfibrils of another particle respectively, (e) and (f) are SEM images showing D-mannitol particle morphology and D-mannitol tablet showing fragmentation of particles after compression at 10 kN, (g) and (h) are AFM topographical images of D-mannitol. The arrow on (g) shows a surface asperity before fragmentation whereas arrows in (h) show the asperity fragmentation and shifting by the effect of tip movement.

Theophylline, on the other hand, showed poor cohesive flow (Carr's index 28-35%) despite its large particle size (96.67 ± 2.25 μm). AFM helped explaining this apparent contradiction as it showed that theophylline has different trend to the other materials observed in its force-distance approach and retraction curves. These phenomena are discussed in detail in section 2.3.2.4 which shows that theophylline undergoes significant electrostatic charging on the surface and possible liquid bridging, hence could be considered the reason for its rather poor flowability.

Moreover, ibuprofen and D-mannitol showed poor cohesive to very poor flow (Carr's index range 28-40%). Interestingly and coincidently, ibuprofen and D-mannitol had similar adhesion forces (24.45 ± 5.96 nN and 31.88 ± 9.38 nN), surface energies (0.76 ± 0.18 mJ/m^2 and 0.77 ± 0.23 mJ/m^2), particle size (32.15 ± 1.24 μm and 37.78 ± 1.05 μm) and moisture content (0.41 ± 0.35% and 0.4 ± 0.17%) respectively. These similarities potentially led to the close flow behaviour of ibuprofen and D-mannitol.

2.3.2. Compaction mechanisms of excipients/APIs

2.3.2.1. MCC compaction mechanism

The successful application of MCC for direct compression of tablets was first recognized in 1965 in the development of glyceryltrinitrate sublingual tablets which replaced the previously employed tedious moulding process (Richman et al., 1965). The applications of MCC have grown extensively with the introduction of various techniques/strategies to enhance its functionality and overcome limitations (Al-Khattawi and Mohammed, 2013). It undergoes plastic deformation at exceptionally low mean yield pressure (Table 2.2) which enables compaction of tablets using low compression forces. This in turn maintains sufficient internal porosity necessary for fast disintegration of tablets.

MCC was reported previously to undergo H-bonding under pressure which would be responsible for the high tensile strength and low friability of MCC compacts. However, most organic materials will have H-bonding adhesive mechanisms which do not necessarily translate into high tensile strength. It is important to uncover the mechanism for this particular compaction behaviour of MCC to be able to design materials with optimal compression properties.

Research published by Hüttenrauch in 1971 proposed H-bonding between adjacent MCC particles as the mechanism of compaction and adhesion in MCC tablets. This hypothesis was subsequently embraced and accepted by other research groups to explain densification of compacts and the resultant high tensile strength of MCC based formulations. The experimental methodology utilised by Hüttenrauch was built on assessing the difference between disintegration time of MCC tablets in H_2O and D_2O (Deuterium oxide) as the evidence for hydrogen bonding. He hypothesized that MCC tablets would disintegrate faster in light water (H_2O) than in heavy water (D_2O) and that the faster disintegration in H_2O would be attained from the breakage of hydrogen bonds between MCC-MCC particles and respective association of MCC hydrogen atoms with water. In contrast, the disintegration time of MCC tablets in D_2O would be slower due to the anticipated slow kinetic exchange of MCC hydrogen atoms with Deuterium. This hypothesis would be true if a significant difference in disintegration time of MCC tablets was observed. Conversely, when we examined the reported disintegration data, the results showed no statistical significant difference between the disintegration time of MCC tablets in H_2O and D_2O (t-test, $p>0.05$). Therefore, the aforementioned hypothesis cannot be considered true and valid and that the actual mechanism warrants further investigation.

It is also important to note that, in contrast to the Hüttenrauch approach, our research has investigated H-bonding in the dry state (more relevant to the direct compression of tablets) using FTIR by compression of MCC into small compacts (50 mg in weight, 5 mm in diameter) at increasing compression forces (from 5 to 20 kN). The purpose was to investigate whether H-bonding intensity increases upon compression of MCC when the distance between particles is reduced (Hüttenrauch, 1971). Mathematical self-deconvolution and curve fitting of the FTIR broad OH band of MCC between 3000-3500 cm^{-1} (Figure 2.5) revealed 3 main peaks at 3273, 3337 and 3405 cm^{-1}. The first and third peaks were ascribed to cellulose intermolecular hydrogen bonding according to Oh et al. (2005) and Liang and Marchessault (1959). The middle band at 3337 was ascribed to cellulose OH stretching vibrations and intramolecular H-bonding (Liang and Marchessault, 1959; Hinterstoisser et al., 2003). The ratio of OH intermolecular/intramolecular i.e. peak 3273:3337 and peak 3405:3337 were compared between the powder and compacts (5-20 kN). The results showed no change in the 3273:3337 ratio (0.73) between powder and tablets at all compression forces. Similarly, there was no difference in 3405:3337 ratio (0.30) between powder and compacts at all compression forces. The results of FTIR indicated no significant impact of H-bonding mechanism on the densification/bonding between MCC particles in the solid state. Adolfsson et al. (1999) suggested that the forces acting between particles of microcrystalline cellulose cannot be accurately determined/ classified and that it can be possibly described as bonding due to weak attractive forces acting over relatively larger distances.
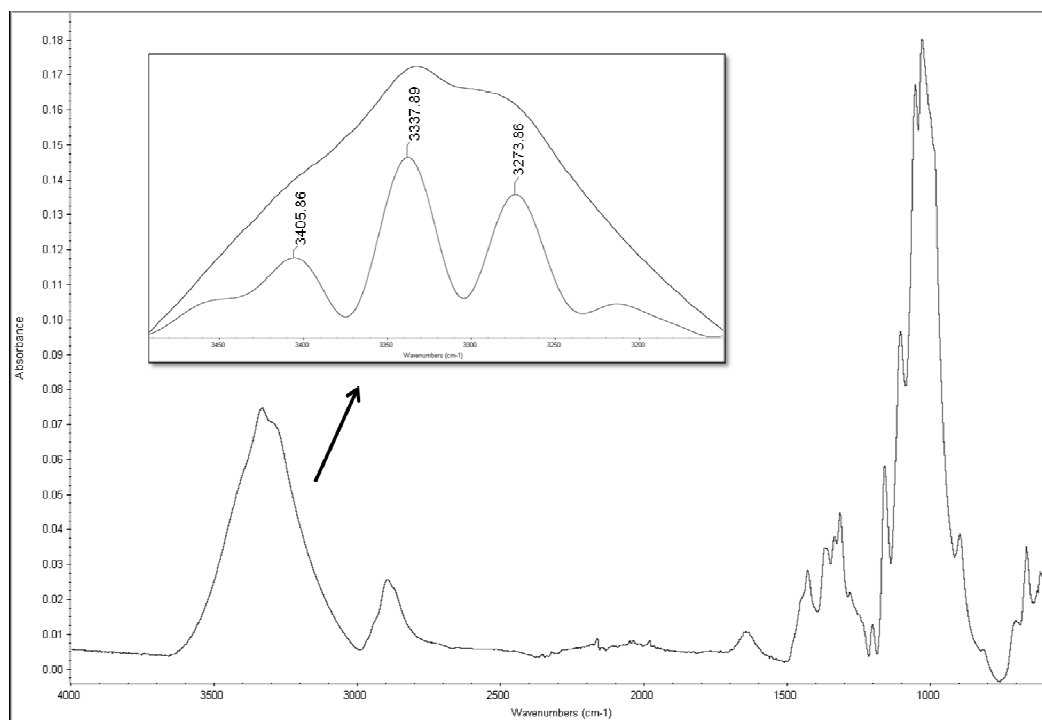
Figure 2.5: ATR-FTIR analysis of MCC. FTIR for MCC showing the full material spectrum and zoomed on mathematically self-deconvoluted OH peaks. Assigned OH peaks were 3273 and 3405 cm^{-1} for intermolecular H-bonding and 3337 cm^{-1} for OH stretching vibrations/intramolecular H bonding. The spectrum is representative of 16 scans per sample (n=3).

Additionally, no evidence could be obtained from AFM to confirm the hypothesis of hydrogen bonding as no extraordinary adhesion force was found when MCC particles interacted with each other. It could be argued that the distance to achieve hydrogen bonding (i.e. 0.2 nm) between the interacting particles was not reached during the AFM particle-particle contact (due to protrusions of microfibrils on the particles' surfaces). However, during the AFM contact mode, an intimate contact between the particle on the cantilever and the one on the plate was achieved to the extent of intercalation sometimes. AFM also confirmed the latter phenomenon between MCC particles which showed an inconsistent adhesion pattern (45.15 ± 23.65 nN) due to irregularity of particles topography resulting in local attachments at different contact points. This was also consistent with the surface energy between MCC-MCC particles (1.39 ± 0.73 mJ/m2) having the highest associated variation.

95

AFM tapping mode analysis showed that MCC is primarily composed of irregularly shaped particles with microfibrillar structure. Furthermore, AFM topographical images clearly showed two important features on MCC particle: microfibrils and large pores/channels in between (Figure 2.4 c and d). The structure of these microfibrils may lead to intercalation with each other during compression (Fox et al., 1963). The microfibril of one MCC particle was suggested to interact with a pore/channel of an opposite MCC particle. The illustration in Figure 2.6 represents this phenomenon where microfibrils of MCC particle (A) intercalate with channels (in between microfibrils) of MCC particle (B).
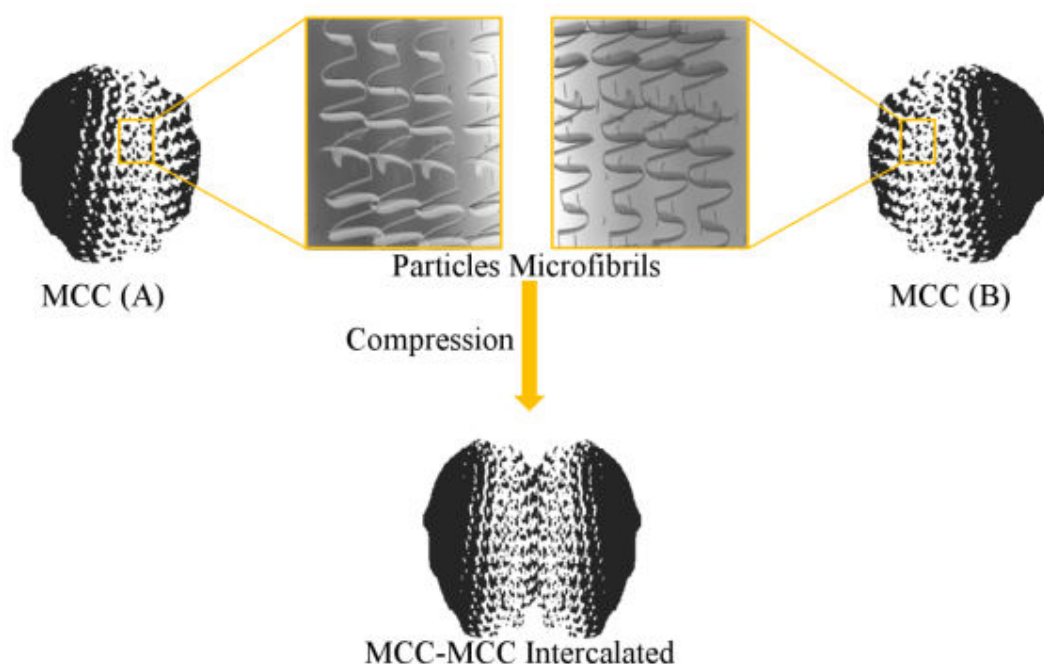
Figure 2.6: An illustration of MCC-MCC intercalation upon compression. The microfibrils of MCC particle (A) intercalate with channels (in between microfibrils) of MCC particle (B).

Analysis of SEM images before and after tableting showed that some particle deformation can be observed, although features of original particles are still noticeable (i.e. agglomerate-like). In fact, the particles after tableting seemed to be closely inserted into each other on the surface (Figure 2.4 a and b).

AFM roughness data (Table 2.2) revealed a much higher roughness for MCC (average roughness Ra of 1079) compared to D-mannitol, ibuprofen and theophylline (333, 273 and 321

respectively). This constitutes another proof for the microfibrillar structure and the rugged surface of MCC that is capable of forming an attachment with another microfibrillar/channel structure on another particle (Karehill and Nyström, 1990 a; Karehill et al., 1990).

XRD diffraction pattern of MCC powder in Figure 2.7 shows a broad amorphous hump in the 14-22° 2θ range, followed by a crystalline peak at 26° and possibly another small amorphous peak at 40°. The occurrence of amorphous regions within MCC is not surprising as the excipient is produced by spray drying which is well known to result in amorphous materials (Hancock and Zografi, 1997). These results were also consistent with our investigation of MCC amorphicity using DSC cyclic mode which showed a glass transition temperature (Tg) at 67.60 ± 0.05°C in the cooling run (Figure 2.8). It was difficult to determine Tg for MCC in the heating run due to interference with moisture evaporation endothermic peaks. These findings were in line with previous results by Szcześniak et al. (2008) who stated that Tg of cellulose is better determined from the cooling runs. In addition, a research by Picker and Hoag (2002) has shown that MCC (Avicel PH-102) has amorphous regions (nearly 30%) using modulated DSC.
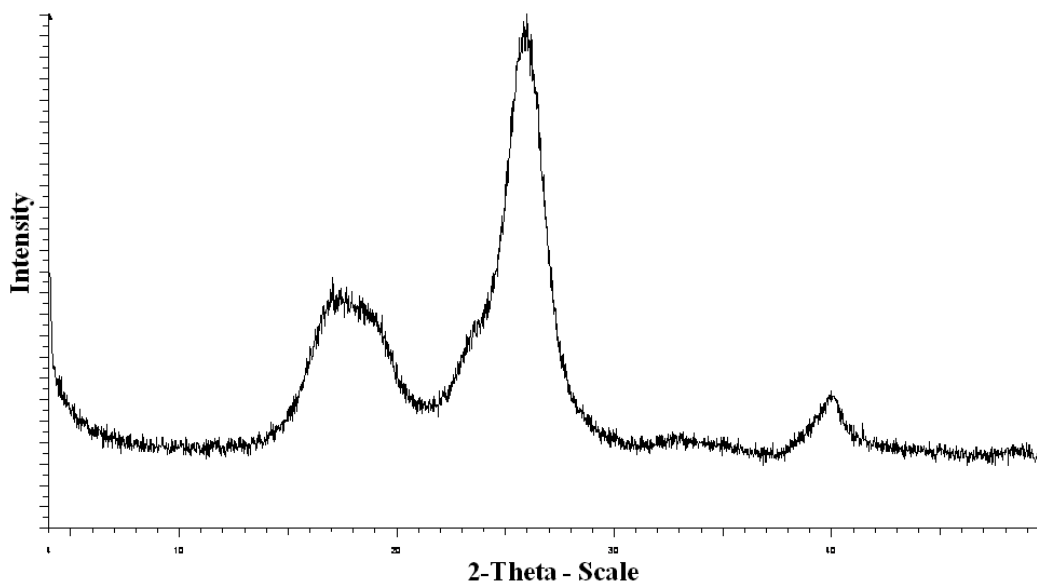
Figure 2.7: MCC XRD pattern. MCC diffraction pattern shows a broad amorphous hump in the 14-22° 2θ range, a crystalline peak at 26° and possibly another amorphous peak at 40°. XRD pattern is representative of triplicate measurements (n=3).
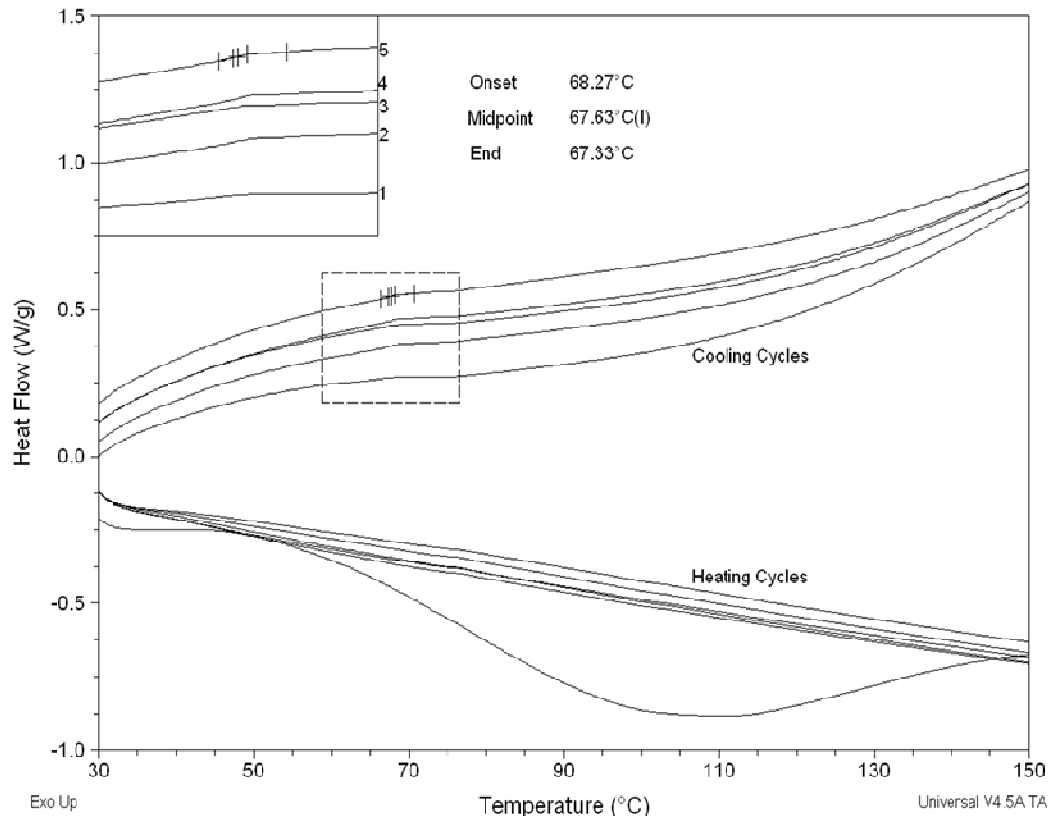
Figure 2.8: DSC thermogram of MCC showing consecutive heating and cooling runs obtained from cyclic mode analysis. The Tg of MCC at 67.63°C is seen in the cooling runs with increased clarity in the run order 1-5 as moisture (3.46 ± 0.17%) was continuously evaporated. DSC thermograms are representative of triplicate measurements (n=3).

Also, as mentioned earlier, MCC showed the lowest mean yield pressure (Py) between the different particles investigated representing the high plasticity of the excipient (Table 2.2). MCC also has undergone a slow decrease in porosity indicating slow rearrangement of particles on the initial part of the Heckel curve prior to bonding by plastic deformation (Figure 2.3) (Alderborn and Nyström, 1996).

To the best of our knowledge, there is no clear explanation supporting the functional behaviour of MCC as a binder. Based on the evidence generated in this study, we would like to propose a "Conglomerate Hypothesis" for the tensile strength and low friability of MCC compacts and associated formulations. In this hypothesis, we suggest that a number of factors act together to yield the high tensile strength and low friability of MCC compacts. The basis for the hypothesis

is also illustrated in Figure 2.9: **(a)** At the initial part of compression, the particles which have *high roughness* are brought closer to each other by the effect of compression force. **(b)** A certain degree of *plastic deformation* inevitably occurs at least due to the presence of *amorphous fraction* within MCC particles which is deformable under pressure. **(c)** Particle's *microfibrils intercalate* with opposite channels of other particles. This intercalation is assisted by the amorphous regions within MCC acting as a 'local binder' enforcing the intimate bonding, whereas some molecular bonding (such as by H-bonding) is also bound to happen due to the nature of cellulose and amorphous domains within MCC.
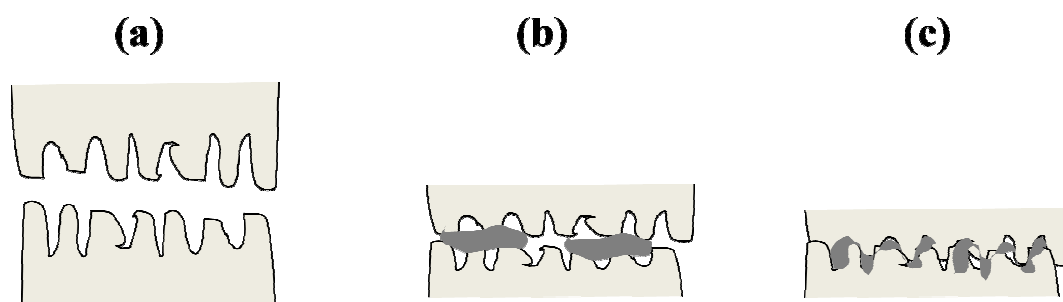
Figure 2.9: An illustration of the proposed compaction mechanism of MCC. **(a)** The particles are brought closer to each other by the effect of compression force. **(b)** A certain degree of plastic deformation occurs due to the presence of amorphous fraction (dark grey) within MCC particles which is deformable under pressure. **(c)** Particle's microfibrils intercalate with opposite channels of other particles.

The resultant strong contact between particles could possibly result in minimizing the stress relaxation experienced during compact release from the die. This hypothesis is supported by the following arguments: 1) Evidence obtained from AFM contact mode that intercalation is occurring between MCC-MCC (i.e. variation in adhesion force), AFM tapping mode (structural microfibrils and channels), SEM analysis of particles before and after tableting, roughness data for MCC obtained from AFM (which showed 3 times higher roughness compared to the other materials and was a further confirmation of the rugged microfibrillar nature of MCC). 2) Plasticity data for MCC (low mean yield pressure of 625 MPa using out-of-die Heckel profile)

indicating deformability largely due to the presence of amorphous fraction observed through XRD and DSC. The amorphous form contributes to plasticity as it is known to be deformable under pressure and less prone to fragmentation (Gonnissen et al., 2007).

2.3.2.2. D-mannitol fragmentation behaviour

D-mannitol is a widely used excipient in the development of ODT formulations as it offers a creamy mouthfeel upon disintegration of the tablet and a sweet taste (Yoshinari et al., 2003). Compared to MCC, D-mannitol has lower compactability when used in tablet formulations resulting in more friable tablets. This disadvantage of D-mannitol originates from fragmentation under pressure leading to the formation of weak compacts. Furthermore, our previous research suggested that the longitudinal/columnar shaped particles of D-mannitol (Figure 2.4 e) are implicated in its low compactability (Al-Khattawi et al., 2012). Heckel analysis was performed to check for the type of deformation mechanism derived from bulk tablet testing. The results showed a high value for mean yield pressure (Table 2.2) which indicates that densification of D-mannitol is more difficult to accomplish in comparison with other excipients such as MCC.

The mechanism of D-mannitol deformation under pressure was further studied using SEM (of powder and tablet) and AFM. SEM images of D-mannitol show a longitudinal particle with multiple surface crystallites and asperities (Figure 2.4 e). From Figure 2.4 e and f, it can be seen that D-mannitol did not retain its particle morphology and size (38 - 50 μm) after compression and that the tablet is composed of smaller particles/aggregates (approximately 5 – 10 μm). This is an indication of fragmentation which occurs by propagation of cracks in particles resulting in breakage and diminution of particle size by the effect of pressure.

To further support the fragmentation pattern, AFM topographical analysis was carried out which showed a considerable number of surface asperities that are susceptible to damage when minimal force is applied using the AFM cantilever (Figure 2.4 g and h). During tapping mode, some of the surface features shifted to other areas or fragmented into smaller pieces due to

movement of the scanning probe on the surface. This is a further confirmation of the brittleness of D-mannitol which supports the data of SEM as well as Heckel plot analysis. Moreover, the adhesion force and surface energy obtained for D-mannitol (31.88 ± 9.38 nN, 0.77 ± 0.23 mJ/m^2) were comparable to that of other fragmenting materials such as ibuprofen (24.45 ± 5.96 nN, 0.76 ± 0.18 mJ/m^2) discussed in section 2.3.2.3. This signifies the commonalities between fragmenting materials adhesion pattern which is low when compared to that of MCC and theophylline or their pair combinations.

D-mannitol exists as three polymorph modifications: I (also denoted β) thermodynamically stable crystal form which is monotropically related to mod II (also denoted α) while III (also denoted δ) is the metastable form that reverts to mod I or II upon heating. The compaction properties of the three modifications were reported by Burger et al. (2000) which showed differences in behaviour under pressure. It is useful to investigate whether the D-mannitol used in this research corresponds to any of these crystal forms and whether that has impacted the results outlined above. For this reason, DSC was used first to identify the polymorphic form of D-mannitol which presented a melting peak at 168.43 ± 0.06°C. This melting point indicates that the polymorphic form is either mod I or II as mod III has much lower melting point (Figure 2.10 b) (Burger et al., 2000). This was followed by comparison of FTIR spectra obtained for D-mannitol (Figure 2.11) with those of reference spectra from Burger et al. (2000). This showed that D-mannitol used in this investigation was mod I (The FTIR bands which are specific for Mod I polymorph are 1209, 1077, 1018, 959 and 929 cm^{-1}). The compactability of this polymorph was reported to be lowest compared to the other two forms and the diewall friction generated during compression was the highest (Yoshinari et al., 2003). This is in line with results obatined from AFM, SEM and Heckel plot which revealed fragmentation of the particles under pressure. Despite that, fragmentation could be argued to increase hardness by generation of new clean surfaces and more contact points as could be seen with lactose. However, fragmentation of mannitol leads to the generation of fine particulates leading to increased die wall friction and associated compaction issues (Yoshinari et al., 2003; Burger et

al., 2000). For this reason, D-mannitol is usually granulated to produce directly compressible grades with better compaction characteristics or by co-processing with adjuvants that mask the undesirable properties (Yoshinari et al., 2003; Soh et al., 2012).
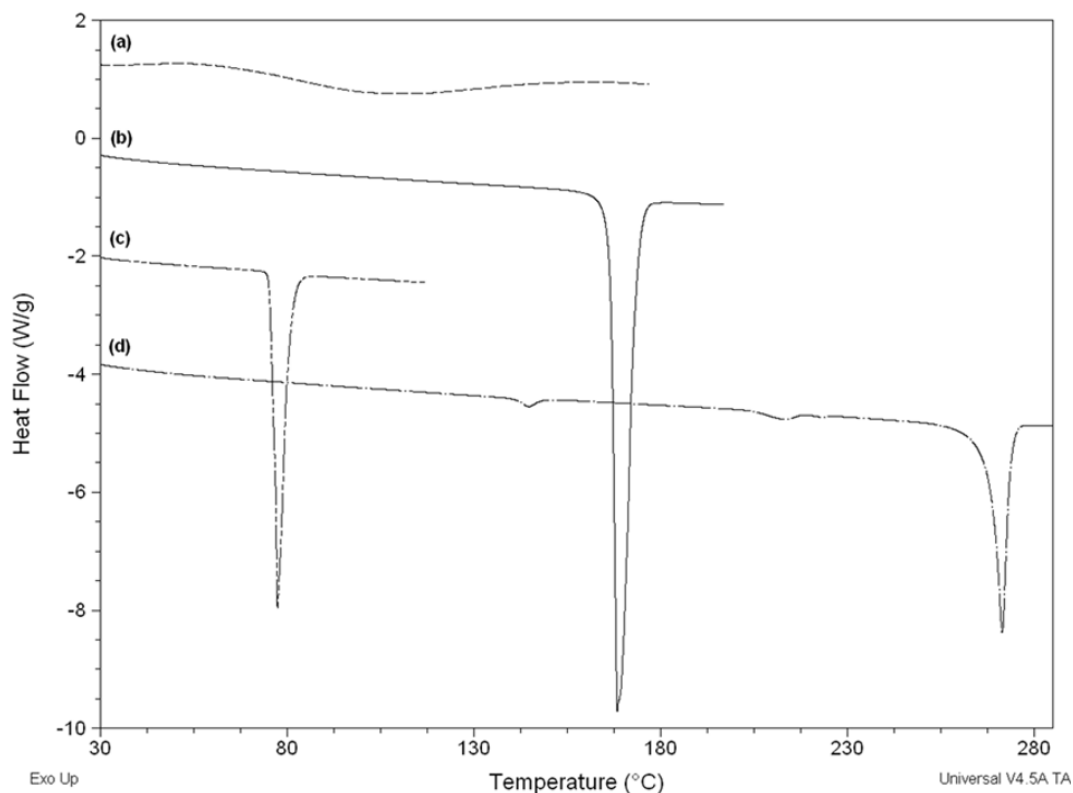
Figure 2.10: Overlaid DSC thermograms of (a) MCC (b) D-mannitol(c) ibuprofen and (d) theophylline. DSC thermograms are representative of triplicate measurements (n=3).
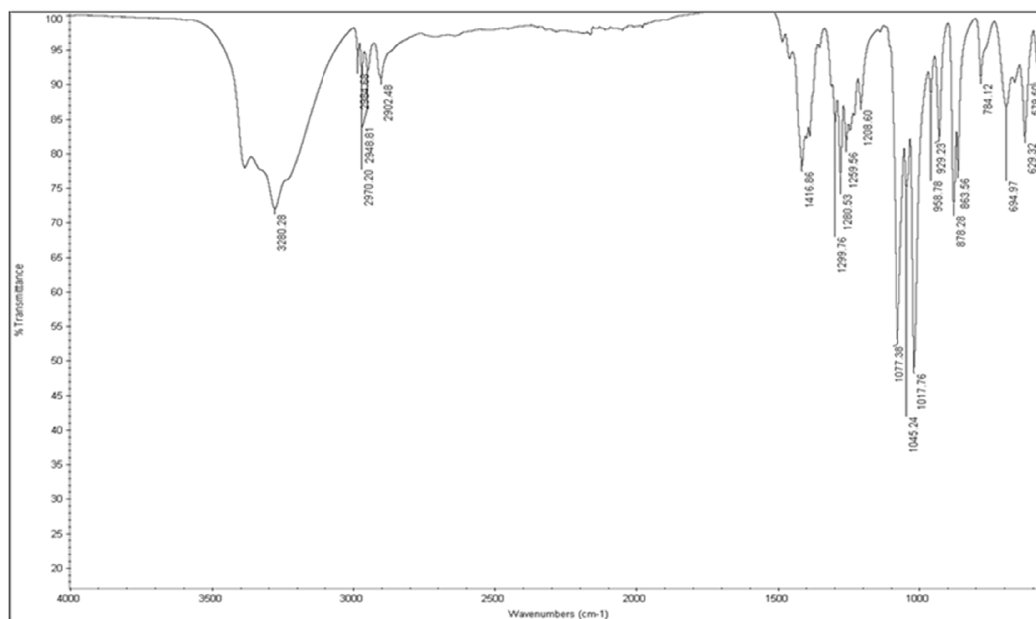
Figure 2.11: FTIR spectrum of D-mannitol. The bands 1209, 1077, 1018, 959 and 929 cm^{-1} were assigned for mod I polymorph of the excipient. The spectrum is representative of 16 scans per sample (n=3).

2.3.2.3. Ibuprofen physico-mechanical deformation

Ibuprofen is a widely used NSAID (Non-steroidal anti-inflammatory drug) which has inherent formulation difficulties such as poor compaction and low water solubility (Whelan et al., 2002). In the crystalline state it presents a sharp melting peak at 77.40 ± 0.08°C identified using DSC (Figure 2.10 c). Previous evidence showed that crystal habit modification has a great influence on the mechanical properties of ibuprofen although no enantiotropic polymorphs could be identified for the pure drug (Romero et al., 1993; Garekani et al., 2001). It was reported in a research by Nesic et al. (1990) that ibuprofen consolidates by brittle fracture/fragmentation and that plastic deformation is unlikely to occur. As a result, researchers have employed different approaches to improve the compaction properties of the drug including addition of binders or co-crystallisation with plastic deforming materials (Gohel et al., 2007).

To elucidate the densification mechanism, SEM and AFM were performed to analyse the exact cause of poor compaction. It is well recognized that particle shape affects mechanical properties of plastically deforming and not of fragmenting materials (Alderborn et al., 1988). However, from this work we found that particle shape potentially plays a role in densification of fragmenting materials. This conclusion arises from the fact that ibuprofen which is classified as a brittle material only undergoes fragmentation on the surface while bulk of particle is intact as noticed from SEM images before and after compaction (Figure 2.12 a and b).
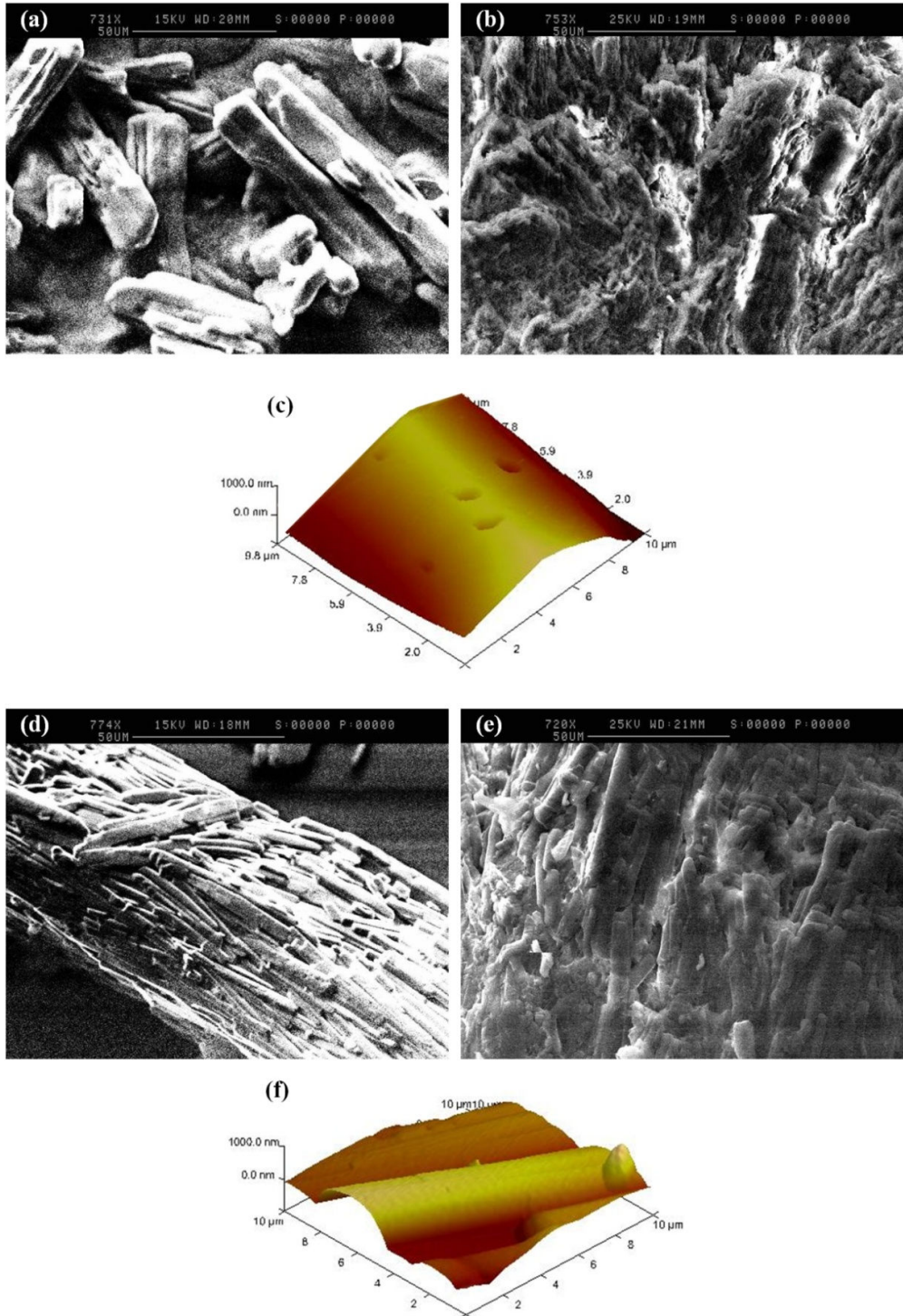
Figure 2.12: Micro and nano structural features of ibuprofen and theophylline from SEM and AFM.(a) and (b) are SEM images for ibuprofen powder (smooth) and tablet (surface fragmentation while particles still retain their elongated shape) respectively, (c) AFM image showing ibuprofen particle smooth surface although few dips can also be seen which might occurred due to surface fragmentation of the drug, (d) and (e) show SEM images for theophylline particle and theophylline tablet respectively (drug crystallites are compacted on each other in theophylline), (f) AFM topographical image showing theophylline surface crystallites. The crystallite in the middle of the image is cylindrical and has a smooth surface.

105

In accordance, analysis of ibuprofen topography exposed the presence of "pit-hole" like features on relatively smooth particle surface (Figure 2.12 c). These dips were formed due to indentation of the surface of ibuprofen by the cantilever during analysis especially the material suffers surface fragmentation as shown from the SEM images.

In 2002, Martino et al. affirmed that fragmentation contributes towards densification of ibuprofen, yet, it has a limited effect on tabletability and compressibility and is not the sole mechanism for densification. Furthermore, Marshall et al. (1993) had previously studied the effect of punch velocity on the densification mechanism of ibuprofen. The results of that study showed a compression-dwell time dependency relationship which is a characteristic of plastic deforming materials and not of fragmenting materials. The authors also suggested a mechanism involving a balance between plastic and elastic deformation during compression depending on tablets' axial recovery/velocity relationship.

Using AFM, when the surface of one ibuprofen particle was indented with another particle on the same region, a noticeable decrease in the adhesion force was firstly observed before reaching a constant value (Figure 2.13). The decrease in adhesion force between indentations 1-3 indicates that the surface of the particle is flattening under applied pressure leading to reduced adhesion force (from 55.9 - 29.2 nN). The deformation of ibuprofen surface is expected as the material showed fragmentation on the surface observed from the SEM image after compression compared to that before compression. As the surface indentation continued, constant adhesion force was obtained between 4-6 (28 - 27.4 nN) signifying that the probe has reached the dense core of the particle whereby no further flattening of surface occurs (i.e. no more propagation of fragmentation) and consequently a plateau was observed.
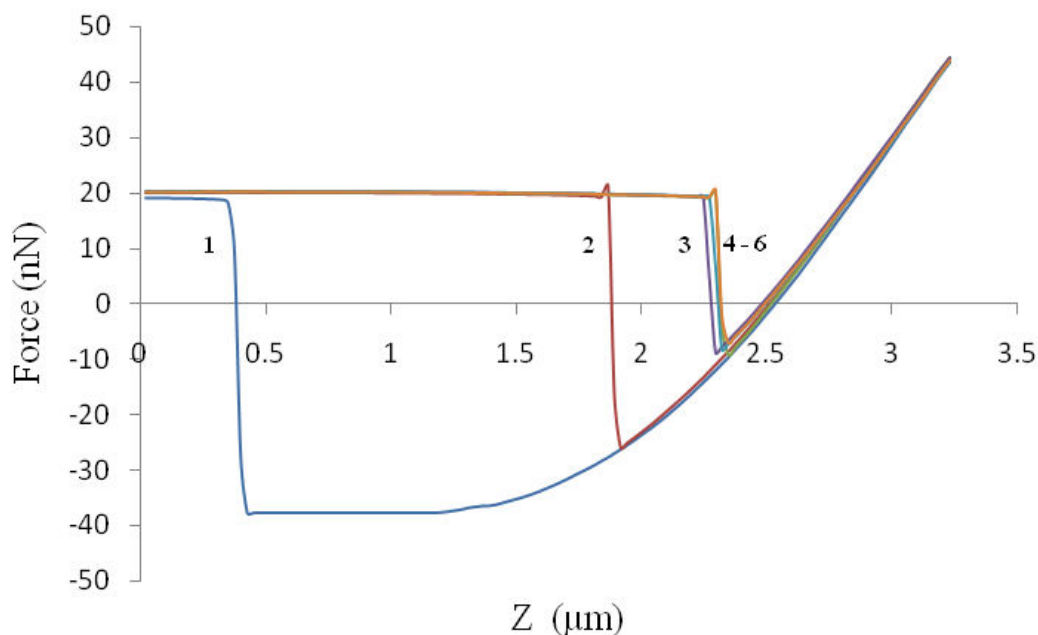
Figure 2.13: Changes in AFM adhesion force upon indentation of ibuprofen particle. The graph shows the retraction part of the curve used to obtain adhesion force. The force was decreased upon subsequent indentations (from 1 to 3) followed by a constant force indicated by the overlap at indentations 4 to 6. The approach curves are not shown for image clarity purposes.

In addition, the overall cohesion force (24.45 ± 5.96 nN) and surface energy (0.76 ± 0.18 mJ/m^2) obtained for ibuprofen-ibuprofen (Table 2.1) represents the fragmentation pattern of ibuprofen which is a proposed surface phenomenon that consequently results in lower adhesion at the interface between particles. Furthermore, SEM shows that the elongated nature of ibuprofen particle could still be seen after compression which suggests that the material has enough elastic property to retain the original elongated habit (Figure 2.12 b). Moreover, elongated particles were described previously to have poor compactability due to low interparticulate adhesion (Kaialy et al., 2010).

The densification of ibuprofen was not attributed to molecular forces i.e. due to physical bonding forces between particles as the adhesion curve was similar (shape and not magnitude of force) to that of a typical curve shown in Figure 2.1 a, which indicates no distinct attractive molecular forces between interacting ibuprofen particles. Additionally, the moisture content within ibuprofen is relatively low (0.41 ± 0.35%) which reduces the chances of formation of

liquid bridges between particles. Therefore, the mechanism of deformation of ibuprofen under pressure was identified based on AFM and SEM data. These showed that the drug undergoes physico-mechanical deformation rather than molecular based interactions and that fragmentation happened on the surface followed by elastic/plastic deformation of the core.

2.3.2.4. Theophylline molecular bonding mechanism

Theophylline is a bronchodilator which is highly water soluble and requires release modulation using sustained-release tablet formulation. The drug exhibits polymorphism and exists as theophylline monohydrate or three anhydrous forms. The polymorphic modification used in this investigation is anhydrous theophylline II. Although the drug particle is known to deform plastically under pressure, it was also reported that crushing strength of tablets containing theophylline with other excipients was low (Herting and Kleinebudde, 2007).

The AFM results (approach curve in Figure 2.14) showed that the drug particle which is attached on the AFM cantilever was pulled by an attractive force towards another theophylline particle from a vertical distance of approximately 3 μm. The attractive force caused the probe to 'snap' to the surface earlier than the expected time of contact in the absence of such force. This interesting jump-to-contact effect was also noticeable when theophylline adhesion was tested against MCC and D-mannitol (however, the distance for initiation of the pulling effect was less than 1 μm for both). The distance at which this effect commenced indicated that a long range distance force was involved in the pulling effect. The inter-atomic forces between the two particles are either van der Waals or electrostatic forces. The latter is the most likely force contributing to the jump-to-contact effect as the van der Waals forces are relatively weak forces and cannot contribute to the extent of bending of the AFM probe. Therefore, the unique intermolecular effect observed with theophylline was attributed to electrostatic forces which are, also, why this drug undergoes poor flowability during processing and tableting (Lam and Newton, 1992; Pather et al., 1998).
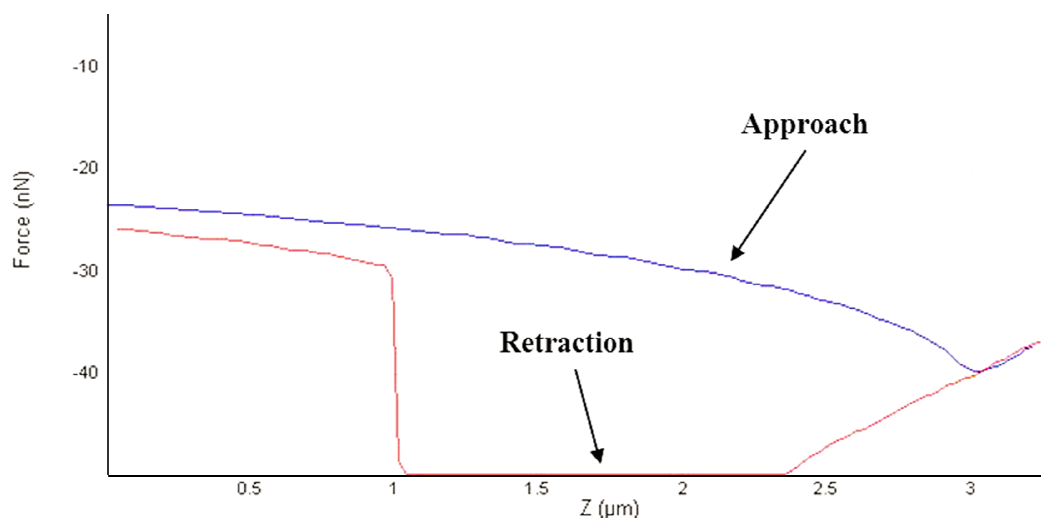
Figure 2.14: AFM force-distance curve for theophylline. The approach component shows a noticeable pulling effect (concave downward curve) due to significant electrostatic attraction before contacting the particle on the plate. The retraction component shows a flat part after initial retraction which represents a sticking effect of the probe particle to the particle on the plate. The last part of the retraction curve is snapping off of the particle probe to return to the original position (for comparison refer to Figure 2.1 a for a typical force-distance curve).

Another interesting observation was that theophylline developed an extraordinarily high cohesive force (136.33 ± 26.85 nN) and the highest interfacial energy (2.40 ± 0.53 mJ/m^2) when in contact with another theophylline particle. The two particles on the cantilever tip and on the plate adhered to each other and removal of the functionalised cantilever from the particle on the plate was very difficult. This resulted in a flat base of the retraction curve (due to cantilever reaching maximum deflection capacity) as could be seen in Figure 2.14. This effect is usually attributed to formation of immediate liquid bridges between particles or H-bonding. Anhydrous theophylline has very low moisture content ($0.22 \pm 0.04\%$) as shown from TGA analysis; however, this is not enough reason to exclude liquid bridges as the mechanism of adhesion between theophylline particles. An investigation of thermal events of theophylline using DSC showed the presence of water molecules bound to the drug with a small endothermic peak corresponding for monohydrate form at 213.27°C showing before the anhydrous theophylline melting peak at 270.71 ± 0.89°C (Figure 2.10 d). These results were in accordance with observations made by Suzuki et al. (1989) for thermal events of theophylline polymorphic

forms. In contrast to DSC results, FTIR analysis showed no signs of molecular water within theophylline as the monohydrate form usually shows a distinctive broad peak at 3341 cm^{-1} ascribed to stretching of the hydrogen bonded OH due to presence of water discussed by Seton et al. (2010).

H-bonding was excluded as the cause of adherence between theophylline particles as the hydrogen bonding investigation using FTIR showed no significant difference in intensity at the H-bonding area (3300 - 4000 cm^{-1}) of the spectra recorded for theophylline powder and tablets made at increasing compression forces (5 - 20 kN) (Figure 2.15).
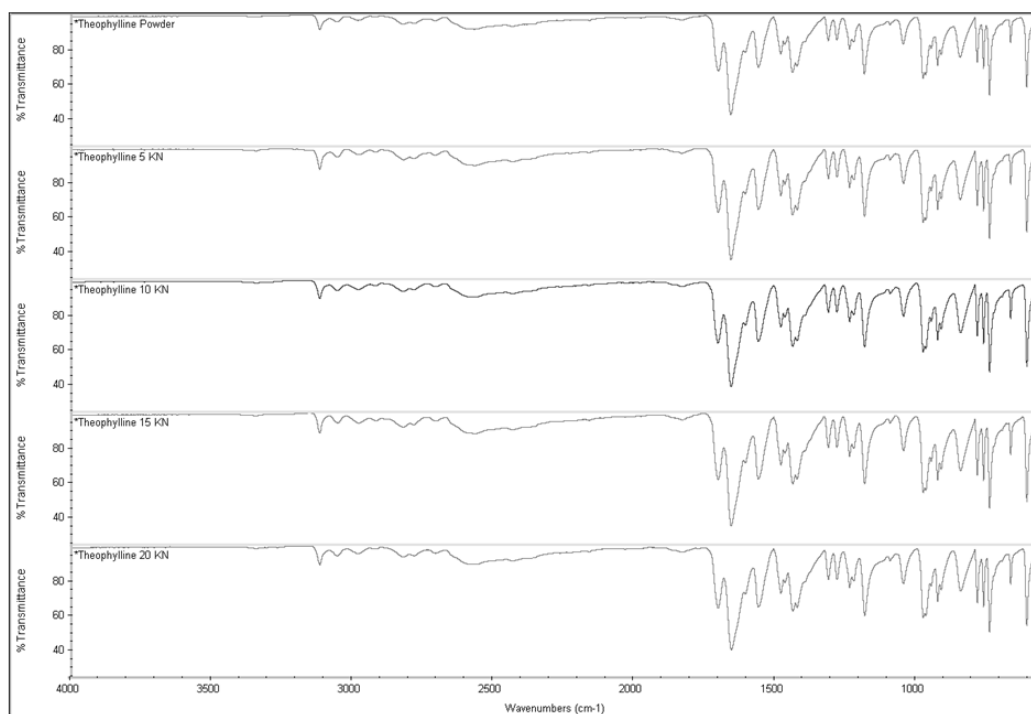
Figure 2.15: ATR-FTIR analysis of theophylline showing the spectra for powder and compacted tablets at increased compression forces (5 – 20 kN). The experimental procedure is the same used for H-bonding investigation of MCC in Figure 2.5. Each spectrum is representative of 16 scans per sample (n=3).

The overall evidence obtained from the above analytical techniques suggests that the adherence of theophylline particles to each other was facilitated by the hydrate form existing within theophylline particles.

AFM and SEM also showed that theophylline is composed of primary smooth surface crystallites (average roughness Ra is 321) that are bound together on a columnar shaped particle (Figure 2.12 d and f) (Suihko et al., 1997; Suihko et al., 2001). The smoothness eliminates the possibility of mechanical intercalation for the high cohesive force between theophylline molecules as intercalation usually happens between particles with irregular/rough asperities (example MCC-MCC).

On the other hand, SEM analysis of particles before and after tableting (Figure 2.12 d and e) showed that large theophylline particle breaks to form individual crystallites which can bond together by plastic deformation to form a strong tablet. The Heckel plot for theophylline (Figure 2.3) shows a profile similar to that of MCC which is representative of plastic deformation.

These findings were consistent with previous research by Picker (1999) suggesting that theophylline only partly fits the Heckel function because of particle fracture and low mean yield pressure. Similarly another research investigation also concluded that theophylline plastic deformation is caused by the slip planes of the drug crystal which are composed of hydrogen bonded columns that provide enhanced flexibility for slip during compaction (Chattoraj et al., 2010).

The cohesion force changes obtained from AFM contact mode analysis confirm the fracture pattern suggested for theophylline at the start of theophylline compression as the data showed a decrease in the force when multiple indentations of theophylline cantilever were carried out on another theophylline particle. From Figure 2.16, it can be seen that a decrease in the vertical (y-axis) component of the adhesion force graph occurred between indentations 1 and 3, however, indentation no. 5 produced a higher cohesive force due to slip of the fragmented surface crystallite.
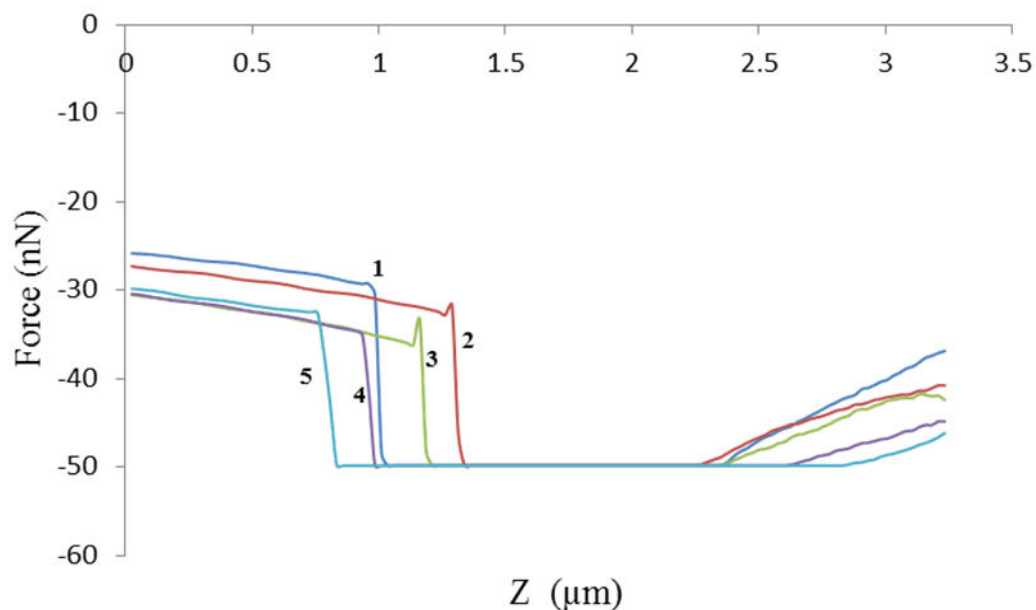
Figure 2.16: Changes in AFM adhesion force upon indentation of theophylline particle. The graph shows the retraction part of the curve used to obtain adhesion force. The force decreased upon subsequent indentations (from 1 to 4) followed by a little increase in force due to slippage of surface crystallite.

2.3.3. Binary and ternary mixtures of excipients and APIs

Pharmaceutical tablets often comprise multiple ingredients in the formulation. In general, very little is known about interparticulate interactions of different materials in tablets that cause mixtures to produce properties different to that of the original individual components (Busignies et al., 2006). AFM provides a valuable tool to understand interparticulate interactions between particles by measuring the adhesion/cohesion forces involved between different pairs of materials.

The AFM results showed that cohesive interaction of D-mannitol and that of MCC were not significantly different (t-test, $p > 0.05$). This could be due to the high standard deviation obtained for MCC (45.15 ± 23.65 nN) possibly due to irregular and rough topography of the excipient resulting in variability of inter-particle intercalation. However, the tabletability results of MCC and D-mannitol (Figure 2.17) showed different results to those observed from AFM as it can be

seen that MCC powder has much higher tabletability, i.e. capacity to transform into tablets, than

D-mannitol due to MCC ductility (Inghelbrecht and Remon, 1998).
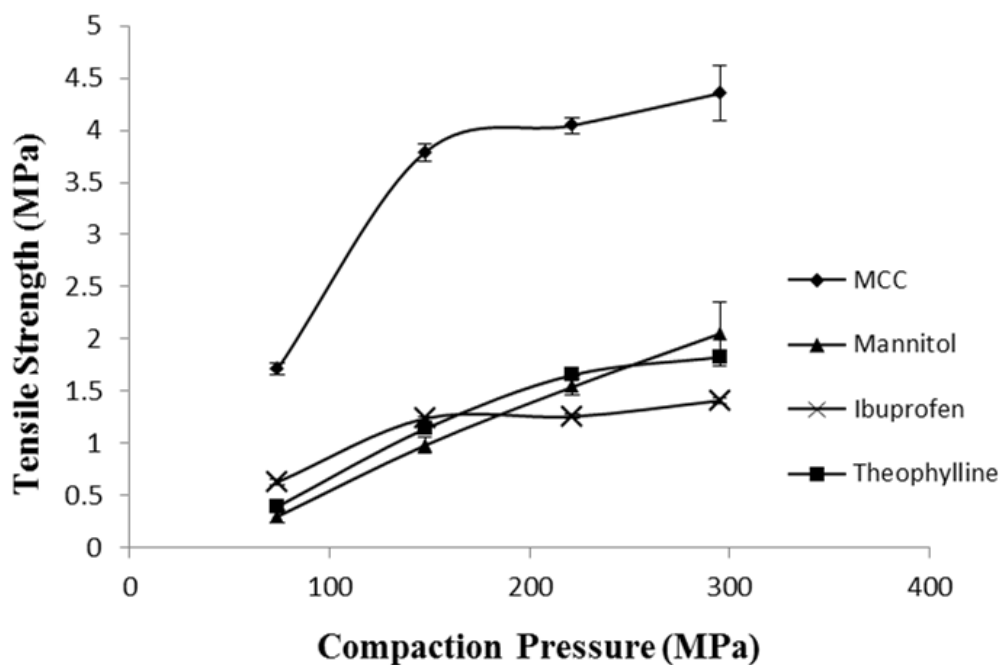
Figure 2.17: Tabletability profile for MCC, D-mannitol, ibuprofen and Theophylline. It represents the capacity of powders to form tablets. Each point represents mean ± SD (n=3).

Furthermore, the interaction of D-mannitol-MCC was low with an adhesion force of 11.22 ± 7.69 nN and surface energy of 0.27 ± 0.19 mJ/m^2 which results in less inter-particle bonding in the binary mixture containing 50% w/w of MCC with D-mannitol (49.5% w/w) compared to pure MCC tablets (Figure 2.18). This in turn led to the development of inter-particle pores which helped fast disintegration of tablets in addition to the intra particle pores within MCC particles. As can be seen from Figure 2.18, a tablet containing D-mannitol and MCC disintegrated faster (19.67 ± 2.52 sec) when the concentration of both excipients was equivalent indicating reduced bonding in tablet due to D-mannitol-MCC weak interaction. Furthermore, hardness of tablets was lowest when MCC concentration was reduced in the tablet as D-mannitol is not capable of forming strong compacts due to fragmentation. Nevertheless, when

the concentration of MCC was increased the hardness and disintegration time increased due to domination of MCC-MCC cohesive interaction (45.15 ± 23.65 nN, 1.39 ± 0.73 mJ/m^2).
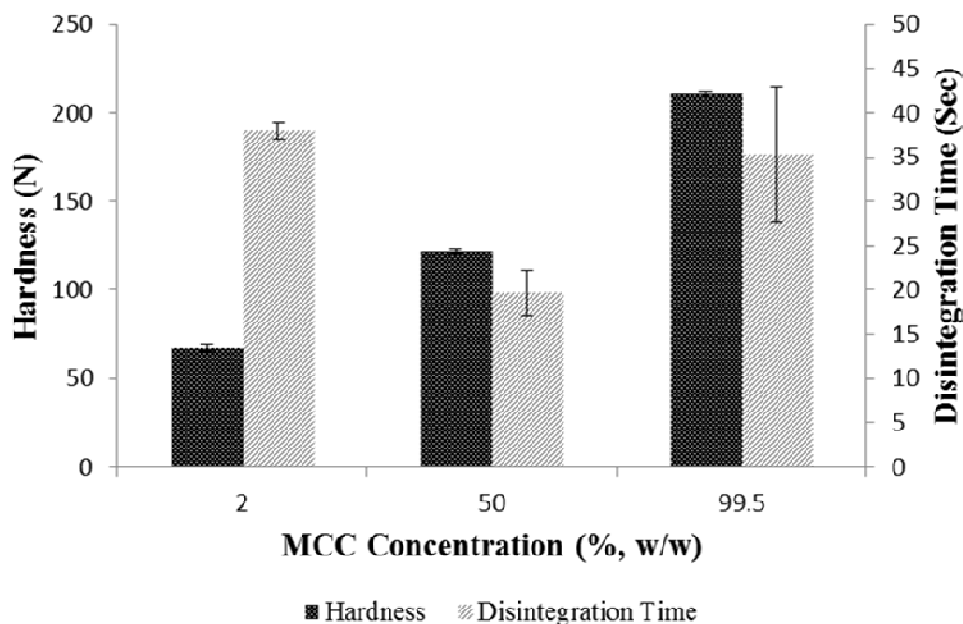
Figure 2.18: Effect of MCC concentration ($2 - 99.5\%$ w/w) on hardness and disintegration time of binary mixture tablets. Tablets were compressed at 20 kN compression force. Results reported as mean $\pm$ SD (n=3).

On the other hand, there was a general trend showing a difference in adhesion force and surface energy between ibuprofen or theophylline with MCC compared to D-mannitol. Statistical analysis showed that a significant difference (t-test, $p<0.05$) exists between D-mannitol-ibuprofen and MCC-ibuprofen. Similarly, there was a significant difference (t-test, $p<0.05$) between D-mannitol-theophylline and MCC-theophylline (Table 2.1). This signifies that D-mannitol and MCC have different bonding characteristics which results in higher adhesive forces for theophylline and ibuprofen when in contact with MCC compared to adhesion effect of the drugs with D-mannitol.

The results for hardness and disintegration time of tablets made from ternary mixtures of 50% w/w MCC, upon varying the concentration of D-mannitol, 1% w/w magnesium stearate and 10-40% w/w of either theophylline or ibuprofen showed that ibuprofen produced harder tablets

than theophylline whereas disintegration was faster for theophylline (Figure 2.19). The results of hardness did agree with the porosity data from Heckel profile (Figure 2.3) as ibuprofen showed better densification than theophylline at the different compaction pressures. In addition, upon increasing concentration of each of theophylline or ibuprofen, a significant increase (ANOVA/Tukey, $p<0.05$) in hardness was noticeable either because of increased cohesive bonding between ibuprofen-ibuprofen or theophylline-theophylline or due to bonding between each of the drugs with MCC. Surprisingly, the results of hardness did not correlate with the extraordinarily high adhesion force (136.34 ± 26.85 nN) and surface energy (2.40 ± 0.53 mJ/m^2) of theophylline observed from AFM. It could be that D-mannitol low hygroscopic character prevented the formation of liquid bridges when theophylline was used in low concentrations (10 - 30% w/w), therefore, no major change in hardness was observed at these levels (Figure 2.19). On the other hand, when D-mannitol was reduced to only 9% w/w, hardness of theophylline tablets increased significantly (ANOVA, $p<0.05$) because of increased availability of theophylline-theophylline liquid bridges. Theophylline tablets disintegrated faster than ibuprofen tablets due to their higher porosity and lower densification (Figure 2.3). Similarly, ibuprofen containing tablets were stronger as a result of fragmentation followed by plastic deformation where tablet strength increased with increasing drug concentration. This is in line with findings from Inghelbrecht and Remon (1998) who stated that highest ibuprofen concentrations result in increased hardness of ibuprofen and MCC tablet.
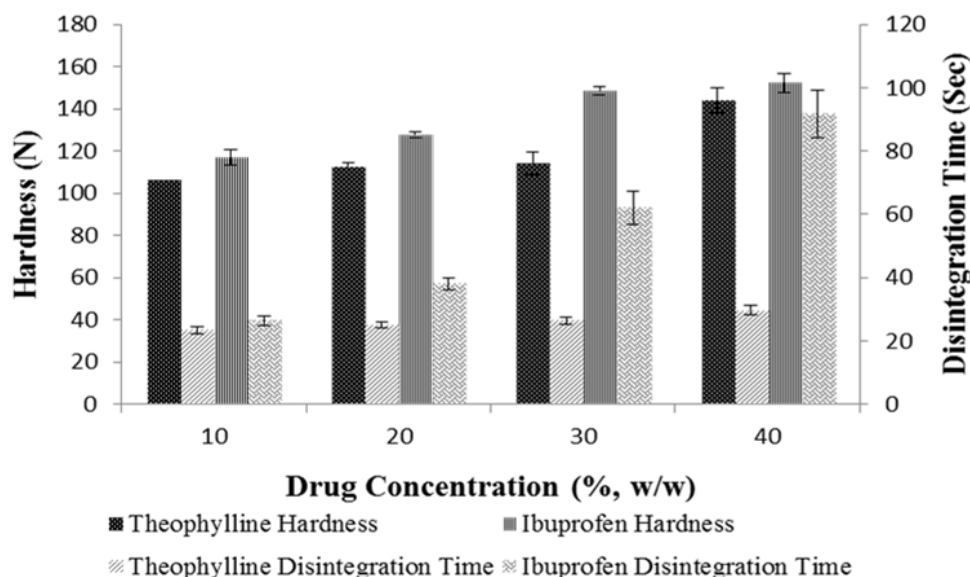
Figure 2.19: Comparison of hardness and disintegration time of ternary mixture tablets of theophylline and ibuprofen. Each drug was compressed with MCC (50% w/w), D-mannitol varying concentration and 0.5% w/w magnesium stearate. Results reported as mean ± SD (n=3).

2.4. Conclusion

The interpretation of tableting behaviour of excipients at the interparticulate level would enable the rational design of ODT formulations via understanding the main factors that contribute to high hardness and fast disintegration which in turn would significantly accelerate product development.

The investigation of few particles (less than 10 μg in total weight) using AFM provided a good approach for the determination of powder densification mechanisms when used alongside other investigative techniques such as SEM.

Flow properties of the materials were mainly dominated by the effect of particle size as well as adhesion profile. The results showed that only MCC exhibited good flow properties whereas the rest of the materials exhibited poor cohesive to very poor flow behaviour.

The high strength of MCC during tableting was suggested to occur as a result of a number of factors acting together. These factors were the high roughness (3 times more than the other

materials investigated), plastic deformation (low Py of 625 MPa), amorphous fraction (30%, Tg at 67.63°C) and intercalation of particle's microfibrils with channels of other particles.

For D-mannitol, the topographic and nano/micro profiling of particles confirmed the fragmentation behaviour of this excipient under pressure. The surface of mannitol was very fragile that asperities were fragmenting and shifting upon even slight movement of the AFM tip.

D-mannitol and MCC showed different bonding characteristics in binary mixtures with APIs. The adhesive forces for theophylline and ibuprofen with MCC were higher than the adhesive forces of the APIs with D-mannitol. This was attributed to the ability of MCC to generate strong bonds with materials due to the mechanism mentioned earlier whereas mannitol fragments and has less binding capacity with other materials.

The preformulation studies carried out in this chapter helped unveil the fundamental mechanisms for functionality of ODT excipients. These results and others from literature formed the scientific basis for carrying out formulation work in the next chapters.

Chapter 3

Development of a Compressed ODT Base

Publications relating to chapter 3

Ali Al-Khattawi, Affiong Iyire, Tom Dennison, Eman Dahmash, Clifford J Bailey, Julian Smith, Chris Martin, Peter Rue and Afzal R Mohammed (2014) Systematic Screening of Compressed ODT Excipients: Cellulosic Versus Non-Cellulosic. *Current Drug Delivery*, 11(4):486-500.

Ali Al-Khattawi, Ahmad Aly, Yvonne Perrie, Peter Rue and Afzal R Mohammed (2012) Multi Stage Strategy to Reduce Friability of Directly Compressed Orally Disintegrating Tablets. *Drug Delivery Letters*, 2(3): 195-201.

3.1. Introduction

Despite the growing popularity and success of ODTs over the last decade, many challenges are still facing the development of these tablets. Firstly, some of the main technologies used to fabricate ODTs (such as freeze drying) produce tablets that disintegrate rapidly yet, they are soft and require expensive peel-off blister packaging (Figure 3.1).
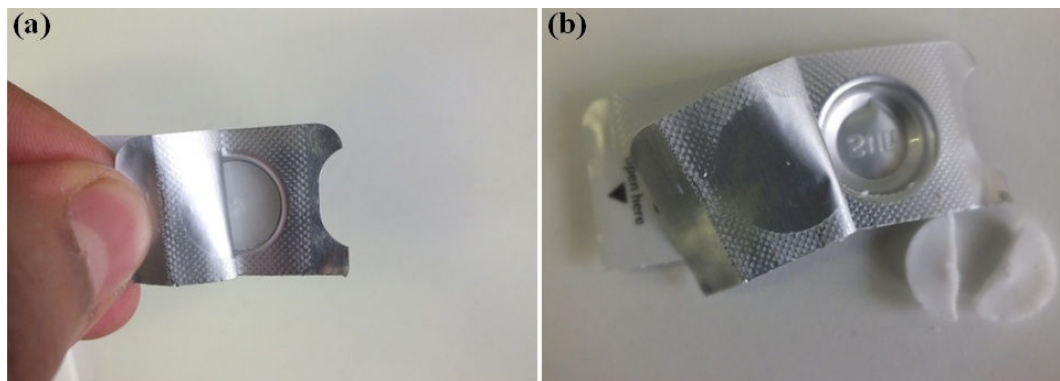
Figure 3.1: Peel-off packaging used for freeze dried ODTs. (a) Shows the intricate mechanism for opening the packaging, (b) shows the weak ODT breaking easily upon opening the packaging.

Secondly, it has never been more important for pharmaceutical companies to find new technologies which are cost-effective and scalable especially because the current processes are time consuming and require the use of special equipments (Sunada and Bi, 2002). For instance, freeze drying of ODTs results in highly porous tablets, due to ice sublimation (Seager, 1998), which in turn have very low mechanical strength (<10 N hardness).

The work in this chapter aims to develop ODTs using a cost-effective direct compression methodology that can be integrated within a conventional tableting plant (Shu et al., 2002). This can also introduce more cost-savings as only standard packaging (blister or bottle) is required for ODTs produced by direct compression.

- The study involves the development of a directly compressible ODT blend (placebo) that has the ability to disintegrate in a matter of seconds (< 30 sec) while retaining good mechanical strength (Hardness > 60 N).

- Dual functional (binder/disintegrant) excipients HPMC and L-HPC were utilised in addition to mannitol as the ODT diluent and magnesium stearate as the lubricant.

- Formulation and process optimization were carried out to assess the optimum levels of excipients and compression forces to develop a successful formulation.

- Further investigation was carried out into the effect of particle size of excipients and different processed mannitol grades on the final ODT properties.

- This was followed by testing the formulated blend and tablets for physico-chemical and mechanical stability over 6 months according to ICH guidelines (ICH, 2003).

3.2. Materials and methods

3.2.1. Materials

D-mannitol and magnesium stearate were purchased from Sigma-Aldrich (Pool, UK). Hydroxypropyl methyl cellulose (HPMC) grade K100M was obtained from Colorcon Ltd. (Kent, UK). Low-substituted hydroxypropyl cellulose (L-HPC) grade NBD-022 was obtained from Shin-Etsu (Tokyo, Japan). Mannitol grades: Mannogem granular (granular), Mannogem AG (Agglomerated) and Mannnogem EZ (spray dried) were obtained from SPI Pharma (Wilmington, USA).

3.2.2. Methods

3.2.2.1. Formulation of tablets to investigate the influence of compression force on tablet properties

2% w/w of HPMC (binder) and 97.6% w/w of mannitol (diluent) were blended using mortar and pestle for 5 min before blending for another 1 min with 0.4% w/w magnesium stearate

(lubricant). The mixture was used to prepare 500 mg flat-faced tablets (13 mm in diameter) using hydraulic tablet press from Specac (Slough, UK). Tablets were compressed between 7 - 40 kN using a dwell time of 1 min to observe the effect of compression force on tablet's hardness, disintegration time and porosity.

3.2.2.2. Formulation of tablets to investigate the influence of binder concentration on tablet properties

HPMC (2-10% w/w) was blended with mannitol (97.6-89.6% w/w) for 5 min using mortar and pestle, followed by blending with magnesium stearate (0.4% w/w) for 1 min. Each powder blend (20 g) was assessed for powder flow properties by measuring the angle of repose and bulk/tapped densities. Same powders were used to prepare two batches of 500 mg tablets (13 mm in diameter) using the hydraulic tablet press. The first batch of tablets was prepared at 15 kN and tested for hardness, disintegration time, porosity and friability. The second batch of tablets was prepared at 30 kN.

3.2.2.3. Formulation of tablets to investigate the influence of a second binder on friability

L-HPC at 0.5 - 2.5% w/w was blended using mortar and pestle with a fixed amount of HPMC (2% w/w) and varying amounts of mannitol (reduced accordingly to 97.1 - 95.1% w/w) for 5 min. Magnesium stearate (0.4% w/w) was added and blending continued for further 1 min. Tablets were prepared (500 mg, 13 mm in diameter) using hydraulic tablet press at a compression force of 15 kN. The tablets were tested for hardness, disintegration time, porosity and friability. From these formulations, 2% w/w L-HPC, 2% w/w HPMC, 95.6% w/w mannitol and 0.4% w/w magnesium stearate formulation was taken forward where compression forces of 15 - 40 kN were used to prepare 500 mg tablets. A control formulation (without HPMC) comprising 2% w/w L-HPC blended with 97.6% w/w mannitol for 5 min, and with 0.4% w/w magnesium stearate for 1 min was made into 500 mg tablets at compression forces 15 - 40 kN. Hardness, disintegration time and friability of the dual binders' formulation (HPMC and L-

HPC) were compared to the single binder formulation (L-HPC) over the compression forces specified.

3.2.2.4. Formulation of tablets to investigate the influence of particle size on friability

Powders of mannitol, HPMC and L-HPC were sieved into fractions according to their particle size distribution. Fractions of fine powders of 95.6% w/w mannitol, 2% w/w HPMC and 2% w/w L-HPC were blended for 5 min using mortar and pestle followed by blending with 0.4% w/w magnesium stearate for 1 min. Similarly, coarse fractions of 95.6% w/w mannitol, 2% w/w HPMC and 2% w/w L-HPC were blended for 5 min using mortar and pestle followed by blending with 0.4% w/w magnesium stearate for 1 min. Tablets (500 mg, 13 mm in diameter) were prepared from the coarse and fine blends at 40 kN using hydraulic tablet press and tested for friability.

3.2.2.5. Formulation of tablets to investigate the use of processed mannitol grades

Three grades of commercial mannitol Mannogem Granular (granular), Mannogem AG (agglomerated) and Mannogem EZ (spray dried) (at a concentration of 95.6% w/w each) were blended separately with 2% w/w HPMC and 2% w/w L-HPC for 5 min followed by blending with 0.4% w/w magnesium stearate for 1 min. Tablets (500 mg, 13 mm in diameter) were prepared at compression forces from 15 to 25 kN using single station automatic tablet press (Minipress) from Riva (Aldershot, UK) then tested for hardness, disintegration time and friability. This was followed by testing the effect of magnesium stearate concentration on tablet (500 mg, 13 mm in diameter prepared at 15 - 25 kN) hardness, disintegration and friability by increasing the concentration of magnesium stearate to 1% w/w while reducing the concentration of mannitol (Mannogem Granular) to 95% w/w and keeping a fixed concentration of HPMC and L-HPC (2% w/w each). Finally, formulations of 50:50, 60:40 and 70:30 granular: powder mannitol (95% w/w) were blended with 2% w/w HPMC and 2% w/w L-HPC for 5 min, followed by blending with 1% w/w magnesium stearate for 1 min. Tablets were made at

compression forces between 15 - 25 kN using the automatic tablet press followed by testing for hardness, disintegration time and friability.

3.2.2.6. Stability studies

Powder samples of optimized blend (70:30 granular: powder constituting 95% w/w alongside 2% w/w HPMC, 2% w/w L-HPC, 1% w/w magnesium stearate) and placebo tablets (same blend composition compressed at 16-17 kN) were tested over 6 months. All samples were incubated in Firlabo SP-BVEHF stability cabinets (Meyzieu, France) at long term (25°C ± 2°C/60% RH ± 5% RH) and accelerated stability (40°C ± 2°C/75% RH ± 5% RH) conditions recommended by ICH Q1A(R2) (ICH, 2003). Samples were monitored at day 0, 14, 30, 60, 90, 120, 150 and 180 by analysing tablets hardness, disintegration time, friability, moisture content (after crushing) and visual inspection. Powder samples were monitored for moisture content using moisture balance, thermal properties using DSC, chemical change using FTIR and visually inspected for any discoloration. Tablets were packed in amber plastic laminate blisters compliant with USP requirements and sealed using foam and roller. Powders were stored in dark conditions using plastic bottles double wrapped with parafilm.

3.2.3.   Assessment of powder flow properties by measurement of angle of repose

The angle of repose measurement was performed using the recommended British Pharmacopeia procedure (British Pharmacopeia Commission, 2012). A powder of approximately 20 g was poured through a funnel into a base free from vibration to form a pile. The funnel was positioned 2 - 4 cm from the top of the powder pile as it was forming. Angle of repose was determined by measuring the height of the pile (h) and diameter of the base (d) then angle of repose (α) was calculated from the equation:

$$\tan \alpha = h \div (0.5 \times d)$$

3.2.4. Assessment of powder flow properties by measurement of bulk and tapped densities

A sample (20 g) of powder was poured into 250 mL volumetric cylinder, initial (bulk) volume was recorded then tapping was carried out sequentially at 5, 10, 500 and 1250 taps until no further change in volume occurred. Bulk density was calculated from the equation: Bulk density = mass of powder/bulk volume while tapped density was calculated from the equation: tapped density = mass of powder / volume of tapped powder. Powder flow properties were assessed based on the values obtained from powder flow indices Carr's Index and Hausner Ratio which were calculated using the following equations (Carr, 1965; Hausner, 1967):

$$\text{Carr}'s \text{ index} = \frac{(\text{Tapped density} - \text{Bulk density})}{\text{Tapped density}} \times 100$$

$$\text{Hausner ratio} = \frac{\text{Tapped density}}{\text{Bulk density}}$$

3.2.5. Tablet hardness

Diametral crushing strength of tablets was measured immediately after compression using 4M tablet hardness tester from Schleuniger (Thun, Switzerland). Tensile strength was calculated using the equation: $\sigma = 2 \times \text{Hardness} / (\pi \times d \times h)$, where σ is the tensile strength, d is the diameter of tablet and h is the tablet thickness.

3.2.6. Tablet disintegration

The disintegration time was determined using the USP moving basket apparatus (USP Convention, 2005). Disintegration test apparatus used was ZT3 from Erweka (Heusenstamm, Germany). A tablet was placed in the disintegration basket (without using a disk) which was raised and lowered at a constant frequency of 30 cycles/min in the disintegration medium. Distilled water (800 mL) maintained at 37°C was used as the medium of disintegration while disintegration time was recorded for one tablet at a time to improve accuracy of recording. Time

of disintegration was recorded when all the disintegrated fractions of tablet passed through the mesh of disintegration basket.

3.2.7. Tablet friability

Friability test was carried out for 8 tablets using friabilator from J. Engelsmann AG (Ludwigshafen, Germany). The procedure involved rotating the drum at 25 rpm for 4 min or 100 revolutions. Each tablet was dedusted carefully before and after the test to remove loose powder. Friability was calculated as percentage loss (%) from original tablets' weight.

3.2.8. Tablet porosity

Tablet porosity was measured using helium multipycnometer from Quantachrome Instruments (Syosset, USA). One tablet was placed in a micro sample cell of the instrument and the true volume V_t was obtained using the equation:

$$V_t = V_C - V_R(P1/P2 - 1)$$

Where V_t is true volume of the sample, V_C is volume of the sample cell, V_R is the known reference volume, P1 is atmospheric pressure and P2 is pressure change during determination. V_t was used to calculate the true density of the tablet by weighing the tablet and substituting the values into:

$$\text{True density} = \text{Weight of tablet/True volume}$$

Porosity (ε) was calculated using the equation:

$$\varepsilon = 1 - (\text{Bulk density/True density})$$

Bulk density was acquired from:

$$\text{Bulk density} = \text{Weight of tablet/Bulk volume}$$

Bulk volume was obtained by measuring the radius (r) and thickness (h) of the tablet using a digital calliper and substituting in the equation for volume of a flat-faced tablet:

$$V = \pi \times r^2 \times h$$

3.2.9. Particle size analysis and separation

Particle size distribution was measured by laser diffraction using particle size analyzer HELOS/BR and dry disperser RODOS with feeder VIBRI/L from Sympatec (Clausthal-Zellerfeld, Germany). The measuring range of the lens was 0 - 175 µm. Approximately 2 g of each powder was placed in the feeder tray and the run started at trigger condition of 2% Copt (optical concentration) for 10 sec with powder dispensing pressure of 3 bar. Volume mean diameter (VMD) was recorded for all powders.

Particle size distribution was also performed using AS 200 mechanical sieves from Retsch (Haan, Germany). A nest of sieves with aperture sizes 355, 250, 125, 90, 75, 63 and 53 µm was stacked upon a collecting pan. The sieves were vibrated at amplitude of 60 for 10 min. Fractions of sieved powders were collected and weighed followed by plotting weight-size distribution curves.

3.2.10. Scanning electron microscopy (SEM)

HPMC powder morphology was examined by scanning electron microscope (SEM) Stereoscan 90 from Cambridge Instruments (Crawley, UK). Approximately 1 mg of HPMC was placed onto a double-sided adhesive strip on an aluminium stub. The specimen stub was coated with a thin layer of gold using a sputter coater Polaron SC500 from Polaron Equipment ltd. (Watford, UK) at 20 mA for 3 min followed by sample examination using SEM. The acceleration voltage (kV) and the magnification can be seen on each micrograph.

3.2.11. Differential scanning calorimetry (DSC)

DSC Q 200, from TA Instruments (Delaware, USA) was used to determine the thermal properties of powders. Accurately weighed sample (3 mg) of optimized blend was transferred into non-hermetically sealed standard aluminium pans and heated in the range of 30–200°C at a rate of 10°C/min under a 50 mL/min nitrogen purge. This was followed by analysis of resulting graphs for melting onset and enthalpy of fusion using TA instruments universal analysis 2000 software (V 4.5A).

3.2.12. Fourier transform infrared spectroscopy (FTIR)

FTIR spectra for excipients and optimized blend were collected in the region of 400-4000 cm^{-1} using Nicolet IS5 FTIR spectrometer equipped with an iD5 attenuated total reflectance (ATR) diamond from Thermo Fisher Scientific (Massachusetts, USA). Approximately 50 mg of each powder was placed on the diamond plate followed by 16 scans /sample (n=3).

3.2.13. Statistical analysis

Student t-test and analysis of variance (ANOVA) followed by post-hoc multiple comparison test (Tukey) were carried out using GraphPad Prism 6.02 software (California, USA). A combination of ANOVA and regression analysis was also used for analysis of stability data. Statistical significance was considered at $p < 0.05$. Where applicable, all results are presented as mean ± SD to account for the noise encountered within the experiments.

3.3. Results and discussion

3.3.1. Influence of compression force on tablet properties

Compression force is the most important process parameter during manufacture of tablets as an increase in compression force is usually accompanied by increase in tensile strength (hardness) of tablets (Sinka et al., 2009). The hardness of tablets made from mannitol (97.6% w/w), HPMC

(2% w/w) and magnesium stearate (0.4% w/w) increased between 6.33 ± 1.15 and 139.33 ± 2.52 N when the compression force was increased between 7 and 40 kN (Figure 3.2). Disintegration time increased slightly when compression forces below 20 kN were used, however, 40 kN produced tablets that disintegrated at significantly (t-test, $p < 0.001$) longer time (Figure 3.3).
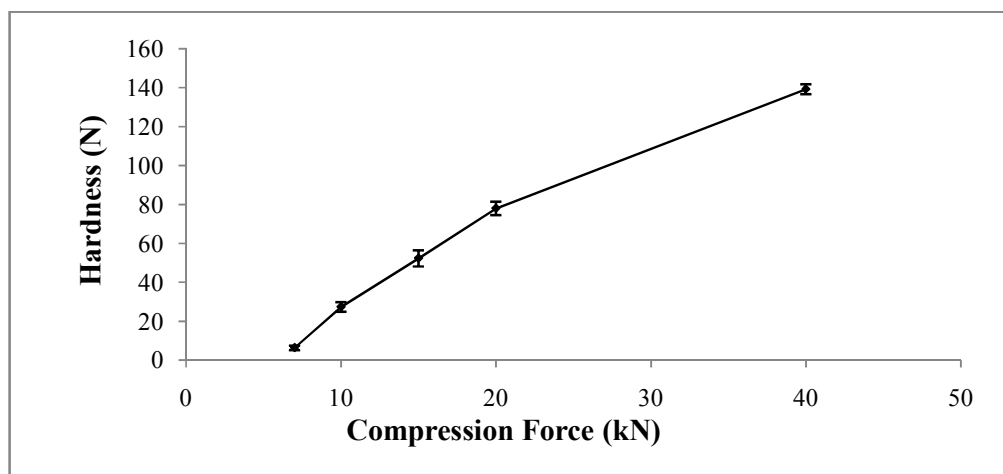
Figure 3.2: Hardness profile of tablets prepared at compression forces between 7 and 40 kN. Tablets (500 mg) contain 2% w/w HPMC, 97.6% w/w mannitol and 0.4% w/w magnesium stearate. Each point represents mean $\pm$ SD (n=3).
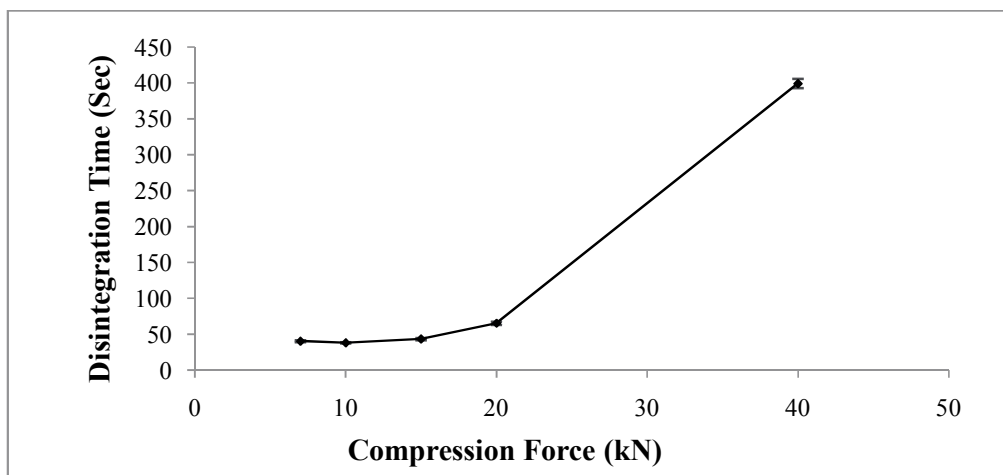
Figure 3.3: Disintegration profile of tablets prepared at compression forces between 7 and 40 kN. Tablets (500 mg) contain 2% w/w HPMC, 97.6% w/w mannitol and 0.4% w/w magnesium stearate Each point represents mean $\pm$ SD (n=3).

Hardness and disintegration were both affected by the increase in compression force possibly as a result of densification of powder bed and particulate deformation by fragmentation of mannitol (discussed in Chapter 2 section 2.3.2.2) and plastic deformation of HPMC (Tatavarti et al., 2008). Factors controlling the type of densification process may include the size and shape of particles as well as their crystal structure (Brittain, 1995). A tabletability profile of the mixture of mannitol, HPMC and magnesium stearate was established by plotting tensile strength of tablets vs. compaction pressure. Tabletability is an important indicator of the powder capacity to be transformed into a tablet of specified strength under the effect of compaction pressure (Sun and Grant, 2001). The results (Figure 3.4) for the blend comprising mannitol (97.6% w/w), HPMC (2% w/w) and magnesium stearate (0.4% w/w) showed a lower tabletability when compared to lactose, which is a common diluent used in the manufacture of conventional tablets (tabletability of lactose by Tye et al. (2004), tensile strength range of 0.1 - 3.5 MPa).
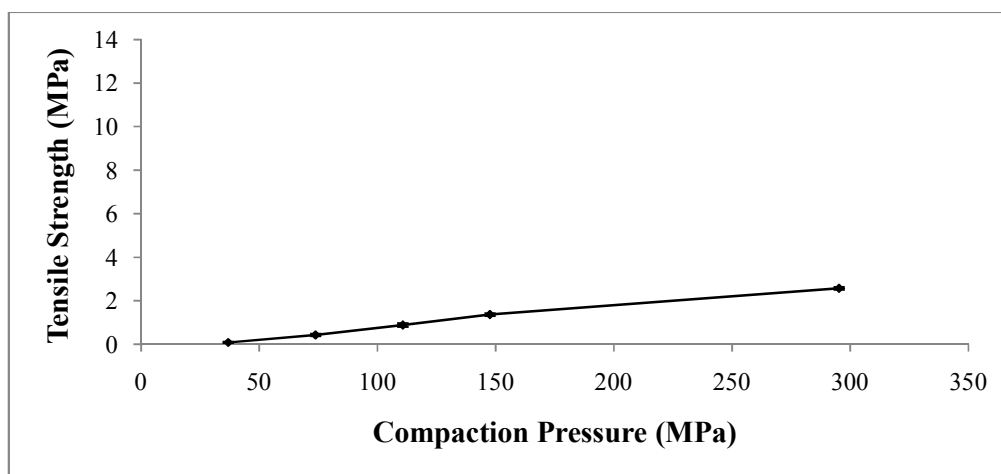
Figure 3.4: Tabletability profile for blend of 2% w/w HPMC, 97.6% w/w mannitol and 0.4% w/w magnesium stearate using hydraulic tablet press. Each point represents mean ± SD (n=3).

The porosity of tablets was measured, followed by plotting compressibility and compactability graphs, to understand the densification mechanism of particles. Compressibility is defined as the ability of a material to undergo reduction in volume as a result of applied pressure while

compactability is the ability of a material to produce tablets with sufficient strength under the effect of densification (Sun and Grant, 2001). The compressibility results (Figure 3.5) were consistent with hardness and disintegration results as the increase in compaction pressure caused a significant decrease in porosity (ANOVA, $p<0.05$) suggesting powder densification and reduction of pores in the formed compacts. The densification resulted in possibly greater bonding and harder tablets while disintegration time was prolonged as the reduction of pores reduces the ability for water to penetrate the tablet.
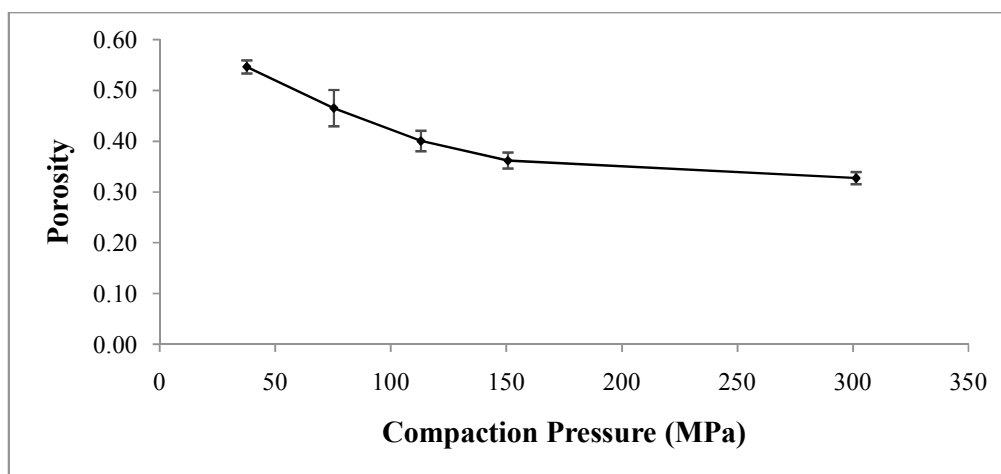
Figure 3.5: Compressibility profile showing the extent of porosity reduction under pressure for blend of 2% w/w HPMC, 97.6% w/w mannitol and 0.4% w/w magnesium stearate using hydraulic tablet press. Each point represents mean ± SD (n=3).

Compactability (Figure 3.6) and tablet thickness data (Table 3.1) showed that increasing the compaction force (and accordingly tensile strength of tablets) resulted in a decrease in porosity. Furthermore, only a slight decrease in porosity and thickness of tablets occurred upon increasing compression force from 30-40 kN (225 - 300 MPa) due to maximum compactability. Hence, any further increase in the tablet's tensile strength would not result in a significant decrease in porosity.
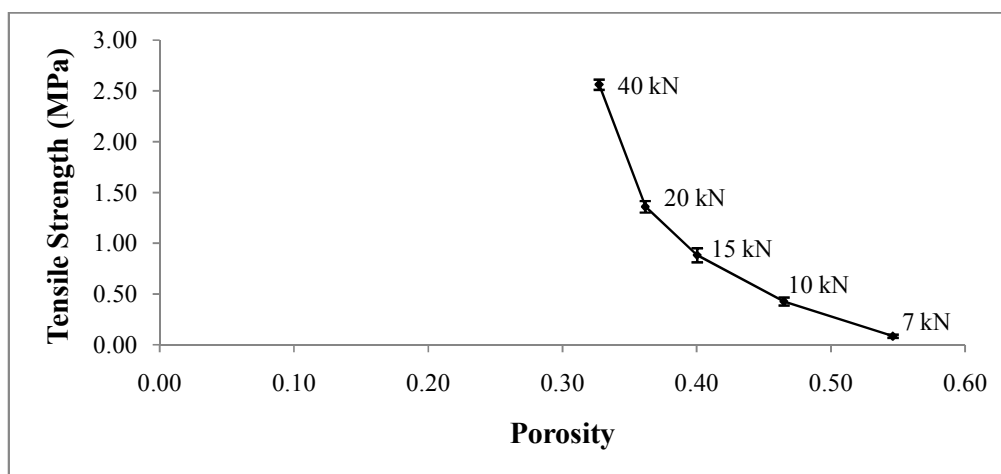
Figure 3.6: Compactability profile showing the ability of a blend of 2% w/w HPMC, 97.6% w/w mannitol and 0.4% w/w magnesium stearate to produce tablets with sufficient strength under the effect of densification. Hydraulic tablet press was used to establish the profile. Each point represents mean ± SD (n=3).

Table 3.1: Tablet porosity and thickness changes under influence of compaction pressure (37.67 – 301.36 MPa) using hydraulic tablet press. Blend composed of 2% w/w HPMC, 97.6% w/w mannitol and 0.4% w/w magnesium stearate. Results reported as mean ± SD (n=3).

Compaction Pressure (MPa)	Porosity	Tablet Thickness (mm)
37.67	0.55 ± 0.01	3.68 ± 0.02
75.34	0.46 ± 0.04	3.15 ± 0.02
113.01	0.40 ± 0.02	2.92 ± 0.01
150.68	0.36 ± 0.02	2.82 ± 0.01
301.36	0.33 ± 0.01	2.67 ± 0.01

Overall, the powder blend comprising 2% w/w HPMC, 97.6% w/w mannitol and 0.4% w/w magnesium stearate showed a slightly lower tabletability (tensile strength, 0.1 - 2.2 MPa) than lactose (tensile strength, 0.1 - 3.5 MPa), higher porosity (0.33 - 0.55) than microcrystalline cellulose (0.09 - 0.28) even at high compression forces, while compactability was lower than that of lactose and microcrystalline cellulose (tabletability, compressibility and compactability data for lactose and MCC by Tye et al. (2005)). Although tablets retained high porosity which is important to enhance water penetration and disintegration of tablets, their tensile strength was

insufficient. 15 kN was chosen as the compression force to be used in the next experiment as it showed a balance between hardness of 52.33 ± 4.16 N and a disintegration time of 43 ± 1.53 sec. The other compression forces used were either accompanied by low hardness (27.33 ± 2.52 N at 10 kN) or long disintegration time (65.33 ± 2.31 sec at 20 kN) which are not desirable properties for an ODT according to US FDA (FDA CDER, 2008). The tablet properties could be enhanced further by optimisation of binder (HPMC) quantity which was carried out in the following stage.

3.3.2. Effect of binder (HPMC) concentration on powder flow and tablet properties

Flow properties were assessed before the tableting was carried out for the different HPMC concentrations (2-10% w/w). Good flow properties are a prerequisite for the successful manufacturing of tablets as it affects blending, content uniformity, tablet compression and scale-up operations (Sarraguca et al, 2010). Powder flow properties of blends containing different amounts of HPMC (2 - 10% w/w) with mannitol (89.6 – 97.6% w/w) and magnesium stearate (0.4% w/w) were assessed by measuring the angle of repose, Hausner ratio and compressibility index (Carr's index). The results showed no significant difference (ANOVA, $p > 0.05$) between the angle of repose of powders (Table 3.2) as they were all in the range of 31 – 40° which represents good to fair flow (Aulton, 2007).

Table 3.2: Flow properties for powders composed of mannitol 89.6 – 97.6% w/w, 2-10% w/w HPMC and 0.4% w/w magnesium stearate. Tests used were angle of repose and bulk and tapped density measurements. Hausner ratio and Carr's index were calculated from bulk and tapped densities. Results reported as mean ± standard deviation (n=3).

HPMC Conc. (% w/w)	Angle of Repose (°)	Hausner Ratio		Compressibility Index (Carr's Index, %)	
2	33.67 ± 2.52	1.37 ± 0.03	Poor	27.17 ± 1.88	Poor, fluid
4	39.30 ± 1.15	1.63 ± 0.11	Very very poor	38.55 ± 3.89	Very poor
6	36.17 ± 2.19	1.43 ± 0.04	Poor	29.97 ± 1.84	Poor, cohesive
8	34.37 ± 5.10	1.48 ± 0.08	Very poor	32.19 ± 3.81	Poor, cohesive
10	40.37 ± 2.05	1.44 ± 0.01	Poor	30.60 ± 0.67	Poor, cohesive

Hausner ratio and Carr's index were used to obtain the flow properties of powders. In contrast to angle of repose, the results for Hausner ratio and Carr's index showed statistically significant differences (ANOVA, $p < 0.05$). It can be seen from Table 3.2, the powder blends exhibited poor to very poor flow ranging from poor fluid powder (2% w/w HPMC) to cohesive powders (4, 6, 8 and 10% w/w HPMC). According to Hausner (1967), powders which have poor flow need agitation or vibration to improve flow whereas powders with very poor or very very poor flow require greater agitation or special hopper. 2% w/w HPMC powder showed the most fluid behaviour and the best flow properties between the powders tested which could be attributed to the lower concentration of HPMC (a cohesive binder) that aids powder flow (Chowhan, 1980). SEM showed that HPMC has a long fibre-like morphology with some particles present as clusters (Figure 3.7). This may have negatively affected the overall flowability of the powder blend. In fact, previous research has shown that particle elongation (e.g. fibrous particles) can be related to increased friction and poor flow properties (Podczeck and Mia, 1996).
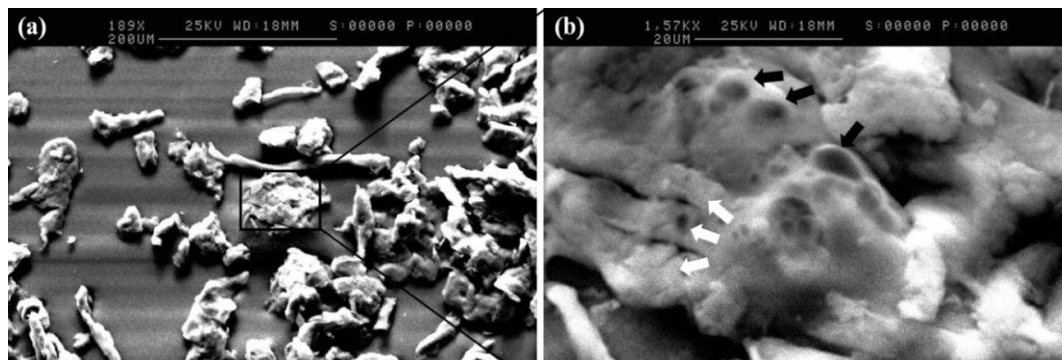
Figure 3.7: SEM of HPMC K100M. (a) shows long fibrous morphology of HPMC, 200 μm view at 189X magnification. (b) zoomed area showing HPMC clustered fibres (marked by white arrows) and areas swollen due to moisture (black arrows, discussion in section 3.3.4), 20 μm view at 1,57KX magnification.

Tablets were prepared at 15 kN from the blend containing different concentrations of HPMC (2-10% w/w). The purpose was to investigate the effect of binder concentration on tablet's hardness, disintegration time, porosity and friability. As a binder, HPMC was expected to increase the hardness of tablets when its concentration was increased between 2 and 10%, however, the results showed no significant difference in hardness (ANOVA, $p > 0.05$) (Figure 3.8). To investigate the anomaly in the results, another batch of tablets containing same levels of HPMC (2 - 10%) was prepared at a different compression force (30 kN). The results showed a gradual increase in hardness upon increasing HPMC concentration when the compression force was increased to 30 kN (Figure 3.9). The findings of the experiment are in agreement with a previous research carried out by Tatavarti et al. (2008) who found that HPMC has a significant elastic recovery at compression pressures less than 150 MPa (20 kN) and at slow compression speeds (1 mm/s). Elastic recovery is the expansion of tablet during decompression stage which occurs as a result of stored elastic energy in the compacted material (Haware et al., 2010). The force used to prepare the first batch of tablets (15 kN or 113 MPa) was less than the level stated by Tatavarti et al. (20 kN or 150 MPa) possibly explaining the lack of significant change in hardness. On the other hand, when 30 kN compression force was used permanent deformation occurred above the elastic limit of the material, as a result, hardness increased with increase in HPMC concentration.
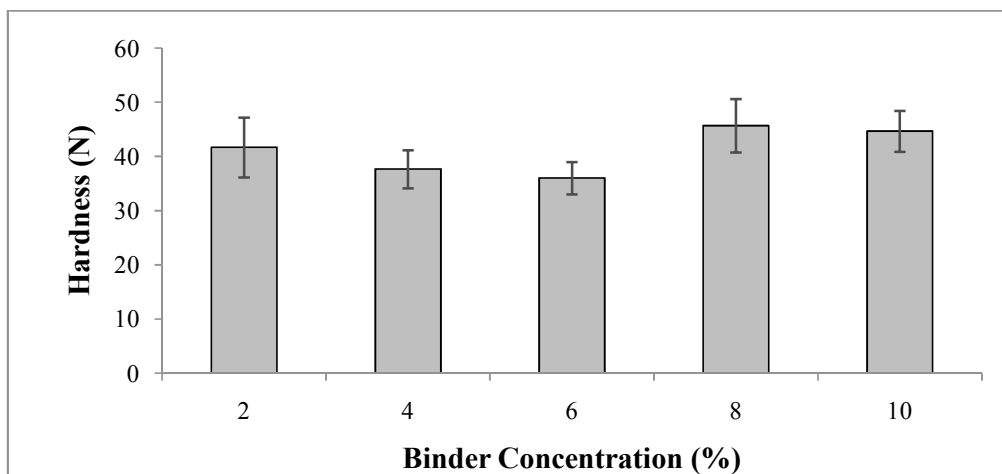
Figure 3.8: Hardness profile of tablets prepared at 15 kN from 2 - 10% w/w HPMC, mannitol and magnesium stearate using hydraulic tablet press. The results showed no significant difference in hardness (ANOVA, p>0.05) upon increase in binder (HPMC) concentration. Each point represents mean ± SD (n=3).
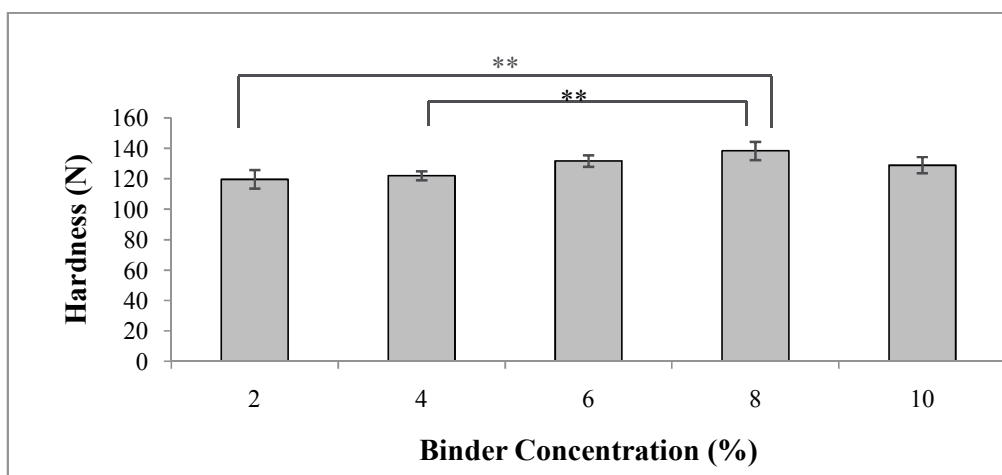
Figure 3.9: Hardness profile of tablets prepared at 30 kN from 2 - 10% w/w HPMC, mannitol and magnesium stearate using hydraulic tablet press. The results showed gradual increase in hardness upon increase in binder (HPMC) concentration. Each point represents mean ± SD (n=3).

Investigation was continued to test the tablets made at 15 kN for disintegration, porosity and friability. A gradual increase in disintegration time was observed when the concentration of HPMC was increased from 2 - 10% w/w (Figure 3.10) possibly due to the formation of gel matrix of HPMC (Avalle et al., 2011). Previously, researchers (Maggi et al., 1999; Ishikawa et al., 2000; Siepmann and Peppas, 2001) investigated the effect of HPMC concentration on the formation of matrix tablets used for sustained drug release. The concentration of HPMC

required to form a gel matrix was between 10 and 80% w/w whereas a concentration lower than 10% w/w resulted in tablet disintegration. The disintegration of HPMC-containing tablets (at 2% w/w) happens due to the low amount of polymer particles inside the tablet which would not allow the formation of a continuous gel layer upon hydration. Instead, these particles swelled generating pressure that caused disintegration of the tablet (Heng, 2001). Observation of the tablet shape during disintegration also confirmed the tendency towards matrix formation when the concentration of HPMC was increased. A sample of tablets was separately withdrawn after 20 sec from the start of disintegration test and checked for increase in diameter due to matrix formation (Figure 3.11).
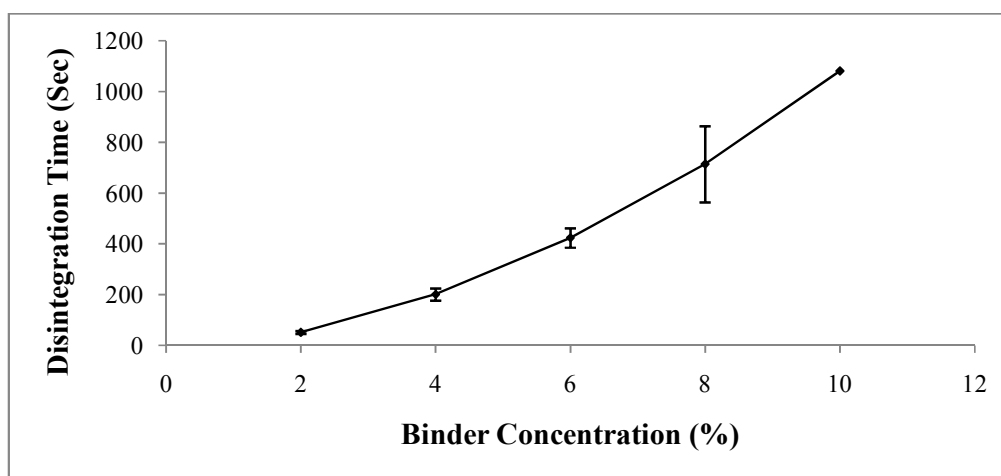
Figure 3.10: Disintegration profile of tablets prepared using different binder concentration (HPMC 2 - 10% w/w) with mannitol and magnesium stearate. Hydraulic tablet press was used to prepare tablets at 15 kN. Each point represents mean ± SD (n=3).
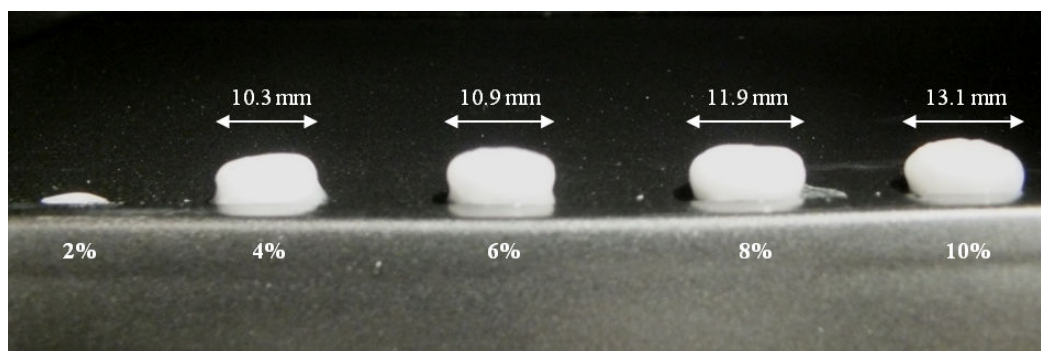
Figure 3.11: Image for tablets containing 2-10% w/w HPMC (in addition to mannitol and magnesium stearate) showing the tendency for gelation at higher concentrations. Diameter was measured for each tablet withdrawn from disintegration test after leaving to hydrate/disintegrate for 20 sec.

The porosity results (Figure 3.12) showed that the higher concentration of HPMC resulted in a linear decrease of porosity. This confirmed the role of HPMC as a binder where increasing its concentration in the binary mixture of mannitol has led to considerable reduction of inter-particle pores upon densification.
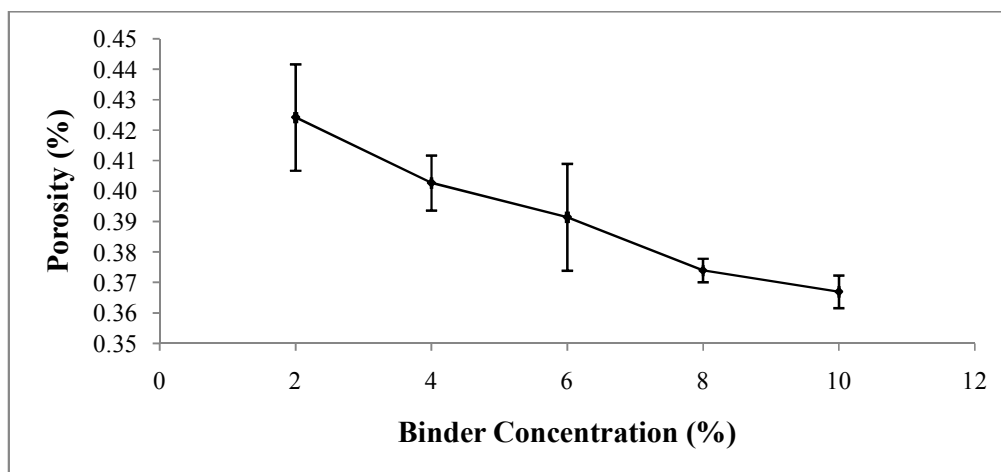
Figure 3.12: Porosity profile for tablets containing 2 - 10% w/w HPMC with mannitol and magnesium stearate. Tablets were prepared using hydraulic tablet press at 15 kN. Each point represents mean ± SD (n=3).

Friability testing is important as tablets are continuously subjected to abrasion and mechanical stresses during packaging, transportation and patient handling (Huyhnh-Ba, 2009). Low friability levels are essential to ensure physical integrity of the tablet and correct dose of the drug. Friability of tablets prepared using different levels of HPMC (2 - 10% w/w) at a fixed compression force (15 kN) was higher than 1% which is beyond the acceptable limit according to BP and USP (Figure 3.13). In addition, one tablet was broken when the lowest concentration (2% w/w HPMC) was used due to inferior binding capacity at lower concentration. Hence, Figure 3.13 shows the friability data for only four concentrations from 4 - 10% w/w without 2% w/w HPMC tablets. The results showed a continuous decrease in friability with increasing binder concentration which affirmed the role of HPMC as a binder. By examining the trend in Figure 3.13, it is reasonable to assume that friability would decrease below 1% if the concentration of HPMC is increased beyond the levels tested, however, this approach may not

be feasible as it will prolong the disintegration time of tablets which contradicts with the objective of developing a fast disintegrating formulation.
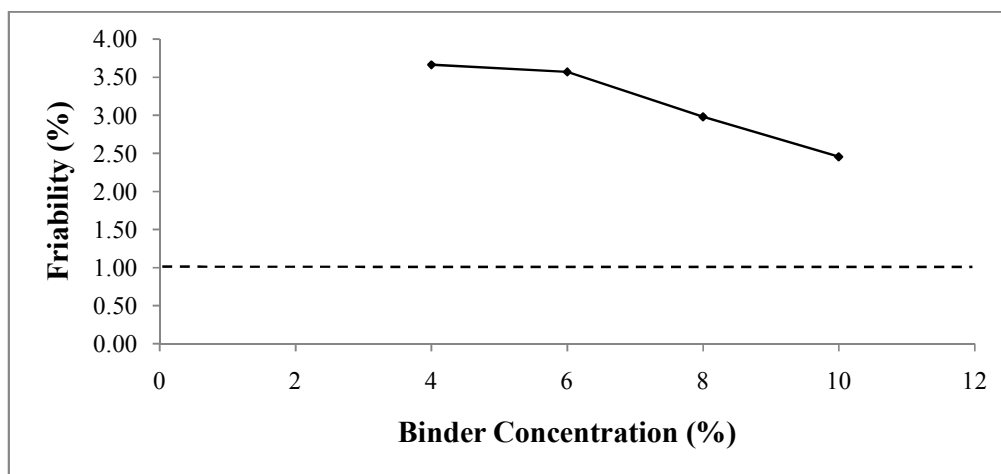
Figure 3.13: Friability profile for tablets prepared from different HPMC concentrations (4 - 10% w/w), mannitol (89.6 – 95.6% w/w) and magnesium stearate (0.4% w/w). 2% w/w HPMC concentration was not shown as the tablets broke during the test. Hydraulic tablet press was used to prepare the tablets at 15 kN. The dashed line represents 1% which is the accepted friability level according to pharmacopeia. Each point represents a batch of 8 tablets (n=1).

Although 2% w/w HPMC tablet was broken during friability testing, it was taken forward to the next stage as it retained the best balance between hardness and disintegration among the formulations tested.

3.3.3. Strategies to reduce friability of tablets

3.3.3.1. Influence of addition of a second binder on friability and other ODT properties

With only few exceptions, tablet friability is inversely related to tablet hardness: the higher the hardness value, the lower the friability value (Sheskey and Dasbach, 1995). L-HPC which is a binder/disintegrant was added to the formulation containing mannitol, HPMC and magnesium stearate in order to address high friability of the resultant compacts (Shimizu et al., 2003 b). As a binder, L-HPC may help to overcome friability by increasing tablet hardness while as a

disintegrant it may reduce the disintegration time further. In addition, it was reported by Tabata et al. (1994) that addition of L-HPC reduced friability without delaying tablet disintegration.

L-HPC was incorporated in various concentrations ranging from 0.5 - 2.5% w/w with a fixed amount of first binder HPMC (2% w/w), various concentrations of mannitol (95.1 - 97.1% w/w) and fixed concentration of magnesium stearate (0.4% w/w). At a compression force of 15 kN, the tablets showed no significant difference (ANOVA, p>0.05) in hardness between the different concentrations of L-HPC (Table 3.3). On the other hand, tablets made with two binders (L-HPC and HPMC) were harder (52.33 ± 5.03 – 53.33 ± 7.57 N) than the tablets made from single binder (HPMC), (36 ± 3 – 46 ± 4.93 N) when the same compression force was applied (15 kN). L-HPC was reported to consolidate under pressure by plastic deformation which could be the reason for the increased hardness of tablets (Humbert-Droz et al., 1982). Sano et al. (2013) reported that the hardness of ODTs containing L-HPC NBD grades were high even without further processing due to provision of higher degree of homogeneity and improved tablet mouldability.

Table 3.3: Properties of tablets prepared from 0.5 - 2.5% w/w L-HPC, 2% w/w HPMC, mannitol and magnesium stearate. Hydraulic press was used to prepare the tablets at 15 kN. Results reported as mean ± standard deviation (n=3) except for friability (n=1).

L-HPC Concentration (%)	Hardness (N)	Disintegration Time (sec)	Porosity	Friability (%)
0.5	52.33 ± 5.03	43.33 ± 2.08	0.50 ± 0.02	2.7
1.0	53.33 ± 4.16	41.00 ± 1.00	0.46 ± 0.01	2.7
1.5	52.33 ± 2.08	36.33 ± 3.21	0.44 ± 0.01	2.7
2.0	53.33 ± 7.57	45.33 ± 6.81	0.40 ± 0.03	2.26
2.5	52.67 ± 2.08	42.33 ± 4.04	0.43 ± 0.01	3

Disintegration time upon addition of L-HPC (Table 3.3) was significantly reduced (ANOVA, p<0.05) compared to the formulation containing HPMC only (51.67 ± 5.51 sec). Theoretically,

L-HPC could increase the hardness of tablets by plastic deformation while it could reduce the disintegration time due to its high swelling capacity (Alvarez-Lorenzo et al., 2000 a). Nevertheless, results showed that varying L-HPC concentration (0.5 – 2.5% w/w) did not have an impact on hardness and disintegration of tablets (Table 3.3). Porosity testing (section 3.2.8) was carried out at the different concentrations of L-HPC (0.5 - 2.5% w/w) to investigate this lack of change in hardness and disintegration. Accordingly, the results showed decreased porosity when more L-HPC was used in the formulation (ANOVA, p<0.001). The decrease in porosity could not be related to the constant hardness and disintegration time upon using different concentrations of L-HPC. Another study carried out in our laboratory confirmed the amount of L-HPC needed to show a significant increase in hardness of mannitol based tablets as not less than 2% and not more than 8% w/w. The study also reported no further decrease in disintegration time of mannitol based tablets even at L-HPC concentrations close to 10% w/w (Al-Khattawi et al., 2014 a). These observations were related to the elastic deformation of cellulosic excipients at low compression forces which was reported previously by York (1983) and Tatavarti et al. (2008).

Friability decreased as the hardness of tablets improved after inclusion of L-HPC. The 2% w/w HPMC tablets could not survive the friability test as one tablet was broken whereas when L-HPC was added, friability decreased to 2.26% with 2% w/w L-HPC in the formulation. The formulation which retained the lowest friability (2% w/w HPMC, 2% w/w L-HPC, 95.6% w/w mannitol and 0.4% w/w magnesium stearate) was taken forward for comparison with a control formulation which contained 2% w/w L-HPC, 97.6% w/w mannitol and 0.4% w/w magnesium stearate at different compression forces.

3.3.3.2. Influence of increasing compression force on friability and other ODT properties

The effect of compression force on tablet properties and specifically on friability was investigated as previous research showed that friability depends on the level of compression force and its effect on tablet surface properties (Riippi et al, 1998). In this experiment,

compression forces between 15 and 40 kN were used to compress tablets composed of 2% w/w HPMC, 2% w/w L-HPC, 95.6% w/w mannitol and 0.4% w/w magnesium stearate followed by assessment of friability, hardness and disintegration time. Figure 3.14 shows the effect of increasing compression force on the combined formulation of HPMC and L-HPC and on control L-HPC formulation. A clear trend could be seen whereby increasing compression force decreased friability for both formulations, although HPMC and L-HPC formulation produced less friable tablets probably due to the combined synergistic effect of two binders.
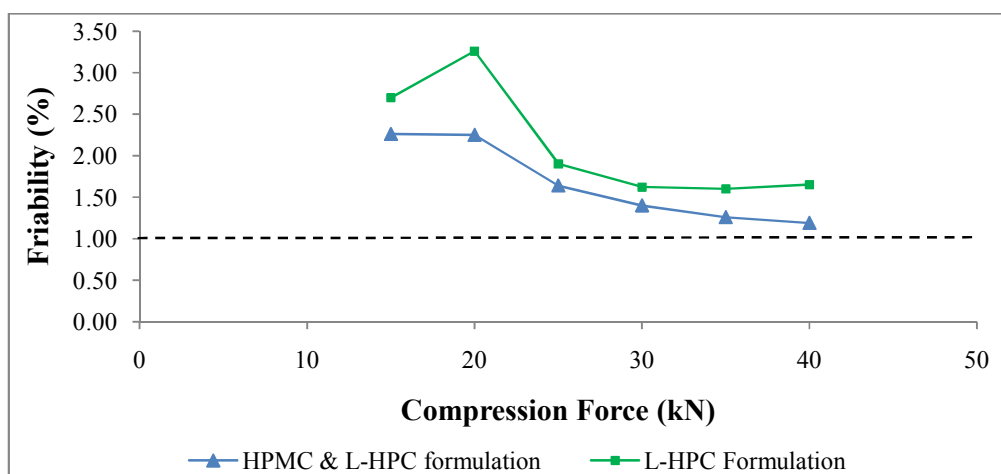
Figure 3.14: Comparison of friability profile for combined formulation (HPMC and L-HPC) and control formulation (L-HPC) at different compression forces (15 – 40 kN). The dashed line represents 1% which is the acceptable friability level according to pharmacopeia. Each point represents a batch of 8 tablets (n=1).

Hardness of tablets made at same compression forces was only significant (ANOVA/Tukey, $p < 0.05$) at the highest compression force (40 kN) in which HPMC and L-HPC combined formulation produced significantly harder tablets than control L-HPC formulation (Figure 3.15).
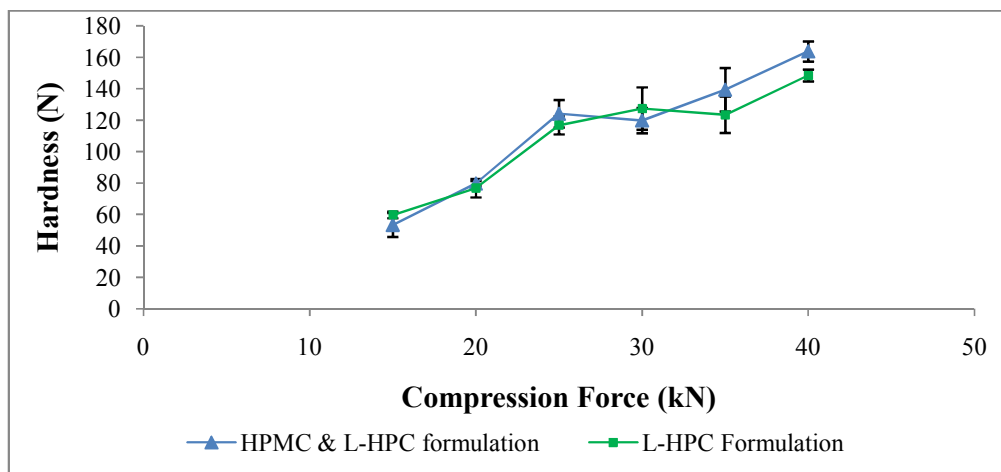
Figure 3.15: Comparison of hardness profile for combined formulation (HPMC and L-HPC) and control formulation (L-HPC) at different compression forces (15 – 40 kN). Each point represents mean ± SD (n=3).

The results of friability and hardness were consistent with the findings of Chowhan et al. (1982) who reported that it is possible to reduce tablet friability at higher crushing strengths (hardness). However, acceptable friability levels of < 1% were not obtained even at the highest compression force (40 kN). This friability issue was associated with the weak crystal strength of the diluent (D-mannitol) which undergoes fragmentation under high pressure (Bolhuis and Chowhan, 1996). Indeed, our preformulation work reported in Chapter 2 highlighted the issue of fragmentation and confirmed its mechanism. This has resulted in considerable amounts of loose powder on the surface and edges of mannitol based tablet, which upon friability testing wear off the tablet surface and edges easily (Figure 3.16). In order to overcome the high friability and to lower it to less than 1% (currently 1.19% for tablets made at 40 kN), other grades of mannitol can be used in conjunction with the current formulation composition.
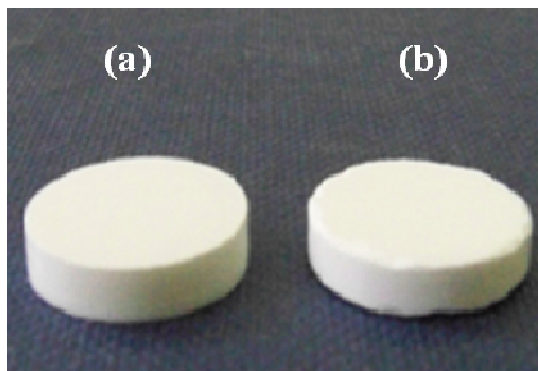
Figure 3.16: Mannitol-based ODT. (a) before and (b) after friability test (weight loss of 1.19%).

It was necessary to assess the disintegration time of tablets as the strategy used to reduce friability by increasing compression force might affect tablet disintegration time. Furthermore, a study by Martino et al. (2005) showed that disintegration time of tablets (mannitol based) containing different L-HPC grades could be dependent on concentration as well as the compression force used. In our study, results showed a significant difference (ANOVA/Tukey, $p < 0.05$) in disintegration time between combined formulation (2% w/w HPMC and 2% w/w L-HPC) and control formulation (2% w/w L-HPC) at the different compression forces except at 30 kN where no significant difference was observed (Figure 3.17).
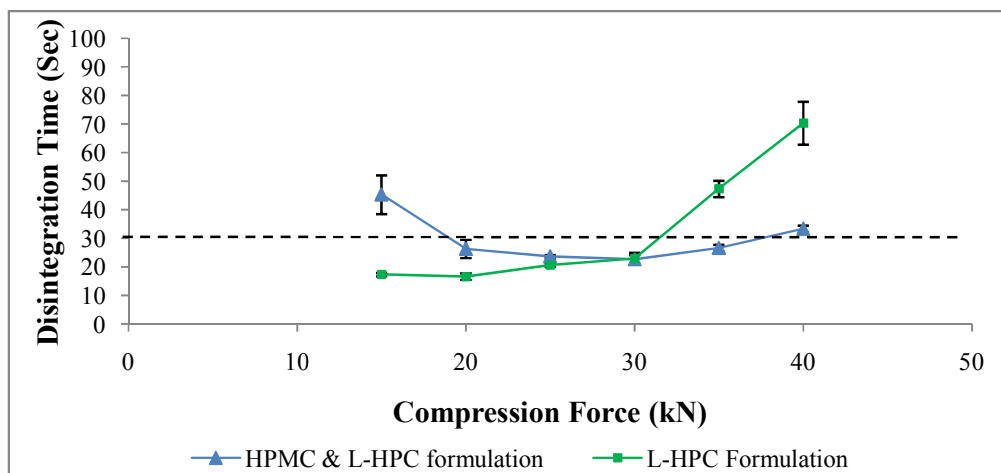
Figure 3.17: Comparison of disintegration profile for combined formulation (HPMC and L-HPC) and control formulation (L-HPC) at different compression forces (15 − 40 kN). The dashed line represents 30 sec which is the USP recommended disintegration time for ODTs. Each point represents mean ± SD (n=3).

From Figure 3.17, the higher disintegration time of combined HPMC and L-HPC formulation at the low compression forces (<30 kN) was consistent with lower friability (Figure 3.14) which may indicate better binding. On the other hand, at the highest compression forces (>30 kN), L-HPC formulation exhibited longer disintegration time (47.33 ± 2.89 − 70.33 ± 7.51 sec compared to 26.67 ± 1.15 − 33.33 ± 1.15 sec for combined formulation) possibly due to high plasticity and change of structural characteristics of L-HPC above 30 kN. It was reported from investigations carried out by our group (Al-Khattawi et al., 2014 a) that L-HPC under high compression forces results in increase in the proportion of crystalline content. The results were evaluated using XRD scans by varying the compression force and it is likely that this change results in higher densification which in turn gives rise to longer disintegration time.

The high compression forces (35 and 40 kN) did not compromise the disintegration time of combined formulation (HPMC and L-HPC) tablets as they still retain a quick disintegration profile of 26.67 ± 1.15 -33.33 ± 1.15 sec which is well within the limits (FDA CDER, 2008). The possible mechanism underlying the fast disintegration of combined HPMC and L-HPC formulation could be based on Superdisintegration. The maximum swelling of L-HPC upon contact with water was reported to be 10 times that of MCC (Gissinger and Stamm, 1980). The structural backbone of L-HPC is made of cellulose (Figure 3.18) which is insoluble in water having low substitution of hydroxypropoxy hydrophilic groups on the glucose subunits (Martino et al., 2005). This low substitution with hydrophilic groups causes the polymer to swell (Figure 3.19) but not dissolve upon contact with water, and hence results in the disintegration of the tablet. In addition, the swelling of HPMC could be considered another factor contributing to the breakage of tablet due to expansion (Heng, 2001).
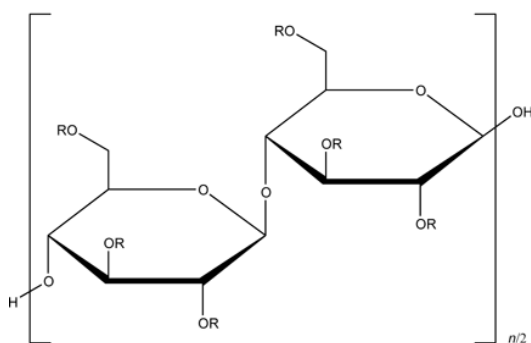
R = H or Hydroxypropoxy group $CH_2CH(CH_3)OH$

Figure 3.18: Structure of L-HPC. H or $CH_2CH(CH_3)OH$ are attached to the cellulosic backbone, composed of repeating glucose subunits, via R-O-R linkages (Hapgood and Obara, 2009).
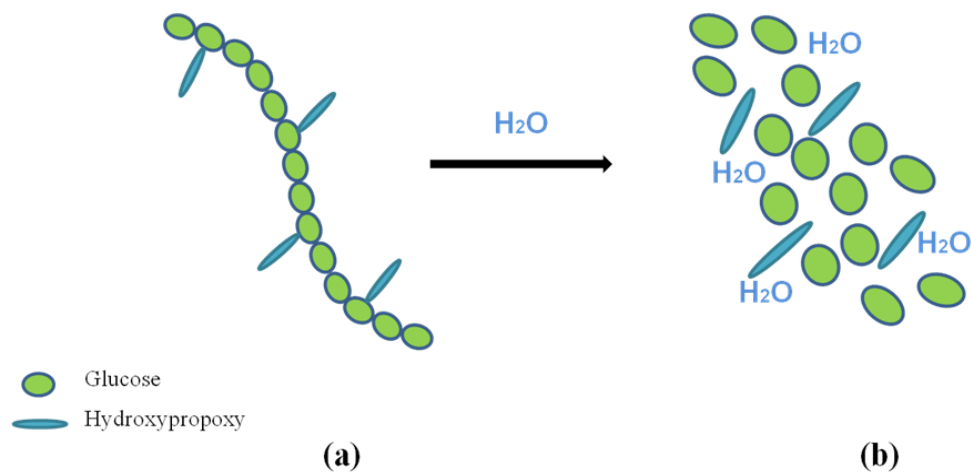
Figure 3.19: Superdisintegration by L-HPC. (a) intact polymer with low hydroxypropoxy hydrophilic groups substitution. (b) polymer swelled as water associates itself with the hydroxypropoxy groups.

3.3.3.3. Effect of particle size of excipients on friability of ODTs

To further develop ODT with acceptable levels of friability, an investigation into the role of particle size of excipients was carried out. Particle size distribution of mannitol, HPMC and L-HPC was determined followed by size separation into coarse and fine fractions and tableting of similar size fractions (i.e. coarse mannitol, HPMC and L-HPC together and vice versa). Particle

145

size distribution of mannitol was bimodal, that is two size populations 0 - 75 μm and 90 - 250 μm (Figure 3.20, also appendix A).
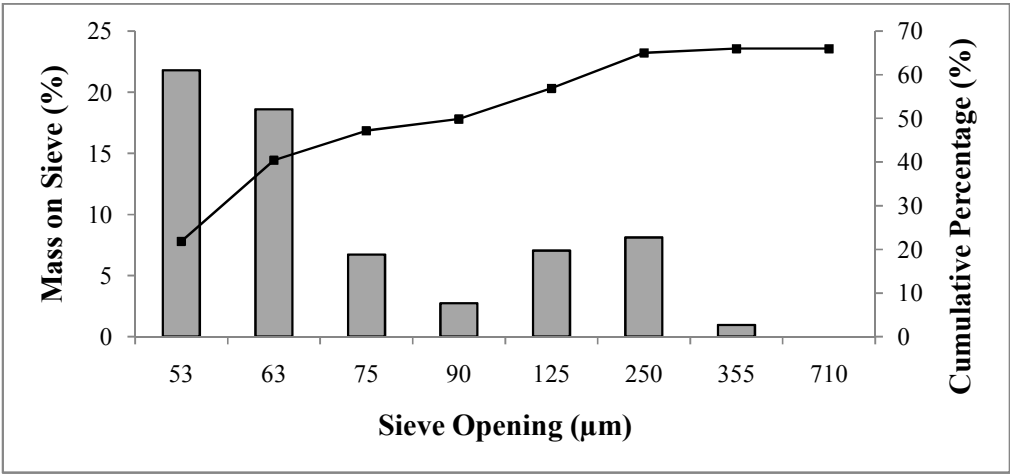
Figure 3.20: Mannitol particle size histogram and cumulative distributions established by mechanical sieves (53 – 710 μm) showing bimodal distribution (two size populations 0 - 75 μm and 90 - 250 μm).

HPMC also showed a bimodal distribution with two particle size ranges 0-75 μm and 90-125 μm (Figure 3.21, also appendix A).
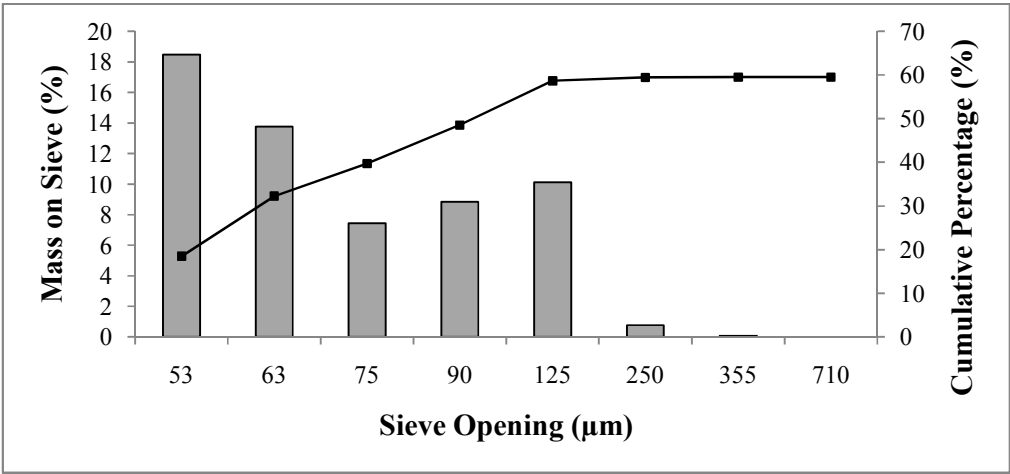
Figure 3.21: HPMC particle size histogram and cumulative distributions established by mechanical sieves (53 – 710 μm) showing bimodal distribution (two populations 0-75 μm and 90-125 μm).

Unlike mannitol and HPMC, L-HPC was a micronized grade with small amount of coarse particles resulting in unimodal particle size distribution between 0 and 125 µm (Figure 3.22, also appendix A).
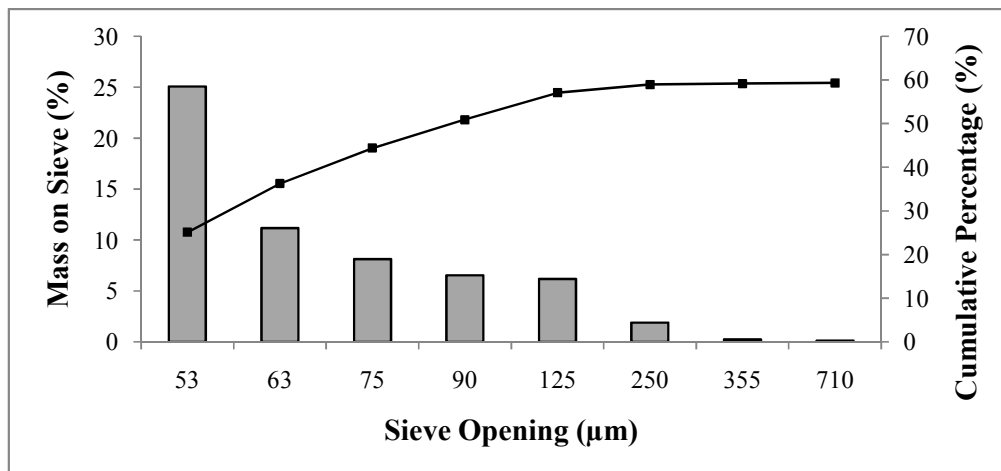
Figure 3.22: L-HPC particle size histogram and cumulative distributions established by mechanical sieves (53 – 710 µm) showing unimodal distribution with one population (0 -125 µm).

Tablets made from blend of coarser fractions of mannitol 95.6% w/w (90 - 250 µm), HPMC 2% w/w, (90-125 µm) and L-HPC 2% w/w (0 - 125 µm) with 0.4% w/w magnesium stearate showed a friability of 1.06% while tablets made from fine particles (0 - 75 µm for mannitol, 0-75 µm for HPMC and 0 -125 µm for L-HPC) of the same excipients showed a slightly higher friability of 1.12%. Results showed a reduced friability for the blend made of the coarser particles compared to the blend made from fine particles although the difference was very small (0.06%). Further experiments using a grade of mannitol which has larger particle size may demonstrate the effect of particle size on friability as both mannitol size populations used in this experiment are classified as very fine (X_{50} for mannitol used is 49.84 µm which is less than 125 µm threshold for very fine particles) according to BP (British Pharmacopeia Commission, 2012).

3.3.3.4. Effect of using different grades of mannitol on friability of ODTs

Due to low mechanical strength of mannitol crystal, it suffers from fragmentation under the influence of compaction pressure (Fukuoka et al., 1993). This is an undesirable property since it is usually accompanied by low compressibility and high friability for the tablets. Granular mannitol can improve the friability profile of tablets as it has better compressibility than the powder form. Yoshinari et al. (2003) developed a wet granulation process for mannitol and investigated the properties of the granulated excipient during compaction. Their investigation showed that mannitol particle size and specific surface area were likely to be the major contributing factors towards improved compaction behaviour. In this study, tablets were prepared from commercial grades of mannitol (granular, agglomerated and spray dried) blended with 2% w/w HPMC, 2% w/w L-HPC and magnesium stearate (0.4 or 1% w/w). These mannitol grades were claimed to be suitable for direct compression therefore, the influence on friability, hardness and disintegration time of tablets was investigated.

3.3.3.4.1. Properties of tablets prepared from granular, agglomerated and spray dried mannitol

Tablets prepared from granules are known to be stronger than those prepared from powders (Juppo et al., 1995). The grades of mannitol used in this stage were granulated by the manufacturer using high shear granulation (granular mannitol), fluidised bed agglomeration (agglomerated mannitol) and spray drying (spray dried mannitol). Each of the grades was blended with 2% w/w HPMC, 2% w/w L-HPC and 0.4% w/w magnesium stearate before tableting. Using automatic press, all grades showed linear increase in hardness with increasing compression force between 15 and 25 kN (Figure 3.23). Spray dried mannitol produced the strongest tablets (ANOVA/Tukey, $p<0.05$) because of its consolidation by plastic deformation. This is attributed mainly to the generation of mannitol polymorphs with superior deformation characteristics (more detailed description of spray dried mannitol tableting functionality is found in Chapter 4). Furthermore, tablets made from spray dried mannitol were harder (143.67

± 8.50 - 197.33 ± 10.07 N) than powder mannitol tablets (53.33 ± 7.57 - 124 ± 8.72 N) used in previous experiments.

Furthermore, granular mannitol resulted in stronger tablets than fluidised agglomerated mannitol (Figure 3.23) because of high shear granulation technique which produces relatively strong granules (Rumpf, 1962). Granular mannitol also showed better hardness (93.67 ± 7.57 N - 159.67 ± 19.04 N) than tablets made of powder mannitol. On the other hand, agglomerated mannitol showed almost similar hardness to powder mannitol especially at 15 and 20 kN, but much lower hardness at 25 kN. It could be that powder mannitol started to deform plastically at this compression force.
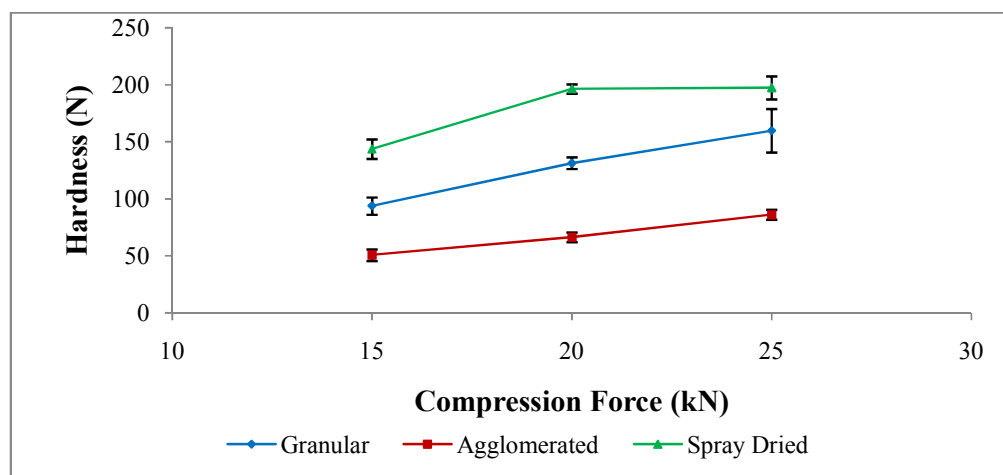
Figure 3.23: Hardness profiles for granular, agglomerated and spray dried mannitol upon different compression forces (15 – 25 kN). Tablets were prepared using automatic tablet press. Each point represents mean ± SD (n=3).

Spray dried mannitol showed longer disintegration time (ANOVA/Tukey, $p<0.01$) than the other two grades because of the more compact tablets formed by plastic deformation (Figure 3.24). However, there was no significant difference (ANOVA, $p>0.05$) in disintegration time between granular and agglomerated mannitol at the different compression forces. Investigation of the porosity of tablets containing granular mannitol (0.44 ± 0.01 – 0.37 ± 0.01 at 15-25 kN) showed it was higher than that of agglomerated mannitol (0.38 ± 0.01 – 0.33 ±

149

0.01 at 15-25 kN). This in turn resulted in the relatively similar disintegration time to the agglomerated mannitol tablets (Figure 3.24). This meant that granular mannitol with HPMC and L-HPC has good tableting functionality as it can provide higher hardness and sufficient tablet porosity for reasonable disintegration.
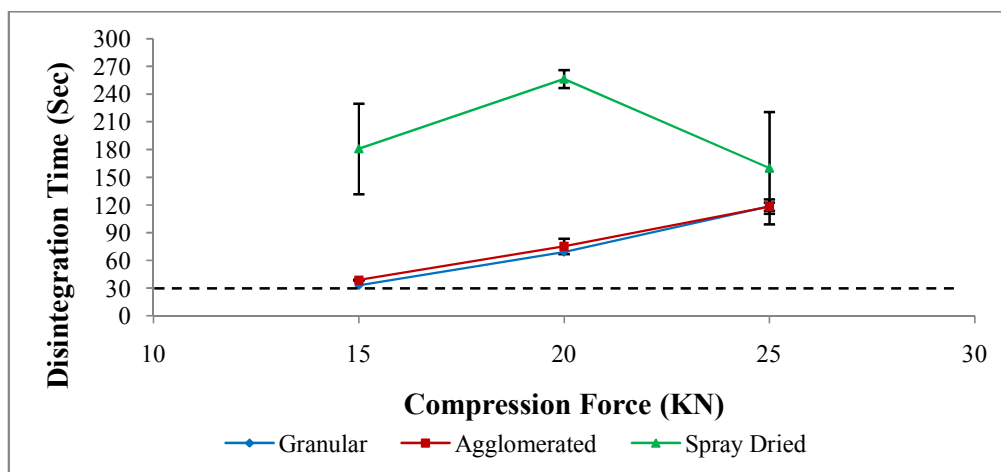
Figure 3.24: Disintegration profiles for granular, agglomerated and spray dried mannitol upon different compression forces (15 – 25 kN). Tablets were prepared using automatic tablet press. Each point represents mean ± SD (n=3).

Spray dried mannitol showed the best friability profile (Figure 3.25) between the three grades (0.77 and 0.9% at 20 and 25 kN respectively) due to the high hardness of its tablets. Granular mannitol could only achieve low friability (0.81%) at the highest compression force of 25 kN while agglomerated grade produced mechanically weaker tablets which in turn failed to achieve satisfactory friability levels. This is because fluidized bed process produces agglomerates that have lower mechanical strength than granules produced by high shear mixing (Smith and Nienow, 1983). In comparison with powder mannitol, all three processed mannitol grades produced tablets with lower friability at lower compression forces. This is due to improved compressibility, lower fragmentation, improved deformation characteristics and higher surface area for binding (Yoshinari et al., 2003).
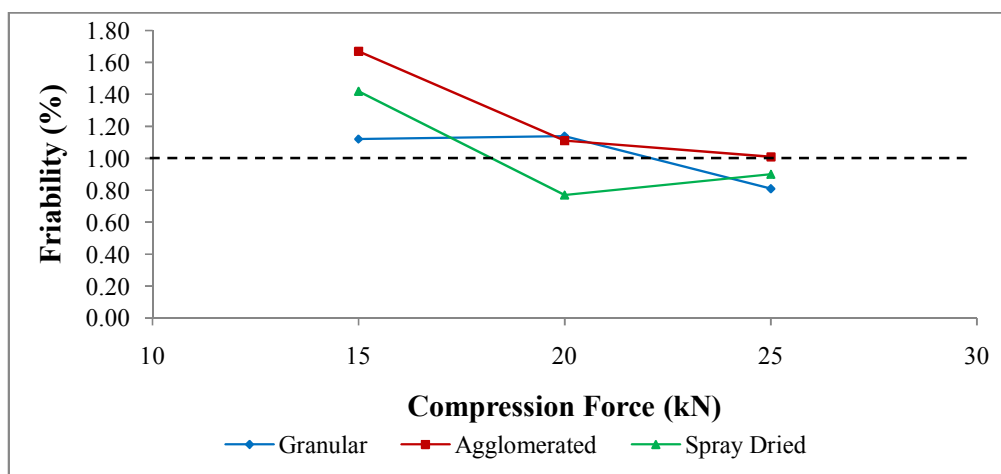
Figure 3.25: Friability profiles for granular, agglomerated and spray dried mannitol upon different compression forces (15 – 25 kN). Tablets were prepared using automatic tablet press. Each point represents a batch of 8 tablets (n=1).

3.3.3.4.2. Influence of lubricant concentration (magnesium stearate) on tablet properties

Optimising magnesium stearate level was important to improve tablet properties and reduce friability. Magnesium stearate is used to prevent powder sticking to the dies and punches of the tablet machine (Zuurman et al., 1999). However, it can negatively affect mechanical strength by forming a lubricant film around the particles during mixing, which in turn affects inter-particle bonding (Strickland et al., 1956). The film is also hydrophobic which can reduce wettability and delay tablet disintegration (Bolhuis et al., 1981).

Increasing magnesium stearate from 0.4-1% w/w for the tablets made at 20 kN showed a significant (t-test, $p < 0.05$) negative effect on tablet hardness. This confirmed that the higher amount of magnesium stearate potentially reduces tablet hardness (Figure 3.26). On the other hand, no significant difference was observed at the low and high compression forces due to sticking of 0.4% lubricant tablets resulting in greater variation of hardness.
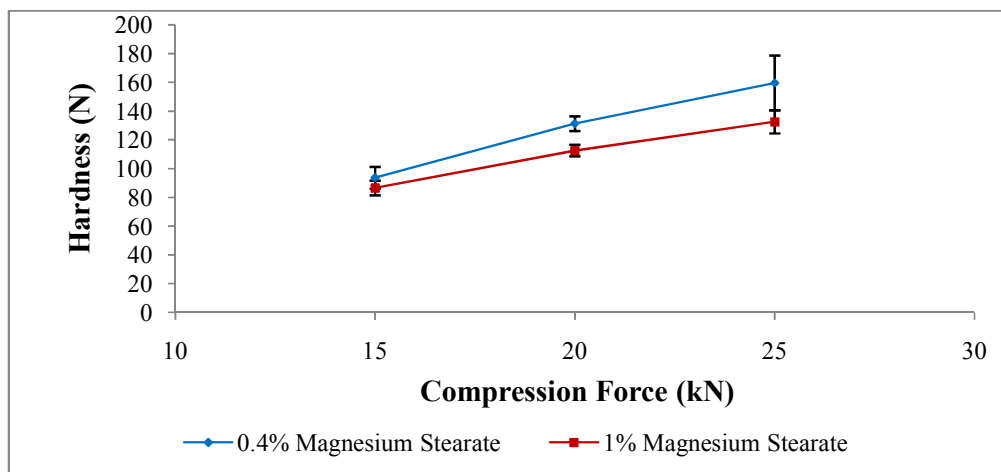
Figure 3.26: Effect of magnesium stearate (lubricant) level on tablet hardness. Automatic tablet press was used to prepare tablets containing 0.4 and 1% w/w magnesium stearate with mannitol (granular), HPMC and L-HPC at different compression forces (15 – 25 kN). Each point represents mean ± SD (n=3).

No significant difference (ANOVA, $p>0.05$) of increasing magnesium stearate concentration (from 0.4 -1% w/w) on disintegration time was observed at 15-20 kN (Figure 3.27). It could be that mannitol as well as HPMC and L-HPC required more pressure to reach to the plastic region where negative effects of lubrication may start to appear (Bolhuis et al., 1975; Zuurman et al., 1999). In accordance, the highest compression force (25 kN) has shown the effect of lubrication (reducing wettability) whereby an increase in disintegration time occurred. Overall, it could be that the low mixing time of excipients with magnesium stearate (1 min) has limited the negative effects and prevented dramatic increases in disintegration time.
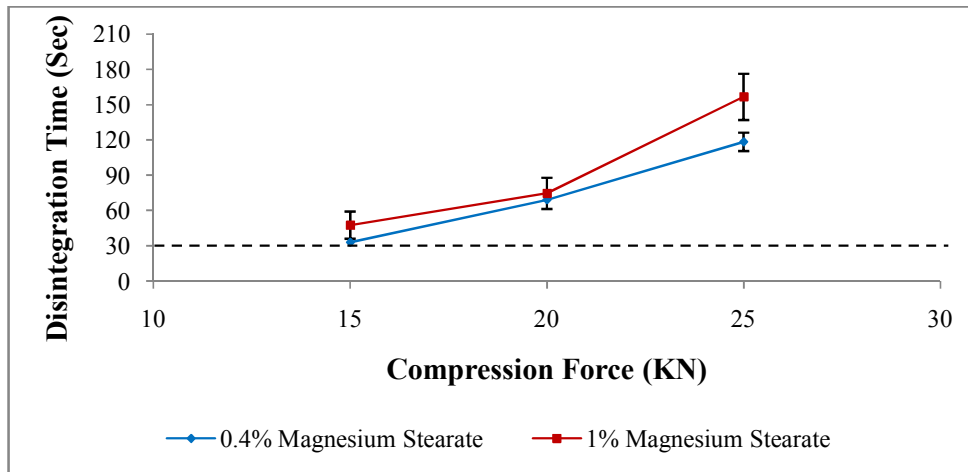
Figure 3.27: Effect of magnesium stearate (lubricant) level on tablet disintegration. Automatic tablet press was used to prepare tablets containing 0.4 and 1% w/w magnesium stearate with mannitol (granular), HPMC and L-HPC at different compression forces (15 − 25 kN). Each point represents mean ± SD (n=3).

Increasing magnesium stearate from 0.4-1% w/w generally had a positive effect in reducing friability (Figure 3.28). Increasing magnesium stearate was reported earlier to reduce internal friction and improve flowability of powders (Podczeck and Mia, 1996). This in turn may have resulted in lower die-wall friction and enhanced powder bonding on the tablet surfaces.
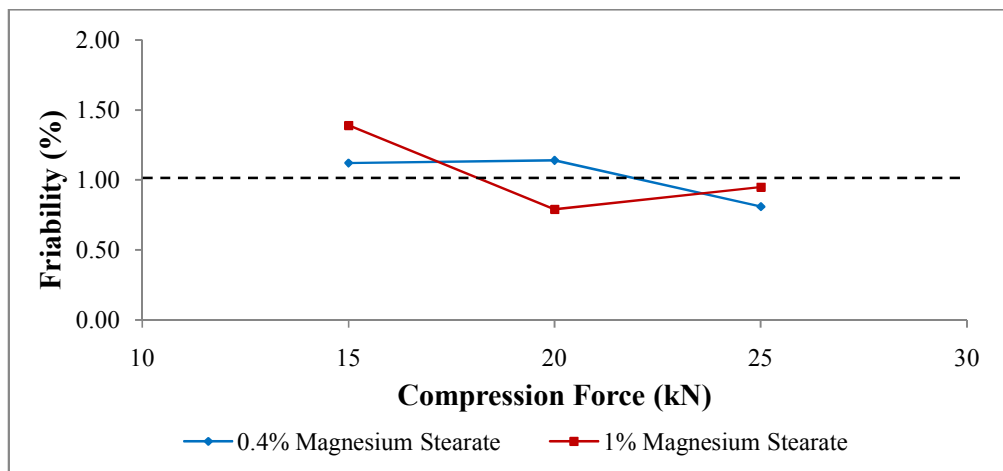
Figure 3.28: Effect of magnesium stearate (lubricant) level on tablet friability. Automatic tablet press was used to prepare tablets containing 0.4 and 1% magnesium stearate with mannitol (granular), HPMC and L-HPC at different compression forces (15 − 25 kN). Each point represents a batch of 8 tablets (n=1).

153

In conclusion, 1% w/w magnesium stearate was deemed necessary when using automatic tablet press as it reduced sticking and improved powder processability.

3.3.3.4.3. Influence of blending granular and powder mannitol on tablet properties

Using the automatic press, tablets composed of 95% w/w granular and powder mannitol at 50:50, 60:40 or 70:30 ratios, alongside 2% w/w HPMC, 2% w/w L-HPC and 1% w/w magnesium stearate were prepared. The purpose was to exploit the properties of granules (such as good compressibility to lower the friability) and of powder mannitol (such as rapid disintegration) in ODT development. The effect on hardness, disintegration time and friability was compared to a totally granular formulation composed of 95% w/w granular mannitol, 2% w/w HPMC, 2% w/w L-HPC and 1% w/w magnesium stearate. Results showed that totally granular mannitol tablets were significantly harder (ANOVA, $p < 0.05$) than 50:50, 60:40 and 70:30 granular: powder mannitol tablets (Figure 3.29). This demonstrates that granular mannitol has better compressibility than powder form. The latter statement was confirmed by Juppo et al. (1995) who reported that mannitol granules form a more complicated system than powder mannitol as they densify by plastic deformation in addition to fragmentation. The results also demonstrated that by decreasing the amount of powder mannitol, the mechanical strength of tablets increased (ANOVA/Tukey, $p < 0.05$) between 50:50 and 70:30 granular: powder at 20 kN due to reduction in the negative impact of mannitol powder fragmentation.
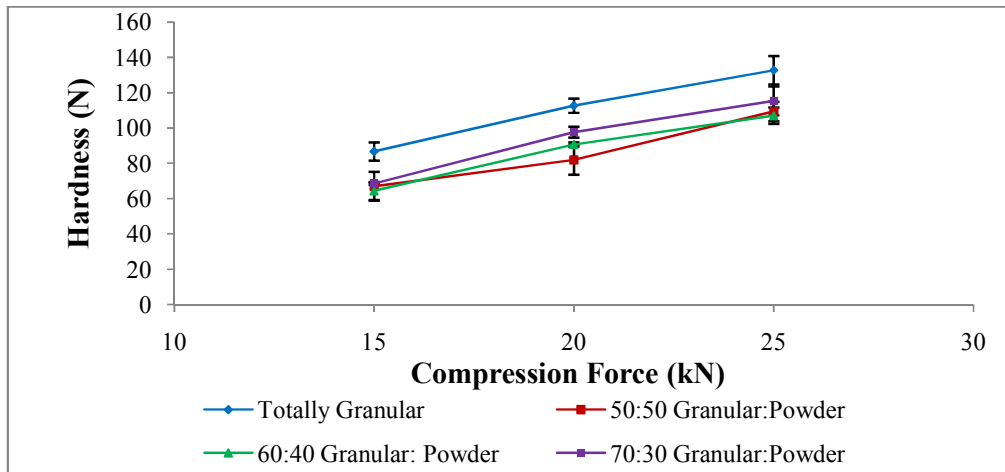
Figure 3.29: Comparison of hardness profile of totally granular mannitol tablets and 50:50, 60:40, 70:30 granular: powder mannitol tablets. Automatic tablet press was used to prepare tablets at 15 - 25 kN. Each point represents mean ± SD (n=3).

Furthermore, the disintegration time of granular mannitol tablets was significantly longer (ANOVA, $p < 0.05$) than 50:50, 60:40 and 70:30 granular: powder mannitol tablets. The disintegration time of granular mannitol tablets was longer because they are more compact tablets due to plastic deformation. All the tablets made from 50:50, 60:40 and 70:30 granular: powder mannitol exhibited much quicker disintegration because they were less compacted; hence, water penetration was easier (Figure 3.30).
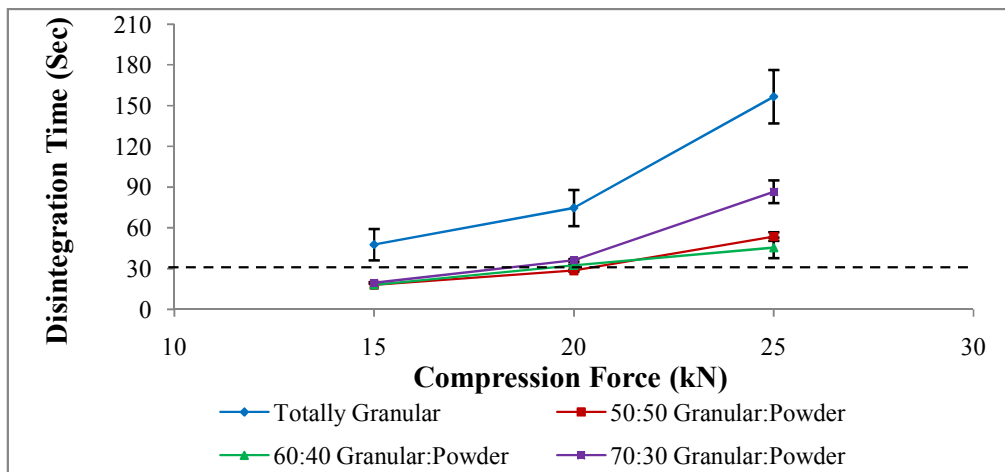
Figure 3.30: Comparison of disintegration profile of totally granular mannitol tablets and 50:50, 60:40 and 70:30 granular: powder mannitol tablets. Automatic tablet press was used to prepare tablets at 15 - 25 kN. Each point represents mean ± SD (n=3).

The results of friability showed an inverse relationship with hardness (Sheskey and Dasbach, 1995) i.e. granular mannitol produced harder tablets (Figure 3.29) therefore, friability (%) was lower (Figure 3.31). Furthermore, 50:50 and 60:40 granular: powder mannitol blend produced weaker tablets (Figure 3.29) than 70:30 and totally granular mannitol tablets at 20 kN thus friability was considerably higher (Figure 3.31).
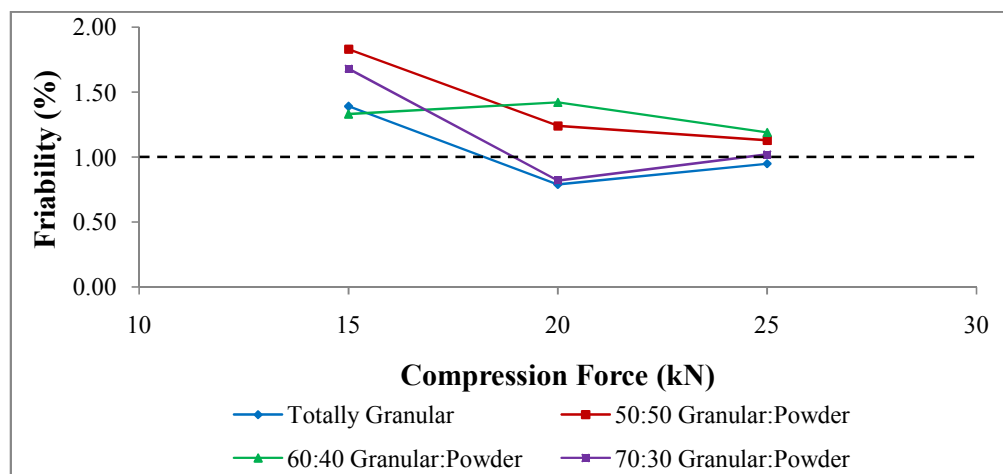
Figure 3.31: Comparison of friability profile of totally granular mannitol tablets and 50:50, 60:40 and 70:30 granular: powder mannitol tablets. Automatic tablet press was used to prepare tablets at 15 - 25 kN. Each point represents a batch of 8 tablets (n=1).

In conclusion, it was reasonable to suggest a blend of 95% w/w (70:30 granular: powder) mannitol along with 2% w/w HPMC, 2% w/w L-HPC and 1% w/w magnesium stearate could achieve the objective of good tablet hardness (such as > 60 N), acceptable friability (<1%) and fast disintegration (<30 sec) if tablets were prepared at 16-17 kN. In fact, this formulation was attempted and proved successful in achieving a hardness of 76.33 ± 1.53 N, a friability of 0.66%, and a disintegration time of 26 ± 2 sec. Therefore, this formulation was considered compliant with the FDA guidelines for ODTs (FDA CDER, 2008).

156

3.3.4. Stability studies over 6 months

Stability studies were carried out for the optimized powder blend (70:30 granular: powder mannitol constituting 95% w/w alongside 2% w/w HPMC, 2% w/w L-HPC and 1% w/w magnesium stearate) and placebo tablets (same blend composition compressed at 16-17 kN) over 6 months. The powders and tablets were incubated at the ICH recommended conditions: long term stability at 25°C/60% RH and accelerated stability at 40°C/75% RH as the formulation was intended for room temperature storage (ICH, 2003; Huynh-Ba, 2009).

The disintegration time of tablets showed no significant change (ANOVA, $p>0.05$) over 6 months of storage at 25°C/60% RH ($26 \pm 2 - 33.67 \pm 3.06$ sec) which complies with USP specifications for disintegration of ODTs (Figure 3.32). The tablets incubated at 40°C/75% RH showed different stability profile for disintegration (despite falling within Ph. Eur. limits of <3 min) as there was a significant gradual increase (ANOVA, $p<0.05$) in disintegration time starting at month 4 - 6. The reasons for this behaviour were investigated by comparison with the hardness and friability data as well as thermal/chemical profiling.
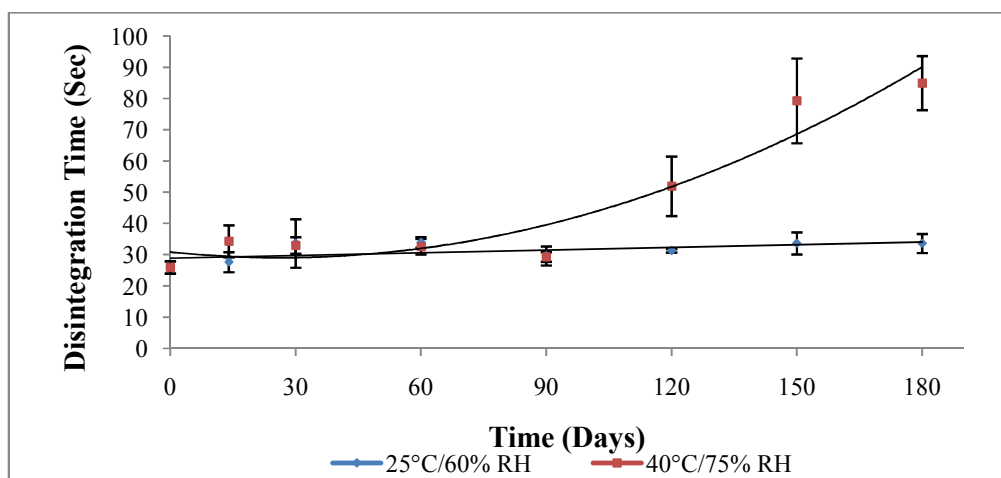
Figure 3.32: Stability profile for disintegration time of tablets (placebo) over 6 months. Tablets were made at 16-17 kN from (70:30 granular: powder mannitol constituting 95% w/w alongside 2% w/w HPMC, 2% w/w L-HPC and 1% w/w magnesium stearate). Disintegration time was assessed using USP basket disintegration apparatus. Linear regression was used to fit the trend line for 25°C/60% RH points. Polynomial regression (2nd order) was used to fit the trend line for 40°C/75% RH points. Each point represents mean $\pm$ SD (n=3).

The tablets stored at both stability conditions showed an increase in hardness up to 90-120 days (3-4 months) followed by a decline at month 5 and 6 (Figure 3.33). The increase in hardness was somehow anticipated as tablets are known to undergo 'ageing' process during storage as previous research has shown (Bhatia and Lordi, 1979). Some of the reasons for the latter process could be the tablets reaching full stress relaxation (part of decompression) after certain time or due to healing of internal structural failures by the effect of moisture (Karehill, and Nyström, 1990 b). However, the decrease in hardness after 4 months was interesting as it may indicate a specific mechanism specifically related to the composition of our formulation. The increase in hardness was higher for the tablets stored at 40°C/75% RH than at 25°C/60% RH for most of the time points assessed. Hence, when subsequent decline in hardness occurred, tablets at 6 months showed higher final hardness of 72.53 ± 1.77 N at 40°C/75% RH compared to 57.57 ± 4.57 N at 25°C/60% RH. These results indicate that physico-mechanical changes were triggered by heat and humidity.
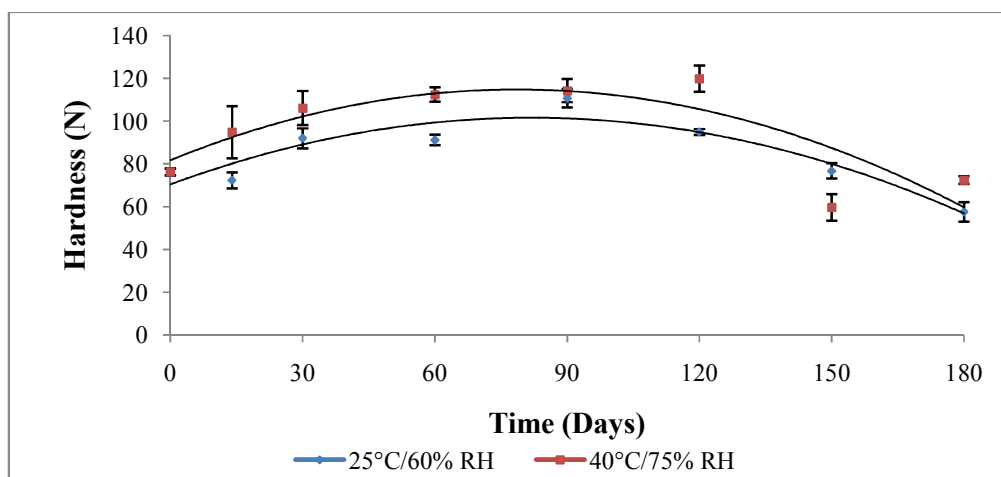
Figure 3.33: Stability profile for hardness of tablets (placebo) over 6 months. Tablets were made at 16-17 kN from (70:30 granular: powder mannitol constituting 95% w/w alongside 2% w/w HPMC, 2% w/w L-HPC and 1% w/w magnesium stearate). Hardness was obtained using diametral crushing strength test. Polynomial regression (2nd order) was used to fit the trend lines. Each point represents mean ± SD (n=3).

Furthermore, the changes in hardness were accompanied by inverse changes in friability as expected. Friability (Figure 3.34) initially declined (to 0.48 and 0.49 from 0.66%) due to

158

increase in hardness (112.53 ± 3.37 and 91.30 ± 2.51 from 76.33 ± 1.53 N), followed by an increase (0.97 and 0.82%) as the hardness of tablets reduced (72.53 ± 1.77 and 57.57 ± 4.57 N) for 40°C/75% RH and 25°C/60% RH respectively. Friability was generally within 1% pharmacopeial limit, however, to prevent future changes of formulation characteristics and to ensure dosage form robustness, further investigation of the changes were carried out. To understand the behaviour of powder blend, moisture content (%), DSC and FTIR data over the 6 months stability period were analysed.
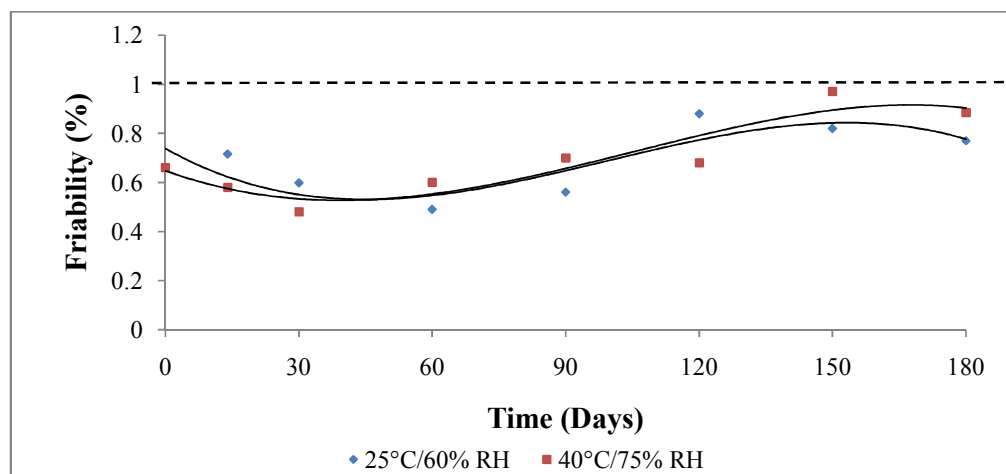
Figure 3.34: Stability profile for friability of tablets (placebo) over 6 months. Tablets were made at 16-17 kN from (70:30 granular: powder mannitol constituting 95% w/w alongside 2% w/w HPMC, 2% w/w L-HPC and 1% w/w magnesium stearate). Dashed line represents acceptable friability limit of 1%. Polynomial regression (2nd order) was used to fit the trend lines. Each point represents a batch of 8 tablets (n=1).

Thermal profiling using DSC showed no significant thermal events in the thermogram of powder blend due to the amorphous nature of HPMC and L-HPC, except for the melting onset of D-mannitol which appeared at 165°C (Appendix A for 6 months DSC data). The latter peak was used as an indicator for thermal changes in the mixture and both onset temperature and enthalpy of fusion data were compared. Over 6 months, DSC investigations showed no significant difference (ANOVA, p>0.05) in melting onset of mannitol or its enthalpy of fusion. Regression analysis was used to analyze the data for Figure 3.35 and Figure 3.36. The results showed no significant difference (linear regression, p>0.05) between the slopes (for 25°C/60%

RH and 40°C/75% RH) and zero. Regression also showed no significant difference (p>0.05) between the slope and intercept of both lines within 95% confidence limits indicating no change in melting onset and enthalpy of fusion between 25°C/60% RH and 40°C/75% RH.
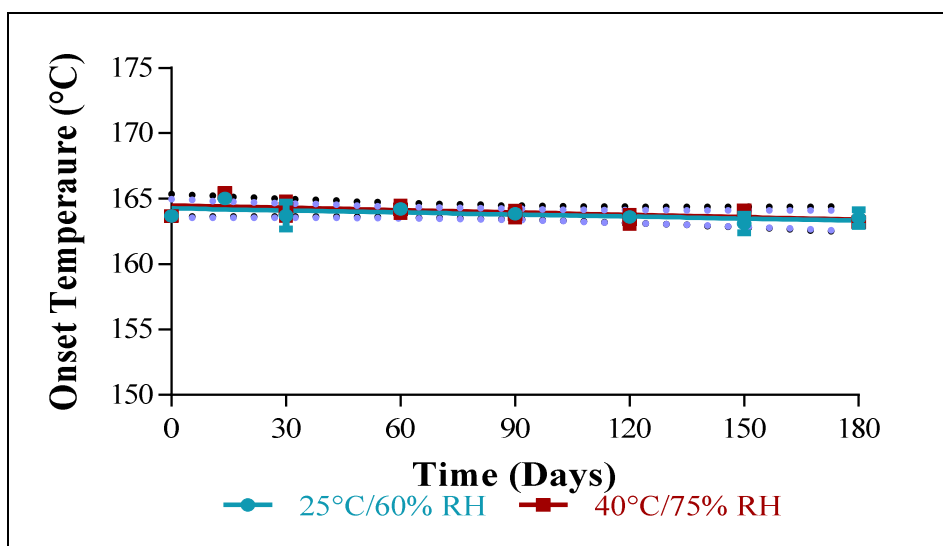
Figure 3.35: Melting onset temperature for mannitol peak over 6 months in a blend composed of 70:30 granular: powder mannitol constituting 95% w/w alongside 2% w/w HPMC, 2% w/w L-HPC and 1% w/w magnesium stearate. Dotted lines represent 95% confidence limits. Each point represents mean ± SD (n=3).
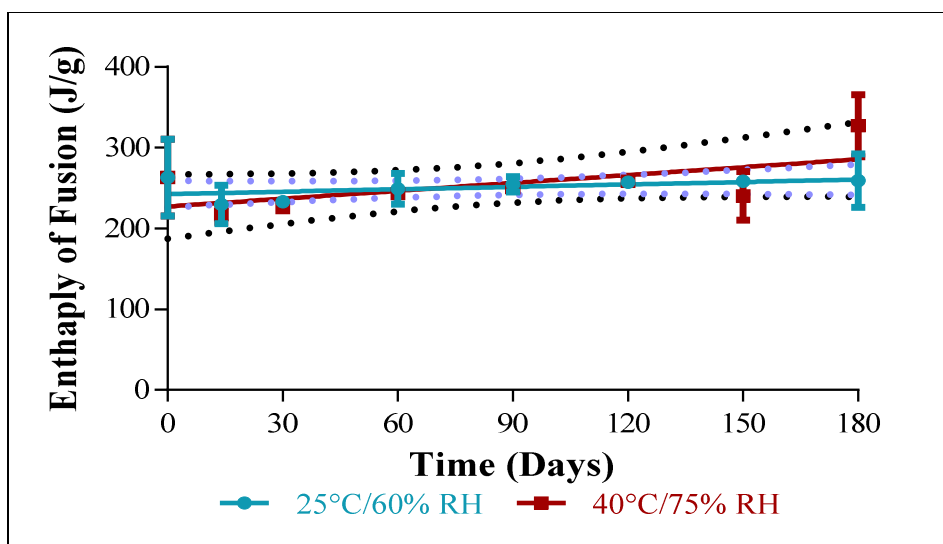
Figure 3.36: Enthalpy of fusion for mannitol peak over 6 months in a blend composed of 70:30 granular: powder mannitol constituting 95% w/w alongside 2% w/w HPMC, 2% w/w L-HPC and 1% w/w magnesium stearate. Dotted lines represent 95% confidence limits. Each point represents mean ± SD (n=3).

Results for moisture content analysis (Figure 3.37) also revealed no significant difference (linear regression, p>0.05) between the slope and intercept of trend lines for powders/tablets incubated at 25°C/60% RH and 40°C/75% RH over 6 months. Therefore, moisture content analysis could not be used to attribute humidity adsorption to the powder/tablet surfaces which possibly led to hardness, friability and disintegration changes.
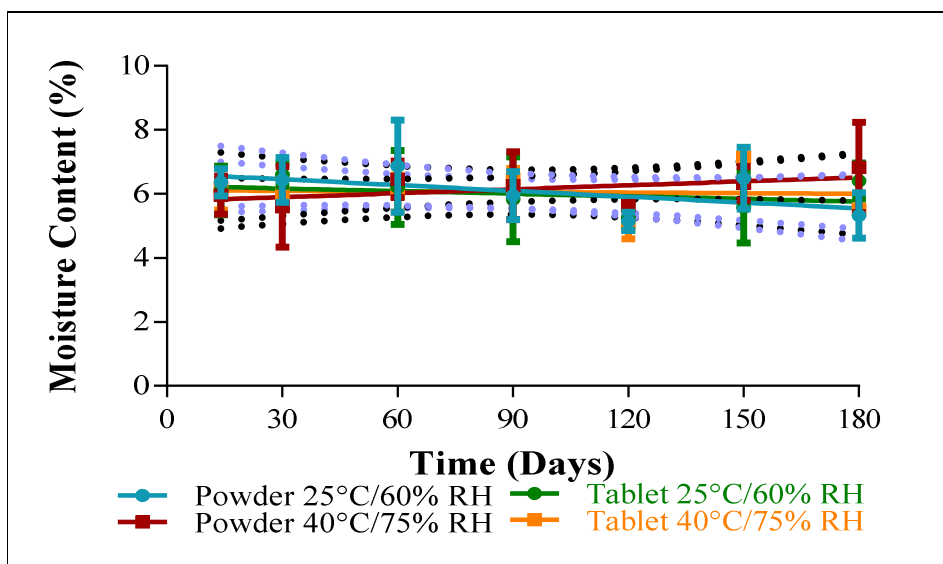
Figure 3.37: Moisture content for powders and tablets at 25°C/60% RH and 40°C/75% RH over 6 months. Powder blend comprised 70:30 granular: powder mannitol (95% w/w) alongside 2% w/w HPMC, 2% w/w L-HPC and 1% w/w magnesium stearate. Dotted lines represent 95% confidence limits. Each point represents mean ± SD (n=3).

FTIR analysis of the powders showed no change in the spectral peaks or their intensity over 6 months in comparison with day 0 (Figure 3.38). The spectra collected were for physical mixtures of mannitol (95% w/w), HPMC (2% w/w), L-HPC (2% w/w) and magnesium stearate (1% w/w). The powder blend showed similar spectrum to mannitol with extra peaks of magnesium stearate (Figure 3.38), for CH_2-CH_3 vibration between $2920 – 2844$ cm^{-1} and for asymmetric stretching corresponding to COO$^-$ at 1572 cm^{-1} (Stulzer et al., 2008). Furthermore, FTIR did not show structural chemical changes of the materials i.e. no new peaks appeared or existing peaks disappeared over 6 months.
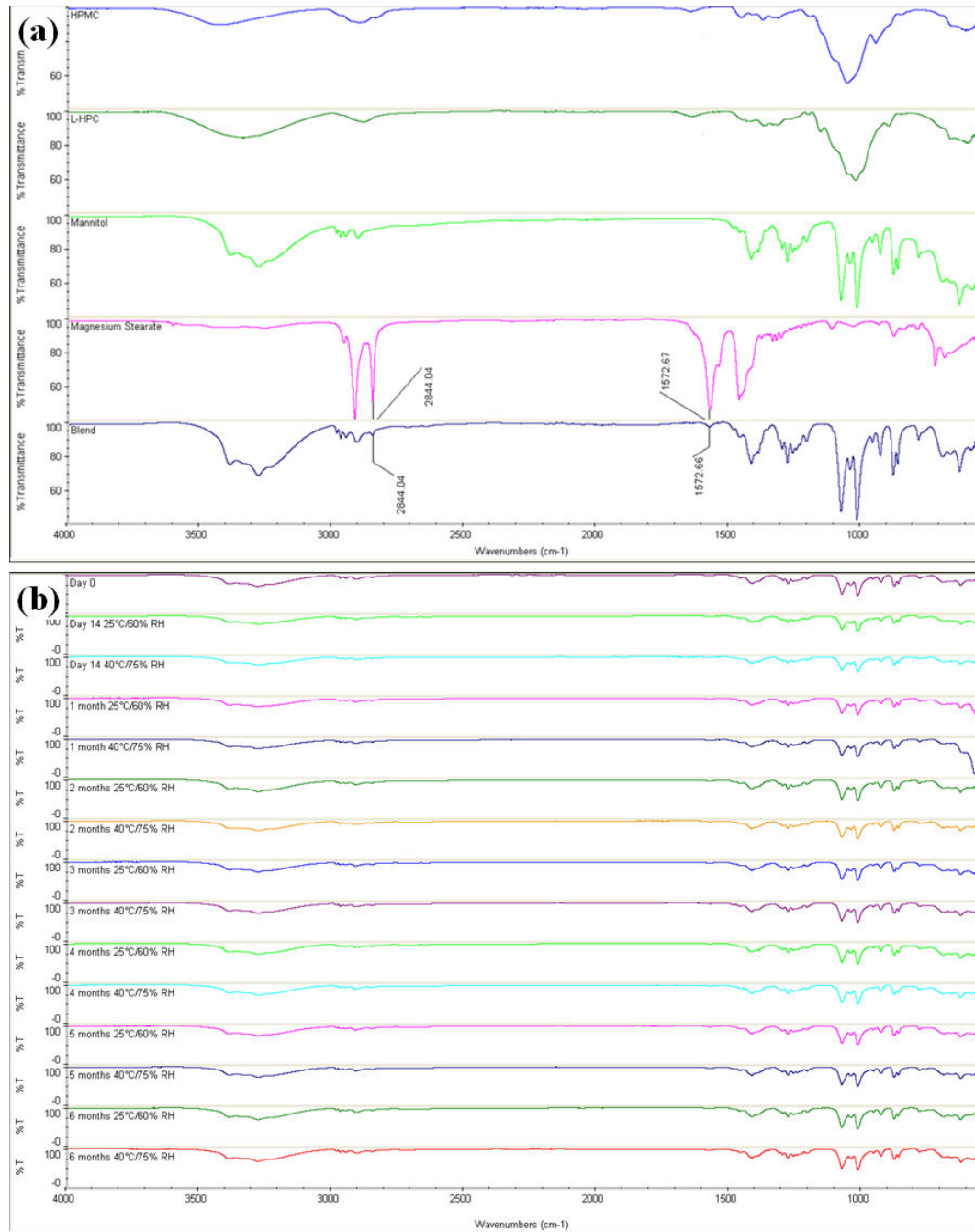
Figure 3.38: FTIR for (a) individual excipients and optimised powder blend and (b) stability data for powders at 25°C/60% RH and 40°C/75% RH over 6 months. Powder blend comprised 70:30 granular: powder mannitol (95% w/w) alongside 2% w/w HPMC, 2% w/w L-HPC and 1% w/w magnesium stearate. Each spectrum is representative of 16 scans per sample (n=3).

The changes in hardness and disintegration time observed earlier could be related to HPMC and L-HPC swelling functionalities. Saravanan et al. (2003) reported a decrease in the release rate

and hardness of HPMC containing tablets upon storage, due to possible ageing of HPMC and gelling. Although not detectable from moisture analysis, it could be that similar phenomenon occurred to our tablets. HPMC may have gelled due to humidity uptake (although at low concentration 2% w/w) forming a network that strengthened the tablet and led to the initial increase in hardness. The subsequent decrease in hardness was possibly due to further moisture uptake by HPMC which led to tablet softening. The disintegration time for the tablets stored at the accelerated condition potentially increased due to the same matrix forming properties of HPMC upon particles slow gelling. SEM in Figure 3.7 b has shown swollen areas on HPMC particle which may relate to moisture sensitivity during sample preparation and possibly support the above explanation.

Additionally, it could be that L-HPC intensified the changes within the tablet internal structure as it provides maximum swelling by virtue of its low hydroxypropoxy content. As mentioned earlier, L-HPC has 10 times more swelling capacity than MCC which in turn may have caused internal structural deformities in the tablet (Gissinger and Stamm, 1980). Alvarez-Lorenzo et al. (2000 b) reported changes in physical attributes of L-HPC containing tablets upon storage under 70% RH. They attributed the changes to moisture-induced swelling of L-HPC polymers. For our tablets, the slower disintegration may also happened due to L-HPC particles swelling and in turn losing their particular superdisintegration property.

The low quantities of both HPMC and L-HPC (2% w/w each) prevented the appearance of any marks such as tablet disintegration inside the packaging, powder/tablet discoloration or significant change in moisture.

Although tablet packaging was USP compliant with claimed UV light and moisture barrier protection, it seemed that it was not adequate to prevent formulation physico-mechanical changes (Appendix A). It is possible that the roller and foam sealing process used was insufficient to isolate and protect the tablets especially from accelerated stability conditions. A

163

heat/pressure sealing process could be used to overcome this issue or by utilizing different type of packaging with better protective characteristics.

3.4. Conclusion

A powder blend suitable for the development of ODTs by direct compression was developed. The optimized blend was made from 70:30 granular: powder mannitol constituting 95% w/w alongside 2% w/w HPMC, 2% w/w L-HPC and 1% w/w magnesium stearate. The mixture complies with FDA guidelines for ODT development when compressed between 16-17 kN (FDA CDER, 2008).

Optimisation of compression force was essential especially when using cellulosic excipients as these undergo significant elastic changes at low compression force. However, the addition of other excipients having plastic properties such as granular mannitol proved to reduce the impact of elasticity of cellulosic excipients. This was demonstrated in the final optimised blend which was compressed at 16-17 kN (low compression force) without any reported issues.

Similarly, optimising the concentration of excipients was essential to produce a fast disintegrating tablet. The use of high HPMC concentrations (> 2% w/w) led to the formation of matrix type tablet due to gelation. On the other hand, using low concentration of HPMC (2% w/w) prevented the formation of a continuous network upon hydration, thus tablets disintegrated quickly due to particles' swelling.

Due to the high friability of mannitol based ODTs, additional binder/disintegrant (L-HPC) was included to increase inter-particle bonding and reduce disintegration time further. The excipient addition led to improved hardness, however, high friability issue persisted due mannitol weak particle and fragmenting nature. As a result, replacement of a proportion of powder mannitol with granular grade was inevitable to enhance ODT mechanical strength and reduce friability below the acceptable limit (1%). The improvement in friability profile happened due to better compressibility of granular mannitol. Furthermore, an optimised ratio of granular: powder

mannitol (70:30) was required to create the balance that achieves suitable tablet hardness while maintaining fast disintegration and acceptable friability.

Optimising lubricant level in ODT was also important to reduce tablet sticking and allow better die filling during direct compression using automatic tablet press. Magnesium stearate at 1% w/w was suitable as it achieved the required lubrication without significantly prolonging disintegration time of ODTs.

Understanding the fragmentation behaviour of mannitol under compression through chapters 2 and 3 will be utilised towards engineering a new mannitol grade with higher hardness and fast disintegration for the development of compressed ODTs (Chapter 4).

Chapter 4

A Pragmatic Approach for Engineering Porous Mannitol and Mechanistic Evaluation of Particle Performance

4.1. Introduction

Mannitol is a versatile excipient with physical state that can be engineered to meet the diverse needs of formulation development (Telang et al., 2003). The last decade has seen the commercial introduction of a number of mannitol products with properties tailored to orally disintegrating dosage forms (Al-Khattawi and Mohammed, 2013). Popularity of mannitol was attributed to many factors including low hygroscopicity, inertness to APIs and patient body and development into robust tablets (Ohrem et al., 2014).

Most non-processed mannitol products suffer poor mechanical properties due to brittle fracture under pressure (Alderborn, 1996; Yoshinari et al., 2003). The development of orally disintegrating tablets (ODTs) requires more than just good binding properties in an excipient (Al-Khattawi and Mohammed, 2013). An ideal ODT excipient would provide favourable disintegration profile (around 30 sec) in addition to high mechanical strength. The fast disintegration property is usually attained by reducing the compression force during tableting thereby increasing inter-particle voids; however, this approach leads to weak and fragile tablets (Fu et al., 2004).

Particle engineering via spray drying may constitute a way for improving internal porosity and physico-mechanical properties of mannitol based ODT by controlling particle characteristics using subliming pore formers (Vehring, 2008). Previous research has shown that ammonium bicarbonate (NH_4HCO_3) sublimes above 50°C and is removed directly during spray drying (Gervelas et al., 2007). This property of NH_4HCO_3 as a pore former was also termed the 'baking powder effect' whereby the material leaves voids in formulated particles due to evolution of $H_2O\uparrow$, $NH_3\uparrow$ and $CO_2\uparrow$ (El-Sherif and Wheatley, 2003). Koizumi et al. (1997) attempted the inclusion of volatile additive Camphor in an ODT base followed by batch vacuum/heating process to sublime the material. Similarly, Roser et al. (1998) developed a porous tablet using ammonium bicarbonate. Despite success in achieving good porosity, the

crushing strength of the produced tablet was insufficient as the increase in porosity was concomitant with a reduction in structural integrity of the compact.

On the other hand, spray drying potentially provides a continuous and cost-effective platform for the production mannitol with enhanced porosity (Masters, 1979). Another added advantage is the tablet mechanical strength improvement after spray drying which is thought to be linked to amorphous material generation or better die rearrangement of particles (Gonnissen et al., 2007; Rojas and Kumar, 2012 b).

Understanding the morphological and physico-chemical/mechanical properties of mannitol during processing is also important as the excipient shows multiple polymorphic phases, e.g. α, β, δ (Kim et al., 1968; Berman et al., 1968; Burger et al., 2000). In fact, spray drying of mannitol may produce one or more polymorphic forms with varying morphologies and properties depending on the temperature of drying or use of adjuvant excipients (Hulse et al., 2009; Maas et al., 2011; Telang et al., 2003).

The primary hypothesis (aim) of this work is built on material processing of mannitol to overcome the significant challenges of low porosity and weak mechanical strength of mannitol based ODT.

- The objective in the current study is to fabricate robust particles of mannitol that would resist brittle fracture during tableting.

- The study will also exploit spray drying particle engineering capability to develop porous particles that can promote tablet disintegration through 'wicking'.

- It will also highlight the effect of the formulation mixture composition and spray drying temperature on the resultant particles tableting functionality.

- Understanding the formation and compaction mechanisms of the fabricated particles will be elucidated using a range of thermal and microscopic techniques.

168

4.2. Materials and methods

4.2.1. Materials

D-mannitol and ammonium bicarbonate were purchased from Sigma-Aldrich (Pool, UK). Both materials were in powder form and used as received.

4.2.2. Methods

4.2.2.1. Preparation of spray dried porous mannitol particles

Particles of mannitol were fabricated by spray drying an aqueous feed solution composed of D-mannitol and ammonium bicarbonate dissolved in distilled water. Preliminary experiments involved using 10-70% w/v D-mannitol and 5 - 20% w/v ammonium bicarbonate. Optimized formula for which most of the characterization was carried out was made using 2:1 ratio, 10% w/v mannitol: 5% w/v ammonium bicarbonate. Laboratory-scale Mini Spray Dryer B-290 from Buchi (Flawil, Switzerland) equipped with 1.5 mm nozzle was used for the procedure. The spray drying conditions were: co-current air flow rate of 670 NormL/h, 90% aspirator rate, 145 mL/h pump rate and inlet temperature of 110 - 170°C. A control formulation was also prepared containing 10% w/v mannitol without ammonium bicarbonate for particle morphology comparison. Process yield (%) was calculated after each run using the equation:

$$\text{Yield (\%)} = \frac{\text{Mass of solids after spray drying}}{\text{Mass of solids before spray drying}} \times 100$$

4.2.2.2. Powder flow assessment by bulk and tapped density measurements

Bulk and tapped densities were measured using a Sotax tap density tester USP II apparatus (Allschwil, Switzerland). The test parameters followed the official USP monograph <616> (USP Convention, 2012 a) except for cylinder volume which was smaller (5 mL) and weight of sample (2 g) due to limited powder quantities. Carr's index and Hausner ratio were calculated for the samples using the equations below:

$$\text{Carr's Index} = \frac{(\text{Tapped density} - \text{Bulk density})}{\text{Tapped density}} \times 100$$

$$\text{Hausner ratio} = \frac{\text{Tapped density}}{\text{Bulk density}}$$

4.2.2.3. Particle size analysis

Particle size of powders was measured by laser diffraction technique using particle size analyzer HELOS/BR and dry disperser RODOS with feeder VIBRI/L from Sympatec (Clausthal-Zellerfeld, Germany). The measuring range of the lens was 0 - 175 μm. Approximately 2 g of each powder was placed in the feeder tray and the run started at trigger condition of 2% Copt (optical concentration) for 10 sec with powder dispensing pressure of 3 bar. Volume mean diameter (VMD) was recorded for all powders.

4.2.2.4. Tablet preparation

A bench-top hydraulic press from Specac ltd. (Slough, UK) was used to compress pure and fabricated mannitol powders into 500 mg, 13 mm flat-faced tablets. Magnesium stearate (0.5% w/w) was added to each formulation followed by compression at 20 kN.

4.2.2.5. Helium pycnometry for true density and porosity measurement

True density and porosity were measured for all the powders/tablets using a helium multipycnometer from Quantachrome Instruments (Syosset, USA). Each powder (1000 mg) or tablet (500 mg) was placed into a micro sample cell and assessed for true volume and in turn true density. True volume V_t was obtained using the equation:

$$V_t = V_C - V_R(P1/P2 - 1)$$

Where V_t is true volume of the sample, V_C is volume of the sample cell, V_R is the known reference volume, P1 is atmospheric pressure and P2 is pressure change during determination.

V_t was used to calculate the true density of the tablet by weighing the tablet and substituting the values into:

$$\text{True density} = \text{Weight of tablet/True volume}$$

Porosity (ε) was calculated using the equation:

$$\varepsilon = 1 - (\text{Bulk density/True density})$$

Bulk density was acquired from:

$$\text{Bulk density} = \text{Weight of tablet/Bulk volume}$$

Bulk volume was obtained by measuring the radius (r) and thickness (h) of the tablet using a digital calliper and substituting in the equation for volume of a flat-faced tablet:

$$V = \pi \times r^2 \times h$$

4.2.2.6. Tablet hardness and disintegration time

Hardness (diametral crushing strength) of tablets was measured using 4M tablet hardness tester from Schleuniger (Thun, Switzerland). Disintegration time was determined for 3 tablets using the USP moving basket apparatus (USP Convention, 2005) from Erweka (Erweka ZT3, Heusenstamm, Germany). A tablet was placed in the disintegration basket (without using a disk) which was raised and lowered at a constant frequency of 30 cycles/min in the disintegration medium. Distilled water (800 mL) maintained at 37°C was used as the medium of disintegration while disintegration time was recorded for one tablet at a time to improve accuracy of recording. Time of disintegration was recorded when all the disintegrated fractions of tablet passed through the mesh of disintegration basket.

4.2.2.7. Heckel profile analysis

In-die Heckel plots were obtained by compressing the powders of pure and fabricated mannitol between 0 - 40 MPa using a Hounsfield materials testing machine from Tinius Olsen (Pennsylvania, USA). The machine was equipped with 13 mm diameter flat-faced punches. Die and punches were externally lubricated with magnesium stearate dispersed in acetone (5% w/v)

prior to each measurement. Each powder (500 mg) was manually filled into the die before starting the compression cycle. The lower punch was stationary during the compression while the upper punch moved at a speed of 6.66 mm/sec. Corrections for tablet thickness and weight were made after each compression cycle to account for punch elastic compressive strains and displacement errors. From the Heckel plot i.e. $\ln(1/(1-D))$ vs. compaction pressure, the slope (K) and intercept (A) of the terminal linear region (above 30 MPa) with the best R^2 value was obtained. Reciprocal of K is the apparent yield pressure (Py) of material. D is the relative density of the compact which equals to the ratio of tablet bulk density to the true density (without pores).

4.2.2.8. Compressive stress/strain curves

Tablets of pure and fabricated mannitol (500 mg, 13 mm diameter) were prepared at 12-30 kN and tested for compressive stress/strain profile using texture analyzer from Brookfield (Massachusetts, USA). The instrument was equipped with 50 kg load cell, TA44 probe (4 mm diameter, cylindrical) and TA-BT KIT table fixture. Test target was 5% deformation in the axial direction without breaking the tablet. Both tablet height and diameter were measured manually before the test (using a digital caliper) and information fed into the instrument software. The test was carried out on the centre of the specimen at a trigger load of 50 g and a probe speed of 3 mm/sec. The stress/strain curves for consecutive loading and unloading cycles were recorded and area in between calculated using GraphPad Prism 6.02 software (California, USA).

4.2.2.9. Scanning electron microscopy (SEM)

The morphology of mannitol powders and tablets cross-sections was examined by scanning electron microscope XL30 FEG ESEM from Philips (Amsterdam, Netherlands). For the powders, approximately 1 mg of each material was sprinkled onto a double-sided adhesive strip on an aluminium stub. For the tablets, each of the 500 mg compacts was dissected with a blade then a thin section was obtained to improve gold coating of the specimen. The specimen stub

was coated with a thin layer of gold using a sputter coater Polaron SC500 from Polaron Equipment ltd. (Watford, UK) at 20 mA for 3 min followed by sample examination using SEM. The acceleration voltage (kV) and the magnification can be seen on each micrograph.

4.2.2.10. Differential scanning calorimetry (DSC)

DSC Q200, from TA Instruments (Delaware, USA) was used to determine the thermal properties of powders. Temperature heat flow was calibrated with Indium (Melting point 156.8°C). Accurately weighed samples (3 mg each) of pure and fabricated mannitol were transferred into non-hermetically sealed Tzero pans. Each sample was heated at 10°C/min from 30 - 200°C under a nitrogen purge (50 mL/min). This was followed by analysis of resulting thermograms using TA instruments universal analysis 2000 software (V 4.5A).

4.2.2.11. Thermogravimetric analysis (TGA)

A thermogravimetric analyzer Pyris 1 TGA from Perkin Elmer (Massachusetts, USA) was used to measure the moisture content (%) and decomposition temperature of pure mannitol, fabricated mannitol and ammonium bicarbonate. Each sample (2 mg) was loaded onto the TGA pan and heated at 10°C/min from 30 - 300°C under nitrogen stream (20 mL/min). Pyris Manager Software (version 5.00.02) was used for analysing the obtained thermograms. Moisture content was calculated between 70 and 120°C.

4.2.2.12. Hot stage microscopy (HSM)

To monitor the drying kinetics and particle formation, HSM was carried out according to the method reported in Maas et al. (2011) using a Nikon Eclipse LV100 polarizing microscope from Nikon Instruments (Amsterdam, Netherlands) equipped with a Linkam hot stage (Surrey, UK). A droplet (4 mm diameter) of mannitol (10% w/v) and ammonium bicarbonate (5% w/v) formulation was placed on a microscope slide pre-heated to the spray drying temperatures 110, 150 and 170°C. Photomicrographs were captured for the crystallization/drying of droplets at the

different temperatures using 1.3 Mega Pixel Moticam camera and software from Motic (Hong Kong, China).

4.2.2.13. X-ray diffraction (XRD)

D2 Phaser X-ray diffractometer from Bruker (Massachusetts, USA) was used for analyzing polymorphic types of mannitol powders and tablets. The angular range (2θ) was $4 - 50°$ with increments steps of $0.02°$ and measured at 0.25 sec/step. Diffractive patterns were generated as counts per step and thereafter analyzed using Eva 18.0.0.0 software (Bruker, AXS). Material Analysis Using Diffraction (MAUD) software 2.49 (Luca Luterotti, University of California, USA) was used to quantify the polymorphic content of the mannitol powders through Rietveld Refinement. Calculated patterns for the mannitol polymorphs were obtained from the Cambridge Crystallographic Data Centre and imported into MAUD as .cif files, obtained XRD patterns were then fitted to the calculated patterns and percentages of each polymorph calculated.

4.2.2.14. Statistical analysis

ANOVA followed by Tukey post-hoc test and student t-test were performed using GraphPad Prism 6.02 software (California, USA). Statistical significant difference was considered at a p value <0.05. Where applicable, all results are presented as mean $\pm$ SD for triplicate measurements to account for the noise encountered within the experiments. For DSC, TGA and XRD, representative thermograms/diffraction patterns were presented out of the triplicate measurements.

4.3. Results and discussion

4.3.1. Morphology, porosity and micromeritic properties

Morphological studies using SEM generally showed spherical particles for fabricated mannitol in comparison with pure mannitol which had a columnar or prismatic rod-shaped particle (Figure 4.1 c, e, g and a). In addition, the formed particles appear to have surface gaps/pores unlike pure mannitol particles. Mannitol sprayed at 110°C (outlet temp. 60°C) (shown in c) has an irregular shape possibly due to incomplete particle formation whereas those made at higher temperatures 150°C (outlet temp. 80°C) and 170°C (outlet temp. 90°C) resulted in spherical particles. Surface pores are evident for particles sprayed at 150°C (e) and less visible in (g) made at 170°C. The role of ammonium bicarbonate in creating surface pores was confirmed by comparing fabricated mannitol morphology to a control formulation (containing no NH_4HCO_3) (b). The latter clearly showed a relatively regular surface with no visible gaps at all.

Initial investigations were carried out to observe the effect of NH_4HCO_3 on porosity. Helium pycnometry measurements showed 14% higher porosity (0.91 ± 0.03) for the powder made from 10% w/v mannitol and 10% w/v NH_4HCO_3 than pure mannitol powder (0.77 ± 0.02). By tableting at 20 kN, the porosity of spray dried mannitol reduced to 0.45 ± 0.03, however, it was still significantly higher (t-test, $p<0.001$) than porosity of tablets made from pure mannitol (0.20 ± 0.002). Furthermore, the reduction of NH_4HCO_3 to 5% w/v (mannitol also at 10% w/v) resulted in further increase of tablet porosity (0.53 ± 0.03) compared to 10% w/v NH_4HCO_3 (0.45 ± 0.03). In fact, an overall 33% enhancement in tablet porosity was achieved with spray dried mannitol (using 5% w/v of NH_4HCO_3) compared to pure mannitol.

The increase in porosity upon reduction of ammonium bicarbonate contradicted the hypothesis that pore former quantity is directly related to porosity. It could be that an optimum amount of ammonium bicarbonate was required to achieve maximum porosity whereby any further increase in the pore former would not cause significant improvement. This may also be related

to the nature of spray drying process whereby heat-mass transfer and particle crust formation is best achieved using an optimal concentration of solids in the feed solution (Reineccius and Bangs, 1985; Re, 1998). In fact, this was confirmed as attempts to use higher amounts of ammonium bicarbonate (up to 20% w/v) and mannitol (up to 70% w/v) did not result in further enhancement of porosity. This was possibly due to increased solid content (i.e. higher density) in formed particles upon increase in spray drying feed concentration.
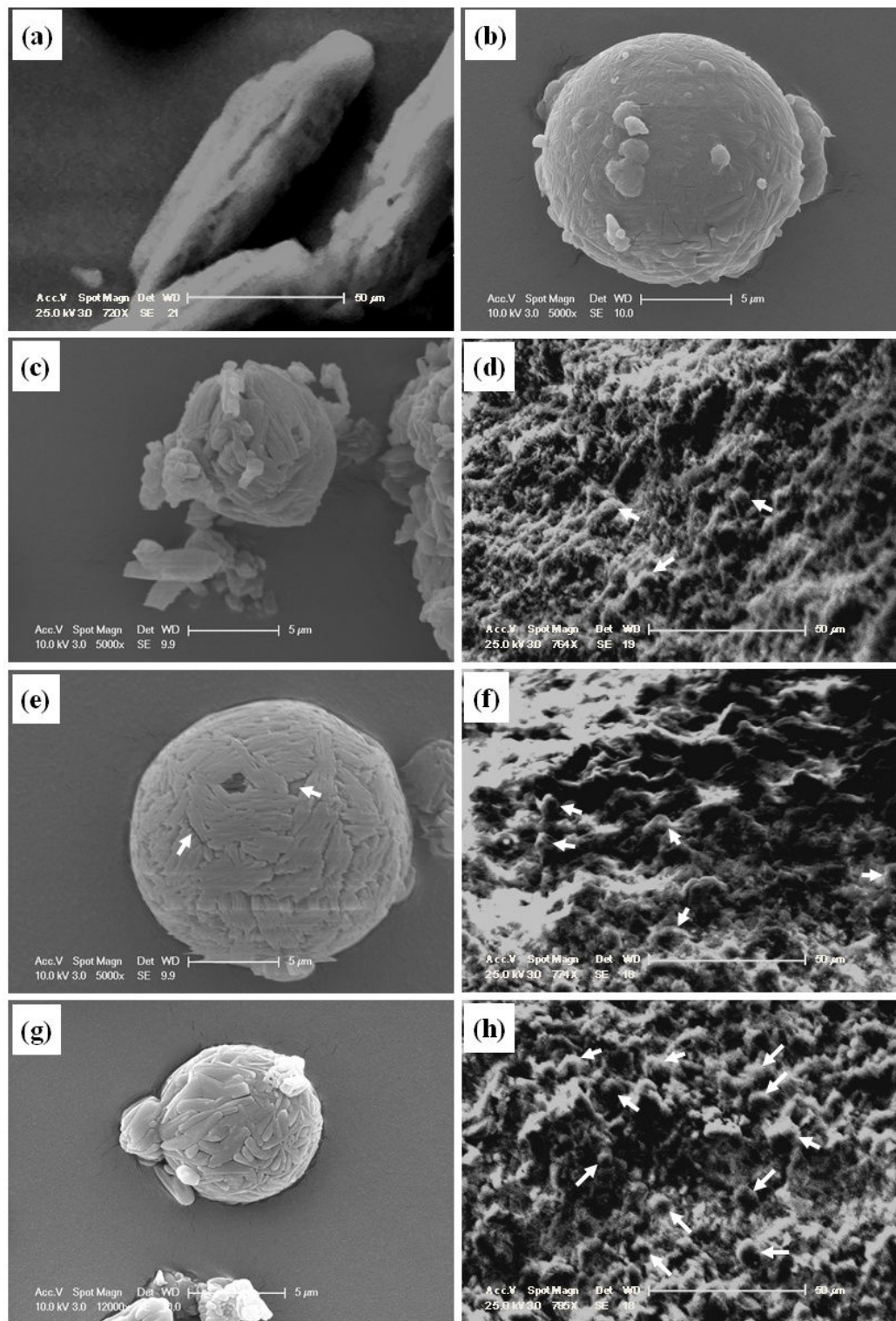
Figure 4.1: SEM showing morphology of mannitol particles and tablets (at 20 kN), (a) pure mannitol powder as control, (b) mannitol spray dried without NH_4HCO_3 as 2nd control, (c) and (d) mannitol sprayed with NH_4HCO_3 at 110°C and compact, (e) and (f) mannitol sprayed with NH_4HCO_3 at 150°C (arrows on gaps) and compact, (g) and (h) mannitol sprayed with NH_4HCO_3 at 170°C and compact, (Arrows in (d),(f),(h) point to spherical particles after tableting). (d), (f) and (h) are images for tablet cross sections obtained using a cutting blade.

Porosity and other micromeritic properties of the powders produced at 110 - 170°C are summarized in Table 4.1. Porosity after tableting was preferred over powders' porosity due to difficulty to accurately measure powder dimensions and bulk volume (Table 4.1). Tablets made from mannitol fabricated at 110 - 170°C showed significantly (ANOVA, $p<0.001$) higher porosity (0.30 ± 0.001 - 0.53 ± 0.03) when compared to pure mannitol tablets (0.20 ± 0.002). This was consistent with the significantly lower (ANOVA, $p<0.001$) true density of spray dried mannitol (1.50 ± 0.003 - 1.54 ± 0.004 g/cm^3) than pure mannitol (1.60 ± 0.002 g/cm^3). The powder made at 170°C showed significantly higher porosity (ANOVA/Tukey, $p<0.05$) than the rest of the powders which was attributed to particles elasticity and resistance to crushing (see discussion on elasticity measurements under 4.3.2).

Analysis of particle size measurements for the processed mannitol when compared to non-processed mannitol showed a significant drop in size (ANOVA, $p<0.001$). Similarly, Carr's index showed an extremely poor flowability (> 40%) while Hausner ratio indicated the powder requires special agitation or hopper (> 1.6). However, these properties are not too dissimilar to the pure mannitol which was on the borderline for extremely poor flow (39.5 ± 1.56) of the Carr's index and has a Hausner ratio above 1.6 indicating requirement of assisted flow.

Table 4.1: Porosity and micromeritic properties of pure and fabricated mannitol (10% w/v mannitol and 5% w/v ammonium bicarbonate) spray dried at 110 - 170°C. Results reported as mean $\pm$ SD (n=3).

Mannitol	Porosity after tableting	Powder true density (g/cm^3)	Particle size VMD (μm)	Carr's index (%)	Hausner ratio	Moisture content (%)	Yield (%)
Pure	0.20 ± 0.002	1.60 ± 0.002	35.41 ± 1.85	39.5 ± 1.56	1.65 ± 0.04	0.12 ± 0.10	-
Sprayed at 110°C	0.30 ± 0.001	1.50 ± 0.003	17.93 ± 1.29	56 ± 1.49	2.27 ± 0.08	0.51 ± 0.43	7.55 ± 4.77
Sprayed at 150°C	0.28 ± 0.01	1.49 ± 0.005	16.03 ± 0.48	68.79 ± 0.14	3.2 ± 0.01	0.23 ± 0.11	41.83 ± 9.03
Sprayed at 170°C	0.53 ± 0.03	1.54 ± 0.004	13.32 ± 0.93	64.77 ± 8.88	2.95 ± 0.67	0.19 ± 0.11	22.77 ± 0.67

Investigation of the moisture content using TGA yielded < 1% moisture content for all the different spray dried powders. Moisture content was inversely proportional to increase in inlet temperature. The yield of the process was lowest at 110°C due to insufficient drying and sticking to drying chamber and highest at 150°C followed by a lower yield again at 170°C (Table 4.1). The latter was attributed to deposition on instrument walls due to proximity to mannitol's melting point (165°C) which renders the material sticky.

4.3.2. Physico-mechanical properties

Results showed that spraying a formulation containing 10% w/v mannitol and 5% w/v ammonium bicarbonate not only provides relatively high porosity (as mentioned above), but also high mechanical strength to the resultant tablets. Spraying the formulation at inlet temperature of 110 - 170°C provided tablet hardness of 258.67 ± 28.89 to 98.53 ± 15.24 N (Table 4.2). This constitutes a 150% increase (ANOVA/Tukey, $p<0.001$) in hardness for mannitol sprayed at 110°C (258.67 ± 28.89 N) and 30% increase (ANOVA/Tukey, $p<0.05$) for mannitol sprayed at 150°C (152.70 ± 10.58 N) compared to pure mannitol (104.17 ± 1.70 N). However, no significant improvement in hardness (ANOVA, $p>0.05$) observed upon using mannitol sprayed at 170°C (98.53 ± 15.24 N). Overall, increasing the inlet temperature resulted in a significant decline (ANOVA, $p<0.001$) in hardness of all tablets. Consequently, the harder tablets made at 110°C and 150°C exhibited significantly longer (ANOVA, $p<0.001$) disintegration times (75.33 ± 2.52 and 49.33 ± 4.51 sec) than weaker tablets made at 170°C (31.66 ± 1.53 sec). Indeed, spray dried mannitol based tablets showed 50 - 77% decrease in disintegration time from 135 ± 5.29 sec for pure mannitol to 75.33 ± 2.52, 49.33 ± 4.51 and 31.67 ± 1.53 sec for mannitol 110, 150 and 170°C respectively.

To understand the differences in mechanical properties, spray dried mannitol was characterized using Heckel profile during tableting (at-pressure) and stress/strain profile for compressed tablets at different compression forces (Table 4.2).

Table 4.2: Physico-mechanical properties of pure and engineered mannitol made at 110 - 170°C. A and Py are intercept and yield pressure from Heckel plot respectively. AUC (area under curve, unit is Mega Joule/m³) enclosed between loading and unloading stress/strain curves. AUC obtained from tablets compressed at 12 - 30 kN. Results reported as mean ± SD (n=3).

Mannitol	Hardness (N)	Disintegration Time (Sec)	Heckel Profile			Stress/Strain Elasticity Profile – AUC Between Loading/Unloading (MJ/m³)			
			A (Intercept)	Py (MPa)	R^2	At 12 kN	At 14 kN	At 20 kN	At 30 kN
Pure	104.17 ± 1.70	135 ± 5.29	1.07 ± 0.02	121.59 ± 5.68	0.999	0.17 ± 0.030	0.04 ± 0.017	0.01 ± 0.004	0.01 ± 0.005
Sprayed at 110°C	258.67 ± 28.89	75.33 ± 2.52	0.87 ± 0.01	233.48 ± 13.52	0.981	0.31 ± 0.024	0.36 ± 0.024	0.42 ± 0.012	0.46 ± 0.017
Sprayed at 150°C	152.70 ± 10.58	49.33 ± 4.51	0.02 ± 0.01	32.30 ± 0.38	0.998	0.21 ± 0.030	0.30 ± 0.035	0.33 ± 0.063	0.48 ± 0.066
Sprayed at 170°C	98.53 ± 15.24	31.67 ± 1.53	0.16 ± 0.06	34.67 ± 2.65	0.999	0.20 ± 0.009	0.25 ± 0.026	0.39 ± 0.019	0.44 ± 0.014

Heckel plot's (Figure 4.2) terminal linear region was used to obtain the apparent yield pressure (Py) and intercept (A) as indicators of powder densification mechanism (Heckel, 1961; Hersey and Rees, 1971). The results (Table 4.2) showed low Py of 32.30 ± 0.38 and 34.67 ± 2.65 MPa for mannitol spray dried at 150 and 170°C respectively which indicate plastic deformation. In contrast, pure mannitol and the one sprayed at 110°C showed significantly (ANOVA/Tukey, $p<0.001$) higher Py of 121.59 ± 5.68 and 233.48 ± 13.52 MPa respectively, indicating brittle fracture. Py value for pure mannitol was close to values reported in literature for mannitol (Roberts and Rowe, 1987 b). Intercept values were significantly lower (ANOVA/Tukey, $p<0.001$) for mannitol 150 and 170°C (0.02 ± 0.01 and 0.16 ± 0.06, respectively) than for pure mannitol and mannitol 110°C (1.07 ± 0.02 and 0.87 ± 0.01, respectively). This was a further confirmation that higher inlet temperatures resulted in more plastic behaviour and lower fragmentation. The high plasticity of mannitol produced at 150 and 170°C explained the high and moderate hardness observed for these materials.

For mannitol made at the lowest temperature 110°C, the fragmentation resulted in stronger tablets possibly due to the formation of new clean surfaces for bonding between particles under compression (Jivraj et al., 2000). An example of this behaviour was also reported for other excipients; particularly lactose which fragments then yields strong tablets with Py of 178 MPa as reported by Roberts and Rowe (1986).
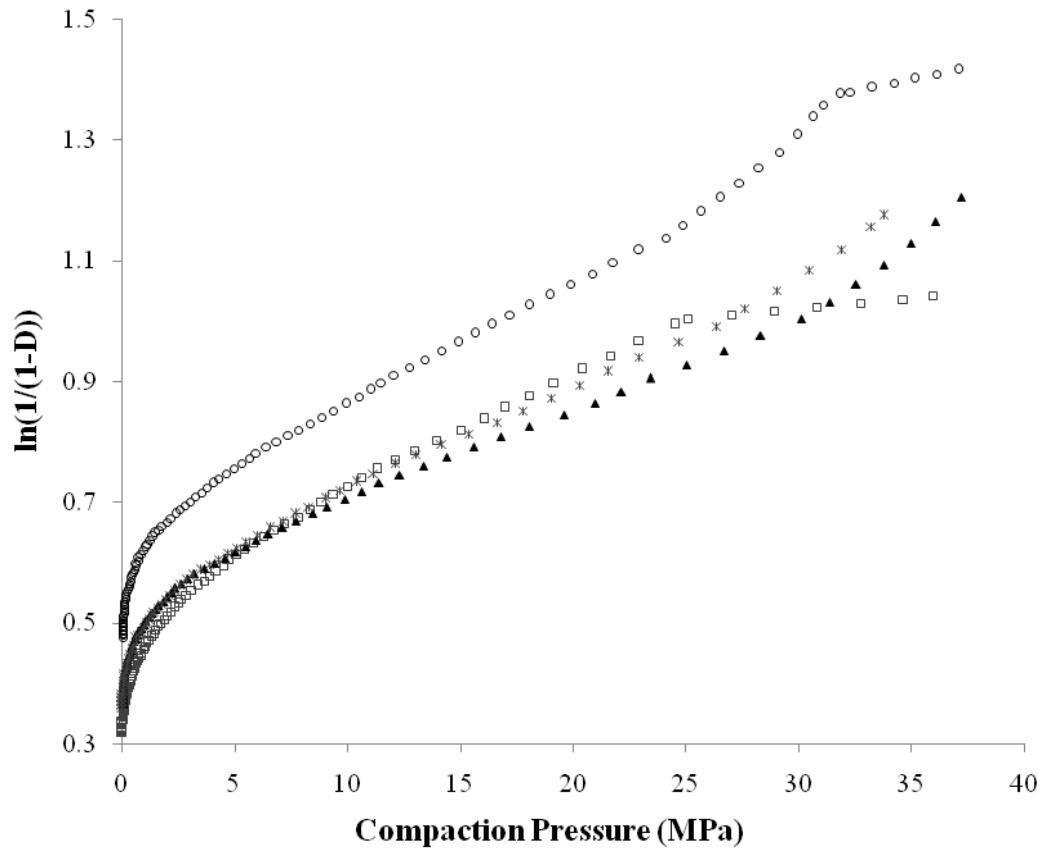
Figure 4.2: Heckel profile of pure and fabricated mannitol particles. Py (yield pressure) and A (intercept indicating rearrangement or fragmentation) obtained from the terminal linear region. R^2 varied between $0.981 - 0.999$. Each line is representative of triplicate measurements (n=3).

SEM of mannitol compacts made at 20 kN showed significant loss of particle morphology in the order of 110°C > 150°C > 170°C. Mannitol spherical particles were more evident with the increase of inlet temperature as shown in the SEM images of tablet cross sections (Figure 4.1 d, f and h, observe the increase in number of arrows). At 110°C, spherical particle morphology was lost due to fragmentation mentioned earlier whereas for 150°C ductile elongation (i.e. plasticity) could be seen especially at the top and bottom of SEM image (Figure 4.1 f). On the other hand, particles fabricated at 170°C seemed to retain spherical morphology (Figure 4.1 h). This particle shape recovery of mannitol made at 170°C indicates axial elastic recovery which is the most plausible explanation for the lower hardness and faster disintegration observed in Table 4.2.

Further confirmation of elastic recovery was derived from the stress/strain curves of each of the compacted specimens. Figure 4.3 shows each material as a compact being strained under pressure (loading) until 5% deformation achieved before load reversal (unloading) takes place where the material undergoes elastic recovery. The initial unloading stage was accompanied with high stress released upon tablet straining before gradual strain release to original probe position. The area under curve (AUC) values between loading and unloading compressive stress/strain cycles at different compression forces are presented in Table 4.2 and shown in Figure 4.3 (highlighted area). This area represents the difference between mechanical (strain) energy per unit volume (MJ/m^3) absorbed/consumed by the material during loading and released during unloading cycles. In the case of mannitol 110 - 170°C, the energy released was higher than the energy consumed which indicates the material exhibited significant elastic recovery (Figure 4.3). The dissipated elastic energy (AUC) increased with the increase in compression force used to make the tablets (Table 4.2). This is a further confirmation of elastic recovery which was consistent with tablet capping observed at higher compression forces (up to 30 kN). In contrast, pure mannitol showed exactly the opposite effect as the mechanical energy difference (AUC) decreased with increase in compression force due to low elastic recovery tendency.
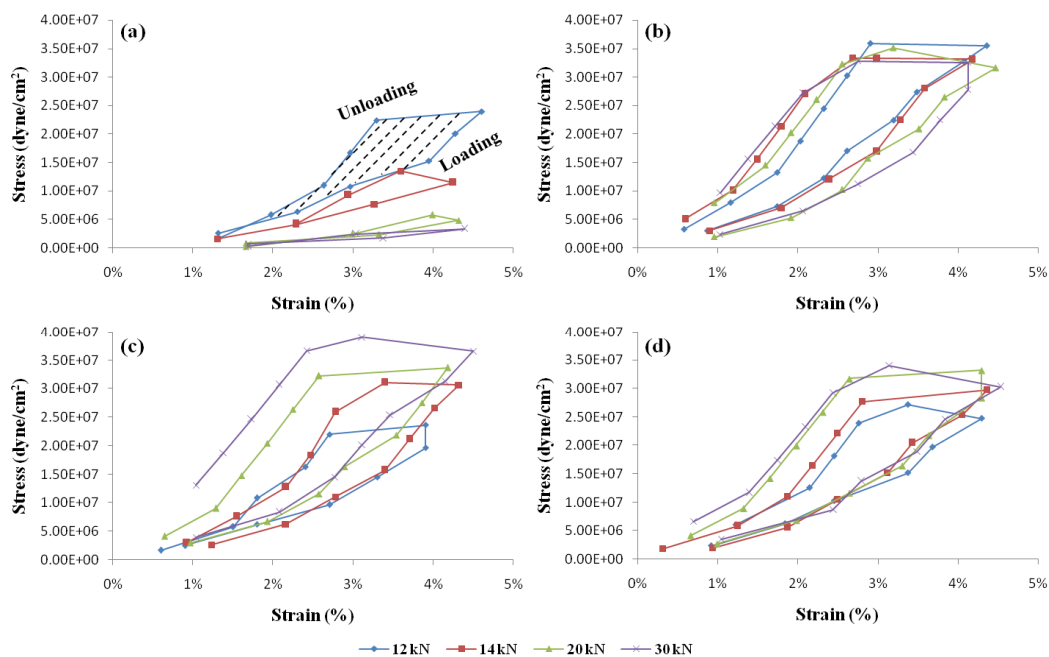
Figure 4.3: Compressive stress/strain loading and unloading curves, (a) pure mannitol tablet, (b) tablet of mannitol made at 110°C, (c) tablet of mannitol made at 150°C, (d) tablet of mannitol made at 170°C. Deformation target was 5% and probe speed 3 mm/sec. Specimens were compressed at 12, 14, 20 and 30 kN before testing. (a) also shows the area under curve (AUC) - highlighted - between loading and unloading which represents elastic strain energy (MJ/m^3). Each loading/unloading profile is representative of triplicate measurements (n=3).

Between the different mannitol batches, the ones sprayed at 150 and 170°C showed no significant difference in strain energy (ANOVA, p>0.05) between each other. Mannitol made at 110°C showed a significantly higher (ANOVA/Tukey, p<0.05) energy released at the low compression force of 12 kN (0.31 ± 0.024 MJ/m^3) than mannitol made at 150 (0.21 ± 0.030 MJ/m^3) and 170°C (0.20 ± 0.009 MJ/m^3), while there was no significant difference (ANOVA, p>0.05) at the highest compression force of 30 kN (0.46 ± 0.017, 0.48 ± 0.066 and 0.44 ± 0.014 MJ/m^3 respectively). This indicated that at the lower compression force (12 kN), mannitol 110°C exhibited higher elastic recovery capacity than mannitol 150 and 170°C that was hampered due to fragmentation at the higher compression force (30 kN).

Generally, the spray dried mannitol particles behaved like 'micro-sponges' that resisted fracture especially in the case of mannitol 150 and 170°C where the air trapped in the pores resisted compressive stress in the axial direction (Antikainen and Yliruusi, 2003). According to Jarosz

184

and Parrott (1982), strains are magnified about regions of low density and upon releasing the force, a mechanical failure may occur which leads to capping. Moreover, the formation of a continuous crust on the particle surface during spray drying (which will be discussed in 4.3.3), also proved to be resistant to crushing, hence the particles in Figure 4.1 (especially h) retained their original shape.

4.3.3. Particle formation mechanisms

The influence of spray drying temperature on particle formation and pore generation was studied using hot stage microscopy. Drying of liquid droplets of the optimum formulation mixture (mannitol 10% w/v and ammonium bicarbonate 5% w/v) at different temperatures (110-170°C) revealed different crystallization kinetics. All the formulations showed bursting gas bubbles indicating NH_4HCO_3 decomposition into $H_2O\uparrow$, $CO_2\uparrow$ and $NH_3\uparrow$ during mannitol particle formation. Particles produced at the lower temperature of 110°C were slightly larger in size (17.93 ± 1.29 µm) than the particles produced at 150 and 170°C (16.03 ± 0.48 and 13.32 ± 0.93 µm) respectively.

At the lowest temperature 110°C, crystallization of mannitol occurred almost instantly (Figure 4.4 a and b) due to the strong tendency of mannitol to crystallize (Yu et al., 1998). The size of the spray dried particles was dependant on the drying temperature and in turn the drying rate. The obtained results are in agreement with Maas et al. (2011), as the low drying temperature (110°C) resulted in faster droplet crust formation/crystallization which upon liquid evaporation forms large crystals.

The formulation dried at 150°C showed different drying kinetics to that of the formulation at 110°C. The droplet formed a smooth continuous crust at the surface with small patches of pores (appear as black dots in Figure 4.4 c and d). Upon puncturing the droplet using a thin needle, the surface layer was removed easily revealing mannitol crystals slowly growing inside the particle (Figure 4.4 e and f). This interesting drying behaviour was attributed to slower

185

crystallization of mannitol particles at this temperature which resulted in better organization of the crystals on the surface of droplet and hence regular shaped spherical particles were formed (SEM in Figure 4.1 e). Particle size was smaller for the particles produced at 150°C in comparison with 110°C, due to both faster drying rate at 150°C and slower crystallization nucleation rate for mannitol. At 170°C, hot stage images were unobtainable due to inability of mannitol to crystallize above its melting point of 165°C resulting in dark images with no features. However, in reality spray drying temperature vary along the chamber and through the cyclone down to the collector. The outlet temperature is always lower than inlet temperature and resulted in crystallization of mannitol between 90 and 100°C.
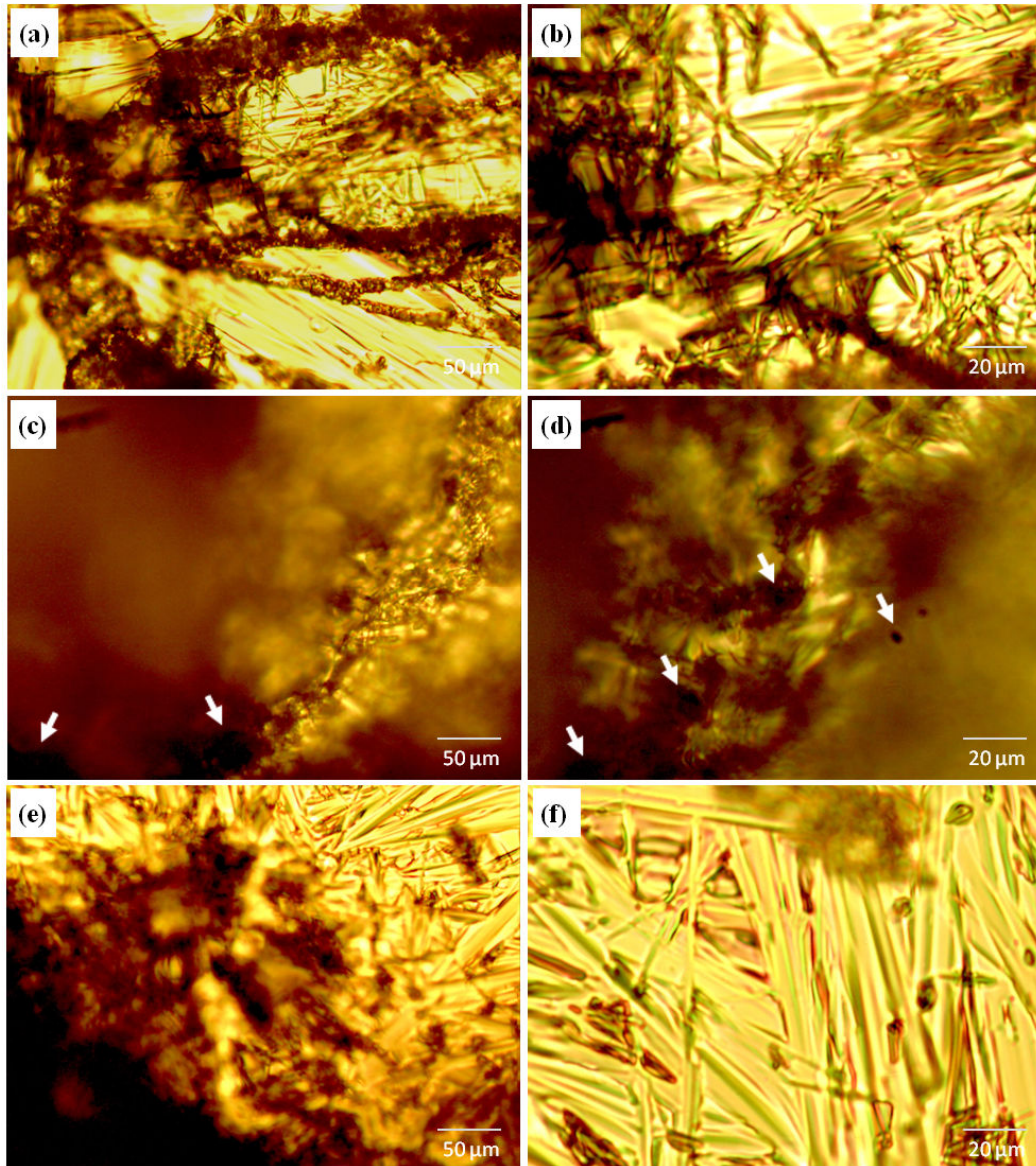
Figure 4.4: HSM images of mannitol (10% w/v) and NH$_4$HCO$_3$ (5% w/v) droplets dried on a preheated hot stage microscope slide at 110°C (a and b), 150°C (c and d), 150°C (e and f) after removal of surface crust using a thin needle to reveal growing crystals. Arrows show surface pores formed during the process.

4.3.4. Thermal and polymorphic properties

Thermal and polymorphic profiling methods (DSC, TGA and XRD) were utilized to understand fabricated mannitol particular physico-mechanical properties. DSC scans showed a 3°C shift (ANOVA, $p<0.001$) in melting onset from 165.51 ± 0.13°C for pure mannitol to 162.18 ± 0.43 - 162.86 ± 0.11°C for mannitol 110-170°C respectively (Figure 4.5). TGA also confirmed a slight

difference between pure and fabricated mannitol (Figure 4.5) as the latter showed a step transition pertinent to weight loss at 166.88°C which was absent from pure mannitol. There was a trend for weight loss at this temperature which followed the order from the highest: 110°C (0.81 ± 0.07%) > 150°C (0.51 ± 0.12%) > 170°C (0.43 ± 0.15%). This in turn confirms the loss was dependant on spray drying temperature and could be explained by volatilization of some entrapped water subsequent to melting of mannitol at 162°C. A further confirmation of this event is the moisture content of fabricated powders which was slightly higher than pure mannitol (Table 4.1). TGA was also used to confirm the decomposition temperature of pure ammonium bicarbonate that was confirmed to occur at 60°C (Figure 4.5).
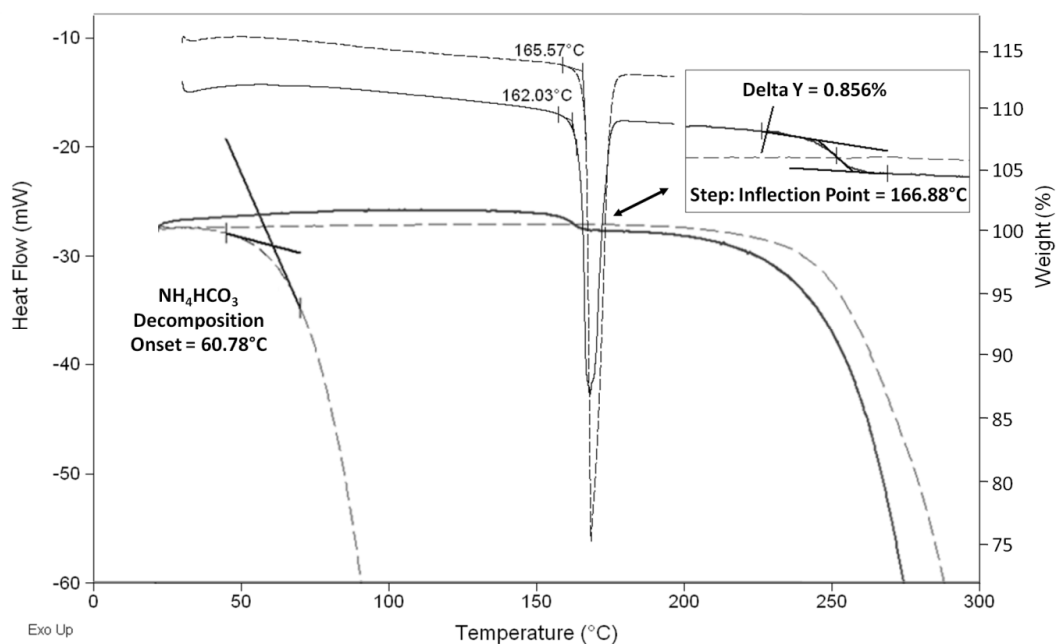
Figure 4.5: Overlaid DSC and TGA representative thermograms of pure mannitol (dashed lines), fabricated mannitol (solid lines) and ammonium bicarbonate (dashed on the left). DSC and TGA thermograms are representative of triplicate measurements (n=3).

DSC also showed a significant increase (ANOVA/Tukey, $p<0.05$) of melting onset upon increase in the spray drying inlet temperature between 110 and 170°C. The small differences in melting onsets (162.18 ± 0.43 to 162.86 ± 0.11°C) were attributed to generation of different polymorphs of mannitol (Burger et al., 2000). No significant difference (ANOVA, $p>0.05$) in enthalpy of fusion was found between the fabricated (243.33 ± 3.84 – 245.53 ± 8.57 J/g for 110

- 170°C) and pure mannitol (246.83 ± 1.40 J/g) powders. This meant that even if different polymorphs existed, they are very closely related as the energy required to melt the materials was almost similar. In fact, similar observation was reported by Burger et al. (2000) for the small energetic differences of D-mannitol β and α polymorphs which were manifested with small differences in heats of fusion.

Using XRD, no amorphous phase was detectable and it was not in the interest to seek more sensitive techniques because mannitol is known to be a poor glass former (Yu et al., 1998). However, XRD confirmed the presence of polymorphic forms as anticipated. Figure 4.6 shows that pure mannitol is crystalline made up of β type whereas mannitol spray dried at 110 - 170°C is also crystalline made up of mixtures of β and α polymorphs. In Figure 4.6, some of the peaks for β polymorph decline in intensity while other peaks appear for α polymorph. No δ polymorph (thermodynamically unstable form) could be observed which is consistent with the DSC results (no melting peak at 155°C).

The observed polymorphic forms have different compression profiles under pressure as reported earlier by Burger et al. (2000), which ultimately contributed to the particular plasticity or fragmentation behaviours. Interestingly, the use of ammonium bicarbonate during spray drying of mannitol led to the appearance of α polymorph in contrast to observations by Hulse et al. (2009) which reported conversion of commercial mannitol (sprayed alone) to β type upon re-spray drying. Despite this, our results agree with Maas et al. (2011) who reported that α polymorph exists alongside β polymorph and that its amount increases with the increase of spray drying outlet temperature.

The generation of β polymorph at low temperatures leads to fragmentation because the particles were formed from large droplets with defined larger surface crystallites and possibly hollow internal structure. This is in turn one reason why it is brittle due to the inside porosity. On the other hand, the generation of α polymorph at higher temperatures leads to more plastic

behaviour due to the formation of internal crystals as well as surface crystals which ultimately compress on each other under the effect of compression pressure.
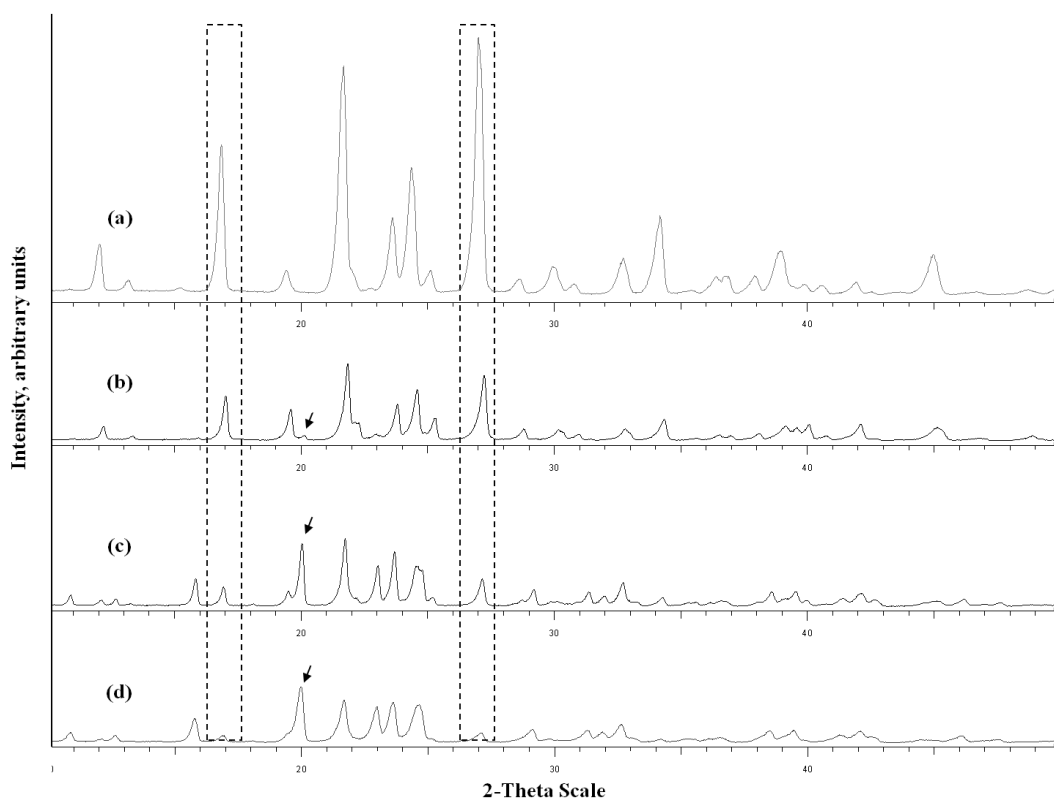
Figure 4.6: XRD for pure and fabricated mannitol powders. (a) pure mannitol, (b) mannitol made at 110°C, (c) mannitol made at 150°C and (d) mannitol made at 170°C. The dashed rectangles show a declining intensity for β polymorph at 2θ 16° and 26°. The arrows show an increased intensity of α polymorph peak at 2θ 20°. Each XRD pattern is representative of triplicate scans (n=3).

As a result, mannitol made at 110°C showed brittle fracture (fragmentation) profile as the mixture has a significant amount of β polymorph (96.77% w/w). However, the high hardness observed could be attributed to the presence of 3.23% w/w α polymorph (appearing at 2θ of 20°) that act, due to lower die friction and better compressibility (Burger et al., 2000), as a binder between the clean surfaces resulting from fragmentation of β polymorph. On the other hand, mannitol made at 150 and 170°C showed high hardness related to the increase in α polymorph (63.2 and 84.1% w/w respectively) which is the predominant polymorph at these temperatures.

XRD patterns obtained for mannitol tablets were not different from the patterns obtained for powders, which confirms that no crystallographic changes have occurred during compression. Additionally, the elastic recovery tendency of mannitol tablets noticed earlier could also be related to the mixture of polymorphic forms and the anticipated change in the strength of the constituent crystals. The resultant mixture of polymorphs potentially led to non-homogeneity and anisotropy of the tablets (Train, 1957; Kandeil et al., 1977; Nyström et al., 1978). Therefore, the tablets exhibited capping tendency at high compression forces despite the radial strength (diametral crushing strength) being quite high.

4.4. Conclusion

Spray drying mannitol resulted in higher porosity due to evaporation of ammonium bicarbonate and increased hardness due to changing particle densification mechanism. The resultant particles retained surface pores produced due to ammonium bicarbonate decomposition and gas expulsion through the forming crust. The porosity significantly increased for both powder and tablets in comparison with pure mannitol and was responsible for the faster disintegration of ODTs due to wicking action.

Spray drying temperature significantly affected the particles' micromeritic, physico-mechanical and polymorphic properties. Tablets made from engineered mannitol showed a significant increase (up to 150%) in hardness and reduction (50 - 77%) of disintegration time in comparison with pure mannitol.

Mannitol particles made at low temperature (110°C) showed densification by fragmentation followed by particle bonding. Fragmentation possibly occurred due to strong tendency of mannitol to crystallize at the low temperature resulting in irregular crystalline particle morphology. The produced particles were also larger (17.93 ± 1.29 μm) than the particles sprayed at the higher temperatures (16.03 ± 0.48 and 13.32 ± 0.93 μm at 150 and 170°C respectively), due to slower drying rate at 110°C, therefore, they were more susceptible to

fracture under pressure. In addition, the polymorphic composition of the powder produced at low temperature revealed it had a significant proportion (96.77% w/w) of β polymorph besides small quantity (3.23% w/w) of α polymorph. The latter acts, due to lower die friction and better compressibility, as a binder between the clean surfaces resulting from fragmentation of β polymorph thereby producing strong tablets.

On the other hand, mannitol particles sprayed at the higher inlet temperatures (150 and 170°C) showed more flexibility under compression (plasticity) due to the formation of a regular crust on the droplet surface during spray drying. The regular crust formation was attributed to slower crystallization of mannitol particles at the higher temperatures which resulted in better organization of the crystals on the surface of droplet and hence regular shaped spherical particles were formed. Furthermore, the produced particles were smaller in size due to the faster drying rate. The high hardness resulted from mannitol particles at high temperatures was also related to further increase in α polymorph which is the predominant polymorph (63.2 and 84.1% w/w at 150 and 170°C respectively) at high temperatures and known to exhibit lower die friction, hence better compressibility. However, the flexibility and relatively high internal porosity, especially at 170°C, resulted in the particles retaining high elastic strain energy. The latter was responsible for elastic recovery tendency observed for the spray dried mannitol particles.

While chapters 3 and 4 dealt with excipients blending/processing and particle engineering to develop ODTs, the next chapter will focus on a different challenge which is the development of modified release microparticles for taste masking and enteric coating within ODT to expand the dosage form applications.

Chapter 5

Aqueous-Based Microencapsulation of Insoluble Drugs for Modified Release ODT Development

5.1. Introduction

Taste masking of unpalatable drugs represents a considerable challenge to the formulator of age-appropriate products (Nunn and Williams, 2005). For ODTs, the formulation process is even more challenging as the currently available technologies utilize multiple coating layers around a drug core to achieve the desired taste masking (Shimizu et al., 2003 a). For instance, formulation of ODTs containing coated/taste masked proton pump inhibitors (PPIs) was attempted previously and has proved to be a very challenging endeavour (FDA, 2011). Omeprazole is unpleasant tasting PPI which is used to inhibit gastric acid secretion in patients suffering from gastro-oesophageal reflux disease (GERD) or stomach ulcers (Lindberg et al., 1990). The current oral formulations of the drug are available as enteric coated pellets/granules filled in a capsule or embedded in a tablet (Joint Formulary Committee, 2012). These dosage forms may not be considered appropriate for paediatrics and geriatrics that have swallowing difficulties (dysphagia). ODT is a promising drug delivery system for omeprazole as it combines the benefits of both tablets (i.e. stability) and liquid formulations (i.e. easily swallowed after disintegration in the mouth).

Many challenges should be addressed during formulation development of an omeprazole ODT. These could be categorized into: (a) drug-specific challenges such as instability in acidic media of stomach and poor water solubility of the drug, (b) general formulation challenges such as development of ODT with optimal particle properties for good mouth-feel and (c) process related challenges such as the development of aqueous process (eco-friendly) using scalable and continuous manufacturing methods.

In this study, hydroxypropyl methyl cellulose acetate succinate (HPMCAS) which is a pH-responsive polymer that is insoluble in the acidic pH of stomach and soluble at near neutral pH (grade HF dissolves at pH 6.8) was investigated for its taste masking/gastro protective properties. The new formulation is anticipated to prevent drug release in the mouth and stomach before reaching the small intestine. When the encapsulated drug is in the small intestine, acidic

groups of HPMCAS ionise causing the polymer to dissolve and release the drug for subsequent absorption (Nagai et al., 1997).

D-α-tocopheryl polyethylene glycol 1000 succinate (TPGS) was used to solubilise omeprazole by formation of micelles in solution. TPGS is a surface-active pharmaceutical excipient that is known for its ability to enhance solubility and permeability of hydrophobic drugs (Mu and Feng, 2003; Sheu et al., 2003). The solubilisation of omeprazole in micelles, would not only improve the physical stability of drug during formulation, but also minimizes interaction with the coating polymer (HPMCAS) solution. TPGS comprises a long hydrophobic chain of α-tocopheryl and a bulky hydrophilic polyethylene glycol (PEG) group (Figure 5.1). When TPGS micelles are formed, the hydrophobic drug (omeprazole) associates itself within the hydrophobic region while a water soluble form of HPMCAS (neutralised using ammonia solution) associates within the hydrophilic region. This will ensure that omeprazole positions itself inside TPGS and HPMCAS layers.

Figure 5.1: Structure of TPGS showing a hydrophobic α-tocopheryl chain on the right side of the molecule and a hydrophilic polyethylene glycol (PEG) group on the left side of the molecule. Both sides (hydrophobic and hydrophilic) are connected by succinic acid (Mu and Feng, 2003).

Upon spray drying, water would evaporate from the formulation solution leading to precipitation of TPGS over omeprazole (serves as a subcoat layer) and the formation of an HPMCAS crust over the TPGS layer (forming an outer protecting layer). An illustration of the microparticle produced is shown in Figure 5.2 whereby the TPGS subcoat helps to prevent chemical interaction of omeprazole with the HPMCAS enteric coating layer.
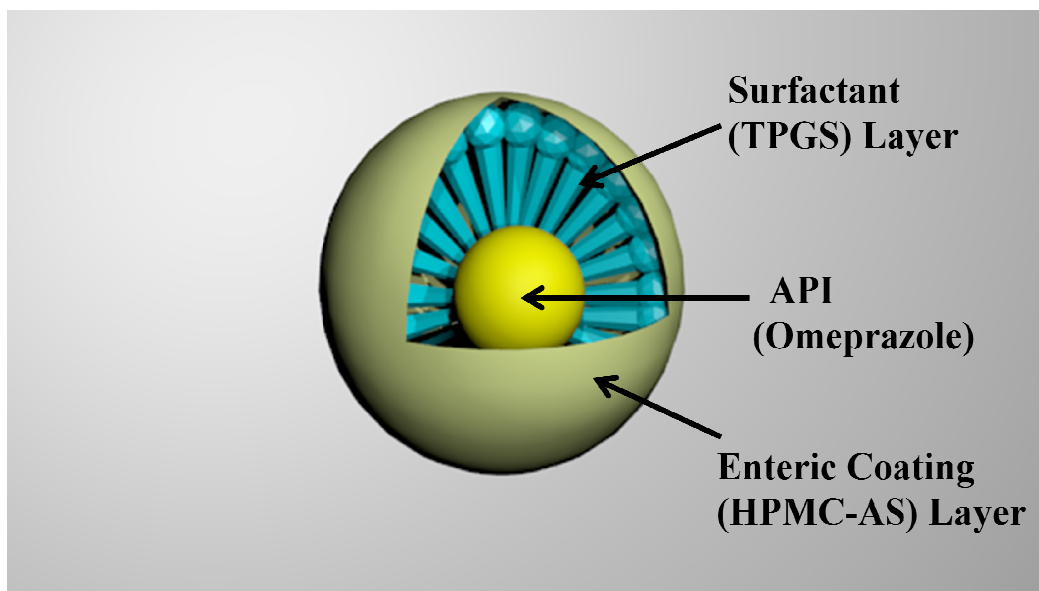
Figure 5.2: An illustration of the final coated microparticle of omeprazole showing the drug in the middle enclosed in a subcoat of TPGS and an outer coating layer of HPMCAS. The microparticle produced would be spherical in shape as a result of spray drying process.

The purpose of this study was to develop taste masked/enteric coated microparticles to be incorporated into ODT formulation for the delivery of insoluble acid sensitive compounds.

- Spray drying was utilised in this study to formulate omeprazole microparticles as a model hydrophobic acid-labile drug.

- Formulation optimisation was carried out in stages to find out the optimal level of each excipient and successful formulation parameters.

- Spray drying process optimisation was carried out using design of experiments (DOE) to enable rational use of process parameters within an optimised design space.

- The resultant encapsulated drug would then be compressed into ODT and its drug release properties assessed.

5.2. Materials and methods

5.2.1. Materials

D-α-tocopheryl polyethylene glycol 1000 succinate (TPGS), phosphate buffered saline (PBS), calcium hydroxide, sodium citrate dihydrate, sodium hydroxide, sodium nitroferricyanide, sodium hypochlorite, phenol and anhydrous dibasic sodium phosphate were purchased from Sigma-Aldrich (Pool, UK). Ammonia solution (ammonium hydroxide), acetonitrile and concentrated hydrochloric acid were purchased from Fisher Chemicals (Loughborough, UK). Omeprazole (Omeprazolum, complies with Ph. Eur., purity of ≥99) was obtained from Fagron (Newcastle upon Tyne, UK). Sodium bicarbonate was purchased from Acros Organics (New Jersey, USA). Hydroxypropyl methyl cellulose acetate succinate (HPMCAS, AQOAT-HF) was obtained from Shin-Etsu (Tokyo, Japan). Methacrylic acid-methyl methacrylate copolymer (1:2) (Eudragit S100) was obtained from Evonik Industries (Darmstadt, Germany). All the chemicals were used without further purification.

5.2.2. Methods

5.2.2.1. Preparation of feed (coating) solution of omeprazole

A multi-stage progressive approach was used to establish omeprazole stability in solution. Formulations containing different combinations of drug and excipients were prepared (Table 5.1) to investigate the effect of pH and formulation excipients on stability of omeprazole. Stage 1 involved dissolving TPGS (20 mg) in 10 mL distilled water at 37°C (melting point of TPGS) followed by cooling the micellar solution to room temperature (20-26°C). Omeprazole (10 mg) was added to the micellar solution of TPGS, stirred for approximately 15 min followed by recording of pH and colour changes.

Stage 2 involved preparation of two solutions/suspensions firstly by adding 74 mg of $CaOH_2$ (basic compound) to TPGS micellar solution (prepared by addition of 20 mg TPGS melted at

37°C in 10 mL distilled water), which was followed by addition of 10 mg omeprazole and stirring for 15 min to obtain a white/cloudy solution. The second solution was prepared by addition of 840 mg of $NaHCO_3$ (basic compound) to a new micellar solution of TPGS (prepared similarly to previous regimen) followed by addition of omeprazole (10 mg) to obtain a white/cloudy solution after stirring for 15 min. pH and colour changes were recorded before taking the second solution to the next stage of formulation development.

Stage 3 involved firstly the addition of Eudragit S100 (100 mg) to a solution prepared from 840 mg $NaHCO_3$, 20 mg TPGS and 10 mg omeprazole in 10 mL distilled water (prepared according to previous regimen), and secondly the addition of HPMCAS (100 mg) to similar solution (840 mg $NaHCO_3$, 20 mg TPGS and 10 mg omeprazole in 10 mL distilled water). Each of the formulations containing either Eudragit S100 or HPMCAS was compared (by monitoring pH and colour changes) to formulations containing same ingredients but without TPGS or without both TPGS and $NaHCO_3$ (Table 5.1).

In Stage 4, $NaHCO_3$ was replaced with ammonia solution to avoid problems related to using sodium in specific patient populations. The presence of sodium ions would be problematic in terms of the final powder properties as sodium ions (from $NaHCO_3$) cannot be easily removed from the produced powder (Alhnan et al., 2011). If sodium is retained in the powder, it could lead to a premature release of the drug (burst effect) from the coated particle (Cruz et al., 2009); furthermore, the formulation would be less suitable for patients with cardiovascular conditions (Geleijnse et al., 2007). Moreover, it was reported that omeprazole/$NaHCO_3$ combination can result in a bitter and unpleasant taste (Whaley et al., 2012). For the above reasons, $NaHCO_3$ was replaced with NH_3 solution to modify pH of the formulation to alkaline as well as to neutralize the enteric polymer rendering it soluble and exploitable for spray drying. 40 mg of TPGS was added to distilled water (20 mL) and stirred at 37°C until dissolved then left to cool down to room temperature. Ammonia solution (50 μL) was added to TPGS micellar solution followed by addition of 20 mg omeprazole. After 15 min of stirring, HPMCAS (1.54 g) was added to

omeprazole micellar solution plus further 1 mL of ammonia to obtain a homogenous polymer solution. This formulation was taken forward to spray drying to produce omeprazole coated microparticles.

5.2.2.2. Spray drying of feed solution to produce omeprazole coated microparticles

The formulation prepared in stage 4 was spray dried using Mini Spray Dryer B-290 from Buchi (Flawil, Switzerland) equipped with lateral outlet glass cylinder and 1.5 mm nozzle. The process parameters included: feed rate 10% (145 mL/h), inlet temperature 180°C, outlet temperature 103-105°C, gas used was air with co-current flow at a rate of 670 NormL/h (55 mm rotameter reading) and aspirator rate 90%. At the end of each run, white to beige powder was collected, weighed and assayed for yield, acid resistance, encapsulation efficiency and particle size.

Table 5.1: Different formulations of omeprazole using TPGS as micelles forming surfactant, HPMCAS and Eudragit S100 as enteric coating polymers, NaHCO$_3$, Ca(OH)$_2$ and NH$_3$ as pH modifiers.

Formulation No.	TPGS % (w/v)	Omeprazole % (w/v)	NaHCO$_3$ % (w/v)	Ca(OH)$_2$ % (w/v)	NH$_3$ % (w/v)	HPMCAS % (w/v)	Eudragit S100 % (w/v)
1	0.2	0.1	-	-	-	-	-
2	0.2	0.1	-	0.74	-	-	-
3	0.2	0.1	8.4	-	-	-	-
4	0.2	0.1	8.4	-	-	-	1
5	0.2	0.1	8.4	-	-	1	-
6	-	0.1	-	-	-	-	0.5
7	-	0.1	-	-	-	0.5	-
8	-	0.1	8.4	-	-	-	0.5
9	-	0.1	8.4	-	-	0.5	-
10	0.19	0.09	-	-	4.38	7.31	-

5.2.2.3. Formulation optimisation

5.2.2.3.1. Influence of drug-to-polymer ratio and solid concentration on microencapsulated powder properties

Feed solutions were prepared according to the previous method stated in stage 4 of 5.2.2.1 using decreasing HPMCAS concentrations (7.31, 4.75, 4.27, 3.80, 3.33 and 2.37%, w/v) with fixed concentrations of omeprazole, TPGS, NH_3 (0.09%, w/v), (0.19%, w/v) and (4.38%, w/v) respectively. The prepared solutions were spray dried following process parameters detailed in 5.2.2.2. Microencapsulated particles were collected and tested for yield, acid resistance, encapsulation efficiency and particle size.

5.2.2.3.2. Influence of TPGS concentration on microencapsulated powder properties

A formulation was prepared according to the previous preparation regimen and spray drying process parameters (in 5.2.2.3.1) except for TPGS which was reduced from 0.19% (w/v) to 0.095% (w/v) to assess the effect of TPGS on microencapsulated powder properties. The concentration of other formulation excipients were 0.09% (w/v) omeprazole, 3.80% (w/v) HPMCAS and 4.38% (w/v) NH_3. Microencapsulated particles were collected and tested for yield, acid resistance, encapsulation efficiency and particle size.

5.2.2.3.3. Effect of reduction of feed solution volume on microencapsulated powder properties

The feed solution volume was reduced from 60 mL to 40 mL, as a result, concentration of excipients increased to 0.14% (w/v) TPGS, 0.14% (w/v) omeprazole, 5.56% (w/v) HPMCAS and 6.42% (w/v) NH_3. The formulation was prepared using the formulation procedure and spray drying parameters from previous experiment (5.2.2.3.2). Microencapsulated particles were collected and tested for yield, acid resistance, encapsulation efficiency and particle size.

5.2.2.3.4. Effect of omeprazole concentration on microencapsulated powder properties

Omeprazole concentration was increased to 0.23% (w/v) and 0.46% (w/v) while other excipients were fixed at 0.14% (w/v) TPGS, 5.56% (w/v) HPMCAS and 6.42% (w/v) NH$_3$. The formulation was made using the same preparation procedure and spray drying conditions from previous experiment (5.2.2.3.3). Microencapsulated particles were collected and tested for yield, acid resistance, encapsulation efficiency and particle size.

5.2.2.4. Spray drying process optimisation using mathematical modelling

Design of experiments (DOE) was carried out using MODDE software version 8 from Umetrics Inc. (New Jersey, USA) to analyse the effects of spray drying process parameters on product/process responses. A Central Composite Face-centred design (CCF) was suggested by the program as a first choice for carrying out experiments/screening of data. The model used is quadratic polynomial which consists of 24 runs and 3 centre points leading to a total of 27 experiments (Appendix B). The factors (independent variables) were inlet temperature, aspirator, spray gas flow and feed rate with three levels (high, medium and low) as shown in Table 5.2 while the recorded responses (dependent variables) were outlet temperature, particle size, encapsulation efficiency, moisture content and yield.

Table 5.2: Independent process variables and their variation levels (also coded) selected for the optimisation of spray drying.

Process parameter	Level		
	High (+1)	Medium (0)	Low (-1)
Inlet temperature (°C)	180	150	110
Aspirator rate (%)	90	70	50
Spray gas flow rotameter reading (mm)	60	50	30
Feed rate (%)	30	20	10

At the end of each run, white to beige powder was collected, weighed and assayed for yield, encapsulation efficiency, particle size and moisture content. The results were fed back into the MODDE software and fitted using partial least squares (PLS) method.

5.2.2.5. Stability study protocol

Powder samples of coated omeprazole (made using 1:45 drug-to-polymer) were incubated in Firlabo SP-BVEHF stability cabinets (Meyzieu, France) at long term (25°C ± 2°C/60% RH ± 5% RH) and accelerated stability (40°C ± 2°C/75% RH ± 5% RH) conditions recommended by ICH Q1A(R2) (ICH, 2003). Samples were monitored at day 0 and 14 by analysing DSC thermograms for thermal changes, FTIR for possible chemical change, HPLC using stability-indicating method for drug concentration or appearance of degradation products, visual inspection for any discoloration and resistance to acid test using 0.1 N HCl. Samples were stored in dark conditions using plastic bottles double wrapped with parafilm.

5.2.2.6. Drug release study

Percentage drug release (%) was performed for loose coated powder (250 mg containing 5 mg omeprazole) and for 500 mg ODT compressed at 16 kN (containing 250 mg at 50% w/w drug loading which equates to 5 mg omeprazole dose) discussed in Chapter 3. Release media, test duration and temperature were in accordance with the USP monograph for omeprazole delayed-release capsules (USP Convention, 2012 b). However, the test was carried out in proportionally smaller volumes (60 mL beaker) to allow for subsequent HPLC quantification. The acid resistance stage was carried out in 27.7 mL of 0.1 N HCl (pH 1.5-2) for 2 h. After withdrawal of a 1 mL aliquot, 22.3 mL of 0.235 M dibasic sodium phosphate (pH 10.4) was added to the 0.1 N HCl medium and adjusted to pH 6.8. Sampling was carried in intervals up to 1 h in buffer stage. Samples were passed through a 0.45 µm nylon filter (Chromacol ltd, Hertfordshire, UK) followed by HPLC analysis using the procedure in 5.2.2.9. Release vessel and replacement

media were equilibrated at a temperature of 37 ± 0.5°C and rotated at 50 RPM. Media were replaced immediately after each sampling aliquot was taken.

5.2.2.7. Scanning electron microscopy (SEM)

SEM of omeprazole microparticles was performed using Stereoscan 90 electron microscope from Cambridge Instruments (Crawley, UK). Approximately 1 mg of microparticles was placed onto a double-sided adhesive strip on an aluminium stub. The specimen stub was coated with a thin layer of gold using a sputter coater Polaron SC500 from Polaron Equipment ltd. (Watford, UK) at 20 mA for 3 min followed by sample examination using SEM. The acceleration voltage (kV) and the magnification can be seen on each micrograph.

5.2.2.8. Differential scanning calorimetry (DSC)

DSC Q 200, from TA Instruments (Delaware, USA) was used for thermal analysis of pure omeprazole, its coated microparticles, HPMCAS and physical mixture at a drug-to-polymer ratio of 1:45. Accurately weighed samples (3 mg each) were transferred into non-hermetically sealed Tzero aluminium pans and heated in the range of 30 - 200°C at a rate of 10°C/min under a nitrogen purge (50 mL/min). This was followed by analysis of resulting graphs using TA instruments universal analysis 2000 software (V 4.5A).

5.2.2.9. High performance liquid chromatography (HPLC)

RP-HPLC analysis was performed based on a method by Alhusban et al. (2011) and Türkoğlu et al. (2003). Two HPLC systems were utilised: a) Thermo Scientific HPLC (Massachusetts, USA) which consisted of SpectraSystem SCM 1000 vacuum degasser, P2000 pump, AS1000 auto sampler and UV6000 Photo Diode Array (PDA) detector for investigation of omeprazole and other formulation excipient peaks. b) HPLC system from Dionex, (also currently owned by Themo Scientific) was used for omeprazole quantification. The system consisted of AS50 autosampler, GP50 gradient pump, and UVD170U detector.

Separation was carried out using Eclipse XDB-C18 reversed phase column, 5 um, 4.6 X 150 mm. The analysis was performed using a fixed flow of 1 mL/min acetonitrile: phosphate buffered saline (PBS) (28:72 v/v, pH 8.38). The run time was 10 min and detection carried out at both 280 nm and PDA 3D mode.

HPLC-PDA analysis involved detecting and confirming omeprazole identity in the coated formulation dissolved in acetonitrile: PBS (28:72, v/v) at 0.5 mg/mL. This phase also involved the investigation of other peaks that appeared in the formulation chromatogram. The concentration of coated formulation dissolved in the mobile phase was increased to 2.5 mg/mL. Furthermore, a number of formulations were made with decreasing concentration of coating polymer (HPMCAS), TPGS, water content and drug: polymer ratio (Table 5.5) to elucidate the identity of formulation peaks.

Omeprazole quantification was carried by dissolving each powder in acetonitrile: PBS (28:72), followed by filtering using 0.45 μm nylon filter (Chromacol ltd, Hertfordshire, UK) and injecting 20 μL into the Dionex HPLC system. Detection was carried out at 280 nm and a calibration curve (R^2 = 0.998) was developed between 5 and 160 μg/mL to assay for the quantity of omeprazole (μg) in mg of spray dried powder. The method denoted (1) was validated for linearity, precision, specificity, LLOD and LLOQ according to ICH Q2(R1) and assessed for stability-indicating capacity under heat/humidity (40°C/RH 75%) and acid degradation (pH 1-2) conditions (ICH, 2005).

The method was revalidated (denoted 2) for change in sample preparation during release study. A calibration curve (R^2 = 0.995) was developed between 5 and 160 μg/mL. The calibration standards were made from pure omeprazole dissolved in 50:50 release medium buffer pH 6.8: (acetonitrile: PBS, 28:72). Calibration standards' pH was 7.47. Validation was carried out according to ICH Q2(R1).

5.2.2.10. Fourier transform infrared spectroscopy (FTIR)

FTIR spectra of omeprazole, coated omeprazole and formulation excipients were captured in the region 400–4000 cm^{-1} using Nicolet IS5 FTIR spectrometer equipped with an iD5 attenuated total reflectance (ATR) diamond from Thermo Fisher Scientific (Massachusetts, USA). Approximately 50 mg of each powder was placed on the diamond plate followed by 16 scans /sample (n=3).

5.2.2.11. Limit of ammonia assay

Ammonia was assayed in the omeprazole coated powder (1:45 drug-to-polymer) using the USP official method (USP Convention, 2012 c). To 4 mL of the sample solution, 0.4 mL of phenol test solution was added followed by 0.4 mL of diluted sodium nitroferricyanide solution, and 1 mL of oxidizing solution (alkaline sodium citrate test solution and sodium hypochlorite solution (4:1)). Dilution with water to 10 mL was carried out, and the sample was allowed to stand for 1 h. The procedure was also performed for a control consisting of ammonia solution.

5.2.2.12. Yield determination

Total yield of the spray drying process was assessed by weighing the mass of powder produced and calculating using the equation below:

$$\text{Yield (\%)} = \frac{\text{Mass of collected particles}}{\text{Mass of solid content in feed solution}} \times 100$$

5.2.2.13. Microparticles resistance to 0.1 N hydrochloric acid and pH threshold test

20 mg of omeprazole microparticle powder was dispersed in 20 mL of 0.1 N HCl then observation for any colour changes continued for two hours. The results were compared against pure omeprazole (20 mg) dispersed in 20 mL of 0.1 N HCl which produced an intense yellow colour suggesting drug degradation (Mathew et al., 1995).

Colorimetric assessment of microparticles in solutions with different pH levels (2-7) was carried out to identify drug release pH threshold. Solutions were prepared by mixing different ratios of 0.1 N HCl (pH 1-2) with phosphate buffered saline (pH 7.2-7.6) and adjusted with 2 N NaOH whenever necessary. Microparticles (20 mg) were added to the solutions (20 mL) and left to stand for 2 h while visual inspection was carried out. The observation criteria were turbidity to indicate insolubility and clarity to indicate solubility of the coating polymer.

5.2.2.14. Encapsulation efficiency determination

Each powder was analysed for omeprazole content using HPLC method described previously in 5.2.2.9. Based on the concentration obtained from HPLC, mass of omeprazole in collected powder was calculated. This was followed by substituting into the equation of encapsulation efficiency (EE%):

$$\text{Encapsulation Efficiency (\%)} = \frac{\text{Calculated mass of drug in coated particles}}{\text{Theoretical mass of drug in coated particles}} \times 100$$

5.2.2.15. Particle size analysis

Particle size was measured by laser diffraction using particle size analyzer HELOS/BR and dry dispenser RODOS with feeder VIBRI/L from Sympatec (Clausthal-Zellerfeld, Germany). The measuring range of the lens was 0 - 175 μm. Approximately 2 g of each powder was placed in the feeder tray and the run started at trigger condition of 2% Copt for 10 sec with powder dispensing pressure of 3 bar. Volume mean diameter (VMD) and particle size distribution were recorded for all powders.

5.2.2.16. Moisture content analysis

Moisture content was quantified using Sartorius moisture balance (Surrey, UK). Approximately 100 mg of microparticles powder was placed in the balance pan where heat was applied at

105°C for a maximum of 2.8 min. The amount of moisture in the spray dried powder was represented by moisture (%) loss from the sample.

5.2.2.17. Statistical analysis

ANOVA and t-test were performed using GraphPad Prism 6.02 software (California, USA). Statistical significant difference was considered at a p value <0.05. Where applicable, all results are presented as mean ± SD for triplicate measurements to account for the noise encountered within the experiments. For DSC and FTIR, representative thermograms/spectra were presented out of the triplicate measurements.

5.3. Results and discussion

A new formulation was developed for taste masking/enteric coating of hydrophobic acid-labile drugs. TPGS was used to form micelles above its critical micelle concentration (CMC) 0.02% w/v (Yu et al., 1999) which can solubilise poorly soluble model drug omeprazole (Tanaka et al., 2009). The drug can be incorporated inside or within the micelles long hydrophobic tails (composed of α-tocopheryl) while the bulky hydrophilic group (composed of polyethylene glycol (PEG)) is exposed to the aqueous environment (Structure of TPGS, Figure 5.1). To the micellar solution, a coating polymer (HPMCAS) was added. As the latter polymer is insoluble in water, NH_3 solution (ammonium hydroxide) was used to neutralize the acidic groups (-COOH of acetyl and succinoyl) of HPMCAS rendering it soluble (structure of HPMCAS in Figure 5.3). No plasticizer was required for neutralised HPMCAS coating process (Anderson et al., 1996). Upon spray drying the prepared solution, water and ammonia evaporated leading to production of a powder of omeprazole coated by inner layer of TPGS and an outer layer of enteric coating polymer (HPMCAS).

Figure 5.3: Structure of HPMCAS showing the sites for substitution with succinoyl and acetyl groups. NH_3 addition neutralised the acidic carboxylic groups rendering the coating polymer (HPMCAS) soluble (Nagai et al., 1997).

PPIs (e.g. omeprazole, pantoprazole, etc.) and other drugs such as duloxetine experience instability during storage when coated directly with enteric coating polymers (Jansen et al., 1997). The acidic moieties (anionic) of HPMCAS tend to react with the drug (cationic) leading to changes in colour as a result of forming degradation products. A separating layer composed of HPMC or PVA has been used previously to overcome this problem (He et al., 2009), however, this has added extra steps of coating using conventional spray coater and also extra drying cycles. In contrast, spray drying potentially forms a microparticle composed of two layers (TPGS as separating layer and HPMCAS as coating layer) in one drying step due to heat-mass transfer (Gharsallaoui et al., 2007). As the surface area of the atomized feed solution is high, quick evaporation of the solvent occurs leading to formation of coating layers around the drug (Figure 5.2). The formation of omeprazole microparticle and its morphology was assessed using SEM. The micrographs (Figure 5.4) show spherical particles as well as agglomerates of approximately 10 μm diameter per particle. Certain degree of agglomeration is inevitable with standard laboratory spray dryers according to Goula and Adamopoulos (2005). This occurs as dehydration conditions do not permit rapid surface solidification before particles collide with each other, leading to agglomeration.
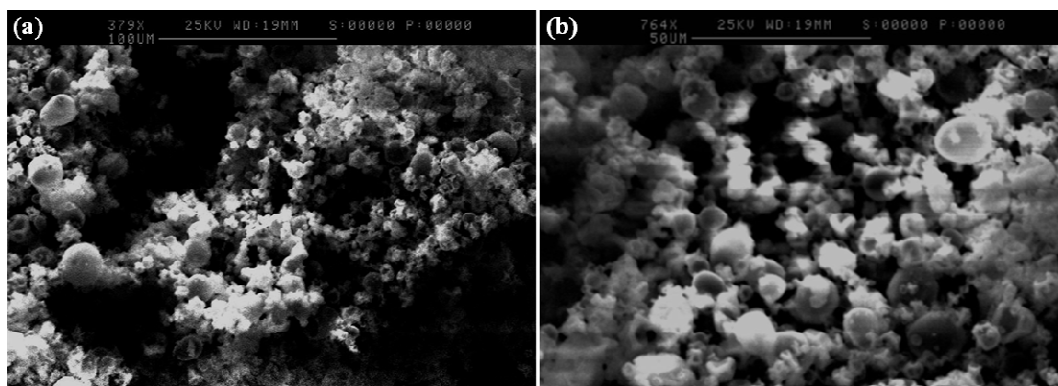
Figure 5.4: SEM images of omeprazole coated particles. (a) 100 µm view at 379X magnification and (b) zoomed image, 50 µm view at 764X magnification.

5.3.1. Influence of formulation excipients on omeprazole stability

Omeprazole was reported for its sensitivity to acidic pH, temperature, humidity and day light (Davidson and McCallum, 1996; Qaisi et al., 2006; Ruiz et al., 1998). It suffers from first-order or pseudo first-order degradation kinetics producing different colours in solution including yellow, purple or dark brown depending on the extent of degradation (Pilbrant and Cederberg, 1985; Mathew et al., 1995). This could be turned into an advantage in the context of formulation development as colour changes may indicate a degradation of the drug and allow the formulator to make changes promptly at early stages of development. In fact, the colorimetric changes were utilised in this work to assess coating efficiency and capacity to prevent drug leakage. Different formulations containing omeprazole were prepared (Table 5.1) followed by recording pH and colour changes. In 0.1 N HCl (pH 1 - 2), omeprazole degraded and a distinctive yellow colour was produced (Figure 5.5 b), this served as a control for comparison during successive formulation stages.
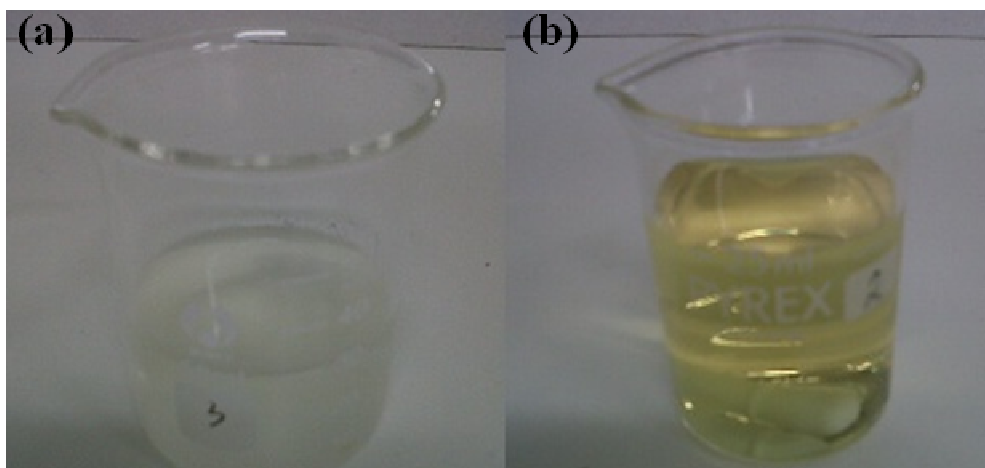
Figure 5.5: (a) Omeprazole coated formulation in 0.1N HCl (no degradation), (b) pure omeprazole in 0.1 N HCl (yellow solution produced in < 5 min indicating degradation).

Omeprazole was tested for its stability in TPGS micellar solution and found to degrade and produce a pink to light brown colour as the pH was around 5. Our observations were in agreement with experiments undertaken by Pilbrant and Cederberg (1985) who confirmed that omeprazole is stable at pH 4 for 10 min, at pH 6.5 for 18 h and at pH 11 for 300 days. In order to overcome this instability, the basic compounds, calcium hydroxide, sodium bicarbonate and ammonia were used to modify the pH (to alkaline) and stabilise omeprazole (See methods section 5.2.2.1). When calcium hydroxide was used, white aggregates formed as a result of addition of its suspension with no change in colour. However, this suspension would not be suitable for spray drying as it may block the feeding tube or nozzle of the instrument. When $NaHCO_3$ was added to TPGS, the pH changed to 8.1 (from 5) and upon addition of omeprazole (the pH changed back to 8.3) the micellar solution was stable for at least 2 hours. The solution produced was cloudy white which could be a micellar solution of omeprazole.

Eudragit S100 or HPMCAS were added to the above micellar solution which contains TPGS, omeprazole and $NaHCO_3$. pH value did not change considerably upon addition of either Eudragit S100 (pH 8.7 from 8.3) or HPMCAS (pH 8.8 from 8.4). The colour of the dispersed

polymers (white original colour of Eudragit and light yellow colour of HPMCAS) in solution did not change over two days of observation. No degradation occurred in the prepared formulations even though Eudragit S100 and HPMCAS contain acidic groups of methacrylic acid, acetic acid and succinic acid which can easily degrade omeprazole. This was further investigated by preparing suspensions of omeprazole and Eudragit S100 and of omeprazole and HPMCAS (without $NaHCO_3$). Both omeprazole suspensions produced a light pink colour after few minutes of preparation and the pH was reduced to 5.5 which confirmed that both Eudragit S100 and HPMCAS caused acidic degradation to omeprazole in the absence of a pH modifier/buffer. In both Eudragit S100 and HPMCAS formulations, the enteric polymers were suspended although solution formation was expected due to the addition of $NaHCO_3$. One possible explanation could be that $NaHCO_3$ only partially/slightly solubilised the enteric polymers as the concentrations of polymers were higher than the equivalent amount of sodium bicarbonate. In addition, when formulations were prepared with lower concentration of enteric polymers; $NaHCO_3$ neutralized the polymers forming a solution (reaction below).

$$R\text{-}COOH \quad + \quad NaHCO_3 \quad \rightarrow \quad R\text{-}COONa \quad + \quad H_2O \quad + \quad CO_2$$

Enteric polymer   Sodium bicarbonate   Polymer salt (soluble)   Water   Carbon dioxide
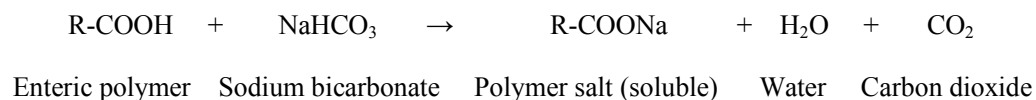
Omeprazole was stable in both formulations of HPMCAS and Eudragit S100 (i.e. no degradation products appeared in the solutions) as the pH was 8.8. In accordance with the above findings, a formulation containing TPGS, omeprazole, Eudragit or HPMCAS and $NaHCO_3$ (as a pH stabilizer and enteric polymer solubiliser) would be suitable for spray drying as it showed good physico-chemical stability and acceptable fluidity (low viscosity). The latter property is important in preventing clogging of the spray nozzle during operation (Rosenberg et al., 1990). $NaHCO_3$ was replaced with ammonia solution to modify the pH and neutralise the enteric polymer solution.

The reaction occurring as a result of addition of NH_3:

$$R\text{-}COOH \quad + \quad NH_3 \; + \; H_2O \quad \rightleftharpoons \quad R\text{-}COO^-NH_4^+ \quad + \quad H_2O$$

Enteric polymer   Ammonia solution   Polymer salt (soluble)   Water
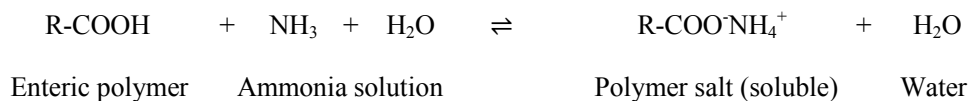
The formulation containing HPMCAS was taken forward to spray drying as the polymer grade used (HPMCAS-HF) contains less acidic moieties (acetyl and succinoyl) than Eudragit S100 which would be beneficial to reduce the interaction of enteric polymer with omeprazole. In addition, it was reported previously that the degradation half life ($t_{1/2}$) of omeprazole in HPMCAS-HF solution is longer (21 h) than in methacrylic acid polymer's solution (8 h) (Riedel and Leopold, 2005 a). During spray drying, water and ammonia evaporate thus dissociation of NH_4^+ from the neutralized polymer salt occur and the coating polymer returns to its initial acidic form (Alhnan et al., 2011). This form would be insoluble in the acidic pH of stomach thereby protecting the drug from degradation.

$$R\text{-}COO^-NH_4^+ \quad + \quad H_2O \quad \rightarrow \quad R\text{-}COOH \quad + \quad NH_3{\uparrow} \quad + \quad H_2O{\uparrow}$$

Enteric polymer salt (soluble)   Water   Enteric polymer   Ammonia and water evaporate
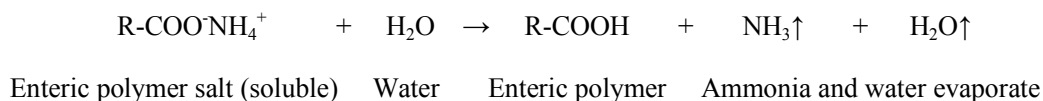
The produced powder was tested in 0.1 N HCl to assess the capacity of microparticles to provide necessary protection from drug acidic degradation. The polymer was successful in protecting the drug from acid as no colour change occurred over 2 h of observation (Figure 5.5 a).

5.3.2. Investigation of omeprazole in formulated microparticles

Differential scanning calorimetry (DSC) is a well established technique for the characterization of microparticles produced by spray drying (Bodmeier and Chen, 1988). DSC was used to investigate if omeprazole existed in the powder collected from spray drying. DSC scan of pure omeprazole (uncoated) showed a clear endothermic transition (melting onset) at 150.58°C

(Figure 5.6) followed by an exothermic peak for recrystallization of the drug at 161.95°C which is in agreement with the results reported by Ruiz et al. (1998). DSC also showed a transition at 64.37°C that looked like an upward baseline shift. This could be related to monotropic solid-solid transition (i.e. irreversible change to more stable form) especially as omeprazole is enantiomeric, shows polymorphism and also contains small amounts of related substances (Six et al., 2001; Council of Europe, 2005 a; Fagron, 2011). In contrast, there was no melting peak corresponding to the drug in the coated powder formulation produced by spray drying. DSC results indicated that either omeprazole did not exist in the coated formulation or converted into amorphous form as spray drying has previously shown to prevent recrystallization (Bhandari et al., 1997). Furthermore, omeprazole itself was reported to undergo crystalline to amorphous transition under processing or dehydration (Ruiz et al., 1998; Murakami et al., 2009). In fact, spray drying of omeprazole with a carrier such as methyl-β-cyclodextrin (MβCD) was reported previously to result in total amorphization of the drug (Figueiras et al., 2007). Nevertheless, a slight endothermic depression at 166.72°C was noticed in the coated formulation which corresponded with the degradation temperature of pure omeprazole (165.39°C).
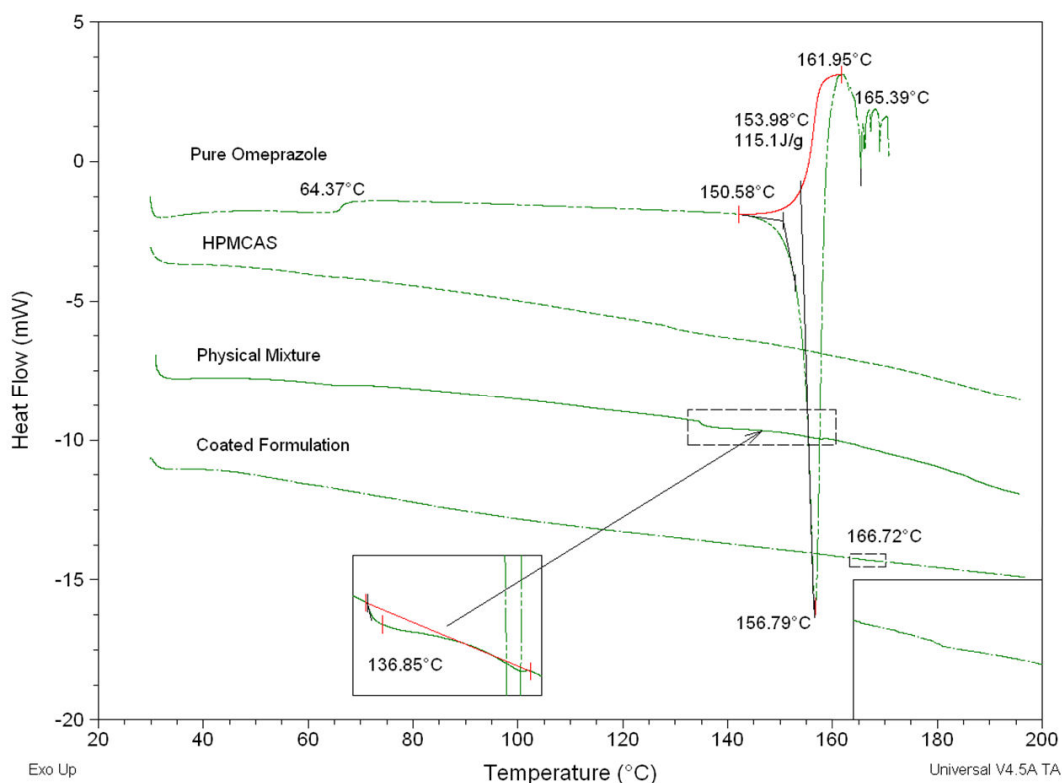
Figure 5.6: Overlaid DSC thermograms for pure omeprazole, coated omeprazole (1:45 drug-to-polymer), HPMCAS and physical mixture (1:45 drug-to-polymer) (3 mg each) heated at 10°C/min between 30-200°C. The figure shows melting onset for pure omeprazole at 150.58°C. Coated omeprazole showed no melting peak (amorphous) but a slight endothermic depression at 166.72°C corresponding to omeprazole degradation. DSC thermograms are representative of triplicate measurements (n=3).

A microencapsulation study conducted by Mu and Feng (2001) reported that spray drying resulted in the formation of amorphous or disordered-crystalline drug phase due to rapid drying of feed solution droplets. Indeed, it was suggested that the disappearance of thermal events in the DSC thermogram of drug may indicate its encapsulation (Ford and Timmins, 1989). The coated omeprazole formulation showed different thermal behaviour to the physical mixture made from the same drug: polymer ratio (1:45) which suggests its encapsulation. The latter showed a broad and weak endothermic event between 134 - 159°C which was attributed to omeprazole melting. The weakness of the signal was caused by the low ratio (1:45) of drug-to-polymer.

HPLC analysis was carried out to confirm the presence of omeprazole in the coated powder formulation. A photodiode array (PDA) detector was used to produce a full scan of UV spectrum at every wavelength. PDA is considered one of the preferred detectors for peak identification during method development and usually used to identify impurities in drugs (Ahuja and Dong, 2005). The coated formulation showed the presence of omeprazole with a peak appearing at 7.06 min (Figure 5.7). This peak was confirmed by running pure omeprazole which showed a peak at similar retention time (7.48 min).
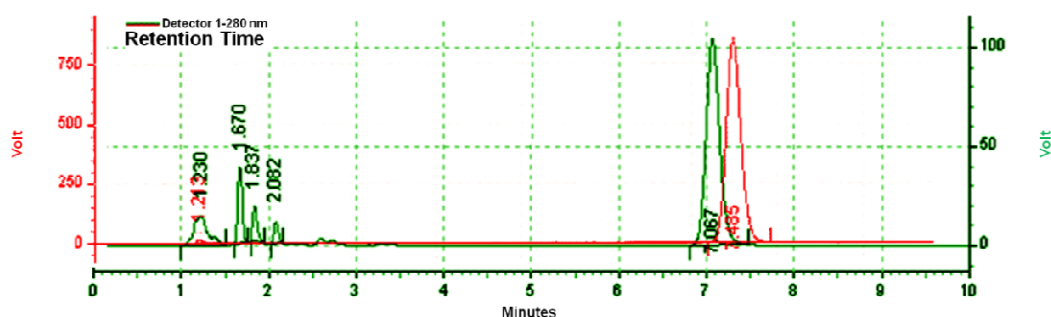
Figure 5.7: Overlaid HPLC chromatograms for pure omeprazole (red) and coated formulation (green) dissolved in acetonitrile: PBS (28:72) at a concentration of 0.5 mg/mL. Omeprazole peak was detected at 7.48 min and for coated formulation at 7.06 min. Peaks at 1.2, 1.6, 1.8 and 2.0 min are related to excipients used in the formulation. UV detection carried out at 280 nm. HPLC analysis was carried out in triplicate (n=3).

The peak of omeprazole at 7 min was also confirmed for identity using the PDA 3D mode (Figure 5.8). The two maximas at 276 nm and 305 nm were in agreement with pharmacopeia values for omeprazole UV maximas (Council of Europe, 2005 a). Furthermore, the PDA spectra also showed the UV absorbance of unknown peaks detected between 1.2-2 min which has different profile to that of omeprazole.
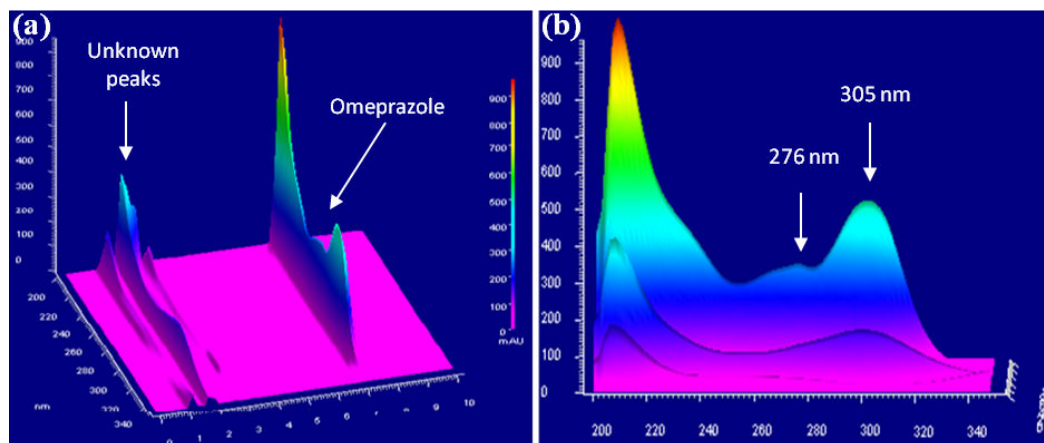
Figure 5.8: 3D view (absorbance vs. wavelength vs. retention time) of coated formulation of omeprazole showing (a) omeprazole and unknown peaks and (b) when figure rotated two maxima appeared for omeprazole at 276 nm and 305 nm while the unknown peaks do not have similar UV absorption maxima.

From HPLC and DSC, a conclusion was drawn that the drug exists in the coated formulation in amorphous form which is less stable than its crystalline form; yet, it could be more soluble in water and probably has better bioavailability (Hancock and Parks, 2000). Another potential advantage of producing amorphous drug is the suitability in direct compression of tablets due to increased plasticity (Yang, 2011). As an example, pharmaceutical excipients such as spray dried lactose have better compressibility than crystalline powder forms (Gohel, 2005). Also, microspheres of a drug with Eudragit or ethylcellulose prepared by spray drying showed increased compaction in comparison with their corresponding physical mixtures (Palmieri et al., 2001).

FTIR for coated omeprazole formulation and pure drug/excipients was also carried out. Figure 5.9 showed no difference between coated formulation and HPMCAS spectra. This resulted from low sensitivity of FTIR to detect omeprazole peak as the drug-to-polymer ratio of the formulation was 1:45. The insensitivity was confirmed when the physical mixture of drug:polymer at 1:45 showed exactly same spectrum as HPMCAS.

Overall, FTIR concluded that no chemical interaction occurred between the formulation components or no degradation product existed in any considerable quantity. FTIR also showed

217

no trace for ammonia (or residual ammonium salts) peaks from the process, anticipated in the region $1525 – 1550$ cm^{-1} corresponding to N-H bond (Alhnan et al., 2011).
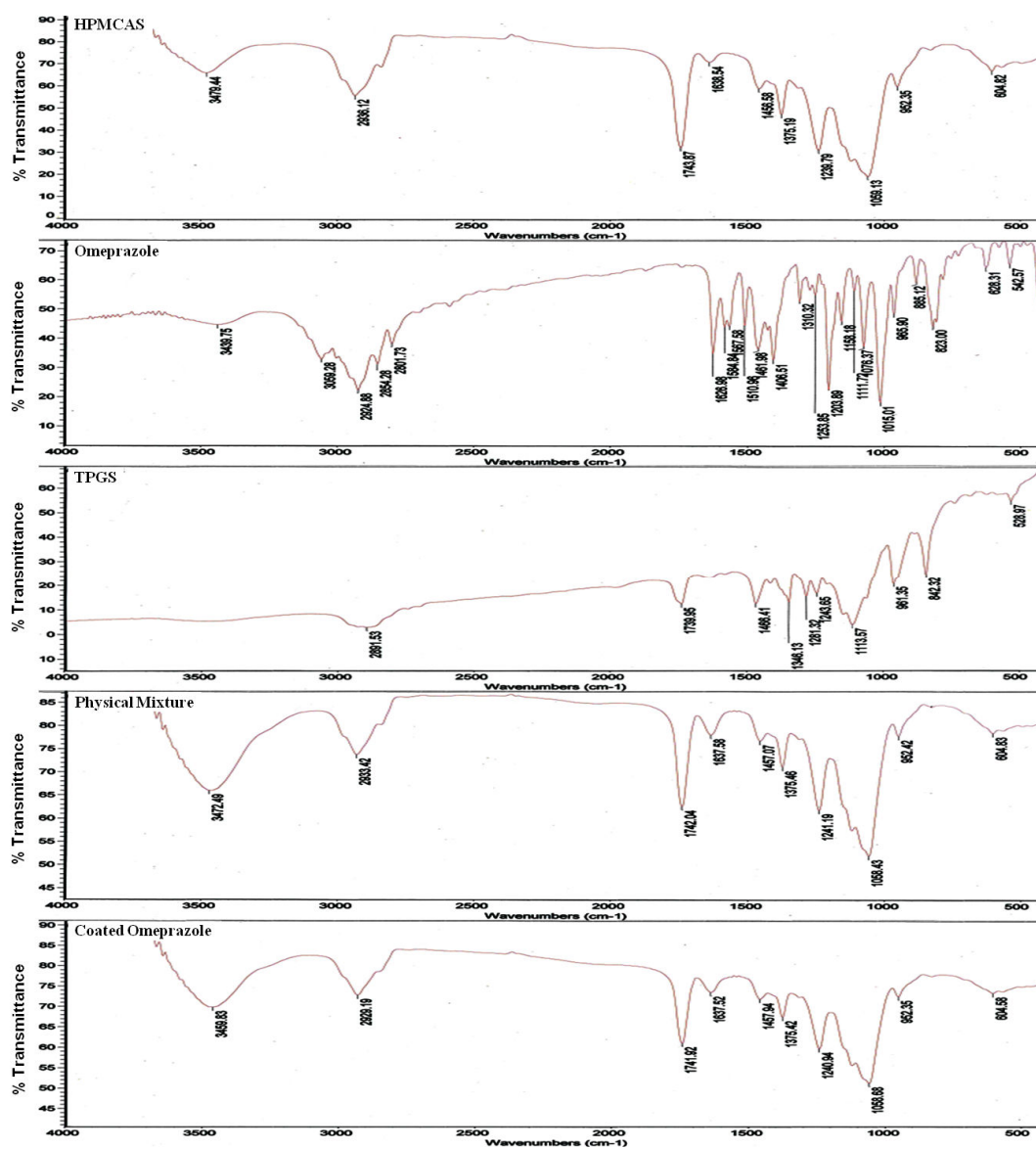
Figure 5.9: Overlaid FTIR of HPMCAS, omeprazole, TPGS, physical mixture (1:45 drug-to-polymer) and coated omeprazole formulation (1:45). No difference was found between pure HPMCAS and coated omeprazole spectra. Each spectrum is representative of 16 scans per sample (n=3).

Limit of ammonia in the omeprazole coated formulation was confirmed using the USP official method (USP Convention, 2012 c). The assay is based on the reaction of ammonia with phenol under alkaline conditions (pH 11-12) in the presence of sodium hypochlorite (oxidizing

solution) and diluted nitroferricyanide solution (catalyst) which results in the formation of indophenol blue (Horn and Squire, 1966; Weatherburn, 1967). The results of the test showed no generation of blue colour in the solution of coated omeprazole after waiting for 1 h (Figure 5.10). This satisfied the official acceptance criterion which is no development of blue colour after leaving the solution for 1 h.
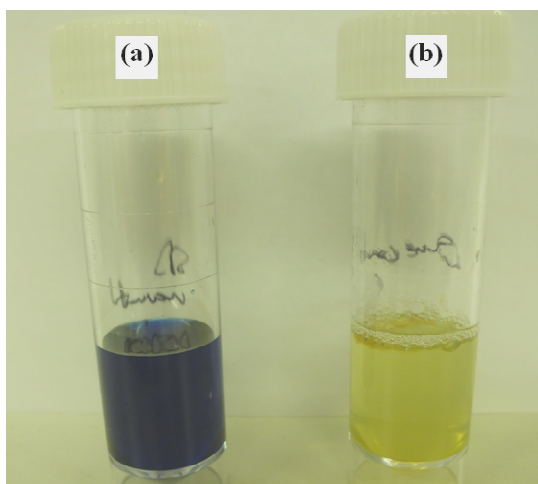
Figure 5.10: Limit of ammonia test after 1 h. (a) control containing ammonia solution (+ve for presence of ammonia), (b) omeprazole coated solution showing no blue colour (-ve for presence of ammonia).

The test is very sensitive (detects down to 0.002% w/v, or 20 ppm) for ammonia in solution (Council of Europe, 2005 b). This confirms that ammonia completely evaporated during spray drying.

HPLC analysis was continued to investigate the peaks at 1.2 min, 1.6 min, 1.8 min and 2.0 min in the coated formulation (Figure 5.7 and Figure 5.8). When the concentration of coated formulation analysed was increased, peak areas for 1.2 – 2 min increased which suggests the peaks relate to the formulation excipients (Table 5.3).

Table 5.3: Coated formulation unknown peaks. Areas increased upon increasing formulation concentration (0.5 – 2.5 mg/mL).

Peak Retention Time (min)	Coated Formulation 0.5 mg/mL	Coated Formulation 2.5 mg/mL
1.23	160426	230934
1.67	141975	471701
1.83	64801	240495
2.08	36366	143019

It was concluded that the peaks which appeared for the coated formulation at 1.23, 1.67 and 1.83 min belonged to HPMCAS because this material was reported to show more than one HPLC peak. This was due to the presence of free carboxylic acids (succinic and acetic acids) in addition to the main polymer and possible generation of these acids upon heat hydrolysis (Dong and Choi, 2008). Decreasing the concentration of HPMCAS in the coated formulation (formulations 1-6 in Table 5.5) led to a decrease in the peak areas of 1.23 − 1.83 min (from 11612 to 4049 at 1.23, from 27594 to 11176 at 1.67 min, from 18396 to 7450 at 1.83 min). On the other hand, the peak at 2.08 min did not decrease in concentration for formulations 1-6 (Table 5.5) and only decreased when TPGS concentration was reduced (formulation no. 7) which indicates it belonged to TPGS (peak area decreased from 9427 − 4534). However, HPLC/UV analysis of solid state mixture of omeprazole and HPMCAS undertaken by Stroyer et al. (2006) showed, in addition to omeprazole peak at 7.5 min, five other peaks which were claimed to be degradation products of omeprazole although identification or proof was not attempted /provided.

5.3.3. Formulation optimisation

5.3.3.1. Influence of drug-to-polymer ratio and solid concentration on omeprazole coated powder properties

HPMCAS concentration was reduced in the formulation before transferring the feed solution to spray drying. This is important to obtain the highest possible drug-to-polymer ratio (omeprazole: HPMCAS) to allow the use of formed powder in ODTs without compromising the total weight of the tablet. However, as the polymer concentration is decreased, the drug would be more prone to degradation by acid (Re, 1998) therefore; a balance between drug-to-polymer ratio and acid resistance and encapsulation efficiency should be studied. To establish encapsulation efficiency, quantification of omeprazole was carried out using HPLC method (1) validated according to ICH guidelines (Table 5.4):
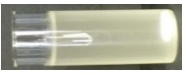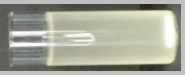
Table 5.4: Validation parameters for HPLC methods. Method (1) for omeprazole in acetonitrile: PBS (28:72) was used for formulation/process optimisation and stability studies whereas method (2) for omeprazole in 50:50 phosphate buffer pH 6.8: (acetonitrile: PBS, 28:72) was used during release study. LLOD and LLOQ represent lower limits of detection and quantification respectively.

Parameter	(1) Omeprazole in acetonitrile:PBS (28:72)	(2) Omeprazole in 50:50 phosphate buffer pH 6.8: (acetonitrile: PBS, 28:72)
Range (μg/mL)	5 – 160	5 – 160
Linearity (R^2 value)	0.998	0.995
Regression line equation	y = 0.197x + 0.617	y = 0.214x + 0.331
Accuracy (%)	98.92	101.50
Intra-day precision (repeatability) (%)	1.86	4.39
Inter-day precision (%)	10.43	-
LLOD (μg/mL)	0.63	1.45
LLOQ (μg/mL)	1.92	4.39
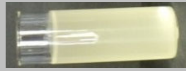
Method (1) demonstrated specificity because it was possible to assay the drug peak (7 min) in the presence of other materials as the UV-Diode array has shown earlier (Figure 5.8). Additionally, specificity was assured by the good resolution between omeprazole peak and other formulation peaks (Figure 5.7) (ICH, 2005). The method also appeared to be stability-indicating because there was no interference between the peak of drug and degradation peaks due to heat/humidity (40°C/RH 75%) and acidic degradation (pH 1-2) (Appendix B Figure B. 2 and Figure B. 3) (FDA, 1998).

Table 5.5 below presents a summary of the coated powder characteristics upon varying HPMCAS concentration and other formulation parameters.

Table 5.5: Properties of omeprazole coated powders containing different HPMCAS concentrations thus different drug: polymer ratios (formulations no. 1 to 6), reduced TPGS concentration (formulation no. 7), reduced solvent volume thus higher solid concentration (formulation no. 8) and increased omeprazole concentration (formulations no. 9 and 10). The properties assessed were yield (%), encapsulation efficiency (EE, %), particle size (µm) and acid resistance.

Formulation no.	HPMCAS % (w/v)	Drug: polymer	Yield (%)	µg Omeprazole /mg powder	EE (%)	Particle size (VMD) µm	Acid Resistance	Sample in 0.1 N HCl Image
1	7.31	1:77	27.37	16.32	35.75	10.28	Cloudy white	
2	4.75	1:50	61.50	16.07	52.4	9.17	Cloudy white	
3	4.27	1:45	62.50	20.08	60.32	8.99	Cloudy white	
4	3.80	1:40	45.69	23.6	46	10.31	Yellow tinge	

223

5	3.33	1:35	30.68	23.3	27.21	9.10	Yellow tinge
6	2.37	1:25	1.40	18.3	0.72	N/A	N/A
7	3.80	1:40	49.33	27.08	57.06	10.49	Yellow tinge
8	5.56	1:40	56.96	25.04	60	9.83	Yellow tinge
9	5.56	1:24	50.21	32.4	41.69	12.23	Cloudy yellow
10	5.56	1:12	59.78	74.68	59.38	9.13	Cloudy yellow

Upon increasing drug-to-polymer ratio, microparticles' yield and encapsulation efficiency increased up at a ratio of 1:45 followed by a decline at ratios 1:40, 1:35 and 1:25 (Figure 5.11). Two main factors might have controlled the process; firstly solid concentration decreased until a point (1:45) whereby further decrease led to loss of product as a result of suction of particles with low solid content by the aspirator. Optimum yield and encapsulation were obtained at 1:45 drug-to-polymer ratio (formulation no. 3 in Table 5.5). This was consistent with literature which suggested that the presence of an optimum solid concentration for each encapsulating material is required to achieve maximum drug retention (Reineccius and Bangs, 1985; Re, 1998). Secondly, the drug would be more susceptible to degradation if the concentration of coating polymer is decreased upon spraying from a solution. This is because in dissolved systems, a drug would migrate with water diffusing out of the capsule shell during drying stage (Wan et al., 1992; Takeuchi et al., 1989). This in turn can cause a loss of encapsulation efficiency of the product leading to lower recoveries.
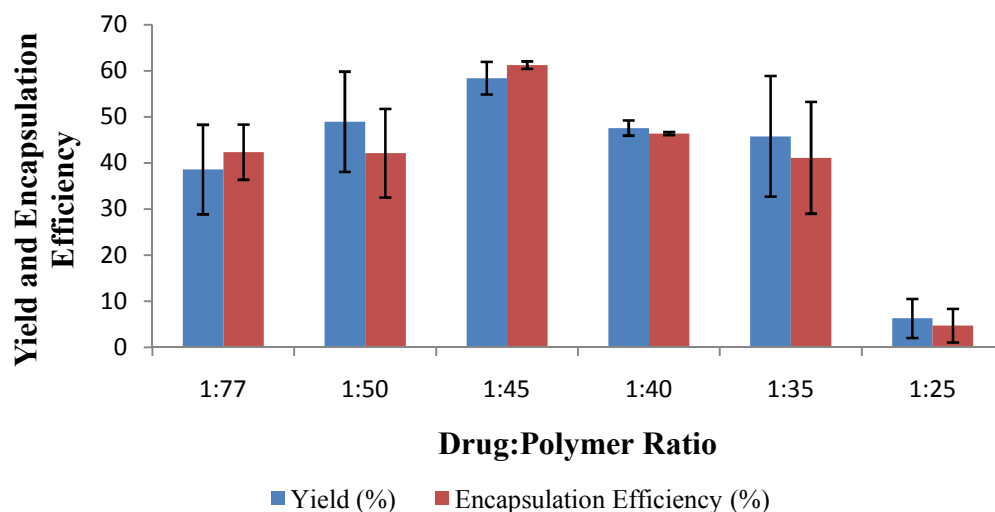
Figure 5.11: Influence of different drug-to-polymer ratios (1:77, 1:50, 1:45, 1:40, 1:35 and 1:25) on yield and encapsulation efficiency of microparticles produced by spray drying. Results reported as mean ± SD (n=3).

From Table 5.5, formulations no. 1 to 3 protected the drug from acid degradation in 0.1 N HCl as no colour change occurred while other formulations (no. 4, 5, 7 and 8) showed a yellow tinge which

may indicate poor drug protection. In addition, formulations no. 9 and 10 experienced the highest degradation as a yellow colour which is distinctive for omeprazole degradation in acid was observed. The extent of acid degradation was dependant on drug-to-polymer ratio which clearly showed that as the ratio increased, extent of degradation increased which was manifested by the increased intensity of yellow colour (Table 5.5).

Particle size of microparticles was mainly dependant on the solid concentration of feed. Decreasing solid concentration in the formulations (via decreasing HPMCAS concentration) resulted in fewer solids in the drops atomized in the spray dryer thus powder particles slightly decreased in size from 10.28 μm for formulation no. 1 to 9.17 μm and 8.99 μm for formulations no. 2 and no. 3 respectively (Masters, 1991; Nath and Satpathy, 1998). When the concentration of solids decreased further (formulation no. 4 and 5 in Table 5.5), more light particles were generated but immediately sucked by the aspirator leading to a powder composed dominantly of heavier particles with a VMD of 10.31 and 9.10 μm respectively.

5.3.3.2. Influence of TPGS concentration on powder recovery

The building of wall deposits in spray dryer is undesirable as it reduces the yield of process, complicates after-use cleaning procedure and in some cases may cause combustion and explosions (Ozmen and Langrish, 2003). TPGS is a tacky material which probably caused the sticking and deposition observed at the interior walls of spray dryer (Figure 5.12). Therefore, concentration of TPGS was reduced by half from 0.19% to 0.095% w/v (formulation no. 7 in Table 5.5) which led to an increase in yield (49.33% from 45.69%) and encapsulation efficiency (57.06% from 46%).

Figure 5.12: Sticking of microparticles at the interior walls of spray dryer. As a result of TPGS tackiness, microparticles sticking occurred on the walls of the instrument leading to degradation of omeprazole (pink colour) and lower process recovery.

5.3.3.3. Effect of reduction of feed solution volume on powder recovery

The volume of feed solution was reduced in an attempt to increase solid concentration which in turn may increase yield (Goula and Adamopoulos, 2004). As expected, both yield and encapsulation efficiency increased to 56.96 % and 60 % respectively (formulation no. 8 in Table 5.5) as the solid concentration was increased. Particle size of produced powder (9.83 µm) was smaller than the previous formulation (10.49 µm) probably due to less encapsulation of drug per mg of powder (25.04 µg/mg) caused by lower micellization of omeprazole.

5.3.3.4. Effect of increasing omeprazole concentration on powder encapsulation efficiency

Formulations no. 9 and 10 (Table 5.5) failed the acid test as a result of their high drug-to-polymer ratios (1:24 and 1:12 respectively) which resulted in incomplete coating and possibly higher precipitation of drug on the outside of polymer crust (Wan et al., 1992). Although omeprazole recovery was reasonable in terms of yield and encapsulation efficiency, however, the coating was

insufficient to prevent the leakage of drug to the acid media. A yellow colour was produced within 10 min of dispersing the coated powders in 0.1 N HCl which indicates degradation of omeprazole.

Overall, formulation no. 3 showed satisfactory properties in terms of yield (62.5 %) and encapsulation efficiency (60.32 %) as well as protection from acid, therefore it was taken forward to process optimization stage.

5.3.4. Process optimisation using design of experiments (DOE)

The influence of spray drying process variables is difficult to assess generally, because of lack of information in the literature and due to the specific drying nature of most materials (Goula and Adamopoulos, 2004; Raffin et al., 2006). Design of experiments (DOE) is a well-established method for identification and optimization of important parameters involved in a process (Yu, 2008). It allows the interpretation and analysis of correlations between dependant and independent variables of the process. DOE forms part of a bigger concept namely, quality by design (QbD) where final product specifications, manufacturing process and critical parameters are included to ease the final approval and the ongoing quality control of a new drug (Maltesen et al., 2008).

Spray drying is a process controlled by multiple factors such as inlet temperature, aspirator, spray gas flow and feed rate. The development of a successful spray dried microparticle would require knowledge of the effect of process parameters on the quality of final product. Furthermore, DOE helps to unveil the main and interaction effects of process parameters.

5.3.4.1. Investigation of statistical data (model verification)

The model was fitted using partial least squares (PLS) regression as the method deals with many responses simultaneously. PLS also provides an advantage of tolerating small amounts of

missing/failed data in the response matrix due to, for example, inaccessibility of a design corner experimentally (Eriksson et al., 2008).

Different statistical tests were carried out to refine the mathematical model by removing outliers. Outliers are responses with values not corresponding to the rest of measurements and are unreasonably different from them possibly occurring due to human error (Miller and Miller, 2005). They can impact the model precision and accuracy and are, therefore, rejected after careful examination. Outlier values were removed using the distance to model (Dmod Y) and N-probability versus normalized residuals plots (Figure 5.13 and Figure 5.14).
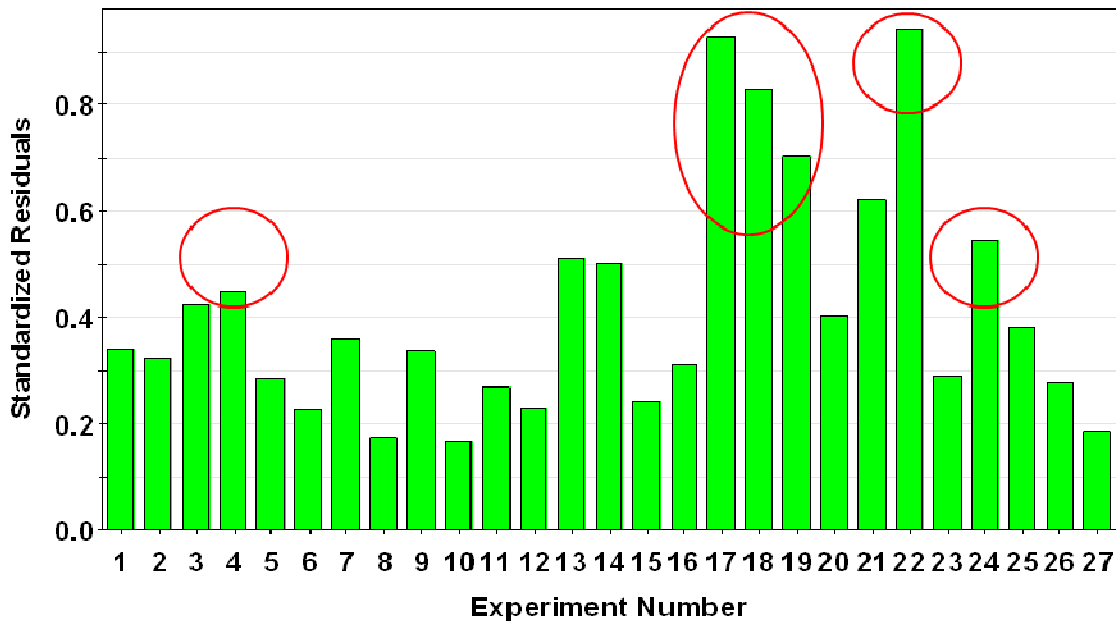
Figure 5.13: Distance to model (Dmod Y) plot showing outliers (in circles) before removal.

Dmod (Y) plot displays normalized residual standard deviations of the responses in proportion to Y model plane. Outliers could be detected and excluded after confirmation with N-probability versus normalized residuals plot. Outliers were removed sequentially starting from the furthest value from response.
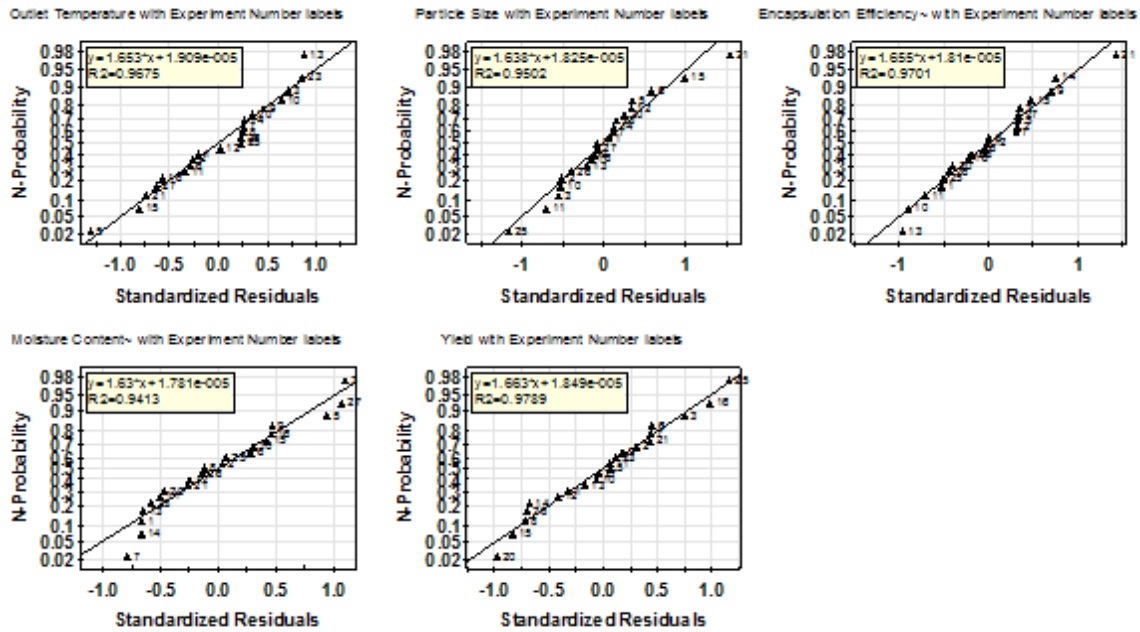
Figure 5.14: N-probability versus normalized residuals plot showing correlation coefficients for responses after removal of outliers.

Experiments 4, 17, 18, 19, 22 and 24 were considered outliers and excluded to obtain linear regression lines with good correlation (Figure 5.14). Furthermore, the squared power of two responses, namely moisture content and encapsulation efficiency, was taken to normalize the residuals versus Y-predicted plot (Appendix B, Figure B. 4) and to avoid funnel pattern due to non-constant variance of these responses.

A lack of fit assessment was carried out as some response values were removed from the model which may affect its validity. Lack of fit plot (Figure 5.15) was used for this purpose which constitutes of three bars: first bar is for standard deviation of lack of fit (i.e. model error in same units as response), second bar is for standard deviation of pure error (i.e. standard deviation of response under same conditions) and third is composed of the value of second bar (pure error) multiplied by critical-F value.
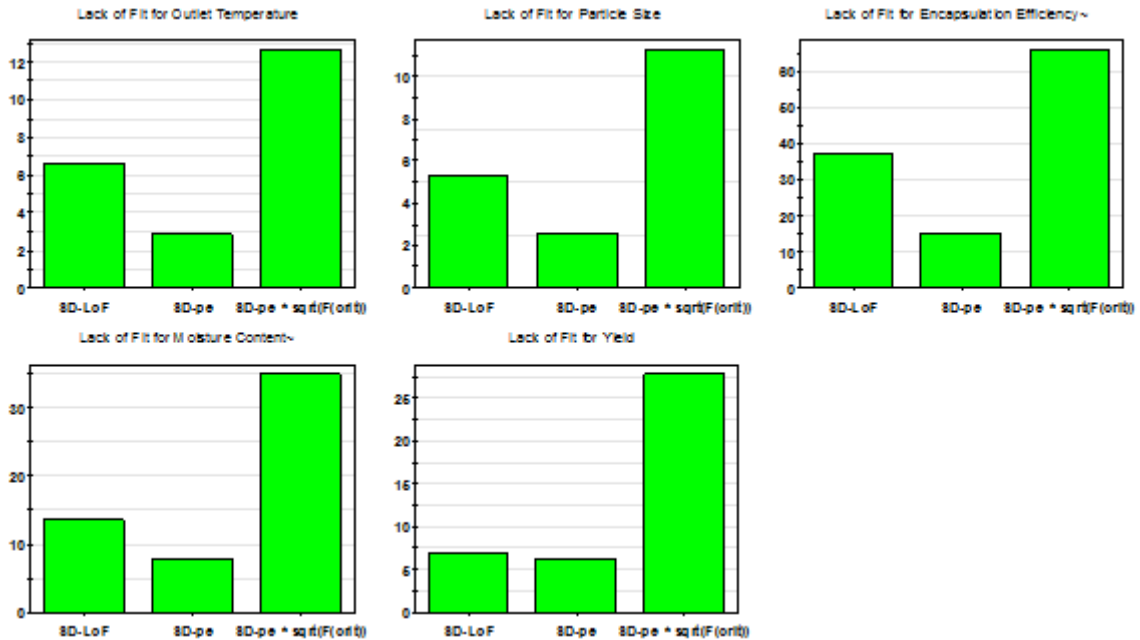
Figure 5.15: Lack of fit plot showing no lack of fit for all responses after removal of outliers. From left, first bar SD-LOF is for standard deviation of lack of fit, second bar is for standard deviation of pure error and third is composed of the value of second bar (pure error) multiplied by critical-F value.

A model with no lack of fit should have the first bar equal or smaller than the third bar. Therefore, all responses showed no lack of fit after removal of outliers. Consequently, the summary plot (Figure 5.16) shows both high reproducibility (80 - 96%) and R^2 (83 - 97%) values. R^2 is the percent of variation in response explained by the model and is a measure of how well the model fits the data. On the other hand, predictability (Q^2) and validity were moderate to high ranging from 39 to 82% for Q^2 and 52 to 83% for validity. The model was correct as the validity was higher than 25% (0.25) which is the minimum threshold below which the model would be incorrect.
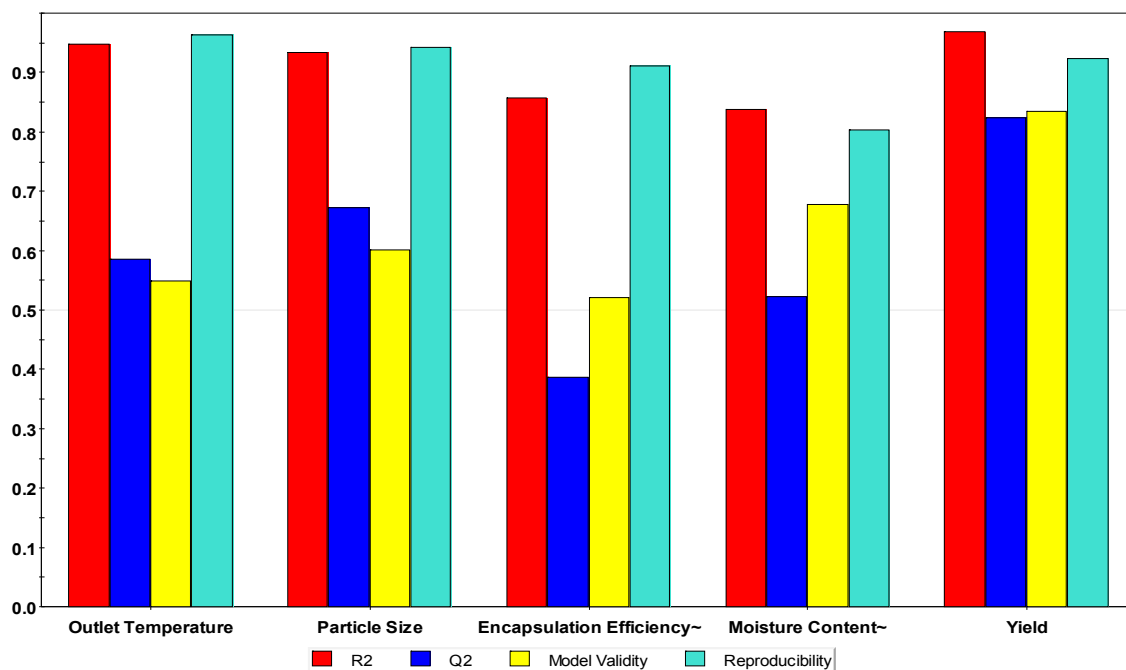
Figure 5.16: Summary plot for PLS model showing high reproducibility and R^2. It also shows moderate to high Q^2 and validity.

5.3.4.2. Analysis of variance (ANOVA) results

ANOVA (Table 5.6) showed that the p value for regression was <0.05 for outlet temperature, particle size and yield while it was insignificant (i.e. >0.05) for encapsulation efficiency and moisture content. The model error due to lack of fit is satisfactory as the p value was >0.05 for all the responses.

Table 5.6: Summary of results obtained from ANOVA of the four responses to test model validity. P is probability and R^2 is the regression coefficient.

	P	R^2
Particle Size		
Regression	0.006	0.933
Lack of Fit	0.204	
Yield		
Regression	<0.0001	0.969
Lack of Fit	0.515	
Encapsulation Efficiency		
Regression	0.064	0.856
Lack of Fit	0.148	
Moisture Content		
Regression	0.09	0.838
Lack of Fit	0.275	
Outlet Temperature		
Regression	0.003	0.948
Lack of Fit	0.165	

5.3.4.3. Influence of process parameters on product properties

5.3.4.3.1. Influence on particle size

Particle size is a crucial product attribute for the successful development of ODTs as it may affect the flow properties of powder as well as mouth-feel upon disintegration. While a relatively large particle is required for good flow properties, a particle size of less than 10 µm may be preferable for optimum mouth-feel as previous research suggested (Tyle, 1993). In accordance, spray drying is a versatile process with the capacity to produce particles of controlled size depending on process parameters and diameter of atomizer nozzle (Elversson and Millqvist-Fureby, 2005).

The assessment of spray drying process parameters showed that size of microparticles was significantly (ANOVA, $p < 0.05$) affected by interaction effect of inlet temperature and spray gas flow rate. The interaction plot (Figure 5.17) is representative of a strong interaction between the two factors because the two lines cross each other.
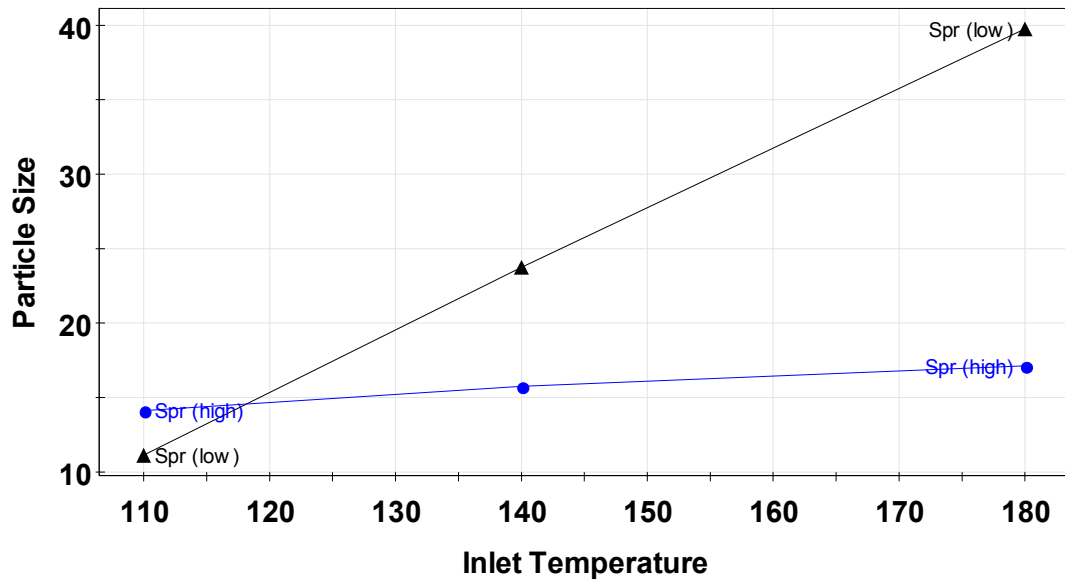
Figure 5.17: Interaction plot of inlet temperature (°C) and spray gas flow rate (rotameter reading in mm) showing strong interaction effect of these factors on VMD size of microparticles (µm).

The interaction plot presents the predicted change in response when one factor changes and the second factor is set at both its high and low level while other process parameters (independent factors) are set at their centre. From the plot, a high spray gas flow (50 – 60 mm rotameter reading or 601 – 742 NormL/h) produces smaller microparticles at different inlet temperatures due to increased dispersion of atomized feed droplets. The opposite occurs when a low spray gas flow (30 – 45 mm rotameter reading or 357 – 536 NormL/h) was used which led to larger droplets with more chance for drying into bigger particles. Response surface modelling (RSM) was used to further investigate the interaction effect between the two process parameters. RSM plot (Figure 5.18) shows that particles with small diameter (< 15 µm) could be produced at lower inlet temperatures

and at various spray gas flow rates. This potentially helps in developing energy efficient process with less power consumed for drying.
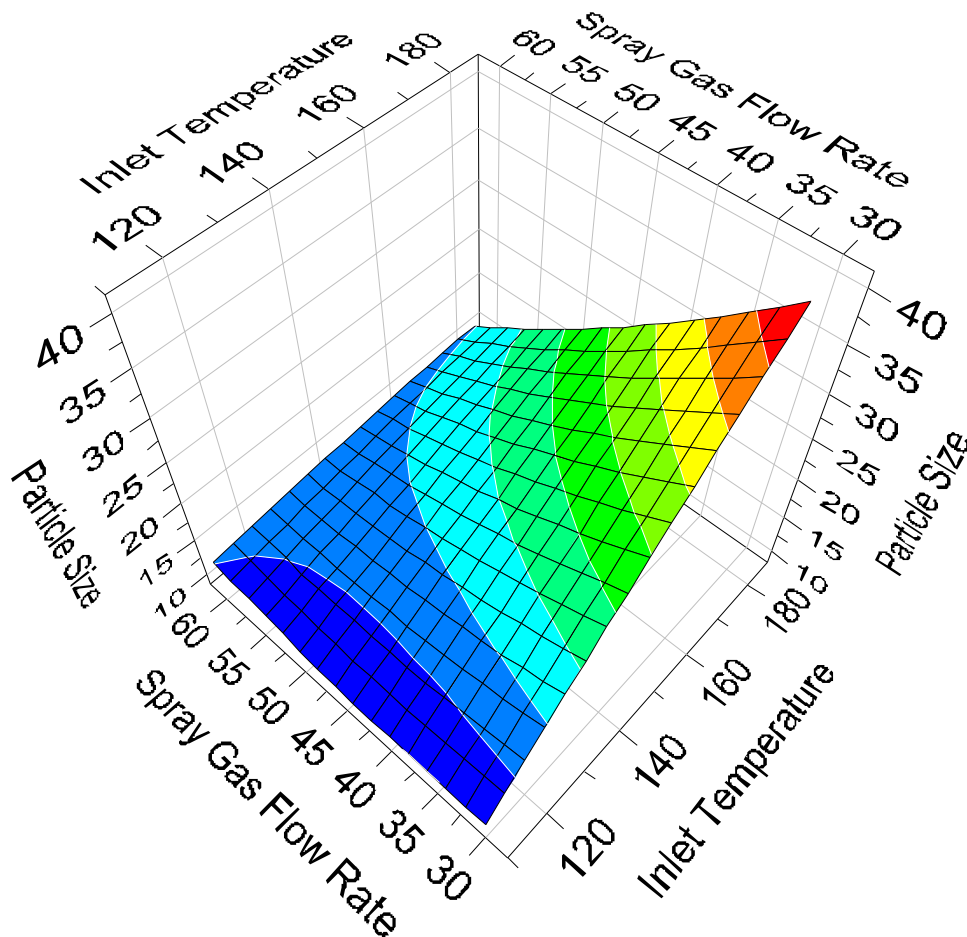
Figure 5.18: Response surface plot showing the interaction between inlet temperature (°C) and spray gas flow (rotameter reading in mm) as dark blue areas and the corresponding effect on microparticles size. The other independent variables (feed rate and aspirator rate) were set at their centre values (20% and 70% respectively).

5.3.4.3.2. Influence on moisture content

High levels of moisture may negatively impact the physico-chemical properties of pharmaceutical solids. It may lead to agglomeration of smaller particles forming irregular larger cohesive aggregates thus affecting powder flow. Furthermore, water provides a suitable growth environment

for microbiological contamination and for formation of unwanted hydrate forms/phase changes (Khankari and Grant, 1995).

The experimental design showed no significant factor (ANOVA, $p > 0.05$) affecting the moisture content of microparticles. This contradicts the general concept that moisture content is reduced with increasing temperature. However, studies have shown similar results for the effect of spray drying process parameters on moisture content. It was reported that none of the main factors were responsible for controlling moisture content and that the quadratic effect of inlet temperature (Inl*Inl) may play a role in controlling this response (Nekkanti et al., 2009; Tewa-Tagne et al., 2007). The loading scatter plot of the PLS model in Figure 5.19 shows that quadratic effect of inlet temperature may have a negative correlation with moisture content as they are positioned opposite to each other on the graph. In other words, when Inl*Inl is increased, moisture content will decrease and vice versa. However, other research suggested that moisture content is influenced by outlet temperature which was not included as a parameter but rather as a response variable in this study (Maltesen et al., 2008).

Figure 5.19: PLS loading scatter plot used to explain the importance of variables and correlation between each other. WC[1] and WC[2] denote for PLS model X weight vector W' and Y weight vector C' in PLS dimension 1 versus 2. Values are distributed around the horizontal and vertical planes with increased importance towards the extremities. Dashed lines are used for the illustration of correlation between variables. The quadratic effect of inlet temperature (Inl*Inl) is highly negatively correlated with moisture content whereas particle size, encapsulation and outlet temperature have lower correlations (respectively) due to being closer to origin. Terms close to each other are positively correlated whereas those opposite to each other are negatively correlated.

5.3.4.3.3. Influence on yield

The yield obtained from spray drying on a laboratory-scale is known to be affected by different factors such as material stickiness, residence time in drying chamber and instrument drying capacity (Maury et al., 2005). However, a well optimized process should provide a reasonable yield in order for the process to demonstrate successful application. Three significant factors affected the yield of the current process, namely: Inlet temperature, feed rate and spray gas flow rate. Results showed that upon increasing inlet temperature, the yield was increased. The results were partly in agreement with Broadhead et al. (1994) as they reported that interaction effect of high inlet

237

temperature and low feed rate produced higher yield. However, in this study only the main effects of inlet temperature (Figure 5.20) and feed rate (Figure 5.21) were significant (ANOVA, $p < 0.05$) and no interaction effect was found. In addition, lack of interaction effect between inlet temperature and feed rate was also confirmed in another study by Ståhl et al. (2002). Generally, a higher temperature would result in a less humid product which in turn reduces the tackiness of the material and improves yield (Figure 5.20).
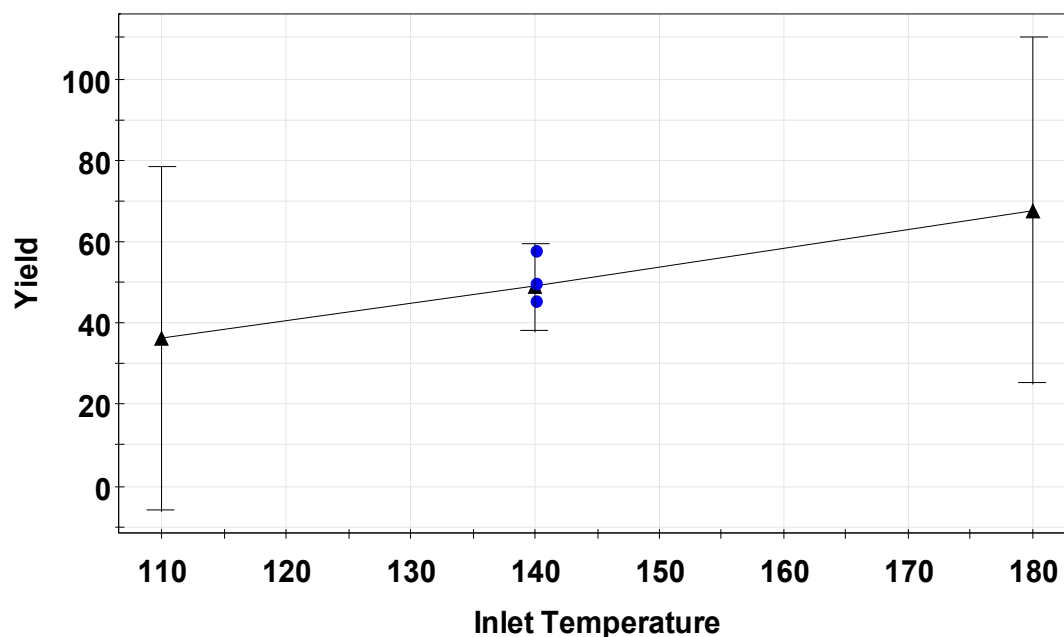
Figure 5.20: Influence of inlet temperature (°C) on yield (%). The blue dots (model centre points) indicate validity of the effect as they fall within the confidence limits of ± 95%.

In addition, a high feed rate (20 – 30% or 290 – 440 mL/h) was found to reduce yield dramatically as spraying more water potentially results in higher moisture content leading to greater deposition on drying chamber walls (Figure 5.21). This could be exacerbated if the operating temperatures are low as it was shown in Figure 5.20 above. On the other hand, a low feed rate may prolong the spray drying run time and slows down the production rate.
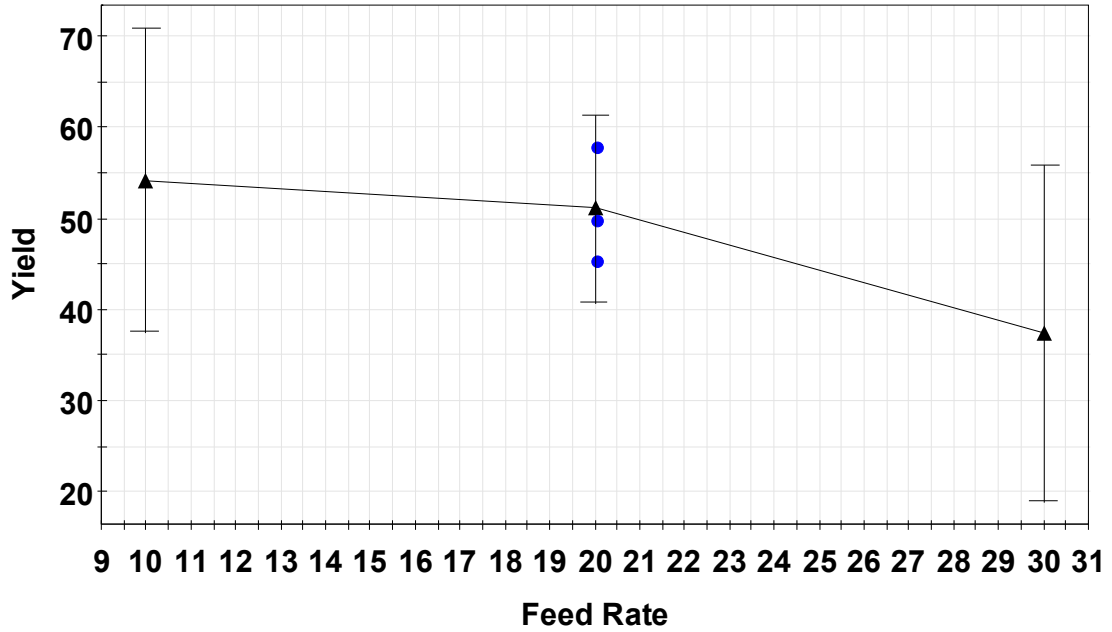
Figure 5.21: The effect of feed rate (%) on process yield (%). The blue dots (model centre points) indicate validity of the effect as they fall within the confidence limits of ± 95%.

The effect of spray gas flow showed an increase of yield when flow rate (rotameter reading) was increased from low to medium (30 - 50 mm, 357 – 601 NormL/h) indicating enough droplet dispersion and drying has occurred. However, when spray gas flow was set at its maximum level (60 mm or 742 NormL/h), yield slightly decreased (Figure 5.22). The latter was explained by the formation of small particles (due to extensive droplets dispersion at the maximum spray gas flow) which were easily sucked by the aspirator causing the lower yield.
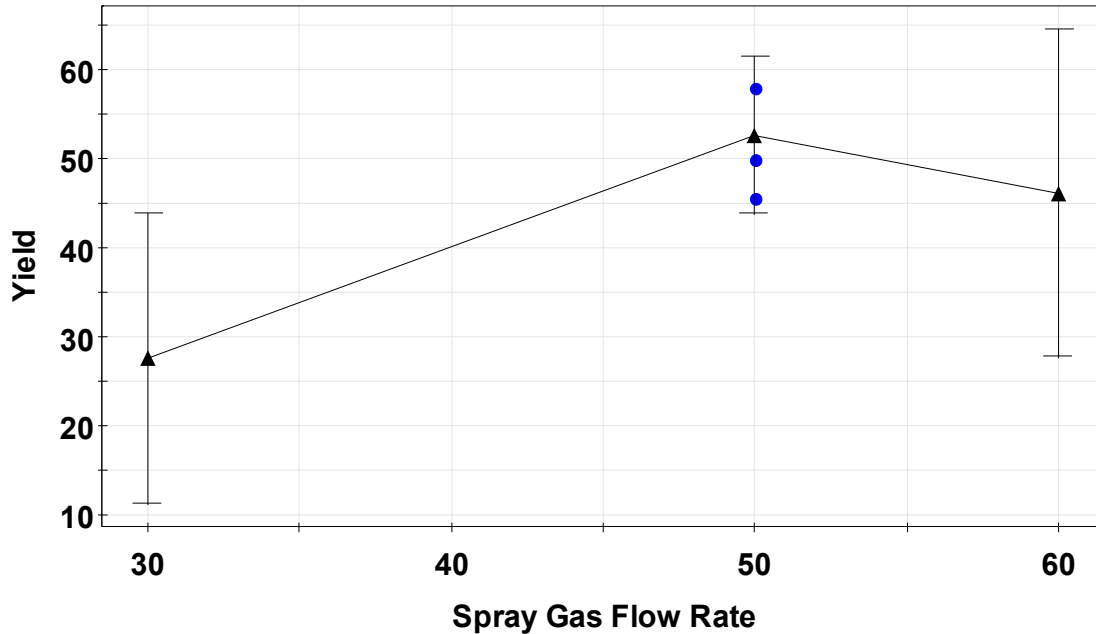
Figure 5.22: The main effect of spray gas flow rate (rotameter reading in mm) on process yield (%). The blue dots (model centre points) indicate validity of the effect as they fall within the confidence limits of ± 95%.

5.3.4.3.4. Effect on outlet temperature

Previous studies reported outlet temperature as the single most important parameter that determines water drying rate (Maa et al., 1998). Furthermore, optimum outlet temperature is required to avoid degradation of product (Broadhead et al., 1994). In accordance, this study included outlet temperature as a response to determine the factors influencing this important parameter.

Two independent variables influenced the outlet temperature namely inlet temperature and aspirator rate. Increasing both factors led to an increase in outlet temperature (Figure 5.23 and Figure 5.24) and was in agreement with Ståhl et al. (2002). Increasing inlet temperature led to increase in the outlet temperature as a result of higher heating energy introduced into the system. On the other hand, outlet temperature showed a linear relationship with increasing aspirator rate because the latter stabilizes the heating environment provided by the inlet via expelling the vaporised water and gases.
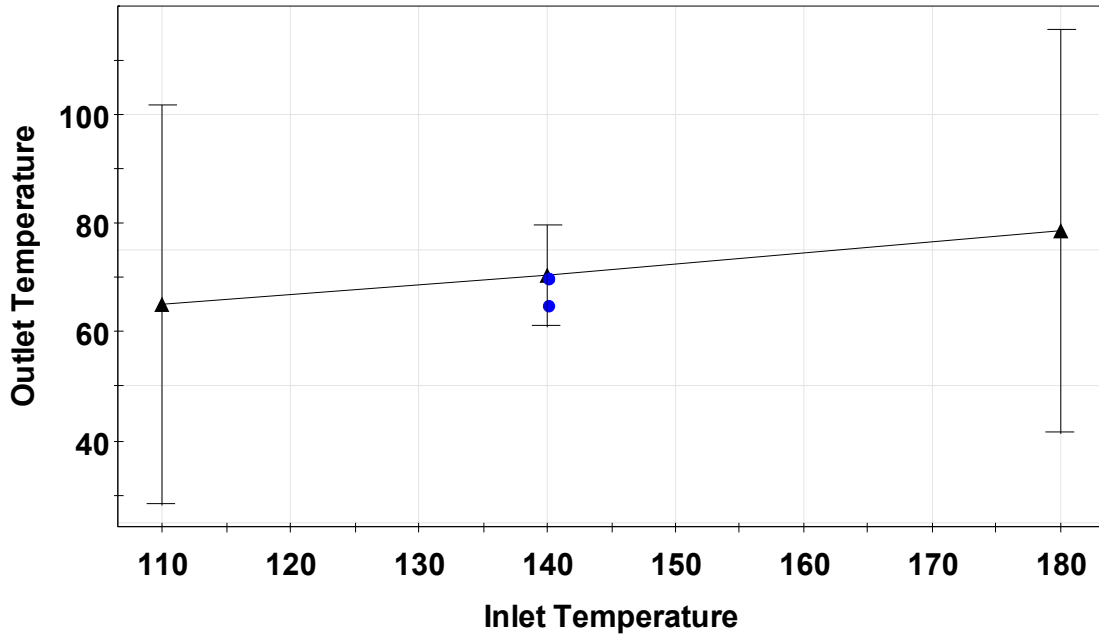
Figure 5.23: Effect of inlet temperature (°C) on resulting outlet temperature (°C). The blue dots (model centre points) indicate validity of the effect as they fall within the confidence limits of ± 95%.
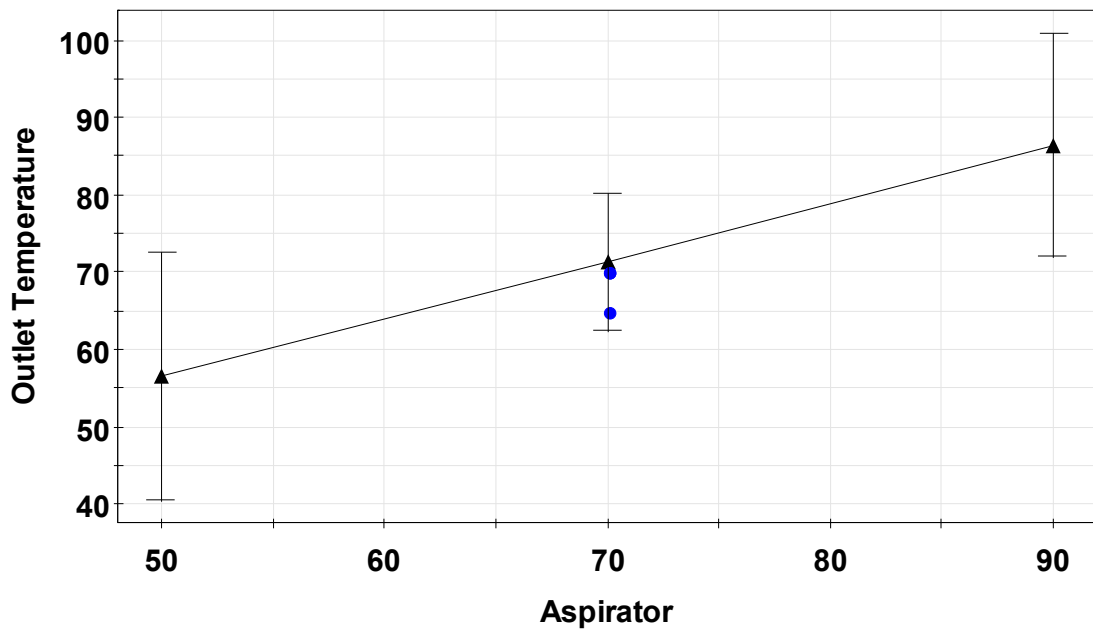
Figure 5.24: Effect of aspirator rate (%) on outlet temperature (°C). The blue dots (model centre points) indicate validity of the effect as they fall within the confidence limits of ± 95%.

5.3.4.3.5. Influence on encapsulation efficiency

Encapsulation efficiency is a measure of the drug loading capacity of microparticles. It is critical to obtain a suitable encapsulation level to ensure development of a successful formulation. No significant effect was found (p>0.05) from ANOVA indicating no dependency between material encapsulation and process parameters. This was somehow anticipated as the encapsulation efficiency of drug inside a polymeric layer primarily depends on the formulation excipients interplay in the liquid dispersion to be spray dried.

5.3.4.4. Process optimisation summary and generation of sweet spot

A valid and reproducible experimental model was fitted using partial least squares (PLS) method. The major factors determining spray dried product quality attributes were identified in order to develop an optimized formulation for omeprazole coated microparticles. The overall PLS score plot expressed as t[1] vs. u[1] (X score vector denoted t' and Y score vector denoted u') (Figure 5.25) showed a positive R^2 of 0.7068 indicating good fit of the experimental data. However, a curvature still could be seen even after removal of outliers which may indicate non linearity in some of the relationships investigated.
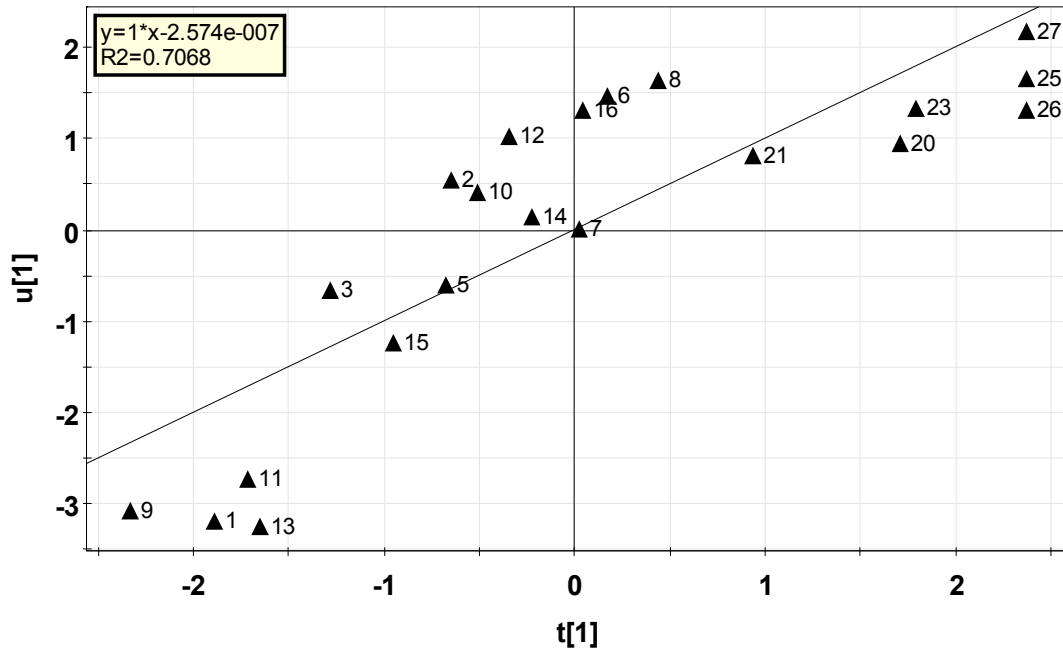
Figure 5.25: t[1] vs. u[1] score plot. A plot used to display the relation between X and Y.

The optimal operable zones within the critical process parameters are illustrated in Figure 5.26. The figure shows the space that could result in optimal yield (> 30%), target particle size (< 20 μm) while maintaining an outlet temperature between 80-110°C. The maximum operable space (red zone) is obtained when the spray gas flow rotameter reading is set at its maximum of 60 mm, the feed is set at its lowest rate of 10% and the inlet temperature can be varied from 127 - 180 °C with aspirator rate ranging from 70 to 90%.
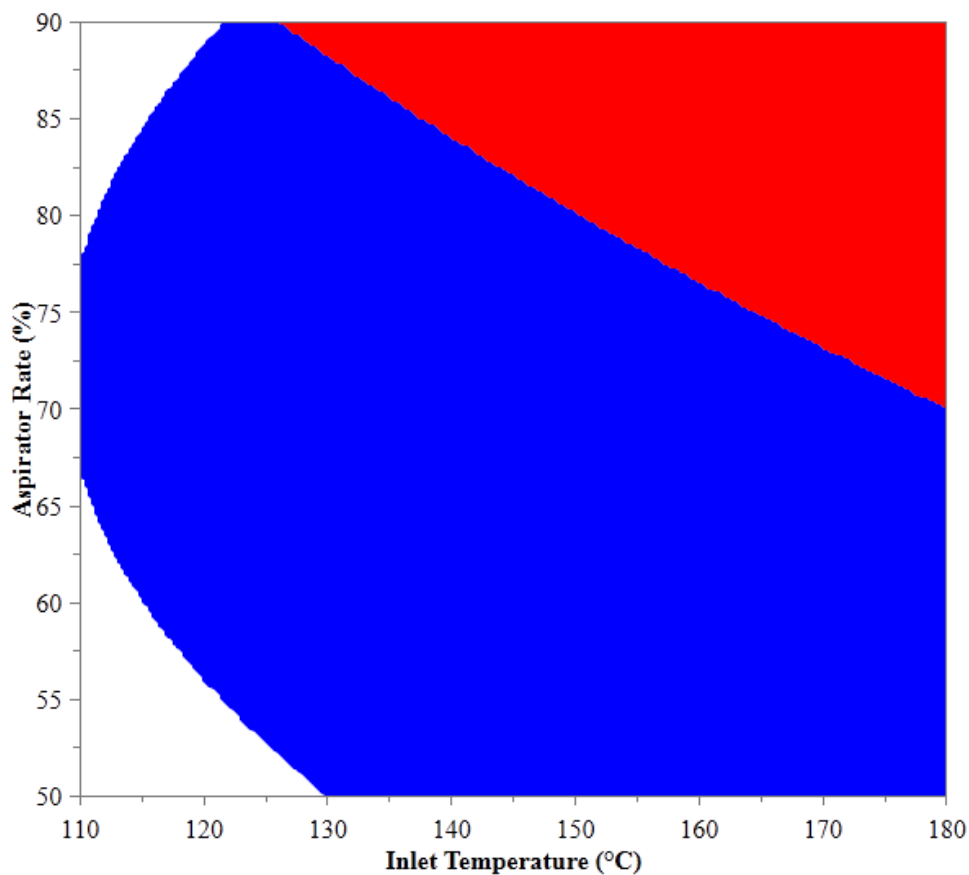
Figure 5.26: Sweet spot for optimal ranges of the critical process parameters (Inlet temperature and aspirator rate) for the desired profile of critical quality attributes (particle size, yield and outlet temperature) while spray gas flow rotameter reading and feed rate were set at 60 mm and 10% respectively. Red zone is the operable zone where all of critical quality attributes are met i.e. yield > 30%, particle size < 20 μm and outlet temperature between 80-110°C. Blue zone is when one or more of the attributes are not met. White zone is the non-operable zone where none of the attributes are met.

5.3.5. Stability of omeprazole coated microparticles for 14 days

Stability was tested for the optimized formulation made from a drug-to-polymer ratio of 1:45 and spray dried within the maximum operable zone conditions (i.e. at inlet temperature of 180°C, spray gas flow rotameter reading of 60 mm (742 NormL/h), feed rate of 10% (145 mL/h) and aspirator rate of 90%). DSC, FTIR, HPLC, visual inspection and acid resistance test were carried out for qualitative and quantitative assessment of the powders. The powders were incubated at the ICH

recommended conditions: long term stability at 25°C/60% RH and accelerated stability at 40°C/75% RH as the formulation was intended for room temperature storage (ICH, 2003; Huynh-Ba, 2009).

DSC was utilized to test for any phase or polymorphic changes during material storage at different conditions. DSC results for 14 days (Figure 5.27) showed no significant change in the powders thermal properties when compared to the original powder tested at day 0. Furthermore, the zoomed region at 166.72°C attributed to omeprazole decomposition also did not change after 14 days at 25°C/RH 60% and 40°C/RH 75% stability conditions.
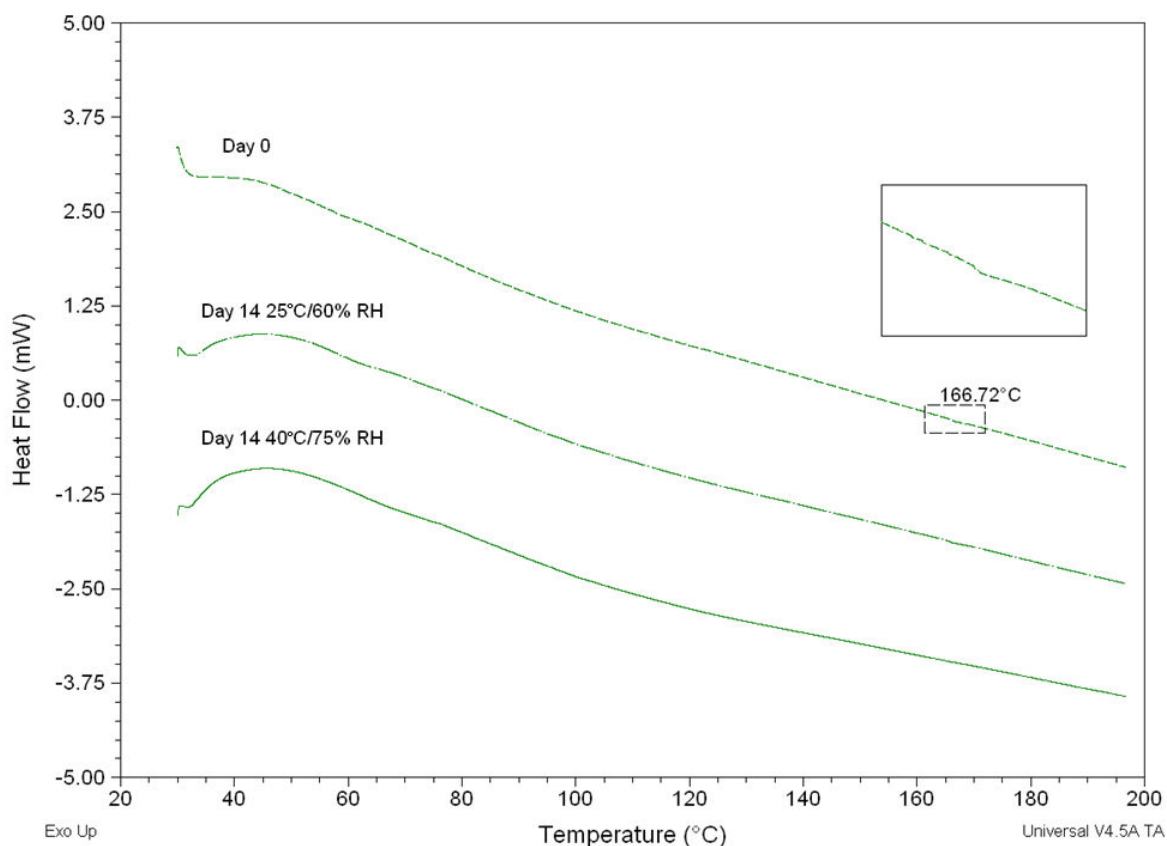
Figure 5.27: DSC stability data for omeprazole coated formulation. Small endothermic depression at 166.72°C is zoomed for day 0 representing decomposition of amorphous omeprazole. No change was observed in this event for day 14 long term (25°C/RH 60%) and accelerated (40°C/RH 75%) stability data. DSC thermograms are representative of triplicate measurements (n=3).

FTIR was used as another confirmative technique for any degradation or chemical change in the formulation assisted by heat or humidity. FTIR results (Figure 5.28) also showed no difference between day 0 and day 14 at both stability conditions and generally there was no spectral difference in all the samples from that of pure HPMCAS. This indicates no formation of degradation products in any significant quantity that can affect the formulation properties even at the higher heating and humidity conditions of the accelerated stability study.
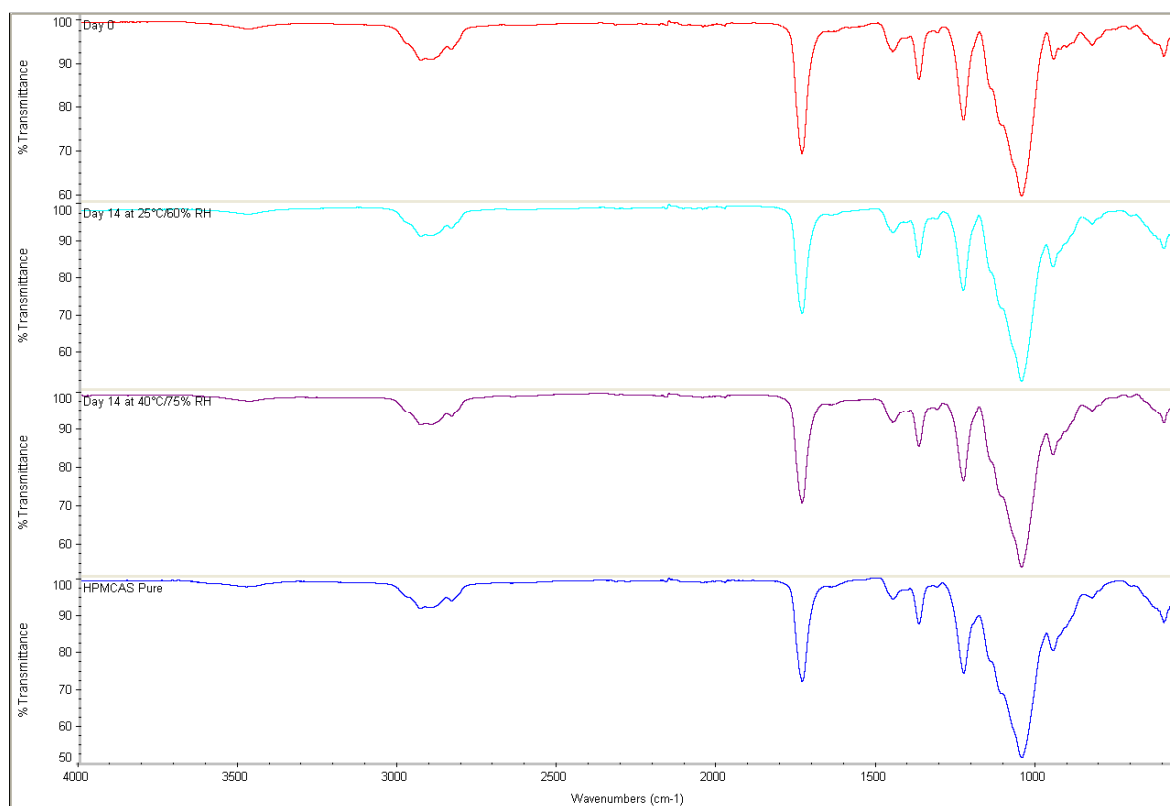
Figure 5.28: FTIR stability data for omeprazole coated formulation. No change was observed between day 0 and 14 spectra at both long term (25°C/RH 60%) and accelerated (40°C/RH 75%) stability conditions. All spectra showed no difference from that of pure HPMCAS. Each spectrum is representative of 16 scans per sample (n=3).

HPLC stability-indicating method (1) (Table 5.4) was used to quantify possible loss or change in the concentration of omeprazole over the 14 days stability period. The results showed no significant change (t-test, $p > 0.05$) in the concentration of omeprazole between day 0 and 14 (14.37 ± 2.58 and

11.86 ± 1.40 µg/mL respectively) for the long term stability at 25°C/60% RH. This indicates the formulation is stable (in the solid state) at room temperature for 14 days.

On the other hand, there was a significant decrease (t-test, $p < 0.05$) in the concentration of omeprazole at the accelerated stability condition (40°C/75% RH) from 14.37 ± 2.58 µg/mL for day 0 to 8.06 ± 0.71 µg/mL for day 14. This loss of concentration was probably caused by degradation of omeprazole at the higher temperature (40°C) and humidity (75% RH). Several articles have mentioned this sensitivity of omeprazole to heat and humidity (Davidson and McCallum, 1996; Türkoğlu et al., 2004; Riedel and Leopold, 2005 b; Markovic et al., 2006). It is unlikely that the drug has lost concentration at accelerated conditions due to light exposure as the stability storage containers were kept in dark conditions.

Visual inspection of the powders (Figure 5.29) showed a slight difference in colour between day 0 (pale white) and 14 (off-white to beige). However, no difference was observed between day 14 long term (25°C/60% RH) and accelerated stability (40°C/75% RH) conditions. Therefore, the change in colour could not explicitly be attributed to temperature or humidity and in fact the change in colour appeared few hours after spray drying the sample. This observation was also reported by the manufacturer of HPMCAS upon using ammonia neutralisation method (Shin-Etsu, 2005). It is possible that small amounts of HPMCAS have undergone hydrolysis (during spray drying or as impurities from the excipient manufacturing process) leading to the generation of cellobiose (disaccharide consists of 2 D-glucose units linked by β(1→4) linkage and has reducing hemiacetal end) units which are engaged in Maillard reaction with N-H group of ammonia. Maillard reaction is also responsible for the slight browning of bread and cakes and generation of some of their flavours. The reaction occurs between reducing sugar moieties and amine groups under elevated temperatures and alkaline conditions (Morales and van Boekel, 1998; Umemura and Kawai, 2007).
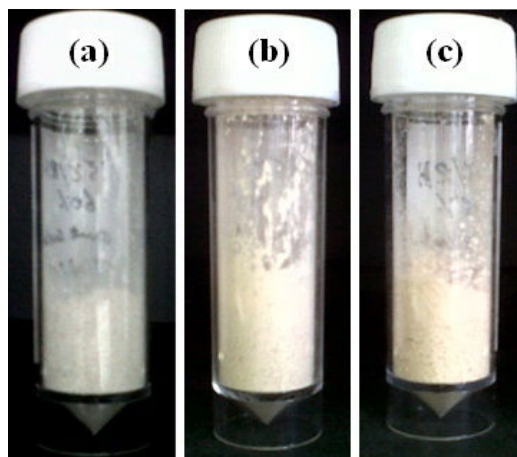
Figure 5.29: Images of omeprazole microparticles at (a) day 0, (b) day 14, 25°C/60% RH and (c) day 14, 40°C/75% RH.

Omeprazole coated powders also exhibited acid resistance over the 14 days period as no appearance of yellow or purple colour was observed.

5.3.6. Drug release from omeprazole microparticles incorporated into directly compressed ODTs

Omeprazole coated microparticles were incorporated (at 50%, w/w) into ODT base (500 mg) prepared from D-mannitol (45%, w/w), HPMC (2%, w/w), L-HPC (2%, w/w) and magnesium stearate (1%, w/w) discussed in Chapter 3. The drug release study was carried out under stirring in a 60 mL beaker instead of the 900 mL USP dissolution vessel due to dilution of drug concentration below the detection/quantification limits of HPLC. Another reason for not using the USP apparatus was the difficulty to assess powder dissolution properties due to clumping in the basket test and floating during the paddle method. In addition, there is no specific official monograph for omeprazole ODT or for ODT dissolution in general, hence the studies were set out to mimic the conditions outlined in omeprazole delayed-release capsules USP monograph (USP Convention, 2012 b). Additionally, the release was carried out at 50 RPM on the finished dosage form (ODT) as well as the bulk intermediate (i.e. loose coated microparticles) according to the FIP/AAPS guidelines for dissolution/*in vitro* release testing of novel/special dosage forms (Siewert et al.,

2003). Acid resistance stage carried out for 2 h in 0.1 N HCl did not result in drug release from the coated microparticles which meant the latter protected the drug from acidic degradation. Upon addition of the alkaline phase and adjusting the release medium to pH 6.8 (Buffer stage), 80% of the drug was released from the loose powder within 30 min (Figure 5.30). According to USP, not less than 75% of the labelled amount of omeprazole must dissolve in 30 min which indicates conformity of the coated powder with the official delayed-release capsules monograph (USP Convention, 2012 b). The coated microparticles inside ODT showed 71% release within 30 min which was not statistically significant (t-test, p>0.05) from the loose coated powder release profile. This indicated that tableting of coated microparticles had no significant negative effect on the release properties of omeprazole. It is possible that the elastic properties of cellulosic excipients HPMC and L-HPC at low compression force of 16 kN (York, 1983) countered the applied tableting stress thus prevented the destruction of microparticles. This represents an advantage over some of the ODT products which employ multiple protective layers (up to 7 layers) around the drug to prevent particle crumbling under pressure (Shimizu et al., 2003 a).
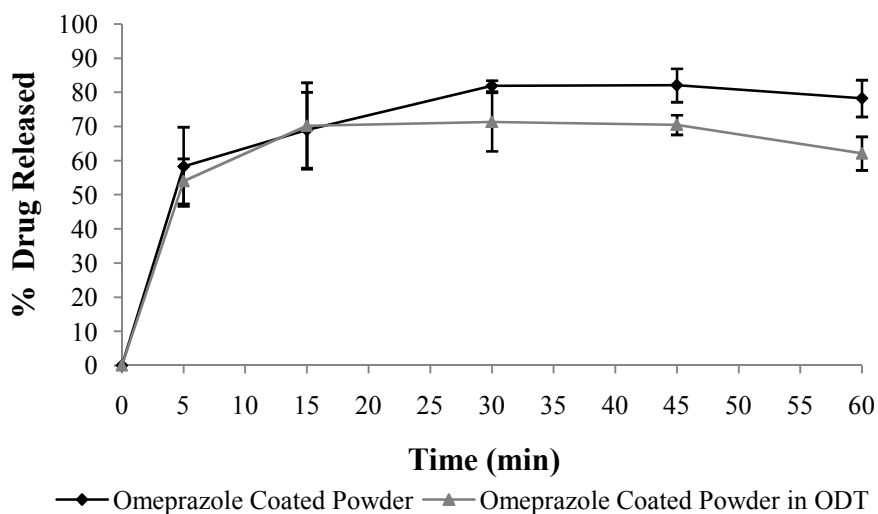
Figure 5.30: Release profile of loose omeprazole microparticles and microparticles incorporated into ODT. Release was carried in buffer of pH 6.8 made by the addition of 0.235 M dibasic sodium phosphate (pH 10.4) to the solution from acidic stage (pH 1.5-2) after 2 h. Release vessel and replacement media were equilibrated at a temperature of $37 \pm 0.5°C$ and stirred at 50 RPM. Each point represents mean $\pm$ SD (n=3).

The threshold at which the drug has started to release from the microparticles (i.e. pH 6.8) was confirmed by dispersing the coated powder in solutions with different pH levels 2-7 (Figure 5.31). The results showed that at the acidic to mildly acidic pH 2-5, HPMCAS formed a cloudy white (2, 3, 4) to beige (5) suspension which contained the drug, nevertheless, when the pH has changed to the intestinal conditions (6-7), the polymer dissolved and cloudiness disappeared. It is worth mentioning here that the light yellow colour at pH 7 has not occurred due to degradation of omeprazole but rather corresponded to the colour of HPMCAS in solution.
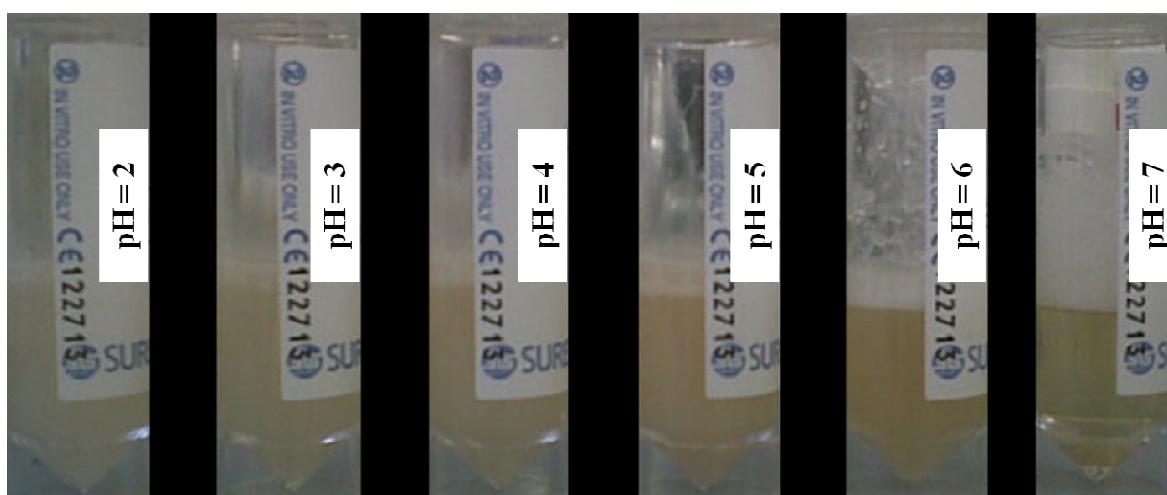
Figure 5.31: Omeprazole microparticles tested in solutions made at pH 2-7 to assess HPMCAS and product dissolution threshold. Solutions were made from mixtures at different ratios of 0.1 N HCl (pH 1-2) with phosphate buffered saline (pH 7.2-7.6) and adjusted with 2N NaOH whenever necessary.

The colorimetric test also served as an indirect method for assessment of taste masking as it covered the pH range of GIT and the mild acidic mouth conditions (pH 5.5-6) of patients with GERD (Bartlett et al., 1996).

Another conclusion from the release and pH experiments, is that neutralisation of HPMCAS using ammonia has not affected the polymer acid protection characteristics. Therefore, this approach can be utilised in different spray drying and coating applications in the future.

5.4. Conclusion

Omeprazole coated microparticles were developed using a simple (two-step), aqueous-based spray drying process with good encapsulation efficiency. The optimum drug: polymer ratio (omeprazole: HPMCAS) in the feed solution of spray drying was found to be 1: 45. This has resulted in the best drug protection properties in acid media and also provided the best yield (60%) and encapsulation efficiency (60%). The attempt to reduce polymer concentration led to a compromised drug protection as the drug leaked out through the polymeric membrane into the acidic medium.

The spray dried microparticles retained small size (< 20 µm) and spherical shape which would be suitable for ODT development as the size and shape of particles play an important role in minimizing gritty mouthfeel. Omeprazole was found to be amorphous in the produced microparticles due to the rapid drying process which prevented recrystallization of the drug.

The coated microparticles showed sufficient resistance to acidic degradation (at 0.1N HCl) and released the drug at intestinal pH (6.8 and above). The microparticles may prove suitable for taste masking because they dissolve above pH 6.8, thus releasing the drug above the mouth salivary pH of 6.2 or even less with patients suffering peptic ulcers/GERD.

Process optimization using DOE provided thorough understanding of the processing conditions that yield the best product quality attributes. The effect of process parameters was significant on particle size, yield and outlet temperature. The results showed an interaction effect between inlet temperature and spray gas flow on particle size. A high spray gas flow produces smaller microparticles at different inlet temperatures due to increased dispersion of atomized feed droplets. Three significant factors affected the yield of the spray drying process, which were inlet temperature, feed rate and spray gas flow rate. Also, the increase of inlet temperature or aspirator rate led to an increase in outlet temperature. On the other hand, changing the process parameters

had no significant effect on encapsulation efficiency and moisture content. The lack of effect on encapsulation efficiency was expected as the encapsulation of the drug inside a polymeric layer primarily depends on the formulation excipients and drug: polymer ratio used. The lack of significant effect on moisture content was mostly influenced by not including outlet temperature as a process parameter, but rather as a response variable in this study.

The microparticles were incorporated into ODT base developed in Chapter 3 and showed no significant difference in the release profile before and after compression. It is possible that the elasticity of cellulosic excipients HPMC and L-HPC at low compression force of 16 kN prevented the destruction of microparticles and premature drug release.

Chapter 6

Conclusion

6.1. Conclusion

ODTs have been acknowledged as one of the most suitable drug delivery systems for the formulation of medicines for children and elderly alongside liquid formulations, chewable tablets, mini tablets and thin films. Despite the interest of the pharmaceutical industry in ODTs, the majority of the formulations currently available are prepared using freeze drying which in turn has limited the growth in the market due to inherent issues such as poor loading capacity for water soluble drugs (as these are generally high dose) and an expensive technology platform. On the other hand, directly compressed ODTs can provide a simple and cost-effective approach. Direct compression also has the benefits of higher content uniformity and a significant reduction in packaging costs. However, the development of ODTs by direct compression requires optimisation of the manufacturing process and composition of the powder blend to obtain reasonable values for hardness, friability, and faster disintegration time.

The domain for excipient and formulation development has already reached a new echelon with the progress made in the availability of multifunctional excipients and ODTs with reasonably high drug pay load respectively. Particle engineering and co-processing approaches are attractive as they create excipients with superior properties by combining favourable properties of different individual excipients. Furthermore, particle engineering offers the opportunity of modifying surface/habit of excipient particles leading to improved physical properties. In addition, processing equipment with continuous production capabilities such as spray drying is widely accessible.

High porosity is the main factor controlling fast disintegration of ODTs besides using a hydrophilic swelling polymer as a disintegrant/superdisintegrant, while excipient compactability being the factor responsible for mechanical strength. Binder/disintegrant systems which offer dual advantages have partly addressed both the requirements.

Although cellulosic excipients were introduced earlier than sugar alcohols for ODT development, a major switch to the latter (especially mannitol) was noticeable due to the unique advantages such as pleasant mouth feel and sweetening characteristics. Nonetheless, the compromise is the mechanical strength with mannitol-based ODT which needs to be improved through alternative strategies in order to meet the final dosage form acceptance criterion (i.e. hardness > 60 N, disintegration time <30 sec and friability <1%). Conversely, cellulosic excipients provide better mechanical properties for ODTs than mannitol due to plastic deformation under pressure and stronger adhesion/inter-particle interactions.

The issue of poor mechanical strength of mannitol in the current thesis was investigated via micro/nanoscopic methods especially using AFM. The results clearly demonstrated that fragmentation of mannitol crystallites was responsible for poor tableting behaviour. AFM and SEM showed multiple surface asperities on the mannitol particle. These surface protrusions fragmented and shifted under slight movement from the AFM tip. In addition, the concomitant adhesion forces and surface energies of mannitol particles were relatively low due to the surface fracture behaviour. Heckel profile analysis also confirmed the brittle fracture of mannitol as material mean yield pressure was very high (Py of 2000 MPa using out-of-die method or 121 MPa using in-die method). This study also enabled the understanding of the interplay of molecular forces that operate between particles which would ultimately uncover the reasons for failure and poor performance encountered during ODT manufacture. For MCC, the bonding property of the excipient was elucidated and found to be related to a number of factors acting together including the high roughness (3 times that of other materials investigated), plastic deformation (low Py of 625 MPa using out-of-die method), amorphous fraction (30%, Tg at 67.63°C) and intercalation of particle's microfibrils with channels of other particles. Furthermore, the adhesive forces for theophylline and ibuprofen with MCC were higher than the adhesive forces of the APIs with D-mannitol. This was attributed to the ability of MCC to generate stronger bonds with materials due to the mechanism mentioned earlier whereas

mannitol fragments and has less binding capacity with other materials. However, the use of MCC in ODTs is restricted to small amounts due the gritty sensation that the excipient leaves in the patient's mouth.

Concomitantly, process/formulation strategies involving the use of mannitol in addition to cellulosic excipients were utilised to produce ODTs. The formulation reported in this thesis required the blending of granular mannitol (plastically deforming) with powder mannitol (fragmenting) at an optimized ratio of 70:30 respectively, to enhance ODT mechanical strength and reduce friability below the acceptable limit (1%). Moreover, the blend contained HPMC and L-HPC (2% w/w each) as dual binders/disintegrants that reduced the friability of the ODT. In fact, the swelling ability of HPMC when used below 10% w/w and of L-HPC when used below 2.5% were the main contributing factors to the fast disintegration of the ODT. The compression force was also a critical factor as a force of 16-17 kN was required to optimise the ODT hardness of > 60 N and a disintegration profile of < 30 sec. Optimising lubricant level in the ODT was also important to reduce tablet sticking and allow better die filling during direct compression using automatic tablet press. Magnesium stearate at 1% w/w was suitable as it achieved the required lubrication without significantly prolonging the disintegration time of ODTs.

Engineering mannitol particle characteristics using spray drying has helped to overcome the poor mechanical properties of mannitol, by producing tablets with upto 150% higher hardness than pure mannitol tablets and 50-77% lower disintegration time. The increased hardness resulted from the change of densification profile of excipient particles. The particles produced at the lower spray drying temperature (110°C) resulted in a fragmentation behaviour that led to subsequent strong bonding due to formation of new clean surfaces. On the other hand, the particles produced at the higher spray drying temperature (150 and 170°C) resulted in plastic deformation which enhanced the tablet compressibility. The fast disintegration profile was attained as the particles of the

fabricated excipient contained pores, which were formed as a result of evaporation of the pore former NH_4HCO_3 during spray drying. This helps in attracting water into the tablet core and promotes disintegration through wicking.

Furthermore, there is still a need for technology platforms with high dilution potential i.e. low amount of excipient generating sufficient mechanical strength. The latter is necessary as FDA guidance for industry recommends a nominal ODT weight of less than 500 mg unless the components are highly water soluble. The produced mannitol excipient potentially satisfies this criterion as the produced tablets contain only mannitol with no other additives, thus reducing the amount of any other functional excipients.

Moreover, the development of taste masking and modified release technologies suitable for ODTs represent an area of major interest. When taste masking is carried out using different approaches, the main criterion is to prevent the contact of the unpalatable API with the taste buds by containing the drug inside a polymeric coating or by complexation to produce a mouth-insoluble product. However, these approaches might affect the dissolution profile of the drug leading to compromised release in the GIT. Similar issues may also be faced if modified release technologies are used alongside the ODT platform to target different parts of the GIT. Accordingly, the complexity and scalability issues of the processes used in the manufacture of these systems have an impact on the final cost of the dosage form.

The ODT modified release methodology discussed in this work provided an aqueous continuous process for encapsulation of the drug within pH-responsive polymer (HPMCAS) that ultimately protect the drug from acidic degradation (pH 1-2) and potentially provides taste masking. The produced particles were small in size (<20 μm) which is necessary to minimize gritty mouthfeel. The process utilised no plasticizers due to film-forming material HPMCAS being totally soluble in ammonia neutralised solution. Moreover, the formulation composition utilised TPGS as a subcoat

that minimizes chemical interaction of the drug with HPMCAS coating layer. The drug: polymer ratio (omeprazole: HPMCAS) which was successful in achieving the highest yield (60%) and encapsulation efficiency (60%) was 1:45. The encapsulated drug transformed from crystalline to amorphous form during the process due to spray drying fast drying/recrystallization rate. The spray drying process was optimised using mathematical design of experiments (DOE) which helped understand the influence of process parameters on product quality attributes.

The lack of cost-effective and reproducible techniques for assessing taste masking of ODTs (and orodispersible dosage forms) is also one of main hurdles in age-appropriate drug development. With the recent regulatory incentives multiple researchers and stakeholders are involved in developing effective taste masking strategies and assessment tools which could have a significant potential for commercialisation in the near future.

Future work

- The development of pharmaceutical particulates with complex structures and functionalities for drug delivery applications. Spray drying could be utilised as one of the techniques due to its potential to precisely control particle size, morphology, porosity and moisture content.

- Modelling the drying behaviour of droplets during spray drying to optimise process parameters based on predictive elements and minimize reliance on empirical approaches.

- Utilising modelling tools such as CFD and other risk assessment strategies to predict and de-risk the scale-up of spray dried formulations.

List of References

ABDELBARY, G. et al. (2004) The preparation of orally disintegrating tablets using a hydrophilic waxy binder. *International Journal of Pharmaceutics*, 278(2), pp. 423-433.

ABDELBARY, G. et al. (2005) Determination of the in vitro disintegration profile of rapidly disintegrating tablets and correlation with oral disintegration. *International Journal of Pharmaceutics*, 292(1-2), pp. 29–41.

ADOLFSSON, Å., GUSTAFSSON, C. and NYSTRÖM, C. (1999) Use of tablet tensile strength adjusted for surface area and mean interparticulate distance to evaluate dominating bonding mechanisms. *Drug Development and Industrial Pharmacy*, 25(6), pp. 753-764.

AHUJA, S. and DONG, M. (2005) *Handbook of pharmaceutical analysis by HPLC*. Amsterdam: Elsevier.

ALDERBORN, G. and NYSTRÖM, C. (1996) *Pharmaceutical Powder Compaction Technology*. New York: Marcel Dekker.

ALDERBORN, G. et al. (1988) Studies on direct compression of tablets. XIX: The effect of particle size and shape on the mechanical strength of sodium bicarbonate tablets. *Acta Pharmaceutica Suecica,* 25(1), pp. 31-40.

ALHNAN, M. et al. (2011) Spray-drying enteric polymers from aqueous solutions: a novel, economic, and environmentally friendly approach to produce pH-responsive microparticles. *European Journal of Pharmaceutics and Biopharmaceutics*, 79(2), pp. 432-439.

ALHUSBAN, F. et al. (2010) Investigation of formulation and process of lyophilised orally disintegrating tablet (ODT) using novel amino acid combination. *Pharmaceutics*, 2(1), pp. 1-17.

ALHUSBAN, F., PERRIE, Y. and MOHAMMED, AR. (2011) Formulation of multiparticulate systems as lyophilised orally disintegrating tablets. *European Journal of Pharmaceutics and Biopharmaceutics*, 79(3), pp. 627–634.

AL-KHATTAWI, A. and MOHAMMED, AR. (2013) Compressed orally disintegrating tablets: excipients evolution and formulation strategies. *Expert opinion on drug delivery*, 10(5), pp.651–663.

AL-KHATTAWI, A. et al. (2012) Multi stage strategy to reduce friability of directly compressed orally disintegrating tablets. *Drug Delivery Letters*, 2(3), pp. 195-201.

Al-KHATTAWI, A. et al. (2014 a) Systematic screening of compressed ODT excipients: cellulosic versus non-cellulosic. *Current Drug Delivery*, 11(4) pp. 486-500.

AL-KHATTAWI, A. et al. (2014 b) Evidence-based nanoscopic and molecular framework for excipient functionality in compressed orally disintegrating tablets. PloS one, 9(7), pp. DOI: 10.1371/journal.pone.0101369.

ALVAREZ-LORENZO, C. et al. (2000 a) Evaluation of low-substituted hydroxypropylcelluloses (L-HPCs) as filler-binders for direct compression. *International Journal of Pharmaceutics*, 197(1-2), pp. 107–116.

ALVAREZ-LORENZO, C. et al. (2000 b) The stability of theophylline tablets with a hydroxypropylcellulose matrix. *Drug Development and Industrial Pharmacy*, 26(1), pp. 13–20.

AMIDON, GE. and HOUGHTON, ME. (1995) The effect of moisture on the mechanical and powder flow properties of microcrystalline cellulose. *Pharmaceutical Research*, 12(6), pp. 923-929.

ANDERSON, N. et al. (1996) *Having duloxetine core, hydroxypropyl methyl cellulose acetate succinate enteric layer*. US5508276 A. USA.

ANTIKAINEN, O. and YLIRUUSI, J. (2003) Determining the compression behaviour of pharmaceutical powders from the force–distance compression profile. *International Journal of Pharmaceutics*, 252(1-2), pp.253–261.

AULTON, M. (2007) *Aulton's pharmaceutics: the design and manufacture of medicines*. 3rd ed. London: Churchill Livingstone.

AVALLE, P. et al. (2011) The use of in situ near infrared spectroscopy to provide mechanistic insights into gel layer development in HPMC hydrophilic matrices. *European Journal of Pharmaceutical Sciences*, 43(5), pp. 400-408.

BARTLETT, DW. et al. (1996) A study of the association between gastro-oesophageal reflux and palatal dental erosion. *British Dental Journal*, 181(4), pp. 125 – 131.

BERGGREN, J. et al. (2004) Compression behaviour and tablet-forming ability of spray-dried amorphous composite particles. *European Journal of Pharmaceutical Sciences,* 22(2–3), pp. 191–200.

BERMAN, HM., JEFFREY, GA. and ROSENSTEIN, RD. (1968) The crystal structures of the α' and β forms of D-mannitol. *Acta Crystallographica Section B Structural Crystallography and Crystal Chemistry*, 24(3), pp.442–449.

BHANDARI, B. et al. (1997) A semi-empirical approach to optimise the quantity of drying aids required to spray dry sugar-rich foods. *Drying Technology*, 15(10), pp. 2509-2525.

BHATIA, R. and LORDI, N. (1979) Conductivity and hardness changes in aged compacts. *Journal of Pharmaceutical Sciences*, 68(7), pp. 896–899.

BHOYAR, PK., BIYANI, DM. and UMEKAR, MJ. (2010) Formulation and characterization of patient-friendly dosage form of ondansetron hydrochloride. *Journal of Young Pharmacists*, 2(3), pp. 240-246.

BI, Y. et al. (1996) Preparation and evaluation of a compressed tablet rapidly disintegrating in the oral cavity. *Chemical and Pharmaceutical Bulletin,* 44(11), pp. 2121-2127.

BI, YX. et al. (1999) Evaluation of rapidly disintegrating tablets prepared by a direct compression method. *Drug Development and Industrial Pharmacy*, 25(5), pp. 571-581.

BODMEIER, R. and CHEN, H. (1988) Preparation of biodegradable poly (±) lactidemicroparticles using a spray-drying technique. *Journal of Pharmacy and Pharmacology*, 40(11), pp. 754–757.

BOEHRINGER MANNHEIM GMBH. (1975) *Preparation of porous tablets*. US3,885,026.

BOLHUIS, G. and CHOWHAN, Z. (1996) Materials for direct compaction. In: ALDERBORN G. and NYSTRÖM C., (eds.) *Pharmaceutical Powder Compaction Technology*. New York: Marcel Dekker, pp. 419-500.

BOLHUIS, GK. et al. (1975) Film formation by magnesium stearate during mixing and its effect on tableting. *Pharmaceutisch Weekblad*, 110(16), pp. 317–325

BOLHUIS, GK., SMALLENBROEK, AJ. and LERK, CF. (1981) Interaction of tablet disintegrants and magnesium stearate during mixing I: effect on tablet disintegration. *Journal of Pharmaceutical Sciences*, 70(12), pp. 1328-1330.

BORA, D., BORUDE, P. and BHISE, K. (2008) Taste masking by spray-drying technique. *AAPS PharmSciTech*, 9(4), pp. 1159-1164.

BOS, CE., VROMANS, H. and LERK, CF. (1991) Lubricant sensitivity in relation to bulk density for granulations based on starch or cellulose. *International Journal of Pharmaceutics*, 67(1), pp. 39-49.

BRITISH PHARMACOPEIA COMMISSION (2012) *British pharmacopoeia*. London: Stationery Office.

BRITTAIN, H. (1995) *Physical characterization of pharmaceutical solids*. New York: Marcel Dekker.

BROADHEAD, J. et al. (1994) The effect of process and formulation variables on the properties of spray-dried beta-galactosidase. *Journal of Pharmacy and Pharmacology*, 46(6), pp. 458-467.

BROWN, D. (2001) Orally disintegrating tablets: taste over speed. *Drug Delivery Technology*, 3, pp. 58-61.

BUCHI (2012) *Nano Spray Dryer B-90* [Online]. Available from: http://www.buchi.com/Nano-Spray-Dryer-B-90.12378.0.html [Accessed 10/02/2012].

BURGER, A. et al. (2000) Energy/temperature diagram and compression behavior of the polymorphs of D-Mannitol. *Journal of Pharmaceutical Sciences,* 89(4), pp. 457-468.

BUSIGNIES, V. et al. (2006) Compaction behaviour and new predictive approach to the compressibility of binary mixtures of pharmaceutical excipients. *European Journal of Pharmaceutics and Biopharmaceutics,* 64(1), pp. 66-74.

BUTT H. (1991) Measuring electrostatic, van der Waals, and hydration forces in electrolyte solutions with an atomic force microscope. *Biophysical Journal*, 60(6), pp. 1438–1444.

CAMESANO, TA. and LOGAN, BE. (2000) Probing bacterial electrosteric interactions using atomic force microscopy. *Environmental Science and Technology*, 34(16), pp. 3354–3362.

CARNABY-MANN, G. and CRARY, M. (2005) Pill swallowing by adults with dysphagia. *Archives of otolaryngology--head & neck surgery*, 131(11), pp. 970-975.

CARR, R. (1965) Evaluating flow properties of solids. *Chemical Engineering*, 72(2), pp. 163–168.

CASTELLANOS, A. (2005) The relationship between attractive interparticle forces and bulk behaviour in dry and uncharged fine powders. *Advances in Physics*, 54(4), pp. 263-376.

CHANG, RK. et al. (2000) Fast-dissolving tablets. *Pharmaceutical Technology*, 24, pp. 52–58.

CHATTORAJ, S., SHI, LM. and SUN, CC. (2010) Understanding the relationship between crystal structure, plasticity and compaction behaviour of theophylline, methyl gallate, and their 1: 1 co-crystal. *Crystal Engineering communications,* 12(8), pp. 2466-2472.

CHAW, KC., MANIMARAN, M. and TAY, FE. (2005) Role of silver ions in destabilization of intermolecular adhesion forces measured by atomic force microscopy in staphylococcus epidermidis biofilms. *Antimicrobial Agents and Chemotherapy,* 49(12), pp. 4853-4859.

CHOWHAN, Z. (1980) Role of binders in moisture-induced hardness increase in compressed tablets and its effect on in vitro disintegration and dissolution. *Journal of Pharmaceutical Sciences*, 69(1), pp. 1-4.

CHOWHAN, Z. et al. (1982) Effect of moisture and crushing strength on tablet friability and in vitro dissolution. *Journal of Pharmaceutical Sciences*, 71(12), pp. 1371-1375.

CIMA LABS. (1991) *Effervescent dosage form and method of administering same.* WO/1991/004757.

CIMA LABS. (1997) *Taste masking microparticles for oral dosage forms*. US5607697A.

CORAPCIOGLU, F. and SARPER, N. (2005) A prospective randomized trial of the antiemetic efficacy and cost-effectivenes of intravenous and orally disintegrating tablet of ondansetron in children with cancer. *Journal of Pediatric Hematology Oncology*, 22(2), pp. 103–114.

COUNCIL OF EUROPE (2005 a) Omeprazole. Strasbourg: European Pharmacopeia. pp. 2146-2148.

COUNCIL OF EUROPE (2005 b) Sodium hydrogen carbonate (Ammonium). Strasbourg: European Pharmacopeia. p. 2437.

CROWLEY, K. et al. (2013) The impact of a poorly-soluble drug on disintegration of orally disintegrating tablets made by different manufacturing technologies. Catalent Pharma Solutions. Available from: http://tablet.catalent.com/var/plain_site/storage/original/application/a4734885037548bc1b121a1ced 0e3b4a.pdf [Accessed 20/02/2014].

CRUZ, L. et al. (2009) High encapsulation efficiency of sodium alendronate in eudragit S100/HPMC blendmicroparticles. *Química Nova*, 32(5), pp. 1170-1174.

DAVIDSON, A. and MCCALLUM A. (1996) A survey of the stability of omeprazole products from 13 countries. *Drug Development and Industrial Pharmacy,* 22(12), pp. 1173-1185.

DAVIES, MJ. et al. (2011) Towards crystal engineering via simulated pulmonary surfactant monolayers to optimise inhaled drug delivery. *International Journal of Pharmaceutics*, 421(1), pp. 1-11.

DAVIS, SS. et al. (1984) A comparative study of the gastrointestinal transit of a pellet and tablet formulation. *International Journal of Pharmaceutics*, 21(2), pp. 167–177.

DEVIREDDY, SR., GONUGUNTA, CS. and VEERAREDDY, PR. (2009) Formulation and evaluation of taste-masked levocetirizinedihydrochloride orally disintegrating tablets. *PDA Journal of Pharmaceutical Sciences and Technology*, 63(6), pp. 521-526.

DONG, Z. and CHOI, D. (2008) Hydroxypropyl Methylcellulose Acetate Succinate: Potential Drug–Excipient Incompatibility. *AAPS PharmSciTech*, 9(3), pp. 991–997.

DOR, PHJM. and FIX, JA. (2000) In vitro determination of disintegration time of quick-dissolve tablets using a new method. *Pharmaceutical Development and Technology*, 5(4), pp. 575-577.

DURIEZ, X. and JOSHI, AA. (2004) Added functionality excipients: an answer to challenging formulations. *Pharmaceutical Technology*, 28, pp. 12-19.

EL-SHERIF, DM. and WHEATLEY, MA. (2003) Development of a novel method for synthesis of a polymeric ultrasound contrast agent. *Journal of biomedical materials research. Part A*, 66(2), pp. 347–355.

ELVERSSON, J. and MILLQVIST-FUREBY, A. (2005) Particle size and density in spray drying—effects of carbohydrate properties. *Journal of Pharmaceutical Sciences*, 94(9), pp. 2049-2060.

EMA CHMP (2006) Reflection paper: formulations of choice for the paediatric population. London: EMA.

EMA EDQM. (2005) Ph. Eur. monographs on tablets. Strasbourg: EMA.

ERIKSSON, L. et al. (2008) *Design of Experiments: Principles and Applications*. 3rd ed. Umea: Umetrics Academy.

EVE, JK. et al. (2002) A study of single drug particle adhesion interactions using atomic force microscopy. *International Journal of Pharmaceutics*, 238(1-2), pp. 17-27.

FAGRON. (2011) *Omeprazolum (omeprazole) certificate of analysis* [Online]. Available from: https://fagron.com/sites/default/files/document/coa_6fd/COA_510767_Omeprazolum_11E31-B07-261885_%28EN%29.pdf [Accessed 20/06/2014].

FANG, F., ADAMS, R., HAHM, HA. (2006) *Desktop disintegration test for orally disintegrating tablets (ODT's): a rapid and simple method for observing the disintegration behavior for the regulatory review scientists in the evaluation of drug applications* [Online]. FDA/Center for Drug Evaluation and Research. Available from: http://www.accessdata.fda.gov/ScienceForums/forum06/K-14.htm [Accessed 23/2/2014].

FDA. (1998) Guidance for industry stability testing of drug substances and drug products. Maryland: FDA Center for Drug Evaluation and Research.

FDA. (2011) Letter to healthcare professionals: communication on lansoprazole delayed-release orally disintegrating tablets manufactured by Teva Pharmaceuticals [Online]. Available from: http://www.fda.gov/Drugs/Drugsafety/ucm251485.htm [Accessed 07/07/2014]

FDA CDER. (2008) *Guidance for industry: orally disintegrating tablets*. Maryland: FDA.

FIGUEIRAS, A. et al. (2007) Solid-state characterization and dissolution profiles of the inclusion complexes of omeprazole with native and chemically modified β-cyclodextrin. *European Journal of Pharmaceutics and Biopharmaceutics*, 67(2), pp. 531-539.

FORD, J. and TIMMINS, P. (1989) *Pharmaceutical Thermal Analysis - Techniques and Applications*. Chichester: Ellis Horwood.

FOX, C. et al. (1963) Microcrystalline cellulose in tableting. *Drug and Cosmetic Industry,* 92, pp. 161-164.

FRANSÉN, N. et al. (2008) Physicochemical interactions between drugs and superdisintegrants. *Journal of Pharmacy and Pharmacology*, 60 (12), pp. 1583–1589.

FU, X. et al. (2012) Effect of particle shape and size on flow properties of lactose powders. *Particuology*, 10(2), pp. 203-208.

FU, Y. et al. (2004) Orally fast disintegrating tablets: developments, technologies, taste-masking and clinical studies. *Critical Review Therapeutic Drug Carrier Systems*, 21(6), pp. 433-475.

FUKAMI, J. et al. (2005) Development of fast disintegrating compressed tablets using amino acid as disintegration accelerator: evaluation of wetting and disintegration of tablet on the basis of surface free energy. *Chemical and Pharmaceutical Bulletin*, 53(12), pp. 1536-1539.

FUKUOKA, E. et al. (1993) Pattern fitting procedure for the characterization of crystals and/or crystallites in tablets. *Chemical and Pharmaceutical Bulletin,* 41(12), pp. 2166–2171.

GAREKANI, HA. et al. (2001) Crystal habit modifications of ibuprofen and their physicomechanical characteristics. *Drug Development and Industrial Pharmacy*, 27(8), pp. 803–809.

GELEIJNSE, J. et al. (2007) Sodium and potassium intake and risk of cardiovascular events and all-cause mortality: the Rotterdam study. *European Journal of Epidemiology*, 22(11), pp. 763–770.

GERVELAS, C. et al. (2007) Direct lung delivery of a dry powder formulation of DTPA with improved aerosolization properties: effect on lung and systemic decorporation of plutonium. *Journal of controlled release,* 118(1), pp.78–86.

Gharsallaoui, A. et al. (2007) Applications of spray-drying in microencapsulation of food ingredients: An overview. *Food Research International*, 40(9), 1107–1121.

GHEBRE-SELLASSIE, I. (1994) *Multiparticulate oral drug delivery*. New York: Marcel Dekker.

GISSINGER, D. and STAMM, A. (1980) Comparative evaluation of the properties of some tablet disintegrants. *Drug Development and Industrial Pharmacy*, 6 (5), pp. 511–536.

GOEL, H. et al. (2008) Orally disintegrating systems: innovations in formulation and technology. *Recent Patents on Drug Delivery and Formulation*, 2(3), pp. 258-274.

GOHEL, M. (2005) A review of co-processed directly compressible excipients. *Journal of Pharmacy and Pharmaceutical Sciences*, 8(1), pp. 76-93.

GOHEL, M. et al. (2004) Formulation design and optimization of mouth dissolve tablets of nimesulide using vacuum drying technique. *AAPS PharmSciTech*, 5(3), pp. 1-6.

GOHEL, MC. et al. (2007) Improving the tablet characteristics and dissolution profile of ibuprofen by using a novel coprocessed superdisintegrant: A technical note. *AAPS PharmSciTech,* 8(1), pp. E94–E99.

GONNISSEN, Y., REMON, JP. and VERVAET, C. (2007) Development of directly compressible powders via co-spray drying. *European Journal of Pharmaceutics and Biopharmaceutics*, 67(1), pp. 220-226.

GOULA, A. and ADAMOPOULOS, K. (2004) Spray drying of tomato pulp: effect of feed concentration. *Drying Technology*, 22(10), pp. 2309-2330.

GOULA, A. and ADAMOPOULOS, K. (2005) Spray drying of tomato pulp in dehumidified air: II. The effect on powder properties. *Journal of Food Engineering*, 66(1), pp. 35–42.

GRIERSON, DS., FLATER, EE. and CARPICK, RW. (2005) Accounting for the JKR–DMT transition in adhesion and friction measurements with atomic force microscopy. *Journal of Adhesion Sciences and Technology*, 19(3), pp. 291-311.

GRYCZKE, A. et al. (2011) Development and evaluation of orally disintegrating tablets (ODTs) containing ibuprofen granules prepared by hot melt extrusion. *Colloids and Surfaces*, 86(2), pp. 275-284.

HANCOCK, B. and PARKS, M. (2000) What is the true solubility advantage for amorphous pharmaceuticals?. *Pharmaceutical Research*, 17(4), pp. 397-404.

HANCOCK, BC. and ZOGRAFI, G. (1997) Characteristics and significance of the amorphous state in pharmaceutical systems. *Journal of Pharmaceutical Sciences*, 86(1), pp. 1-12.

HAPGOOD, K. and OBARA, S. (2009) *Structure of L-HPC* [Online]. Available from: http://www.medicinescomplete.com/mc/excipients/current/1001939614.htm?q=L-HPC&t=search&ss=text&p=2#_hit reference [Accessed 11/01/2012].

HARADA, T. et al. (2006) Evaluation of the disintegration properties of commercial famotidine 20 mg orally disintegrating tablets using a simple new test and human sensory test. *Chemical and Pharmaceutical Bulletin*, 54(8), pp. 1072-1075.

HARMON, TM. (2007) Orally disintegrating tablets: a valuable life cycle management strategy. *Pharmaceutical Communications*. Available from:

http://www.aptalispharmaceuticaltechnologies.com/pdf/EURX_Article_March_2007.pdf [Accessed 13/01/2013]

HAUSNER, H. (1967) Friction conditions in a mass of metal powder. *International Journal of Powder Metallurgy*, 3(4), pp. 7-13.

HAWARE, R. et al. (2010) Evaluation of a rapid approximation method for the elastic recovery of tablets. *Powder Technology*, 202(1-3), pp. 71–77.

HE, W. et al. (2009) Design and in vitro/in vivo evaluation of multi-layer film coated pellets for omeprazole. *Chemical and Pharmaceutical Bulletin*, 57(2), pp. 122-128.

HECKEL, RW. (1961) Density-Pressure Relationships in Powder Compaction. *Transactions of the Metallurgical Society of AIME*, 221, pp. 671–675.

HENG, P. et al. (2001) Investigation of the influence of mean HPMC particle size and number of polymer particles on the release of aspirin from swellable hydrophilic matrix tablets. *Journal of Controlled Release*, 76(1–2), pp. 39–49.

HERSEY, JA. and REES, JE. (1971) Deformation of Particles During Briquetting. *Nature Physical Science*, 230, p. 96.

HERTING, MG. and KLEINEBUDDE, P. (2007) Roll compaction/dry granulation: Effect of raw material particle size on granule and tablet properties. *International Journal of Pharmaceutics*, 338(1-2), pp. 110-118.

HESS, H. (1978) Tablets under the microscope. *Pharmaceutical Technology*, 3, pp. 38-57.

HINTERSTOISSER, B., AKERHOLM, M. and SALMEN, L. (2003) Load distribution in native cellulose. *Biomacromolecules*, 4(5), pp. 1232-1237.

HORN, D. and SQUIRE, C. (1966) The estimation of ammonia using the indophenol blue reaction. *Clinica Chimica Acta*, 14(2), pp. 185–194.

HOWDEN, CW. (2004) Management of acid-related disorders in patients with dysphagia. *American Journal of Medicine*, 117(5A), pp. 44S-48S.

HU, J., JOHNSTON, KP. and WILLIAMS, RO. (2004) Nanoparticle engineering processes for enhancing the dissolution rates of poorly water soluble drugs. *Drug Development and Industrial Pharmacy*, 30(3), pp. 233-245.

HULSE, WL. et al. (2009) The characterization and comparison of spray-dried mannitol samples. *Drug development and industrial pharmacy*, 35(6), pp. 712–718.

HUMBERT-DROZ, P. et al. (1982) Methoderapide de determination du comportement a la compression pour des etude de preformulation. *Pharmaceutica Acta Helvetiae*, 57(1), pp. 136–143.

HÜTTENRAUCH, R. (1971) Identification of hydrogen bonds by means of deuterium exchange demonstration of binding forces in compressed cellulose forms. *Pharmazie,* 26, pp. 645-646.

HUYHNH-BA, K. (2009) *Handbook of Stability Testing in Pharmaceutical Development: Regulations, Methodologies and Best Practices*. New York: Springer Science.

IBAÑEZ, MD. et al. (2007) Safety of specific sublingual immunotherapy with SQ standardized grass allergen tablets in children. *Pediatric Allergy and Immunology*, 18(6), pp. 516-522.

ICH (2003) Stability testing of new drug substances and products. Q1A(R2). Geneva: International conference on harmonisation.

ICH (2005) Validation of analytical procedures: text and methodology. Q2(R1). Geneva: International conference on harmonisation.

ILKKA, J. and PARONEN, P. (1993) Prediction of the compression behaviour of powder mixtures by the heckel equation. *International Journal of Pharmaceutics*, 94(1), pp. 181-187.

INGHELBRECHT, S. and REMON, JP. (1998) Roller compaction and tableting of microcrystalline cellulose drug mixtures. *International Journal of Pharmaceutics*, 161(2), pp. 215-224.

ISHIKAWA, T. et al. (2000) Effect of hydroxypropylmethylcellulose (HPMC) on the release profiles and bioavailability of a poorly water-soluble drug from tablets prepared using macrogol and HPMC. *International Journal of Pharmaceutics*, 202(1-2), pp. 173–178.

ISHIKAWA, T. et al. (2001) Preparation of rapidly disintegrating tablet using new types of microcrystalline cellulose (PH-M series) and low substituted-hydroxypropylcellulose or spherical sugar granules by direct compression method. *Chemical and Pharmaceutical Bulletin*, 49(2), pp. 134-139.

ITO, A. and SUGIHARA, M. (1996) Development of oral dosage form for elderly patients: use of agar as base of rapidly disintegrating oral tablets. *Chemical and Pharmaceutical Bulletin*, 44(11), pp. 2132-2136.

JACOB, S., SHIRWAIKAR, A. and NAIR, A. (2009) Preparation and evaluation of fast-disintegrating effervescent tablets of glibenclamide. *Drug Development and Industrial Pharmacy*, 35(3), pp. 321-328.

JANARDHNAN, S. and SAIN, M. (2011) Isolation of cellulose nanofibers: effect of biotreatment on hydrogen bonding network in wood fibers. *International Journal of Polymer Science,* DOI:10.1155/2011/279610.

JANSEN, P. et al. (1997) Characterization of impurities formed by interaction of duloxetine HCl with enteric polymers hydroxypropyl methylcellulose acetate succinate and hydroxypropyl methylcellulose phthalate. *Journal of Pharmaceutical Sciences.* 87(1), pp. 81-85.

JAROSZ, PJ. and PARROTT, EL. (1982) Factors influencing axial and radial tensile strengths of tablets. *Journal of Pharmaceutical Sciences*, 71(6), pp. 607–614.

JEONG, S. et al. (2010) Fast disintegrating tablets. In: HONG W. and KINAM P, (eds.) *Oral controlled release formulation design and drug delivery: theory to practice*. New Jersey: John Wiley and Sons.

JEONG, SH., Fu, Y. and PARK, K. (2005) Frosta: a new technology for making fast-melting tablets. *Expert Opinion on Drug Delivery*, 2(6), pp. 1107-1116.

JIVRAJ, M., MARTINI, LG. and THOMSON, CM. (2000) An overview of the different excipients useful for the direct compression of tablets. *Pharmaceutical Science and Technology Today*, 3(2), pp.58–63.

JOHN WYETH AND BROTHER LTD. (1981) *Pharmaceutical dosage form packages*. US4,305,502.

JOHNSON, KL., KENDALL, K. and ROBERTS, AD. (1971) Surface energy and the contact of elastic solids. *Proceedings of the Royal Society A,* 324(1558), pp. 301-313.

JOINT FORMULARY COMMITTEE (2012) British National Formulary. London: British Medical Association and Royal Pharmaceutical Society of Great Britain.

JONES, R. et al. (2011) The influence of formulation and manufacturing process parameters on the characteristics of lyophilized orally disintegrating tablets. *Pharmaceutics*, 3(3), pp. 440-457.

JONES, T. (1981) The physicotechnical properties of starting materials used in tablet formulation. *International Journal of Pharmaceutical Technology & Product Manufacture*, 2(2), pp. 17-24.

JOSHI, A. and DURIEZ, X. (2004) Added functionality excipients: an answer to challenging formulations. *Pharmaceutical Technology Excipients and Solid Dosage Forms*, (June), pp. 12-19.

JUPPO, AM. et al. (1995) Compression of lactose, glucose and mannitol granules. *Journal of Pharmacy and Pharmacology*, 47(7), pp. 543–549.

KAIALY, W. et al. (2010) Engineered mannitol as an alternative carrier to enhance deep lung penetration of salbutamol sulphate from dry powder inhaler. *Colloids and Surfaces B: Biointerfaces,* 79(2), pp. 345-356.

KAKUTANI, R., MURO, H. and MAKINO, T. (2010) Development of a new disintegration method for orally disintegrating tablets. *Chemical and Pharmaceutical Bulletin,* 58(7), pp. 885-890.

KANDEIL, A. et al. (1977) The use of hardness in the study of compaction behaviour and die loading. *Powder Technology*, 17(3), pp. 253–257.

KAREHILL, PG. and NYSTRÖM, C. (1990 a) Studies on direct compression of tablets XXI. Investigation of bonding mechanisms of some directly compressed materials by strength characterization in media with different dielectric constants (relative permittivity). *International Journal of Pharmaceutics*, 61(3), pp. 251-260.

KAREHILL, R. and NYSTRÖM, C. (1990 b) Studies on direct compression of tablets. XXII. Investigation of strength increase upon ageing and bonding mechanisms for some plastically deforming materials. International Journal of Pharmaceutics, 64(1), pp. 27–34.

KAREHILL, PG., GLAZER, M. and NYSTRÖM, C. (1990) Studies on direct compression of tablets. XXIII. The importance of surface roughness for the compactability of some directly compressible materials with different bonding and volume reduction properties. *International Journal of Pharmaceutics*, 64(1), pp. 35-43.

KASLIWAL, N. et al. (2011) Formulation, development, and performance evaluation of metoclopramide HCl oro-dispersible sustained release tablet. *Archives of Pharmaceutical Research*, 34(10), pp. 1691-1700.

KAWANO, Y. et al. (2010) Preparation of orally disintegrating tablets for masking of unpleasant taste: comparison with corrective-adding methods. *Yakugaku Zasshi*, 130(1), pp. 75-80.

KECK, CM. and MÜLLER, RH. (2006) Drug nanocrystals of poorly soluble drugs produced by high pressure homogenisation. *European Journal of Pharmaceutics and Biopharmaceutics*, 62(1), pp. 3-16.

KHANKARI, R. and GRANT, D. (1995) Pharmaceutical hydrates. *Thermochimica Acta*, 248(2), pp. 61-79.

KIM, HS., JEFFREY, GA. and ROSENSTEIN, RD.(1968) The crystal structure of the K form of D-mannitol. *Acta Crystallographica Section B Structural Crystallography and Crystal Chemistry*, 24(11), pp. 1449–1455.

KOIZUMI, K. et al. (1997) New method of preparing high-porosity rapidly saliva soluble compressed tablets using mannitol with camphor, a subliming material. *International Journal of Pharmaceutics*, 152(1), pp. 127–131.

KORNBLUM, SS. and STOOPAK, SB. (1973) A new tablet disintegrating agent: cross-linked polyvinylpyrrolidone. *Journal of Pharmaceutical Sciences*, 62(1), pp. 43-49.

KUNO, Y. et al. (2008 a) Effect of preparation method on properties of orally disintegrating tablets made by phase transition. *International Journal of Pharmaceutics*, 355(1-2), pp. 87-92.

KUNO, Y. et al. (2008 b) Effect of the type of lubricant on the characteristics of orally disintegrating tablets manufactured using the phase transition of sugar alcohol. *European Journal of Pharmaceutics and Biopharmaceutics*, 69(3), pp. 986-992.

KYOWA HAKKO KOGYO CO. (1994) *Rotary type tableting machine with lubricant spraying means*. US5700492.

LAM, KK. and NEWTON, JM. (1992) Influence of particle-size on the adhesion behavior of powders, after application of an initial press-on force. *Powder Technology,* 73, pp. 117-125.

LEBOURGEOIS, JP. et al. (1999) Efficacy of an ondansetron orally disintegrating tablet: a novel oral formulation of this 5-HT(3) receptor antagonist in the treatment of fractionated radiotherapy-induced nausea and emesis. Emesis study group for the ondansetron orally disintegrating tablet in radiotherapy treatment. *Clinical oncology (Royal College of Radiologists (Great Britain))*, 11(5), pp. 340-347.

LIANG, CY. and MARCHESSAULT, RH. (1959) Infrared spectra of crystalline polysaccharides. I. hydrogen bonds in native celluloses. *Journal of Polymer Science*, 37(132), pp. 385-395.

LIEBERMAN, HA., LACHMAN, L. and SCHWARTZ, JB. (1989) *Pharmaceutical dosage forms: tablets*. New York: Marcel Dekker.

LINDBERG, P. et al. (1990) Omeprazole: the first proton pumps inhibitor. *Medicinal Research Reviews*, 10(1), pp. 1–54.

MAA, Y. et al. (1998) Effect of spray drying and subsequent processing conditions on residual moisture content and physical/biochemical stability of protein inhalation powders. *Pharmaceutical Research*, 15(5), pp. 768-775.

MAAS, SG. et al. (2011) The impact of spray drying outlet temperature on the particle morphology of mannitol. *Powder Technology*, 213(1-3), pp. 27–35.

MACGREGOR, EA., BRANDES, J. and EIKERMANN, A. (2003) Migraine prevalence and treatment patterns: the global migraine and zolmitriptan evaluation survey. *Headache*, 43(1), pp. 19-26.

MAEDA, A. et al. (2011) Evaluating tamsulosin hydrochloride-released microparticles prepared using single-step matrix coating. *International Journal of Pharmaceutics*, 408(1-2), pp. 84-90.

MAGGI, L. et al. (1999) Formulation of biphasic release tablets containing slightly soluble drugs. *European Journal of Pharmaceutics and Biopharmaceutics,* 48(1), pp. 37–42.

MALTESEN, M. et al. (2008) Quality by design – spray drying of insulin intended for inhalation. *European Journal of Pharmaceutics and Biopharmaceutics*, 70(3), pp. 828–838.

MARKOVIC, N. et al. (2006) Physical and thermal characterisation of chiral omeprazole sodium salts. *Journal of Pharmaceutical and Biomedical Analysis*, 42(1), pp. 25–31.

MARSHALL, PV., YORK, P. and MACLAINE, JQ. (1993) An investigation of the effect of the punch velocity on the compaction properties of ibuprofen. *Powder Technology,* 74(2), pp. 171-177.

MARTINO, P. et al. (2002) Influence of crystal habit on the compression and densification mechanism of ibuprofen. *Journal of Crystal Growth*, 243(2), pp. 345-355.

MARTINO, P. et al. (2005) Evaluation of different fast melting disintegrants by means of a central composite design. *Drug Development and Industrial Pharmacy*, 31(1), pp. 109-121.

MARVOLA, M. et al. (1989) The effect of food on gastrointestinal transit and drug absorption of a multiparticular sustained-release verapamil formulation. *International Journal of Pharmaceutics*, 53(2), pp. 145–155.

MASTERS, K. (1991) *Spray Drying Handbook*. 5thed. Essex: Longman Scientific & Technical.

MATHEW, M. et al. (1995) Stability of omeprazole solutions at various pH values as determined by high-performance liquid chromatography. *Drug Development and Industrial Pharmacy*, 21(8), pp. 965-971.

MAURY, M. et al. (2005) Effects of process variables on the powder yield of spray-dried trehalose on a laboratory spray-dryer. *European Journal of Pharmaceutics and Biopharmaceutics*, 59(3), pp. 565–573.

MCKENNA, A. and MCCAFFERTY, F. (1982) Effect of particle size on the compaction mechanism and tensile strength of tablets. *Journal of Pharmacy and Pharmacology*, 34(6), pp. 347–351.

MESDJIAN, M. et al. (2001) 'Mise au point d'un test de désagrégation in vitro de comprimésorodispersibles'. *STP Pharma Pratiques*, 11(6), pp. 321-324.

MILLER, J. and MILLER J. (2005) *Statistics and chemometrics for analytical chemistry*. 5th ed. Essex: Pearson Education Limited.

MIMURA, K. et al. (2011) Formulation study for orally disintegrating tablet using partly pregelatinized starch binder. *Chemical and Pharmaceutical Bulletin*, 59(8), pp. 959-964.

MISHRA, DN. et al. (2006) Spray dried excipient base: a novel technique for the formulation of orally disintegrating tablets. *Chemical and Pharmaceutical Bulletin*, 54(1), pp. 99-102.

MISHRA, M. and AMIN, A. (2009) Formulation development of taste-masked rapidly dissolving films of cetirizine hydrochloride. *Pharmaceutical Technology*, 33, pp. 48-56.

MIZUMOTO, T. (2008) Development of a modified-release fast disintegrating tablet (Harnal D) containing fine, modified-release particles. *Membrane-Tokyo*, 33(2), pp. 82-84.

MIZUMOTO, T. et al. (2005) Formulation design of a novel fast-disintegrating tablet. *International Journal of Pharmaceutics*, 306(1-2), pp. 83-90.

MIZUMOTO, T. et al. (2008) Formulation design of taste-masked particles, including famotidine, for an oral fast-disintegrating dosage form. *Chemical and Pharmaceutical Bulletin*, 56(4), pp. 530-535.

MORALES, F. and VAN BOEKEL, M. (1998) A Study on Advanced Maillard Reaction in Heated Casein/Sugar Solutions: Colour Formation. *International Dairy Journal*, 8(10–11), pp. 907–915.

MORALES, JO. et al. (2010) Orally disintegrating tablets using starch and fructose. *Pharmaceutical Technology*, 34, pp. 92-99.

MORITA, Y. et al. (2002) Evaluation of the disintegration time of rapidly disintegrating tablets via a novel method utilizing a CCD camera. *Chemical and Pharmaceutical Bulletin,* 50(9), pp. 1181-1186.

MU, L. and FENG, S. (2001) Fabrication, characterization and in vitro release of paclitaxel (Taxol®) loaded poly (lactic-co-glycolic acid) microspheres prepared by spray drying technique with lipid/cholesterol emulsifiers. *Journal of Controlled Release*, 76(3), PP. 239–254.

MU, L. and FENG, S. (2003) A novel controlled release formulation for the anticancer drug paclitaxel (Taxol®): PLGA nanoparticles containing vitamin E TPGS. *Journal of Controlled Release*, 86(1), pp. 33-48.

MURAKAMI, F. et al. (2009) Physico-chemical solid-state characterization of omeprazole sodium: Thermal, spectroscopic and crystallinity studies. *Journal of Pharmaceutical and Biomedical Analysis*, 49(1), pp. 72-80.

NAGAI, T. et al. (1997) Application of HPMC and HPMCAS to aqueous film coating of pharmaceutical dosage forms. In: MCGINITY J. et al. *Aqueous polymeric coatings for pharmaceutical dosage forms*. 2nd edition. New York: Marcel Dekker, pp. 177–225.

NAGAR, P. et al. (2011) Orally disintegrating tablets: formulation, preparation techniques and evaluation. *Journal of Applied Pharmaceutical Science,* 1(4), pp. 35-45.

NAKANO, Y. et al. (2013) Preparation and evaluation of unpleasant taste-masked pioglitazone orally disintegrating tablets. *International Journal of Pharmaceutics*, 446, pp. 160-165.

NATH, S. and SATPATHY, G. (1998) A systematic approach for investigation of spray drying processes. *Drying Technology*, 16(6), pp. 1173-1193.

NAVARRO, V. (2010) Improving medication compliance in patients with depression: use of orodispersible tablets. *Advances in Therapy*, 27(11), pp. 1-11.

NEKKANTI, V. et al. (2009) Spray-drying process optimization for manufacture of drug-cyclodextrin complex powder using design of experiments. *Drug Development and Industrial Pharmacy*, 35(10), pp. 1219-1229.

NESIC, M., CVETKOVIC, N. and POLIC, DA. (1990) Contribution to the knowledge of the consolidation mechanism of ibuprofen-polyvinylpyrrolidone system. *Acta Pharmaceut Jugo,* 40(4), pp. 545-550.

NEWTON, J. et al. (1971) Computer analysis of the relation between tablet strength and compaction pressure. *Journal of Pharmacy and Pharmacology*, 23(S1), pp. 195S-201S.

NOGAMI, H. et al. (1969) Disintegration of the aspirin tablets containing potato starch and microcrystalline cellulose in various concentrations. *Chemical and Pharmaceutical Bulletin*, 17(7), pp. 1450–1455.

NUNN, T. and WILLIAMS, J. (2005) Formulation of medicines for children. *British Journal of Clinical Pharmacology*, 59(6), pp. 674-676.

NYSTRÖM, C. et al. (1978) Measurement of axial and radial tensile strength of tablets and their relation to capping. *Acta pharmaceutica Suecica*, 15(3), pp. 226–232.

Oh, SY. et al. (2005) Crystalline structure analysis of cellulose treated with sodium hydroxide and carbon dioxide by means of X-ray diffraction and FTIR spectroscopy. *Carbohydrate Research,* 340(15), pp. 2376-2391.

OHREM, HL. et al. (2014) Why is mannitol becoming more and more popular as a pharmaceutical excipient in solid dosage forms? *Pharmaceutical development and technology*, 19(3), pp. 257–262.

OKUDA, Y. et al. (2009) A new formulation for orally disintegrating tablets using a suspension spray-coating method. *International Journal of Pharmaceutics*, 382(1-2), pp. 80-87.

OZEKI, Y. et al. (2003) Evaluation of the compression characteristics and physical properties of the newly invented one-step dry-coated tablets. *International Journal of Pharmaceutics*, 267(1-2), pp. 69-78.

OZMEN, L. and LANGRISH, T. (2003) An experimental investigation of the wall deposition of milk powder in a pilot-scale spray dryer. *Drying Technology*, 21(7), pp. 1253-1272.

PALMIERI, G. (2001) Spray-drying as a method for microparticulate controlled release systems preparation: advantages and limits. I. Water-soluble drugs. *Drug Development and Industrial Pharmacy*, 27(3), pp. 195-204.

PARSONS, DS. (1976) Particle segregation in fine powders by tapping as simulation of jostling during transportation. *Powder Technology*, 13(2), pp. 269-277.

PASSERINI, N. et al. (2002) Preparation and characterisation of ibuprofen-poloxamer 188 granules obtained by melt granulation. *European Journal of Pharmaceutical Sciences*, 15(1), pp. 71-78.

PATEL, D. et al. (2008) Design, development, and optimization of orally disintegrating tablets of etoricoxib using vacuum-drying approach. *PDA Journal of Pharmaceutical Science and Technology*, 62(3), pp. 224-232.

PATHER, SI. et al. (1998) Sustained release theophylline tablets by direct compression part 1: Formulation and in vitro testing. *International Journal of Pharmaceutics,* 164(1-2), pp. 1-10.

PICKER, KM. (1999) The use of carrageenan in mixture with microcrystalline cellulose and its functionality for making tablets. *European Journal of Pharmaceutics and Biopharmaceutics,* 48(1), pp. 27-36.

PICKER, KM. and HOAG, SW. (2002) Characterization of the thermal properties of microcrystalline cellulose by modulated temperature differential scanning calorimetry. *Journal of Pharmaceutical Sciences,* 91(2), pp. 342-349.

PIFFERI, G., SANTORO, P. and PEDRANI, M. (1999) Quality and functionality of excipients. *Farmaco*, 54(1-2), pp. 1-14.

PILBRANT, A. and CEDERBERG, C. (1985), Development of an oral formulation of omeprazole. *Scandinavian Journal of Gastroenterology*, 20 (108), pp. 113-120.

PLATTEEUW, JJ. et al. (2004) *Orally disintegrating tablets*. US2004/0265375 A1.

PODCZECK, F. and MIA, Y. (1996) The influence of particle size and shape on the angle of internal friction and the flow factor of unlubricated and lubricated powders. *International Journal of Pharmaceutics*, 144(2), pp. 187–194.

PRESCOTT, J. and BARNUM, R. (2000) On powder flowability. *Pharmaceutical Technology*, 24, pp. 60-85.

PRESCOTT, JK. and HOSSFELD, RJ. (1994) Maintaining product uniformity and uninterrupted flow to direct compression tablet presses. *Pharmaceutical Technology*, 18, pp. 99-114.

QAISI, A. et al. (2006) Acid decomposition of omeprazole in the absence of thiol: A differential pulse polarographic study at the static mercury drop electrode (SMDE). *Journal of Pharmaceutical Sciences*, 95(2), pp. 384–391.

ROSER et al. (1998) *Rapidly soluble oral dosage forms, method of making same, and composition thereof*. US5,762,961.

QUANTACHROME CORPORATION (2009) *Multipycnometer*. [Instruments manual P/N 05034 Rev C]. Florida.

QUE, L. et al. (2006) Evaluation of disintegrating time of rapidly disintegrating tablets by a paddle method. *Pharmaceutical Development and Technology*, 11(3), pp. 295-301.

RAFFIN, R. et al. (2006) Sodium pantoprazole-loaded enteric microparticles prepared by spray drying: Effect of the scale of production and process validation. *International Journal of Pharmaceutics*, 324(1), pp. 10–18.

RAFFIN, R. et al. (2007) Development of HPMC and Eudragit S100® blendedmicroparticles containing sodium pantoprazole. *Pharmazie*, 62(5), pp. 361–364.

RAHMAN, Z., ZIDAN, AS. and KHAN, MA. (2010) Risperidone solid dispersion for orally disintegrating tablet: its formulation design and non-destructive methods of evaluation. *International Journal of Pharmaceutics*, 400(1-2), pp. 49-58.

RE, M. (1998) Microencapsulation by Spray Drying. *Drying Technology*, 16(6), pp. 1195-1236.

REES, JE. and RUE, PJ. (1978) Time-dependent deformation of some direct compression excipients. *Journal of Pharmacy and Pharmacology*, 30(1), pp. 601-607.

REINECCIUS, G. and BANGS, W. (1985) Spray drying of food flavors. III. Optimum infeed concentrations for the retention of artificial flavours. *Perfumer and flavorist*, 10(1), pp. 27-29.

RICHMAN, MD., FOX, CD. and SHANGRAW, RF. (1965) Preparation and stability of GlycerylTrinitratesublingual tablets prepared by direct compression. *Journal of Pharmaceutical Sciences,* 54(3), pp. 447-451.

RIEDEL, A. AND LEOPOLD, C. (2005 a) Degradation of omeprazole induced by enteric polymer solutions and aqueous dispersions: HPLC investigations. *Drug Development and Industrial Pharmacy*, 31(2), pp. 151-160.

RIEDEL, A. and LEOPOLD, C. (2005 b) Quantification of omeprazole degradation by enteric coating polymers:an UV-VIS spectroscopy study. *Die Pharmazie*, 60(2), pp. 126-130.

RIIPPI, M. et al. (1998) The effect of compression force on surface structure, crushing strength, friability and disintegration time of erythromycin acistrate tablets. *European Journal of Pharmaceutics and Biopharmaceutics*, 46(3), pp. 339–345.

ROBERTS, CJ. (2005) What can we learn from atomic force microscopy adhesion measurements with single drug particles?. *European Journal of Pharmaceutical Sciences*, 24(2-3), pp. 153-157.

ROBERTS, RJ. and ROWE, RC. (1985) The effect of punch velocity on the compaction of a variety of materials. *Journal of Pharmacy and Pharmacology,* 37(6), pp. 377-384.

ROBERTS, RJ. and ROWE, RC. (1986) The effect of the relationship between punch velocity and particle size on the compaction behaviour of materials with varying deformation mechanisms. *Journal of Pharmacy and Pharmacology*, 38(8), pp. 567–571.

ROBERTS, RJ. and ROWE, RC. (1987 a) Brittle ductile behavior in pharmaceutical materials used in tabletting. *International Journal of Pharmaceutics*, 36(2-3), pp. 205-209.

ROBERTS, RJ. and ROWE, RC. (1987 b) The compaction of pharmaceutical and other model materials - a pragmatic approach. *Chemical Engineering Science*, 42(4), pp. 903–911.

ROJAS, J. and KUMAR, V. (2012 a) Effect of silicification on the tableting performance of cellulose II: a novel multifunctional excipient. Chemical and Pharmaceutical Bulletin, 60(5), pp. 603-611.

ROJAS, J. and KUMAR, V. (2012 b) Effect of polymorphic form on the functional properties of cellulose: A comparative study. *Carbohydrate Polymers*, 87(3), pp.2223–2230.

ROMERO, AJ., SAVASTANO, L. and RHODES, CT. (1993) Monitoring crystal modifications in systems containing ibuprofen. *International Journal of Pharmaceutics*, 99(2-3), pp. 125–134.

ROSENBERG, M. et al. (1990) Factors affecting retention in spray-drying microencapsulation of volatile materials. *Journal of Agricultural and Food Chemistry*, 38(5), pp. 1288-1294.

RUBICON RESEARCH PRIVATE LTD. (2009) *Orally Disintegrating Tablets*. US2009/0087485 A1.

RUIZ, M. et al. (1998) Determination of the stability of omeprazole by means of differential scanning calorimetry. *Journal of Thermal Analysis and Calorimetry*, 51(1), pp. 29-35.

RUMPF, H. (1962) The Strength of Granules and Agglomerates. In Knepper, W. ed.: From *Agglomeration*. New York: Wiley-Interscience.

SAMMOUR, OA. et al. (2006) Formulation and optimization of mouth dissolve tablets containing rofecoxib solid dispersion. *AAPS PharmSciTech*, 7(2), pp. E167–E75.

SAMPRASIT, W. et al. (2010) Preparation and evaluation of taste-masked dextromethorphan oral disintegrating tablet. *Pharmaceutical Development and Technology*, 17(3), pp. 315-320.

SANO, S. et al. (2013) Design and evaluation of microwave-treated orally disintegrating tablets containing polymeric disintegrant and mannitol. *International Journal of Pharmaceutics*, 448(1), pp. 132-141.

SARAVANAN, M. et al. (2003) Hydroxypropyl methylcellulose based cephalexin extended release tablets: influence of tablet formulation, hardness and storage on in vitro release kinetics. *Chemical and Pharmaceutical Bulletin,* 51(8), pp. 978-983.

SARRAGUÇA, M. et al. (2010) Determination of flow properties of pharmaceutical powders by near infrared spectroscopy. *Journal of Pharmaceutical and Biomedical Analysis,* 52(4), pp. 484-492.

SCHIERMEIER, S. and SCHMIDT, PC. (2002) Fast dispersible ibuprofen tablets. *European Journal of Pharmaceutical Sciences*, 15(3), pp. 295-305.

SEAGER, H. (1998) Drug-delivery products and the Zydis fast-dissolving dosage form. *Journal of Pharmacy and Pharmacology*, 50(4), pp. 375-382.

SEGALE, L. et al. (2007) Formulation design and development to produce orodispersible tablets by direct compression. *Journal of Drug Delivery Science and Technology*, 17(3), pp. 199-203.

SERAJUDDIN, AT. (1999) Solid dispersion of poorly water-soluble drugs: early promises, subsequent problems, and recent breakthroughs. *Journal of Pharmaceutical Sciences*, 88(10), pp. 1058-1066.

SETON, L. et al. (2010) Solid state forms of theophylline: presenting a new anhydrous polymorph. *Crystal Growth Design*, 10(9), pp. 3879–3886.

SHAH, U. and AUGSBURGE, L. (2001) Evaluation of the functional equivalence of crospovidone NF from different sources. II. Standard performance test. *Pharmaceutical Development Technology*, 6(3), pp. 419-430.

SHARMA, V., PHILIP, AK. and PATHAK, K. (2008) Modified polysaccharides as fast disintegrating excipients for orodispersible tablets of roxithromycin. *AAPS PharmSciTech*, 9(1), pp. 87-94.

SHESHALA, R., KHAN, N. and DARWIS, Y. (2011) Formulation and optimization of orally disintegrating tablets of sumatriptan succinate. *Chemical and Pharmaceutical Bulletin*, 59(8), pp. 920-928.

SHESKEY, P. and DASBACH, T. (1995) Evaluation of various polymers as dry binders in the preparation of an immediate-release tablet formulation by roller compaction. *Pharmaceutical Technology,* 19, pp. 98-112.

SHEU, M. et al. (2003) Influence of micelle solubilization by tocopheryl polyethylene glycol succinate (TPGS) on solubility enhancement and percutaneous penetration of estradiol. *Journal of Controlled Release*, 88(3), pp. 355–368.

SHIBATA, Y. et al. (2004) A novel method for predicting disintegration time in the mouth of rapidly disintegrating tablet by compaction analysis using TabAll. *Chemical and Pharmaceutical Bulletin*, 52(11), pp. 1394-1395.

SHIMIZU, T. et al. (2003 a) Formulation study for lansoprazole fast-disintegrating tablet. I. Effect of compression on dissolution behavior. *Chemical and Pharmaceutical Bulletin*, 51(8), pp. 942-947.

SHIMIZU, T. et al. (2003 b) Formulation study for lansoprazole fast-disintegrating tablet. III. design of rapidly disintegrating tablets. *Chemical and Pharmaceutical Bulletin,* 51(10), pp. 1121-1127.

SHIMIZU, T. et al. (2003 c) Formulation study for lansoprazole fast-disintegrating tablet. II. effect of triethyl citrate on the quality of the products. *Chemical and Pharmaceutical Bulletin*, 51(9), pp. 1029-1035.

SHIN-ETSU (2005) *AQOAT: Hydroxypropyl methyl cellulose acetate succinate* [Online]. Available from: http://www.harke.com/fileadmin/images/chemicals/ShinEtsu_Aqoat.pdf [Accessed 01/08/2014].

SHU, T. et al. (2002) Studies of rapidly disintegrating tablets in the oral cavity using co-ground mixtures of mannitol with crospovidone. *Chemical and Pharmaceutical Bulletin*, 50(2), pp. 193-198.

SHUKLA, D. et al. (2009) Fabrication and evaluation of taste masked resinate of risperidone and its orally disintegrating tablets. *Chemical and Pharmaceutical Bulletin*, 57(4), pp. 337-345.

SIEPMANN, J. and PEPPAS, N. (2001) Modeling of drug release from delivery systems based on hydroxypropyl methylcellulose (HPMC). *Advanced Drug Delivery Reviews*, 48(2–3), pp. 139–157.

SIEWERT, M. et al. (2003) FIP/AAPS guidelines for dissolution/in vitro release testing of novel/special dosage forms. Available from: https://www.fip.org/files/fip/BPS/Dissolution/FIP_AAPS_Guidelines%20for%20Dissolution.pdf [Accessed 12/08/2014].

SINKA, I. et al. (2009) The effect of processing parameters on pharmaceutical tablet properties. *Powder Technology,* 189(2), pp. 276–284.

SIX, K. et al. (2001) Investigation of thermal properties of glassy itraconazole: identification of a monotropicmesophase. *Thermochimica Acta*, 376(2), pp. 175-181.

SMITH, P. and NIENOW, A. (1983) Particle growth mechanisms in fluidised bed granulation-II: Comparison of experimental data with growth models. *Chemical Engineering Science*, 38(8), pp. 1233–1240.

SOH, JLP. et al. (2013) Characterization, optimisation and process robustness of a co-processed mannitol for the development of orally disintegrating tablets. *Pharmaceutical Development and Technology*, 18(1), pp. 172-185.

SONNERGAARD, JM. (1999) A critical evaluation of the Heckel equation. *International Journal of Pharmaceutics*, 193(1), pp. 63-71.

SONNERGAARD, JM. (2001) Investigation of a new mathematical model for compression of pharmaceutical powders. *European Journal of Pharmaceutical Sciences,* 14(2), pp. 149–157.

STÅHL, K. et al. (2002) The effect of process variables on the degradation and physical properties of spray dried insulin intended for inhalation. *International Journal of Pharmaceutics*, 233(1-2), pp. 227 – 237.

STANIFORTH, JN. et al. (1981) The design of a direct compression tableting excipient. *Drug Development and Industrial Pharmacy*, 7(2), pp. 179-190.

STEGEMANN, S., GOSCH, M. and BREITKREUTZ J. (2012) Swallowing dysfunction and dysphagia is an unrecognized challenge for oral drug therapy. *International Journal of Pharmaceutics*, 430(1-2), pp. 197-206.

STRICKLAND, W. et al. (1956) The physics of tablet compression IX: fundamental aspects of tablet lubrication. *Journal of the American Pharmaceutical Association,* 45(1), pp. 51–55.

STROYER, A. et al. (2006) Solid state interactions between the proton pump inhibitor omeprazole and various enteric coating polymers. *Journal of Pharmaceutical Sciences*, 95(6), pp. 1342–1353.

STULZER, H. et al. (2008) Compatibility studies between captopril and pharmaceutical excipients used in tablets formulations. *Journal of Thermal Analysis and Calorimetry*, 91(1), pp. 323-328.

SUGIMOTO, M. et al. (2001) The preparation of rapidly disintegrating tablets in the mouth. *Pharmaceutical Development and Technology*, 6(4), pp. 487-493.

SUGIMOTO, M. et al. (2006) Development of manufacturing method for rapidly disintegrating oral tablets using the crystalline transition of amorphous sucrose. *International Journal of Pharmaceutics*, 320(1-2), pp. 71-78.

SUGIURA, T., UCHIDA, S. and NAMIKI, N. (2012) Taste-masking effect of physical and organoleptic methods on peppermint-scented orally disintegrating tablet of famotidine based on suspension spray-coating method. *Chemical and Pharmaceutical Bulletin*, 60(3), pp. 315-319.

SUIHKO, E. et al. (1997) Dehydration of theophylline monohydrate—A two step process. *International Journal of Pharmaceutics*, 158(1), pp. 47–55.

SUIHKO, E. et al. (2001) Dynamic solid-state and tableting properties of four theophylline forms. *International Journal of Pharmaceutics*, 217(1-2), pp. 225-236.

SUMIYA, K. et al. (2000) Preparation and clinical evaluation of orally-disintegrating clonidine hydrochloride tablets for preanesthetic medication. *YakugakuZasshi*, 120(7), pp. 652-656.

SUN, C. and GRANT, D. (2001) Influence of crystal structure on the tableting properties of sulfamerazine polymorphs. *Pharmaceutical Research*, 18(3), pp. 274-280.

SUNADA, H. and BI, Y. (2002) Preparation, evaluation and optimization of rapidly disintegrating tablets. *Powder Technology,* 122(2-3), pp. 188–198.

SUZUKI, E., SHIMOMURA, K. and SEKIGUCHI, K. (1989) Thermochemical study of theophyline and its hydrate. *Chemical and Pharmaceutical Bulletin*, 37(2), pp. 493-497.

SZCZEŚNIAK, L., RACHOCKI, A. and TRITT-GOC, J. (2008) Glass transition temperature and thermal decomposition of cellulose powder. *Cellulose*, 15(3), pp. 445-451.

TABATA, T. et al. (1994) Manufacturing method of stable enteric granules of a new antiulcer drug (lansoprazole). *Drug Development and Industrial Pharmacy,* 20(9), pp. 1661-1672.

TAKEUCHI, H. et al. (1989) Controlled release theophylline tablet with acrylic polymers prepared by spray-drying technique in aqueous system. *Drug Development and Industrial Pharmacy,* 15(12), pp. 1999-2016.

TANAKA, Y. et al. (2009) Nanoparticulation of poorly water soluble drugs using a wet-mill process and physicochemical properties of the nanopowders. *Chemical and Pharmaceutical Bulletin*, 57(10), pp. 1050-1057.

TATAVARTI, A. et al. (2008) Evaluation of the deformation behavior of binary systems of methacrylic acid copolymers and hydroxypropyl methylcellulose using a compaction simulator. *International Journal of Pharmaceutics*, 348(1-2), pp. 46-53.

TELANG, C., SURYANARAYANAN, R. and YU, L.(2003). Crystallization of D-mannitol in binary mixtures with NaCl: phase diagram and polymorphism. *Pharmaceutical research*, 20(12), pp. 1939–1945.

TEWA-TAGNE, P. et al. (2007) Spray-drying nanocapsules in presence of colloidal silica as drying auxiliary agent: formulation and process variables optimization using experimental designs. *Pharmaceutical Research*, 24(4), pp. 650-661.

TEWES, F. et al. (2006) Biodegradable microspheres: advances in production technology. In: BENITA, S., (ed.) *Microencapsulation methods and industrial applications*. 2nd ed. Florida: CRC Press Taylor and Francis Group.

THE BOARD OF REGENTS OF THE UNIVERSITY OF OKLAHOMA. (1996) *Process for making a particulate support matrix for making a rapidly dissolving tablet*. US5,587,180.

TOBYN, MJ. et al. (1998) Physicochemical comparison between microcrystalline cellulose and silicified microcrystalline cellulose. *International Journal of Pharmaceutics,* 169(2), pp. 183-194.

TRAIN, D. (1957) Transmission forces through a powder mass during the process of pelleting. *Transactions of the Institution of Chemical Engineers.*, 35, pp. 258–266.

TÜRKOĞLU, M. et al. (2004) Tableting and stability evaluation of enteric-coated omeprazole pellets. *European Journal of Pharmaceutics and Biopharmaceutics*, 57(2), pp. 279–286.

TYE, C. et al. (2005) Evaluation of the effects of tableting speed on the relationships between compaction pressure, tablet tensile strength, and tablet solid fraction. *Journal of Pharmaceutical Sciences*, 94(3), pp. 465–472.

TYLE, P. (1993) Effect of size, shape and hardness of particles in suspension on oral texture and palatability. *Acta Psychologica*, 84(1), pp. 111-118.

UMEMURA, K. and KAWAI, S. (2007) Modification of chitosan by the Maillard reaction using cellulose model compounds. *Carbohydrate Polymers*, 68(2), pp. 242–248.

USP CONVENTION. (2005) Tablet Disintegration <701>, Maryland: United States Pharmacopeia.

USP CONVENTION. (2012 a) Bulk Density and Tapped Density of Powders <616>, Maryland: United States Pharmacopeia.

USP CONVENTION. (2012 b) Official monographs/Omeprazole Delayed-Release Capsules, Maryland: United States Pharmacopeia, pp. 4113-4114.

USP CONVENTION. (2012 c) Limit of Ammonia, Maryland: United States Pharmacopeia, p. 4649.

VALLE, MD. (2010) Electronic tongues employing electrochemical sensors. *Electroanalysis*, 22(14), pp. 1539–1555.

VAN VEEN, B. et al. (2000) Tensile strength of tablets containing two materials with a different compaction behaviour. *International Journal of Pharmaceutics*, 203(1-2), pp. 71-79.

VARIA, I. et al. (2007) Effect of mirtazapine orally disintegrating tablets on health-related quality of life in elderly depressed patients with comorbid medical disorders: a pilot study. *Psychopharmacology Bulletin*, 40(1), pp. 47-56.

VEHRING, R. (2008) Pharmaceutical particle engineering via spray drying. *Pharmaceutical research*, 25(5), pp. 999–1022.

VERLEY, P. and YARWOOD, R. (1990) Zydis–a novel fast dissolving dosage form. *Manufacturing Chemist*, 61, pp. 36–37.

WAN, L. et al. (1992) Spray drying as a process for microencapsulation and the effect of different coating polymers. *Drug Development and Industrial Pharmacy*, 18(9), pp. 997-1011.

WANG, L., ZENG, F. and ZONG, L. (2013) Development of orally disintegrating tablets of Perphenazine/hydroxypropyl-β-cyclodextrin inclusion complex. *Pharmaceutical Development and Technology*, 18(5), pp. 1101-1110.

WATANABE, Y. et al. (1995) New compressed tablet rapidly disintegrating in saliva in the mouth using crystalline cellulose and a disintegrant. *Biological and Pharmaceutical Bulletin*, 18(9), pp. 1308-1310.

WEATHERBURN, M. (1967) Phenol-hypochlorite reaction for determination of ammonia. *Analytical Chemistry*, 39(8), pp. 971–974.

WHALEY, P. et al. (2012) Stability of omeprazole in SyrSpend SF Alka (reconstituted). *International Journal of Pharmaceutics*, 16(2), pp. 164-166.

WHELAN, MR., FORD, JL. and POWELL, MW. (2002) Simultaneous determination of ibuprofen and hydroxypropylmethylcellulose (HPMC) using HPLC and evaporative light scattering detection. *Journal of Pharmaceutical and Biomedical Analysis*, 30(4), pp. 1355-1359.

WOERTZ, K. et al. (2011) Taste sensing systems (electronic tongues) for pharmaceutical applications. *International Journal of Pharmaceutics*, 417(1-2), pp. 256-271.

XU, J., BOVET, LL. and ZHAO, K. (2008) Taste masking microspheres for orally disintegrating tablets. *International Journal of Pharmaceutics*, 359(1-2), pp. 63-69.

YAN, YD. et al. (2010) Preparation and evaluation of taste-masked donepezil hydrochloride orally disintegrating tablets. *Biological and Pharmaceutical Bulletin*, 33(8), pp. 1364-1370.

YANG, M. (2011) Spray drying pharmaceuticals. *European Pharmaceutical Review*, 16(6), pp. 64-68.

YORK, P. (1983) Solid-state properties of powders in the formulation and processing of solid dosage forms. *International Journal of Pharmaceutics*, 14(1), pp. 1-28.

YOSHINARI, T. et al. (2002) Moisture induced polymorphic transition of mannitol and its morphological transformation. *International Journal of Pharmaceutics*, 247(1-2), pp. 69-77.

YOSHINARI, T. et al. (2003) The improved compaction properties of mannitol after a moisture-induced polymorphic transition. *International Journal of Pharmaceutics*, 258(1–2), pp. 121-131.

YOSHITA, T., UCHIDA, S. and NAMIKI, N (2013). Clinical disintegration time of orally disintegrating tablets clinically available in Japan in healthy volunteers. *Biological and Pharmaceutical Bulletin*, 36(9), pp. 1488-1493.

YU, L. (2001) Amorphous pharmaceutical solids: preparation, characterization and stabilization. *Advanced Drug Delivery Reviews*, 48(1), pp. 27-42.

YU, L. (2008) Pharmaceutical quality by design: product and process development, understanding and control. *Pharmaceutical Research*, 25(4), pp. 781–791.

YU, L. et al. (1999) Vitamin E-TPGS increases absorption flux of an HIV protease inhibitor by enhancing its solubility and permeability. *Pharmaceutical Research*, 16(12), pp. 1812-1817.

YU, L., MISHRA, DS. and RIGSBEE, DR.(1998) Determination of the glass properties of D-mannitol using sorbitol as an impurity. *Journal of pharmaceutical sciences*, 87(6), pp. 774–777.

ZENG, F. et al. (2013) Formulation and in vivo evaluation of orally disintegrating tablets of clozapine/hydroxypropyl-β-cyclodextrin inclusion complexes. *AAPS PharmSciTech*, 14(2), pp. 854-860.

ZUURMAN, K. et al. (1999) Effect of magnesium stearate on bonding and porosity expansion of tablets produced from materials with different consolidation properties. *International Journal of Pharmaceutics*, 179(1), pp. 107–115.
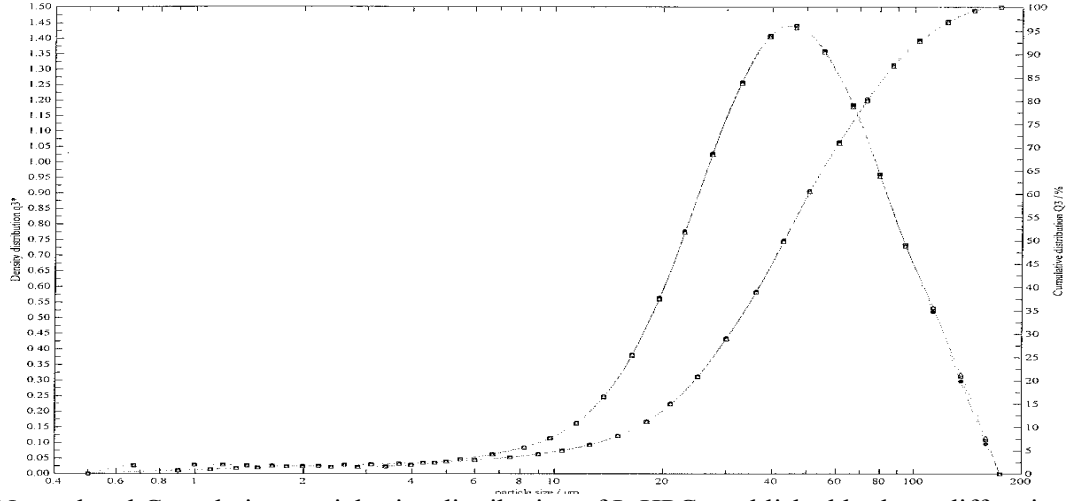
Appendices

Appendix A.
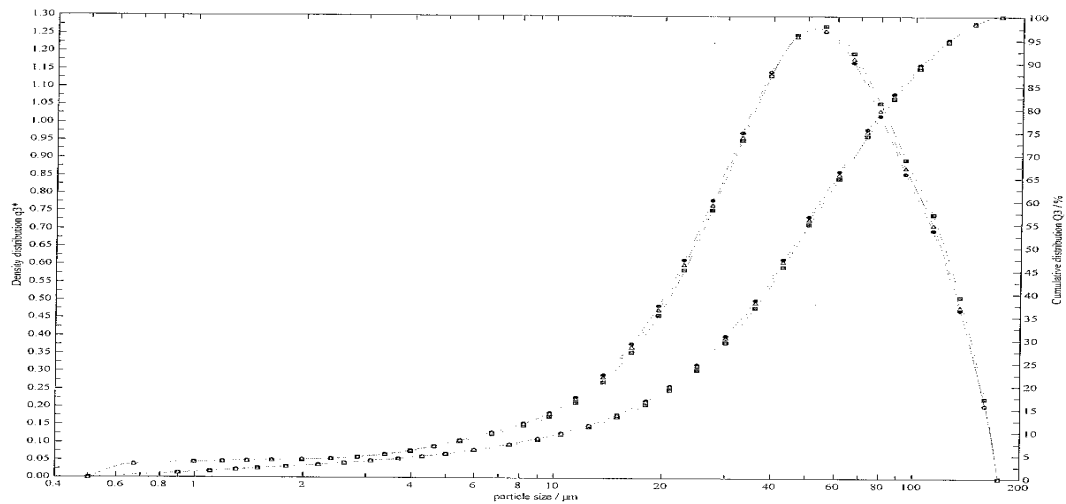

A. 1: Normal and Cumulative particle size distribution of mannitol established by laser diffraction (0 – 175 µm) showing incomplete distribution due to existence of coarse particles.
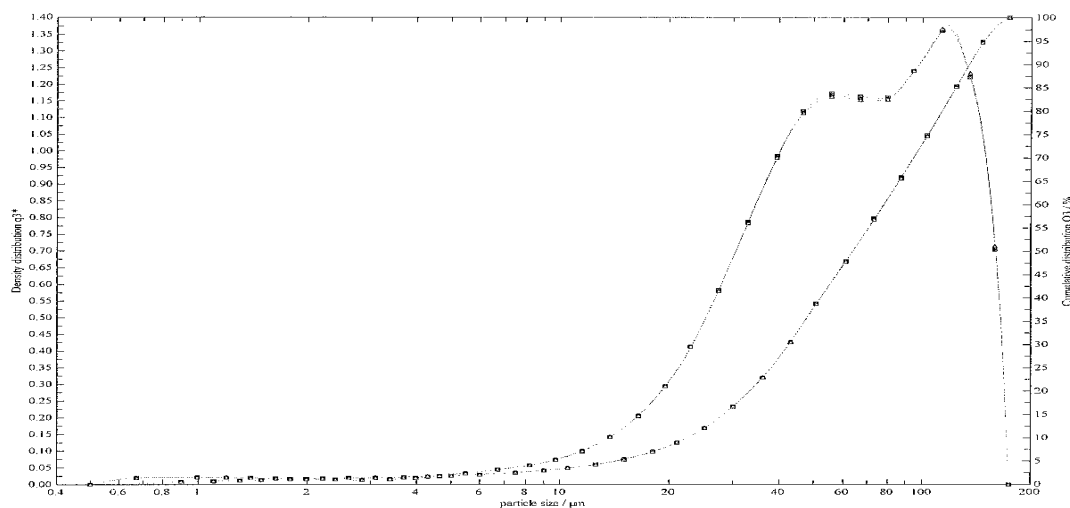

A. 2: Normal and Cumulative particle size distribution of HPMC established by laser diffraction (0 – 175 µm) showing incomplete distribution due to existence of coarse particles.
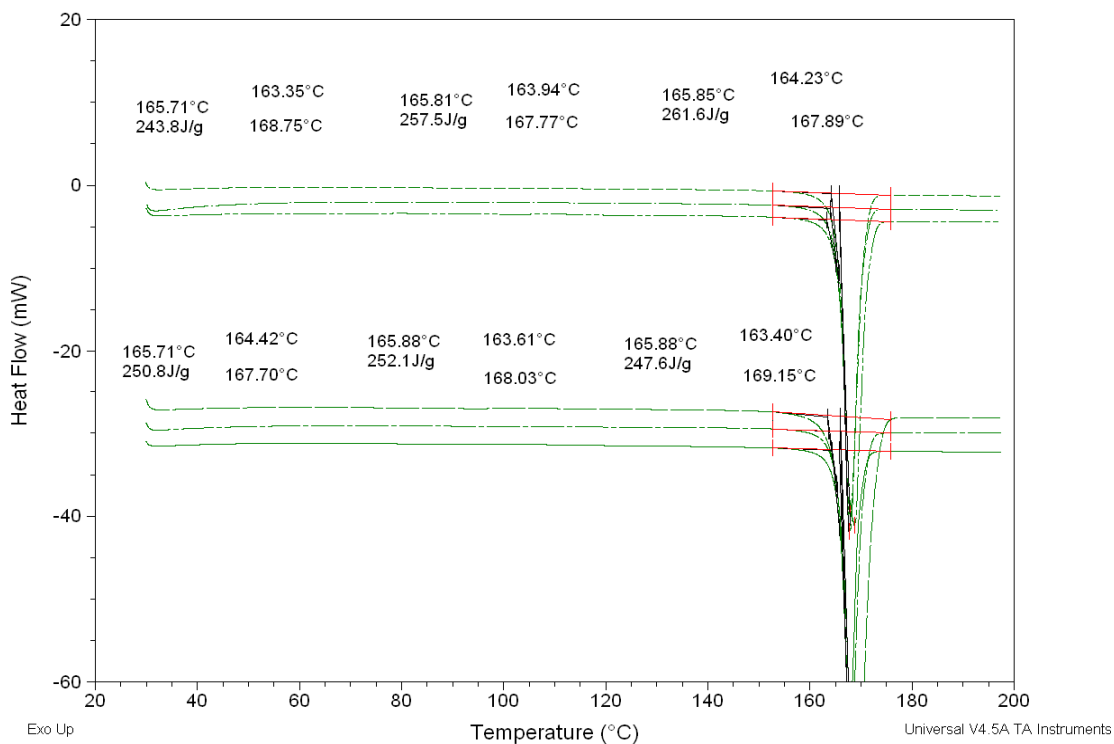
A. 3: Normal and Cumulative particle size distribution of L-HPC established by laser diffraction (0 − 175 µm) showing unimodal distribution between 0 and 125 µm.
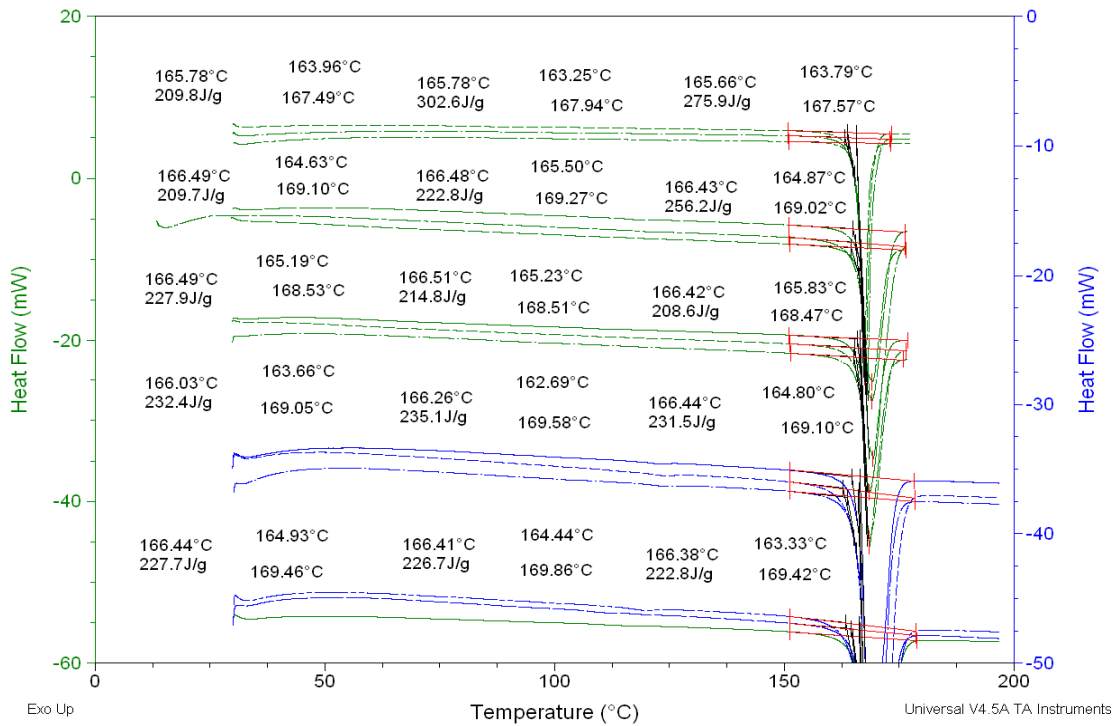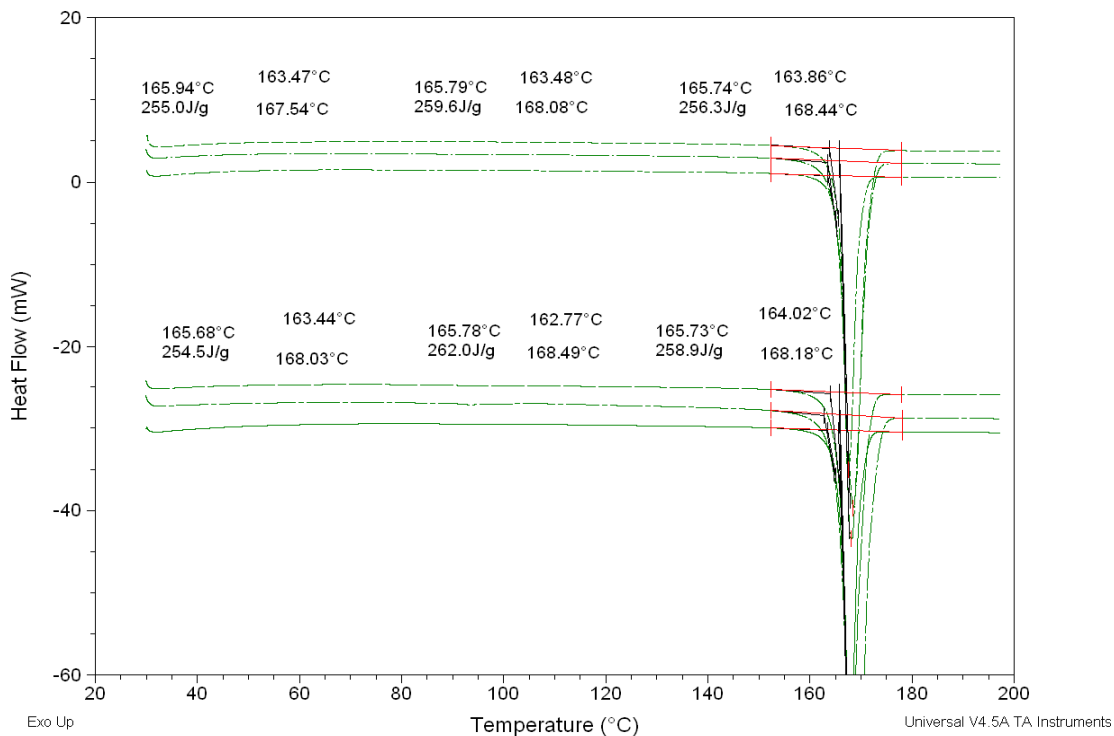

A. 4: DSC stability profile (1 month) at 25°C/60% RH and 40°C/75% RH.

283
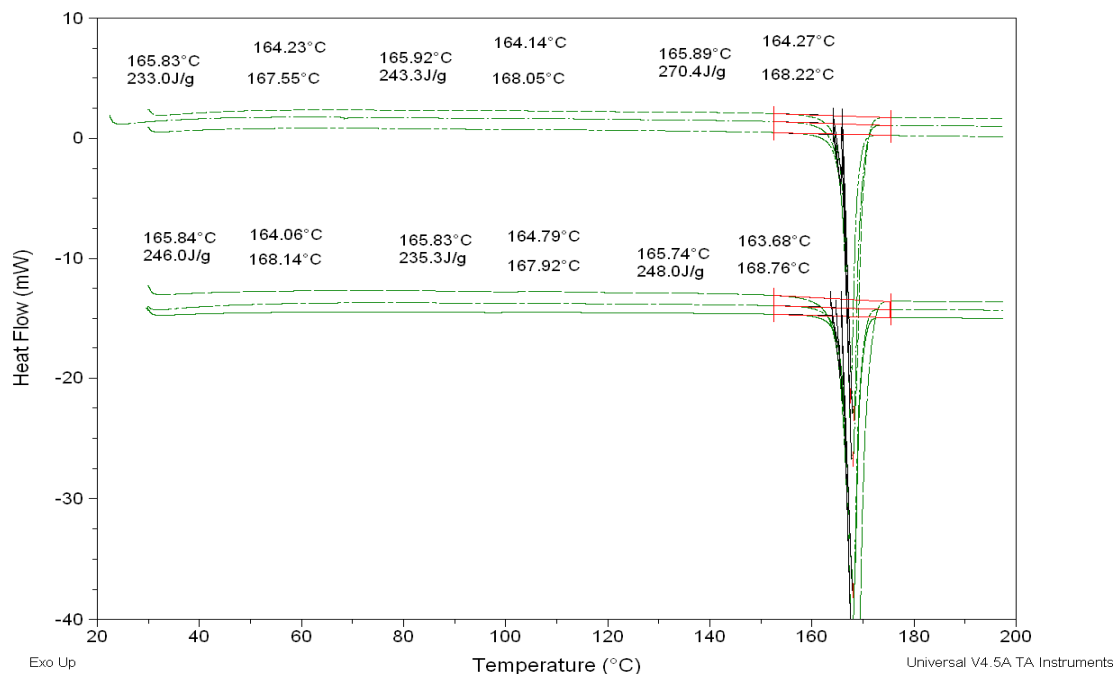
A. 5: DSC stability profile (2 months) at 25°C/60% RH and 40°C/75% RH.

A. 6: DSC stability profile (3 months) at 25°C/60% RH and 40°C/75% RH.

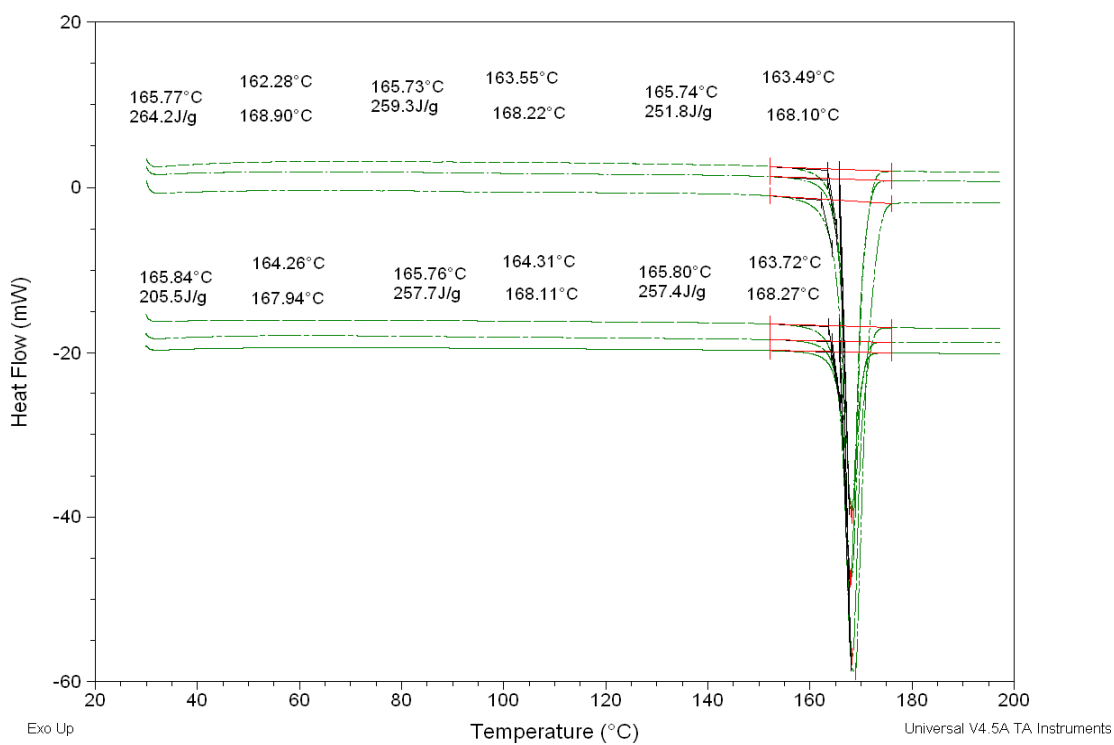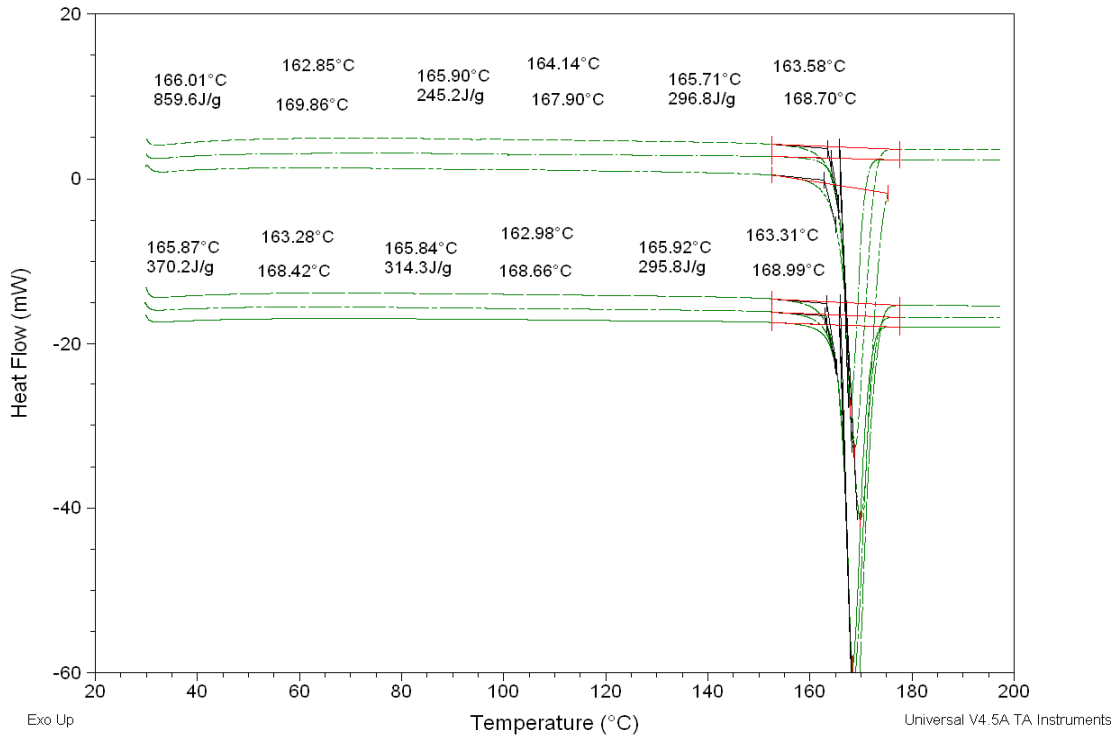284

A. 7: DSC stability profile (4 months) at 25°C/60% RH and 40°C/75% RH.

A. 8: DSC stability profile (5 months) at 25°C/60% RH and 40°C/75% RH.

A. 9: DSC stability profile (6 months) at 25°C/60% RH and 40°C/75% RH.
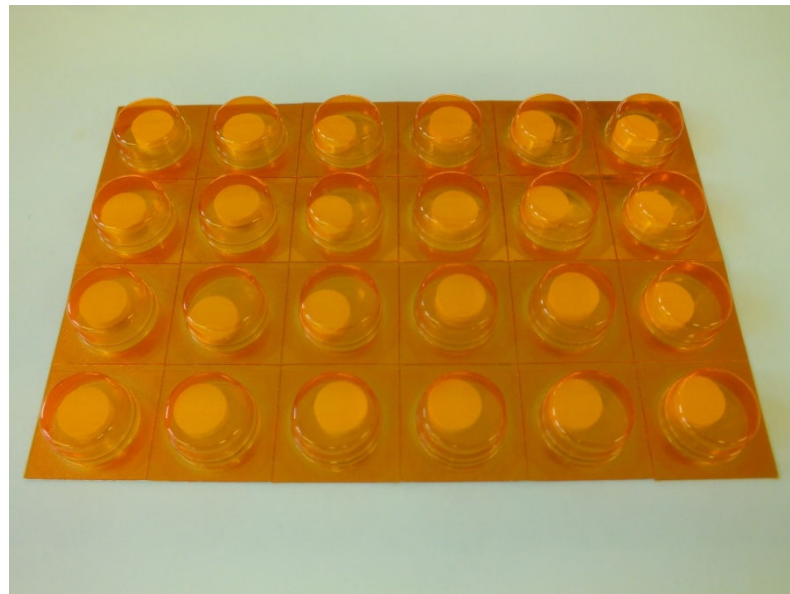

A. 10: Amber blisters meet USP requirements for protection of light sensitive medication. Combination of blister and label provides the highest in moisture barrier protection properties and meets USP Class A package requirements which is a one-year expiration date from the date of packaging.

286

Appendix B.

B. 1: DOE worksheet showing the experimental process parameters and obtained responses. Total of 27 experiments (24 + 3 centre points).

| Exp No	Exp Name	Run Order	Incl/Excl	Inlet Temperature	Aspirator	Spray Gas Flow Rate	Feed Rate	Outlet Temperature	Particle Size	Encapsulation Efficiency	Moisture Content	Yield
1	N1	9	Incl	110	50	30	10	52	0	0	0	0
2	N2	8	Incl	180	50	30	10	62	22.97	5.78283	6.42	33.29
3	N3	23	Incl	110	90	30	10	84	0	8.61346	5.8	8.02
4	N4	6	Excl	180	90	30	10	100	33.09	10.4593	0	10.17
5	N5	24	Incl	110	50	60	10	46	6.16667	8.61346	6.01	18.47
6	N6	7	Incl	180	50	60	10	62	7.21333	11.4905	6.03	65.31
7	N7	25	Incl	110	90	60	10	77	8.56	9.27858	5.52	25.48
8	N8	11	Incl	180	90	60	10	98	7.97667	9.69621	5.86	64.86
9	N9	19	Incl	110	50	30	30	60	0	0	0	0
10	N10	5	Incl	180	50	30	30	67	29.3533	6.09992	6.67	14.16
11	N11	22	Incl	110	90	30	30	82	0	0	0	0
12	N12	20	Incl	180	90	30	30	101	36.4433	7.63382	6.02	15.45
13	N13	12	Incl	110	50	60	30	48	0	0	0	0
14	N14	3	Incl	180	50	60	30	50	7.27667	14.4487	4.69	27.56
15	N15	13	Incl	110	90	60	30	60	9.09333	7.67378	5.36	0
16	N16	18	Incl	180	90	60	30	78	9.75	11.7148	6.16	46.04
17	N17	27	Excl	110	70	50	20	65	12.8733	13.7875	7.67	29.3
18	N18	14	Excl	180	70	50	20	82	13.88	6.93519	6.13	42.53
19	N19	15	Excl	140	50	50	20	49	10.5733	12.5346	8.94	36.42
20	N20	26	Incl	140	90	50	20	85	15.1233	8.12042	6.47	35.62
21	N21	10	Incl	140	70	30	20	70	30.9033	8.53612	5.88	28.78
22	N22	4	Excl	140	70	60	20	70	0	8.70626	10.08	35.17
23	N23	17	Incl	140	70	50	10	77	13.11	8.42784	6.41	54.75
24	N24	21	Excl	140	70	50	30	51	11.83	0	7.11	31.28
25	N25	2	Incl	140	70	50	20	70	11.8033	8.18036	7.19	58
26	N26	1	Incl	140	70	50	20	70	15.34	8.3041	7.01	45.55
27	N27	16	Incl	140	70	50	20	65	16.7933	9.69621	8	50

287
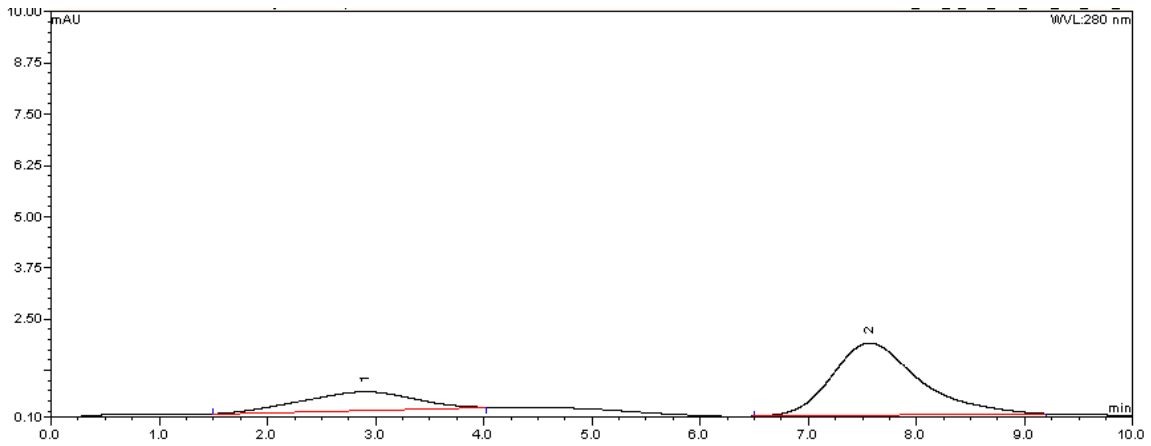
B. 2: HPLC chromatogram showing no interference between omeprazole peak (7 min) and degradation product peak (2 min) at 40°C/RH 75% stress condition.
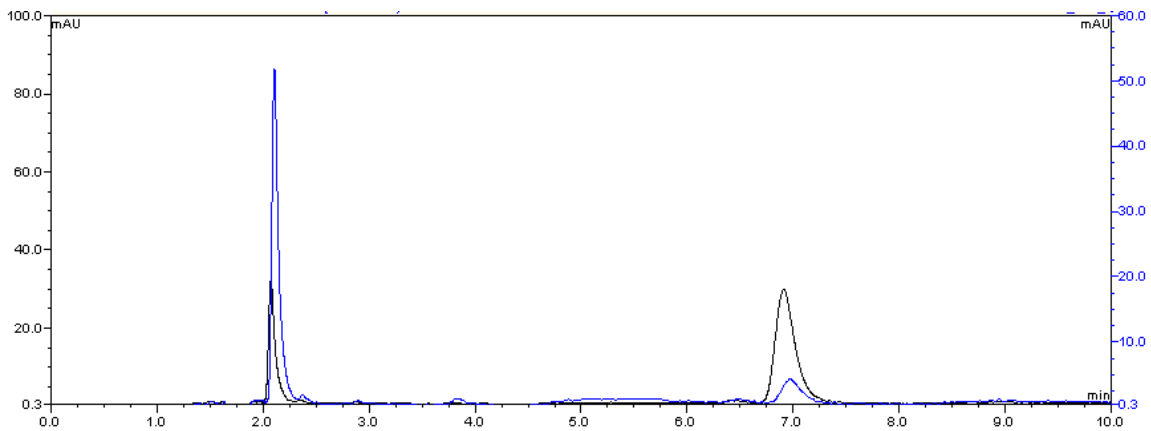
B. 3: HPLC chromatogram showing no interference between omeprazole peak (7 min) and degradation product peak (2 min) at pH 1-2 stress condition.
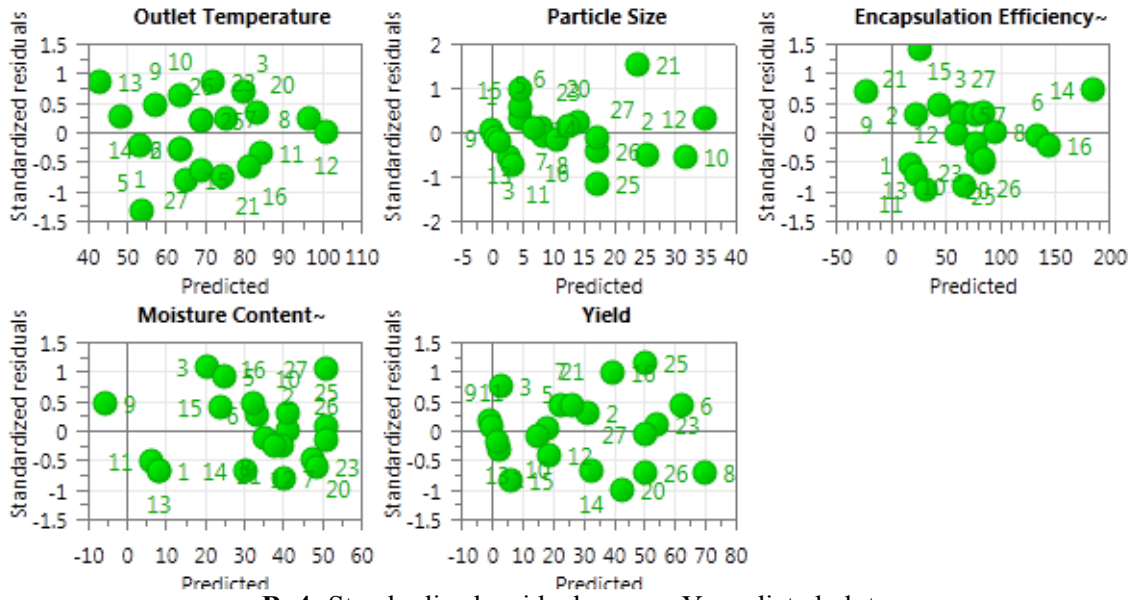
B. 4: Standardized residuals versus Y-predicted plot.